UNIVERSIDAD DE SEVILLA

FACULTAD DE BIOLOGÍA

Departamento de Bioquímica Vegetal y Biología Molecular

TESIS DOCTORAL

IDENTIFICACIÓN Y CARACTERIZACIÓN DE GENES IMPLICADOS EN LA SÍNTESIS Y MODIFICACIÓN DE LÍPIDOS DE OLEAGINOSAS.

Doctorando:

Antonio Javier Moreno Pérez

Tutor:

Dr. Francisco Javier Cejudo Fernández

Directores:

Dr. Enrique Martínez Force

Dr. Joaquín Jesús Salas Liñán

Trabajo presentado para optar al grado de Doctor por el Licenciado

Antonio Javier Moreno Pérez

Fdo. Antonio Javier Moreno Pérez

Vº Bº

El Tutor:

Dr. Francisco Javier Cejudo Fernández
Catedrático de la Universidad de Sevilla

Fdo. Dr. Francisco Javier Cejudo Fernández

Los Directores

Dr. Enrique Martínez Force
Investigador Científico
Instituto de la Grasa (CSIC)

Dr. Joaquín Jesús Salas Liñán
Científico Titular
Instituto de la Grasa (CSIC)

Fdo. Dr. Enrique Martínez Force

Fdo. Dr. Joaquín J. Salas Liñán

Sevilla, Septiembre de 2010

A mis padres y a Irene,
por su cariño y apoyo

Tras finalizar la redacción de mi tesis doctoral me gustaría agradecer a todas aquellas personas que me han ayudado de alguna manera a terminar con buen fin mi trabajo.

En primer lugar me gustaría agradecer a mis directores de tesis, Enrique Martínez Force y Joaquín J. Salas Liñán, por darme la oportunidad de seguir formándome y transmitirme su entusiasmo por la ciencia.

Gracias Quique por ser algo más que un jefe, por estar siempre dispuesto a echarme una mano, por tus consejos y sobre todo por confiar en mí.

Gracias Quino por ayudarme durante todo el trabajo y por demostrarme que ser buen científico no está reñido con ser sevillista.

A Rafael Garcés, por estar siempre ahí cuando lo he necesitado y darme la oportunidad de formar parte de este magnífico grupo.

Al Dr. Francisco Javier Cejudo, por acceder a la tutoría de mi tesis.

Al Instituto de la Grasa y en especial a su director, Francisco Millán, por poner a mi disposición todo lo necesario para realizar esta tesis.

También quisiera agradecer a todos los miembros de mi grupo, sin los cuales nunca podría haber llegado a escribir estas líneas.

A Damián y Juan Diego, por ser algo más que mis compañeros de laboratorio, por ser mis amigos. Muchos años juntos, muchos recuerdos, muchos momentos buenos y otros tantos menos buenos. Espero no dejar de teneros a mi lado porque gente buena como vosotros es la que te empuja a seguir hacia delante. Gracias amigos.

A Irene, por ser como eres y hacer más amenos mis días con nuestros momentos musicales.

A Adrián, por ser un buen amigo, prestarme su ayuda incondicional y por ser el tío con más arte de Los Palacios.

A Alicia, por ser una maravillosa compañera y amiga. Ha sido un placer poder trabajar contigo.

A Mónica, por todos sus buenos consejos, apoyo y por toda la información "premamá" extra que me llevo.

A Arantxa, Bárbara y Marisol, por ser simplemente magníficas. Gracias por la alegría que me habéis transmitido.

A Javi y Loubna, por enseñarme en mis primeros pasos en la ciencia, por tener paciencia conmigo y por compartir tantos buenos momentos.

A Mª Carmen, por sus buenas palabras y por cuidar de mí en todo momento.

A Diana y Noemí, por todo lo que me enseñaron en el tiempo que compartimos.

A los chicos del coro, Miguel Ángel y Miriam, por aportar el toque culto a nuestro grupo.

A José Antonio, por su apoyo y por estar siempre dispuesto a jugar al futbol conmigo.

A todo el grupo del Dr. Ian Graham de la Universidad de York por el buen trato que me dieron durante mi estancia en su laboratorio y en especial a Fabián Vaistij por aguantarme durante todo ese tiempo.

A Luisa Hernández, por enseñarme tantas y tantas cosas, por darme siempre buenos consejos, por su ayuda en los momentos difíciles y por ser una buena amiga.

A Justo, por ser un gran apoyo aquí dentro, por nuestros madrugones para ponernos "más fuertes que el vinagre" y sobre todo por descubrirme que hay cosas que nunca cambiarán con el tiempo.

A Rosario, por toda su ayuda y dedicación.

Al resto de miembros del Instituto de la Grasa, a Lourdes, Almudena, Elena, Cristina, Mª Ángeles, Javi, Mere, Mª Mar, Mª Carmen, Juanma, Lola, María, Araceli, Ana, Carmen, Mercedes… y otros tantos, por ser mi segunda familia durante estos años y por todos los ratos divertidos que hemos vivido juntos.

A mis amigos, los de aquí y los de allá, en especial a Carlos y Roman, por ayudarme a ver que existían más cosas que la tesis durante estos años.

A mis "suegris", por tratarme tan bien y hacerme uno más de su familia.

A todas mis cuñadas, por su gran cariño.

A mis hermanos, por apoyarme y ser pieza fundamental en mi vida. Gracias por no fallarme nunca.

A mis padres, gracias por la educación que me habéis dado, por vuestra preocupación y todo el cariño que me demostráis a diario. Gracias a vuestro esfuerzo y sacrificio he logrado ser lo que soy.

Por último, quisiera agradecérselo y dedicárselo a Irene, por ser la verdadera causante de que me dedique a esto. Por disfrutar con mis buenos momentos y levantarme de los malos. Por orientarme y mimarme. Gracias Irene por ser mi estrella.

ÍNDICE

ABREVIATURAS

ACC	Acetil-CoA carboxilasa
ACP	Proteína transportadora de acilos
ACS	Acil-CoA sintetasa
AGL	Ácidos grasos libres
BCCP	Biotina carboxilasa
CPT	Colina fosfotransferasa
d18:0	Esfinganina
d18:1^4	Esfingosina
DAG	Diacilglicerol
DAGAT	Diacilglicerol aciltransferasa
DDF	Días después de floración
DGTA	Diacilglicerol:diacilglicerol transacilasa
DGDG	Digalactosildiacilglicerol
DH	β-hidroxiacil-ACP dehidratasa
DSQG	Diacilsulfoquinovosilglicerol
ENR	Enoil-ACP reductasa
FAD2	Oleato desaturasa microsomal
FAD3	Linoleato desaturasa microsomal
FAD6	Oleato desaturasa plastidial
FAD7/8	Linoleato desaturasa plastidial
FAS	Ácido graso sintasa
FatA	Acil-ACP tioesterasa tipo A
FatB	Acil-ACP tioesterasa tipo B
GPAT	Glicerol-3-fosfato aciltransferasa
G3P	Glicerol-3-fosfato
KDS	3-cetohidroxiesfinganina
KAS	β-cetoacil-ACP sintasa
KR	β-cetoacil-ACP reductasa
LPA	Ácido lisofosfatídico
LPAAT	Lisofosfatidil aciltransferasa
LPC	Lisofosfatidilcolina
LPCAT	Lisofosfatidilcolina aciltransferasa
MAG	Monoacilglicerol

MGDG	Monogalactosildiacilglicerol
PA	Ácido fosfatídico
PAP	Fosfatidato fosfatasa
PC	Fosfatidilcolina
PDAT	Fosfolípido:diacilglicerol aciltransferasa
PE	Fosfatidiletanolamina
PG	Fosfatidilglicerol
PI	Fosfatidilinositol
PSer	Fosfatidilserina
RE	Retículo endoplásmico
SAD	Estearil-ACP desaturasa
t18:0	Fitoesfingosina
TE	Acil-ACP tioesterasa
TAG	Triacilglicerol

INTRODUCCIÓN

1. PLANTAS OLEAGINOSAS

Las plantas oleaginosas son vegetales cuyas semillas o frutos acumulan aceite. En el desarrollo de esta tesis se ha llevado a cabo el estudio de genes y enzimas implicadas en el metabolismo lipídico de distintas plantas oleaginosas.

1.1.Girasol

1.1.1. Aspectos generales

El girasol (*Helianthus annuus* L.) es una planta anual dicotiledónea perteneciente a la familia de las *Compuestas*, que crece bien en climas templados (Figura 1). Por su alto contenido de aceite en la semilla (38-52%) es una típica planta oleaginosa.

En los últimos años, el cultivo del girasol ha experimentado un importante desarrollo, triplicándose la superficie mundial dedicada a su cultivo desde 1961 hasta 2004, pasando de 6,6 a 21,3 millones de hectáreas (MHa) (Figura 2). Y, prácticamente, casi cuadriplicado su producción, pasando de 6,8 a 26,2 millones de toneladas (MT) (Figura 2). Como se puede observar en la Figura 2, esta tendencia ascendente, tanto de la producción mundial como de la superficie cultivada, se mantiene durante los últimos años, aunque cabe señalar que en España se ha producido en este mismo periodo, comprendido entre 1990 y 2005, un ligero descenso en ambos parámetros, como se aprecia en la Figura 3 (Faostat, 2009; http://faostat.fao.org/).

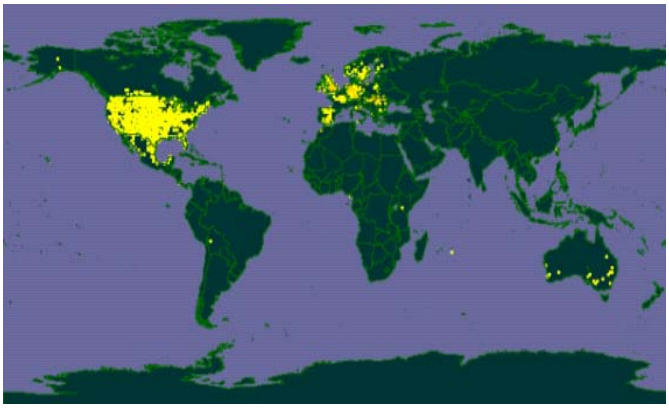

Figura 1. Distribución mundial del cultivo de girasol. En amarillo se indican las zonas de cultivo.

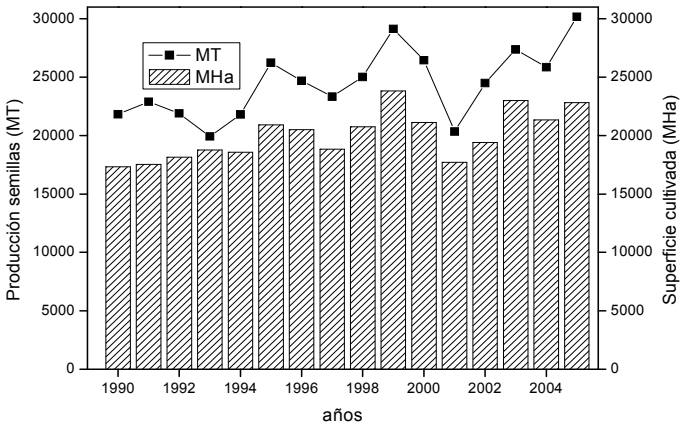

Figura 2. Evolución de la superficie cultivada y la producción mundial durante los últimos años. (Faostat, http://faostat.fao.org/**).**

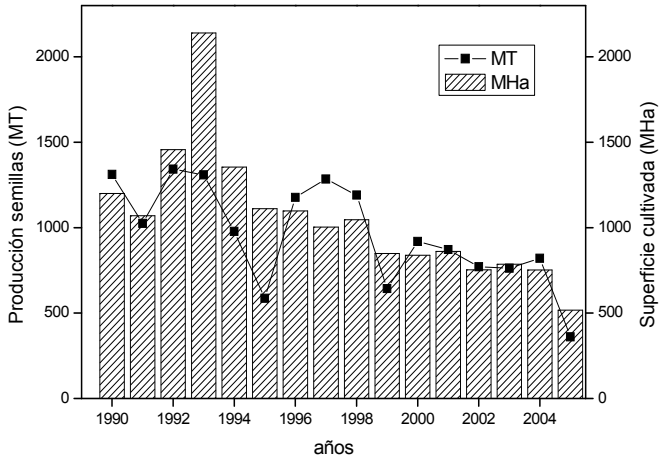

Figura 3. Evolución de la superficie cultivada y la producción en España durante los últimos años. (Faostat, http://faostat.fao.org/**).**

Las razones del éxito de este cultivo pueden resumirse en dos, el girasol es una planta rústica de fácil cultivo y tiene una buena adaptación a una gran variedad de suelos. Su aceite ha encontrado, desde el primer momento, una excelente acogida entre los consumidores y ha obtenido el respaldo de científicos y dietistas, especialmente como sustitutivo de las grasas de origen animal. La relativa sencillez de las técnicas industriales para su extracción, así como su fácil conservación, son otras de las ventajas para su industrialización y su comercio (Alba y Llanos, 1990).

Actualmente, el girasol es una de las cinco oleaginosas para consumo humano más cultivadas en todo el mundo.

1.2.2. Historia, origen y botánica de Helianthus annuus L.

El girasol pertenece al orden Synandrales, familia Asteridae, género Helianthus y especie *H. annuus*. El nombre latino del género alude a la forma y aspecto de la inflorescencia y el de la especie a la característica de anualidad del ciclo vegetativo-reproductivo de la planta. Se trata de una planta anual, con un desarrollo vigoroso en todos sus órganos. El género Helianthus comprende 68 especies, de las que *H. annuus* tiene la mayor extensión geográfica y es la más variable del género. Dentro de esta especie existen numerosos tipos o subespecies cultivadas como plantas ornamentales, oleaginosas y forrajeras.

En cuanto al origen del girasol actual, algunos autores piensan que Helianthus, con un número de cromosomas n=17, procede de la hibridación de dos especies ancestrales del género Viguiera, con n=8 y n=9 (Jackson y Murray, 1983). Así se produjo un híbrido con 17 cromosomas que pasó a tener 34 al duplicarse espontáneamente evitando la inestabilidad en meiosis. De esta forma, aunque se comporte como un diploide en general, hay que tener en cuenta la posibilidad de un posible origen tetraploide y de que existan cromosomas homeólogos.

Las variedades de girasol cultivadas en el mundo son el resultado de un largo proceso de adaptación a distintos ambientes y de selección, dirigida normalmente a la obtención de plantas con mayor contenido en aceite.

1.1.3. Morfología y fisiología

La raíz es del tipo pivotante y con un sistema de raíces secundarias de las que nacen las terciarias, que exploran el suelo en sentido horizontal y vertical. Normalmente, la longitud de la raíz principal sobrepasa la altura del tallo. La raíz cuando tropieza con obstáculos desvía su trayectoria vertical y deja de explorar las capas profundas del suelo, llegando a perjudicar el desarrollo del cultivo y, por tanto, el rendimiento de la cosecha.

El tallo es cilíndrico y de consistencia semileñosa y maciza en su interior con un diámetro variable entre 2 y 6 cm y una altura hasta el capítulo entre 40 cm y 2 m. La superficie exterior del tallo es rugosa, asurcada y vellosa; excepto en su base. En la madurez, el tallo se inclina en la parte terminal debido al peso del capítulo.

Las hojas son alternas, grandes, trinervadas, largamente pecioladas, acuminadas, dentadas y de áspera vellosidad tanto en el haz como en el envés. El número de hojas varía entre 12 y 40, según las condiciones de cultivo y la variedad. El color también es variable y va de verde oscuro a verde amarillento.

La inflorescencia consiste en un disco de 10 a 40 cm de diámetro (según variedades y condiciones de cultivo), que puede ser plano, cóncavo o convexo. El capítulo del girasol cultivado es solitario, rotatorio y está rodeado por brácteas involucrales. El número de flores varía entre 700 y 3000 en variedades para aceite y hasta 6000 o más en variedades de consumo directo. Está formado por un tejido de naturaleza esponjosa en el que se insertan las flores que nacen sobre su cara superior (Figura 4A). El verticilo o anillo exterior del capítulo está formado por flores liguladas, estériles y dispuestas radialmente (Figura 4B: e), con una función de exhibición y atracción visual para los insectos polinizadores. Las flores propiamente dichas son las tubulosas, que están en el interior del capítulo y forman círculos espirales desde el centro (Figura 4B: a-d). Estas flores están formadas por un ovario inferior, dos sépalos, una corola en forma de tubo compuesta por cinco pétalos, y cinco anteras unidas a la base del tubo de la corola.

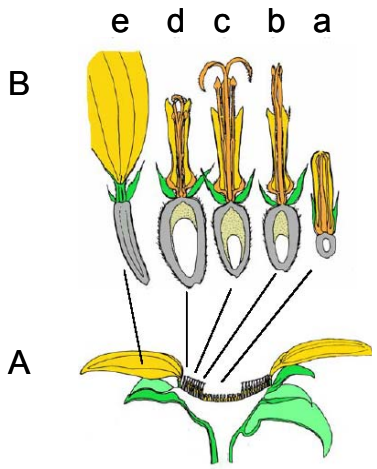

Figura 4. Representación esquemática de una inflorescencia de girasol. A. Sección longitudinal de un capítulo de girasol; **B**. Flores liguladas (e) y tubulosas en diferentes estadíos de desarrollo: antes de abrirse (a); abriéndose (emergencia de estambres) (b); abierta (c) y después de fecundada (d). Modificado de Alba y Llanos (1990).

El fruto es un aquenio de tamaño comprendido entre 3 y 20 mm de largo, 2 y 13 mm de ancho, y 2,5 y 5 mm de grueso (Figura 5). Las flores del centro del capítulo generalmente no se transforman en frutos. El pericarpio (envuelta exterior del fruto) es duro y fibroso, y queda pegado a la semilla menos en sus aristas. La membrana seminal crece con el endospermo y forma una película fina que cubre el embrión de la semilla y asegura la adherencia entre pericarpio y semilla. Los cotiledones representan la reserva energética de la semilla, y entre éstos está la gémula.

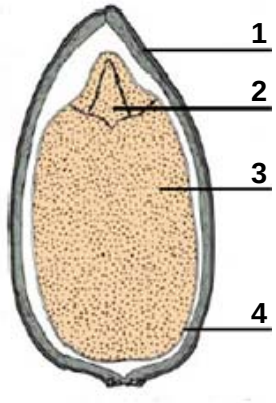

Figura 5. Sección longitudinal de un aquenio de girasol. 1. Pericarpio; 2. Gémula; 3. Cotiledón; 4. Membrana seminal.

La duración del ciclo del girasol depende de la variedad y el momento de la siembra, y se divide en varias etapas (Alba y Llanos, 1990).

La germinación y emergencia van desde la siembra hasta la aparición de los cotiledones. En función de la humedad y la temperatura puede durar de 10 a 30 días. La formación de las primeras hojas va desde la emergencia hasta la aparición de 4-5 pares de hojas. Durante esta fase se produce un rápido crecimiento de la raíz, lo que condiciona el posterior vigor de la planta. En esta etapa, la disponibilidad de agua es muy importante, siendo perjudicial tanto la falta como el exceso de ésta. Esta fase dura entre 15 y 25 días. A partir de este momento, tiene lugar la fase de crecimiento más activa y de máxima absorción de elementos minerales del suelo, que dura hasta el principio de la floración. Cuando se forma el botón floral es cuando la planta es más sensible al estrés hídrico. Esta fase tiene una duración de entre 40 y 50 días. La floración comprende todo el periodo en el que las flores se van abriendo.

Las primeras flores en abrir son las de la parte exterior del capítulo y continúa con la apertura de los anillos exteriores hacia el centro, a razón de 1 a 5 anillos diarios.

En esta etapa se determina el número de flores que van a convertirse en semillas. En este momento la planta es muy sensible a la falta de agua y a las temperaturas elevadas. Las flores liguladas (pétalos amarillos) que rodean el capítulo se secan y empiezan a caerse un día después de abrirse las últimas flores del centro del capítulo. El proceso tarda en completarse de 10 a 12 días. La polinización y fecundación, llevada a cabo por insectos, es generalmente alógama (fecundación cruzada entre flores distintas). Los óvulos una vez fecundados reciben sustancias de reserva hasta que se convierten en semilla madura.

La fase de maduración de la semilla va desde el final de la floración, hasta el estado de madurez fisiológica. Durante este periodo, se llena la semilla y se produce la biosíntesis del aceite. Ésta finaliza cuando la semilla tiene aproximadamente un 40% de humedad. El periodo de maduración puede durar entre 35 y 50 días.

1.2. Ricino

1.2.1. Importancia y distribución del cultivo de ricino

Las dos terceras partes de la producción mundial de grasas y aceites se obtienen de semillas de oleaginosas, y dentro de éstas, el ricino como cultivo oleaginoso contribuye sólo al 0,5% de la producción mundial de grasas y aceites vegetales, según los datos de la FAO. Sin embargo, el aceite de ricino es uno de los 5 aceites vegetales más utilizados por la industria. El ricino es cultivado por su alto contenido de aceite en semilla (55%). Dicho aceite es la principal fuente natural del ácido ricinoleico pudiendo alcanzar el 85% del total de ácidos grasos. Su aceite se utiliza ya sea directamente o tras previas transformaciones químicas. Los usos más importantes para éste son la fabricación de barnices, coberturas protectoras, lubricantes de alto grado, etc.

En los últimos 20 años la producción mundial de semillas de ricino, según los datos de la FAO (FAOSTAT), se ha mantenido relativamente estable (Figura 6), con aproximadamente un millón de toneladas métricas de semillas por año y distribución centralizada fundamentalmente en India (Figura 7). En España no se han encontrado datos oficiales en FAOSTAT de la producción de dicho cultivo. Ello se debe a que dicho cultivo no es común en nuestro país. Pero aún así, el ricino está totalmente

adaptado a las condiciones climáticas de Andalucía, creciendo de manera silvestre en multitud de lugares.

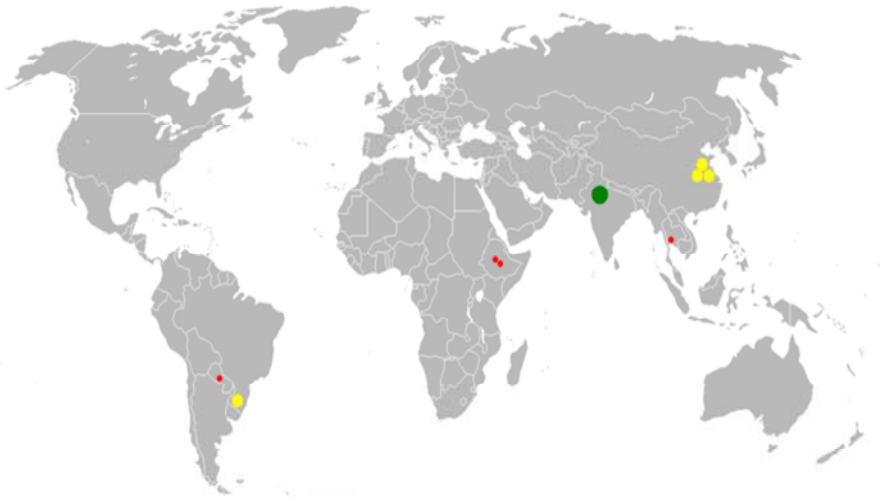

Figura 7. Distribución mundial del cultivo de ricino. Los datos mostrados se refieren al porcentaje de la India, que es el productor mayoritario con 730.000 Toneladas. En verde se muestra el 100%; en amarillo el 10%; y en rojo el 1%.

1.2.2 Historia, origen y botánica de Ricinus communis L.

El ricino (*Ricinus communis* L.) es miembro de la familia *Euphorbiaceae*. Se trata de un género monotípico, siendo *R. communis* la única especie conocida. Es diploide y todos las variedades tienen el mismo número de cromosomas (2n=20), aunque alguna vez se ha informado de polimorfismo cromosomal, y se cree que la especie podría ser un alopoliploide con un número básico de x=5 (Weiss, 1983; Atsmon, 1989).El nombre Ricinus deriva del término latino que designa a la garrapata de la oveja mediterránea (*Ixodes ricinus*), por el gran parecido físico de su fruto con el del insecto (Weiss, 1983). En español también se le conoce con el nombre de "Higuerilla", "Higuereta" y "Tártago". La domesticación del ricino se pierde en la historia. Las referencias más tempranas de su uso por el hombre se encuentran en Egipto (4000 A.C.) (Weiss, 1983; Bonjean, 1991), donde su aceite era usado como combustible en las lámparas (Weiss, 1983). En India, hay referencias de su uso en lámparas por los indígenas desde el 2000 A.C., donde se describen dos variedades, una de semilla roja y la otra blanca. El aceite fue utilizado, y aún lo es, en medicina local

como laxante, pero también para el tratamiento de la piel. Las hojas se utilizaron tradicionalmente como alimento para el gusano de seda (Weiss, 1983; Bonjean, 1991).

1.2.3. Descripción de la planta

La planta de ricino tiene una alta capacidad de adaptación, crece con éxito en zonas tropicales, sub-tropicales y también en zonas mediterráneas, pero es susceptible a las heladas, especialmente en los primeros estadios de desarrollo. El color de las plantas de ricino varía desde el rojo intenso al verde. Los tallos, hojas y frutos pueden estar cubiertos por cera. El fruto es una cápsula trilobular, con tres semillas y distintos grados de dehiscencia (Figura 8). Estas cápsulas pueden ser espinosas, glabras o intermedias.

Figura 8. Estadíos de maduración de semillas de ricino. A, fruto encapsulado verde; B, fruto encapsulado seco; C, detalle de la apertura de la cápsula y semilla.

Las semillas muestran una gran variabilidad genética en el dibujo, tamaño, forma y color (Atsmon, 1989; Brigham, 1993). Normalmente no presenta latencia, pero su tasa de germinación cae drásticamente después de 2 o 3 años si no son almacenadas en frío y baja humedad (Atsmon, 1989).

La planta de ricino puede variar de uno a varios metros de altura, pudiendo ser genéticamente enana, semi-enana o alta. Posee grandes hojas lobuladas, que se asemejan a las de una palma. Aunque se cultiva como una planta anual, es perenne (Weiss, 1983; Atsmon, 1989; Brigham, 1993).

El tallo principal se encuentra terminado por el primer racimo o racimo primario, el cual es frecuentemente el más largo de la planta. El racimo primario suele darse normalmente en los nudos más jóvenes después del sexto al décimo nudo. En los cultivos antiguos, los racimos pueden aparecer del octavo al decimosexto nudo.

Después de la aparición del racimo, se originan ramificaciones en el nudo por encima del racimo. El número de ramificaciones depende del espacio disponible por la

planta y en algunos casos del cultivar. En condiciones de cultivo en campo, se producen dos o tres ramificaciones a la vez, pero generalmente en el siguiente orden: la primera ramificación se da inmediatamente por debajo del racimo primario, la segunda en el nudo segundo y la tercera en el nudo tercero por debajo del racimo primario. Los primeros racimos formados en las ramificaciones son comúnmente llamados "segunda generación de racimos". Posteriormente otras ramificaciones se generarán en los nudos justo por debajo de los racimos de la segunda generación. Esta secuencia de desarrollo continúa tanto tiempo como la planta permanezca viva y creciendo activamente. Por lo tanto, el desarrollo de racimos a lo largo de un eje es secuencial, haciendo posible para una misma planta encontrar el desarrollo de racimos desde el estadío de yema a completamente maduros.

La inflorescencia, normalmente monoica, está formada por un racimo con un eje central y ramificaciones laterales que se diferencian en flores unisexuales, con flores masculinas (estaminadas) en la base de la inflorescencia (racimo), y femeninas (pistiladas) sobre las anteriores (Weiss, 1983; Atsmon, 1989; Brigham, 1993).

El ricino es una planta de polinización abierta, principalmente anemófila, pero las abejas, y quizás otros insectos, pueden ser también vectores de polinización, con tasas de polinización cruzada que varían desde un 35% hasta el 70%, pudiendo llegar incluso al 90%.

1.2.4. Mejora genética del ricino

La variabilidad genética en las poblaciones silvestres de ricino es enorme, lo que ha hecho posible encontrar caracteres deseados como indehiscencia, precocidad, estructura delgada, semilla grande y dos tipos de feminidad. A su vez, gracias al reducido efecto de depresión endogámica y a la herencia relativamente simple de los caracteres de interés económico, ha sido posible una rápida mejora del cultivo (Atsmon, 1989). Como en otros cultivos oleaginosos, el principal objetivo de mejora en ricino es incrementar el rendimiento en aceite y, por lo tanto, de semillas por hectárea. Para ello, además de seleccionar plantas más vigorosas, las estrategias incluyen la selección para una alta proporción de flores femeninas por racimo, un mayor número de racimos por plantas, y/o un mayor peso de semilla (Weiss, 1983; Atsmon, 1989).

Un sistema de mejora llevado a cabo en los últimos años se basa en la obtención de líneas androestériles para así poder obtener un mayor rendimiento de aceite y

semillas (Brigham, 1993). La disponibilidad de líneas androestériles es indispensable para la producción de semilla híbrida, de la cual se obtienen plantas híbridas F_1 que presentan mayores rendimientos debido a la dominancia de los caracteres como el número de nudos en el primer racimo, peso de la semilla, número de semillas por racimo, mayor contenido de aceite en la semilla, y de la distribución uniforme de las flores pistiladas a lo largo de la inflorescencia (Weiss, 1983; Brigham, 1993).

1.3 Macadamia

1.3.1. Origen y botánica

El género *Macadamia* pertenece a la familia Proteaceae, perteneciente a su vez al orden Proteales. La familia Proteaceae consta de 80 géneros y unas 1700 especies, que se distribuyen por el hemisferio sur, ocupando áreas de origen gondwánico y sus fragmentos. La mayor concentración de diversidad de taxones se encuentra en Australia y Sudáfrica. El género *Macadamia* consiste en 10 especies pero sólo dos, *Macadamia tetraphylla* L. Johnson y *Macadamia integrifolia* Maiden & Betche, son cultivadas por sus nueces comestibles (McHargue, 1996). *Macadamia integrifolia* es originaria de la zona de selva tropical del sudeste de Queensland, Australia, donde crece cerca de riachuelos. Por otro lado *Macadamia* tetraphylla, además del sudeste de Queensland también es nativa del nordeste de Nueva Gales del Sur, Australia. En zonas donde ambas especies coexisten pueden aparecer híbridos naturales.

La macadamia era un importante alimento para los aborígenes australianos. El cultivo comercial de la nuez se inició en los años 30 en Hawái y se impulsó en los 60 en Australia. En la actualidad el cultivo de macadamia se ha extendido a muchos otros países (Tabla 1).

Tabla1: Producción mundial de macadamia en toneladas métricas de grano. Datos provenientes de la Asociación Sudafricana de Cultivadores de Macadamia (www.samac.org.za)

País	Producción mundial de grano de macadamia (Toneladas métricas)				
	2004	2005	2006	2007	2008
Australia	12600	10000	12200	11600	10500
Sudáfrica	3063	4205	4480	4902	5600
EEUU (Hawái)	4750	5200	5500	3750	3750
Kenia	1650	1800	2052	2000	2000
Malaui	1150	1595	1100	1468	1523
Guatemala	1000	1200	1250	1230	1250
Brasil	500	665	750	900	750
Costa Rica	250	200	100	200	200
Zimbabue	-	225	208	100	100
Otros	200	400	400	450	450
Total mundial	25163	25490	28040	26600	26123

1.3.2. Características del árbol

Se encuentra en forma natural en los bosques lluviosos tropicales o subtropicales. Su forma y tamaño varían, alcanzando entre 10 a 20 m de altura en lugares boscosos, sin embargo, solo alcanza los 10 m en áreas abiertas. La madera es de veta gruesa y dura, pero las ramas son quebradizas y se desenganchan y caen fácilmente.

1.3.3. Características del racimo floral

El tamaño de los racimos florales puede variar entre 13 y 23 centímetros de longitud, nacen de las axilas de las hojas o de lugares desde donde éstas han caído. Los frutos se originan de un pequeño porcentaje de las flores del racimo floral, presentándose en pares, a lo largo de la inflorescencia. Esto permite obtener alrededor de 10 a 12 frutos por estructura floral, siendo raro encontrar más de 20 (Figura 9).

Figura 9: Estructura del árbol de macadamia y su racimo floral.

1.3.4. Características de la nuez

La nuez corresponde a una drupa globosa contenida en un pericarpio que se abre por una sutura. La semilla es simple, y está cubierta por una cáscara muy dura. La parte comestible es el embrión, de color blanco cremoso, que mide entre 2,0 a 2,8 centímetros de diámetro. Contiene un 80% de aceite y 4 % de azúcar, base peso seco. En la Figura 10 se muestra una nuez de macadamia abierta. En la parte superior de la imagen se encuentra el pericarpio y en la parte inferior la pulpa de la nuez dentro de la cáscara dura.

Figura 10: Nuez de macadamia abierta donde se diferencian el pericarpio, la cáscara y la pulpa de la nuez.

1.3.5. Diferencias entre variedades de macadamia

Tanto las dos variedades de macadamia anteriormente mencionadas, *Macadamia tetraphylla* y *Macadamia integrifolia*, como sus híbridos tienen importancia como

cultivos comerciales. Las principales diferencias entre las dos variedades se muestran en la Tabla 2.

Tabla 2: Principales características distintivas entre *Macadamia tetraphylla* y *Macadamia integrifolia*.

Características	*M. integrifolia*	*M. tetraphylla*
Disposición de las hojas	Usualmente 3 por nudo	Usualmente 4 por nudo, algunas veces 2 hasta 8.
Hojas adultas	Bordes lisos con 4 a 14 espinas con extremo romo. Sésiles.	Bordes serrados y siempre espinoso extremo. Pecioladas.
Brote nuevo	Verde pálido o cremosas blancas	Rosados a rojizos, ocasionalmente amarillento-verdoso.
Flores	Racimos de 10 a 20 cm de largo. Color blanco a cremosa.	Racimos de 17 a 28 cm de largo. Color rosado a rojizo, Ocasionalmente blanco a cremosas. Muy fragantes.
Producción	Produce fruta de los 3 a los 7 años.	Producción de los 2 a los 4 años.
Época de cosecha	En otoño, durante un largo periodo de seis meses a todo el año.	Caída rápida durante 6 a12 semanas.
Cáscara	Gruesa, firme, brillante, adherida a la nuez. Requiere máquina para despedrarla.	Delgada, firme, opaca, se abre al madurar. Muchas nueces caen sin la Cáscara.
Concha	Lisa o suave y redondeada, dura, gruesa, densa, quebradiza, fácil de romper.	Rugosa y levemente elíptica, dura, delgada y menos densa. Los extremos más firmes que los laterales.
Madera	Moderadamente densa, quebradiza.	Densa, dura fuerte, rara vez se quiebra o parte.
Semillas	Menos dulces, textura blanda.	Dulce, textura firme. Algo más variable en calidad.
Enfermedades	Susceptible a *Phytophtora cinamonii* (Pudrición radicular).	Menos susceptible.
Temperatura	Menos resistente al frío y al calor extremo. Requiere de temperaturas altas para obtener máximas calidad.	Más resistente al frío y fuerte al calor

En la Figura 11 se ponen de manifiesto las diferencias existentes entre las hojas de *Macadamia tetraphylla*, *Macadamia integrifolia* y su híbrido.

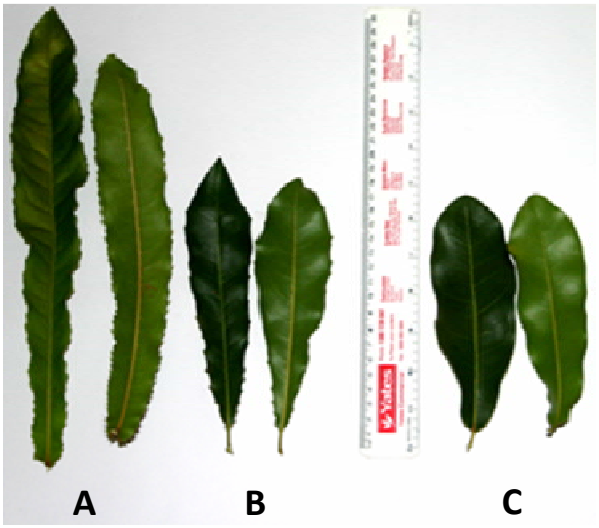

Figura 11: Hojas de macadamia. A: *M. tetraphylla* (sésil, larga y con margen serrado). B: Híbrido de *M. tetraphylla* x *M. integrifolia* (peciolada, longitud menor y margen menos serrado). C: *M. integrifolia* (peciolada, más corta y de margen liso). Modificado de Gitonga et al. (2008)

1.3.6. Usos y propiedades

Las nueces de macadamia comestibles tienen un alto contenido en grasas (73-80%) aunque también son ricas en proteínas y minerales. El aceite de la macadamia adquiere un interés especial ya que contiene altos niveles de ácidos grasos monoinsaturados, especialmente de ácidos grasos monoinsaturados n-7 como el ácido palmitoleico ($16{:}1^{\Delta 9}$) y el cis-vaccénico ($18{:}1^{\Delta 9}$), los cuales convierten el aceite de macadamia en beneficioso para nuestra salud (Maguire et al., 2004). De este modo, una ingesta regular de nueces de macadamia o de aceite proveniente de éstas produce un descenso de los niveles de colesterol LDL (Garg et al., 2003; Griel et al., 2008). También existen evidencias de un posible efecto antitumoral del aceite de macadamia (Hayatsu et al., 1988) y de efectos beneficiosos sobre el sistema cardiovascular (Harrison y Somerset, 2004). Por otro lado, el aceite de macadamia, por su composición, es ampliamente usado en cosméticos como un sustituto vegetal al aceite de visón y también cumple los estándares necesarios para ser usado como biolubricante (Garcés et al. 2010).

2. LÍPIDOS DE PLANTAS: ESTRUCTURA Y DISTRIBUCIÓN

2.1. Naturaleza y función de los lípidos

Se denominan lípidos a los componentes biológicos derivados de los ácidos grasos. Éstos son constituyentes esenciales de la célula viva y componen un grupo químico variado y heterogéneo. Los lípidos son biomoléculas que poseen un alto grado de insolubilidad en agua siendo, en cambio, fácilmente solubles en disolventes orgánicos no polares, que son empleados para extraerlos de las células y los tejidos.

Al igual que en el resto de seres vivos, los lípidos desempeñan importantes funciones biológicas en las plantas (Harwood, 1996):

i) Poseen un papel estructural fundamental, ya que son los componentes básicos de las membranas celulares, que actúan como barreras delimitando tanto las células como los compartimentos celulares. Asimismo, en estas membranas tienen lugar importantes funciones para la célula como la captación de luz, las reacciones de transporte de electrones o la generación de ATP;

ii) Sirven como material de reserva. Las especies vegetales oleaginosas acumulan lípidos en la semilla o el fruto, generalmente en forma de triacilgliceroles (TAG), que constituyen una importante materia prima tanto en la industria alimentaria como química;

iii) Están implicados en procesos biológicos fundamentales, como la transducción de señal actuando como precursores en la síntesis de hormonas como el ácido jasmónico y de segundos mensajeros como el inositol fosfato, la fotoprotección, la modificación post-traduccional de proteínas, el reconocimiento celular, la especificidad de especie, la inmunidad de los tejidos y la adaptación al frío;

iv) Actúan como cubierta protectora en la superficie de muchas plantas, como es el caso de las ceras, la cutina y la suberina.

2.2. Ácidos grasos

2.2.1. Definición y clasificación

Los ácidos grasos son biomoléculas orgánicas formadas por una cadena hidrocarbonada larga que contiene un número par de átomos de carbono y un grupo

carboxilo terminal (Coultate, 1996). Son compuestos insolubles en agua y ricos en energía. Se clasifican según:

- La longitud de la cadena:

  Ácidos grasos de cadena corta: 4-6 carbonos.

  Ácidos grasos de cadena media: 8-12 carbonos.

  Ácidos grasos de cadena larga: 14-18 carbonos.

  Ácidos grasos de cadena muy larga: 20 o más carbonos.

- El número y posición de los dobles enlaces:

  Saturados: no presentan ningún doble enlace, siendo moléculas lineales.

  Insaturados: tienen un doble enlace (monoinsaturados) o más de un doble enlace (poliinsaturados). Los dobles enlaces suelen ser de configuración cis, y cuando hay más de uno, suelen estar separados por grupos metileno.

2.2.2. Nomenclatura

Los ácidos grasos se pueden nombrar de diferentes formas. La mayoría de ellos tienen un nombre común, pero además, todos ellos se pueden nombrar mediante la nomenclatura sistemática y la abreviada. La nomenclatura sistemática sigue las reglas adoptadas por la IUPAC, donde se indica la longitud de la cadena y el número, posición y configuración de los dobles enlaces contando el número de átomos de carbono a partir del grupo carboxilo (Δ). En la nomenclatura abreviada el ácido graso se simboliza por dos números separados por dos puntos, indicando el primero la longitud de la cadena y el segundo el número de dobles enlaces. A continuación, se indica la posición en la que se encuentra el doble enlace, ya sea contando el número de átomos de carbono a partir del grupo carboxilo (Δ) o a partir del grupo metilo terminal (n ó ω). Finalmente, se indica la configuración *cis* (c) o *trans* (t) del doble enlace.

2.2.3. Ácidos grasos más frecuentes en la naturaleza

Los ácidos grasos son abundantes como componentes fundamentales de los lípidos, pero en estado libre (no esterificados) sólo aparecen en pequeñas cantidades. En la naturaleza existe una gran diversidad de ácidos grasos, pero no todos tienen la misma

importancia. Aunque se han aislado unos 300 tipos distintos de ácidos grasos, los más comunes sólo tienen entre 12 y 22 átomos de carbono (Tabla 3).

Tabla 3. Ácidos grasos más comunes en los lípidos de reserva

Nombre común	Nombre sistemático	Nombre abreviado
Láurico	Dodecanoico	12:0
Mirísrico	Tetradecanoico	14:0
Palmítico	Hexadecanoico	16:0
Palmitoleico	Cis-9-hexadecenoico	16:1 ω7c
Esteárico	Octadecanoico	18:0
Oleico	Cis-9-octadecenoico	18:1 ω9c
Linoleico	Cis,cis-9,12-octadecadienoico	18:2 ω6c,9c
α-linolénico	Cis,cis,cis-9,12,15-octadecatrienoico	18:3 ω3c,6c,9c
γ-linolénico	Cis,cis,cis-6,9,12-octadecatrienoico	18:3 ω6c,9c,12c
Aráquico	Eicosanoico	20:0
Gadoleico	Cis-11-icosenoico	20:1 ω9c
Behénico	Docosanoico	22:0
Erúcico	Cis-13-docosenoico	22:1 ω9c
Lignocérico	Tetracosanoico	24:0

Los ácidos grasos considerados mayoritarios, que constituyen en la mayoría de los casos más del 95 % del total, son el palmítico, esteárico, oleico, linoleico y α-linolénico (Harwood, 1979). Además de los ácidos grasos mencionados en la Tabla 3, existen también ácidos grasos con estructuras poco frecuentes, característicos de determinados grupos o especies vegetales. Estos ácidos grasos presentan dobles enlaces en posiciones poco comunes, triples enlaces, ramificaciones, sustituyentes como grupos hidroxi, epoxi, anillos de ciclopropeno, etc.

2.2.4. Estructura tridimensional

Como se muestra en la Figura 12, los dobles enlaces con isomería cis (B) introducen "codos" en las cadenas hidrocarbonadas, afectando con ello a sus propiedades físicas como, por ejemplo, el punto de fusión. No sucede lo mismo con los dobles enlaces en configuración trans (C), que no introducen más que un pequeño ángulo en la cadena, lo que supone un cambio menor en las propiedades físico-químicas

del compuesto y su comportamiento es más parecido al de los ácidos grasos saturados (A). Por ejemplo, el ángulo que introduce el doble enlace cis en la molécula del ácido oleico, hace que su punto de fusión baje desde 69ºC del ácido esteárico hasta 16ºC. El doble enlace trans, sin embargo, no distorsiona tanto la molécula, por lo que, el punto de fusión se mantiene en 44ºC.

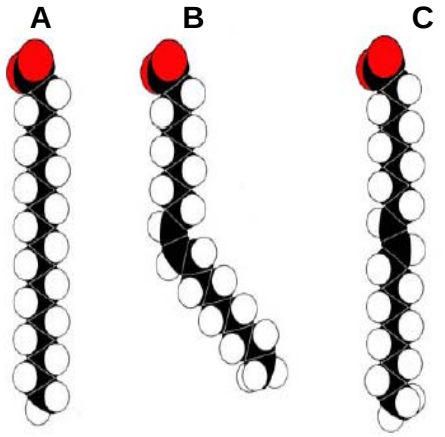

Figura 12 Estructura de los ácidos grasos y puntos de fusión: A) esteárico (18:0), B) oleico (18: 1ω9c ó18:1Δ^{9c}) y C) elaídico (18: 1ω9t ó 18:1 Δ^{9t}).

2.3. Lípidos vegetales

2.3.1. Acilglicéridos

Los acilglicéridos, también llamados grasas neutras, son glicerolípidos compuestos por una molécula de glicerol esterificada por uno, dos o tres ácidos grasos. Son solubles en disolventes apolares y su densidad es menor que la del agua.

En los monoacilgliceroles (MAG) hay un solo ácido graso esterificando a la molécula de glicerol en las posiciones *sn*-1, *sn*-2 o *sn*-3 (Figura 13). Existen, por tanto, tres formas isoméricas: los 1(3)-MAG y 2-MAG. Hasta muy recientemente no se les ha asignado a los MAG una función metabólica definida en los vegetales (Stobart et al., 1997). Los diacilgliceroles (DAG) tienen esterificadas dos posiciones (1,2-DAG, 2,3-DAG y 1,3-DAG). Los 1,2-DAG de configuración L se han descrito como importantes intermediarios en el metabolismo lipídico. Los 2,3-DAG y los 1,3-DAG sólo se encuentran en cantidades trazas. Los TAG tienen esterificadas las tres posiciones del glicerol. Cuando tienen un solo tipo de ácido graso se denominan TAG

simples y si contienen dos o más ácidos diferentes se llaman TAG mixtos o compuestos. Pueden existir muchas formas isoméricas.

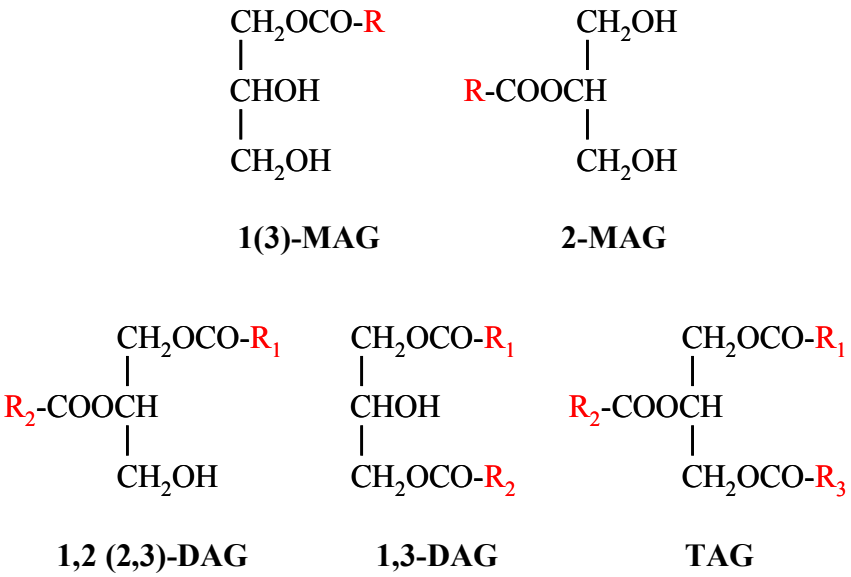

Figura 13. Estructura de los acilglicéridos. R = ácido graso.

De todos los lípidos, los TAG son los componentes mayoritarios de los aceites vegetales y, por tanto, su composición de ácidos grasos determina las propiedades tecnológicas y nutricionales de los mismos. Los MAG y los DAG se consideran compuestos minoritarios.

2.3.2. Fosfolípidos

Los fosfolípidos son otro grupo de glicerolípidos, siendo los compuestos más abundantes en las membranas celulares, mientras que en otras localizaciones celulares y en grasas y aceites sólo aparecen en pequeñas cantidades. Se caracterizan por tener la molécula de glicerol esterificada por dos ácidos grasos (Figura 14), mientras que la tercera posición está esterificada por una molécula de ácido fosfórico. Además, el ácido fosfórico se encuentra esterificado por un alcohol, que constituye un grupo de cabeza polar, confiriéndole carácter anfipático a la molécula. Los distintos fosfolípidos se diferencian en el tamaño, forma y carga eléctrica de sus grupos de cabezas polares.

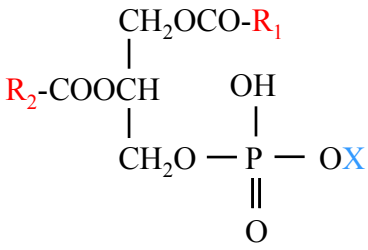

Figura 14. Estructura de los fosfolípidos. R = ácido graso, X = alcohol esterificado.

El compuesto primario de los fosfolípidos es el ácido fosfatídico (PA), que contiene un grupo de cabeza no polar, ya que no posee el alcohol esterificado. Se encuentra en pequeñas cantidades en las células, pero es un intermediario importante en la biosíntesis de los fosfolípidos y TAG. La fosfatidilcolina (PC), la fosfatidiletanolamina (PE) y la fosfatidilserina (PSer), contienen en su cabeza polar un aminoalcohol y pueden interconvertirse entre sí mediante varias reacciones enzimáticas (Dörmann, 2005). Los fosfolípidos más abundantes en plantas son PC y PE, los cuales representan más del 50 % de los glicerolípidos presentes en las membranas extraplastidiales. Mientras que PE no se encuentra en las membranas plastidiales, PC forma parte, además, de las membranas de la envuelta externa del cloroplasto. PSer es un fosfolípido minoritario en plantas, y, al igual que PE, no se encuentra en membranas cloroplásticas. El fosfatidilinositol (PI), que lleva un grupo inositol, se detecta en pequeñas cantidades en casi todas las membranas de las células vegetales. Sin embargo, mientras que su presencia en las membranas extraplastidiales está generalmente aceptada, la identificación de PI en las membranas tilacoidales no se ha confirmado. A pesar de que PI es un glicerolípido minoritario, juega un importante papel en la transducción de señal en las células, ya que es el precursor de los segundos mensajeros inositol trifosfato y DAG. El fosfatidilglicerol (PG), cuyo grupo de cabeza polar es una molécula de glicerol, es el único fosfolípido presente tanto en las membranas tilacoidales, como en las membranas extraplastidiales (Dörmann, 2005).

El fosfolípido más complejo es la cardiolipina o difosfatidilglicerol, que está constituido por una molécula de PG en la que el grupo 3'-hidroxilo de la segunda molécula de glicerol se encuentra esterificado por una molécula de PA. El esqueleto de la cardiolipina contiene tres moléculas de glicerol unidas mediante dos puentes fosfodiéster, los dos grupos hidroxilo de los gliceroles externos se hallan esterificados

por ácidos grasos. Su localización está restringida a las membranas internas mitocondriales.

2.3.2.1 Degradación de fosfolípidos. Fosfolipasas D.

La degradación de los fosfolípidos se da por acción de enzimas denominadas fosfolipasas. Las fosfolipasas están agrupadas en cuatro grupos distintos (fosfolipasa A_1, fosfolipasa A_2, fosfolipasa C y fosfolipasa D) dependiendo de la posición del fosfolípido en la que actúe (Figura 15). De todas ellas, la fosfolipasa D (PLD) aparece como la predominante en los tejidos de plantas. PLD cataliza la hidrólisis del enlace fosfodiéster terminal del fosfolípido generando PA y un grupo de cabeza hidrofílica libre.

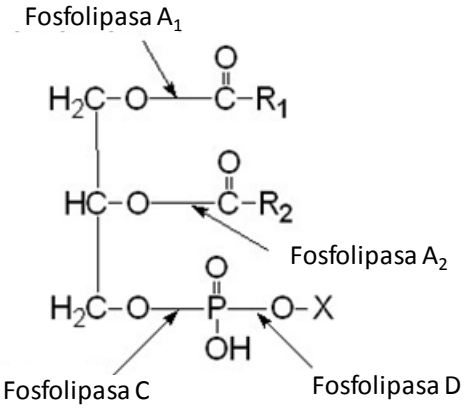

Figura 15. Sitios de acción de las fosfolipasas A_1, A_2, C y D.

La actividad enzimática correspondiente a una PLD fue caracterizada por primera vez en extractos de zanahorias como una actividad lecitinasa capaz de liberar colina de mezclas de fosfolípidos de plantas (Hanahan et al., 1947). La primera clonación y expresión de una PLD perteneció a un cDNA de la planta de ricino (Wang et al., 1994). Desde entonces, varios cDNAs de PLDs han sido clonados de otras especies de plantas, levaduras, roedores y humanos. PLDs de plantas están clasificadas en seis familias génicas denominadas PLDα, β, γ, δ, ζ y ε (Wang, 2000 y 2005) (Figura 16).

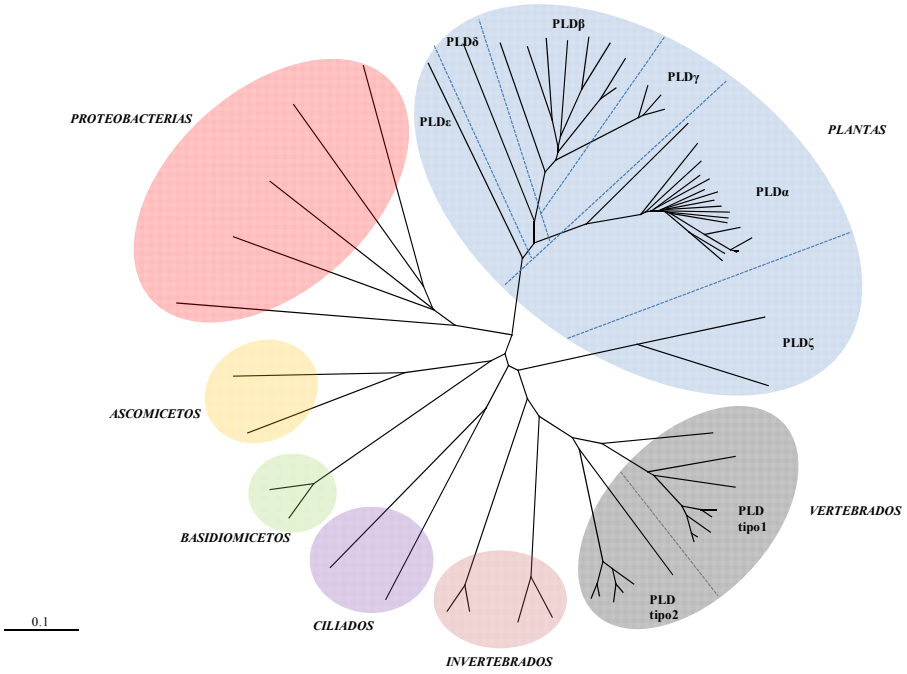

Figura 16. Análisis filogenético de las PLDs. Dentro de las PLDs de plantas se pueden diferenciar las seis familias génicas: PLDα, β, γ, δ, ζ y ε.

Todas las PLDs, a excepción de PLDζ, comparten una organización estructural común compuesta por un dominio de unión a fosfolípidos dependiente de Ca^{2+} (dominio C2) y dos motivos catalíticos HxKxxxxD típicos de enzimas de plantas que metabolizan fosfolípidos. Este tipo de enzimas además de estar relacionadas con el catabolismo e intercambio de lípidos de membrana, juegan un papel fundamental en la transducción de señales durante el metabolismo de la planta.

El bloque II de esta tesis se centrará en la clonación y caracterización funcional de la PLDα de girasol.

2.3.3. Glicolípidos

Los glicolípidos son otra clase de glicerolípidos que se diferencian de los fosfolípidos en que en lugar del grupo polar unido al grupo fosfato, presentan un azúcar en la tercera posición de la molécula de glicerol esterificada por dos ácidos grasos (Figura 17). Dentro de los glicolípidos destacan los galactolípidos, que presentan una (monogalactosildiacilglicerol, MGDG) o dos (digalactosildiacilglicerol, DGDG) moléculas de galactosa en el grupo de cabeza polar. Estos glicolípidos

representan el 85 % de los glicerolípidos presentes en las membranas cloroplásticas y contienen elevadas proporciones de ácidos grasos poliinsaturados, como los ácidos α-linolénico y hexadecatrienoico (Block et al., 1983). También en las membranas cloroplásticas se encuentran los sulfolípidos, que contienen una molécula de sulfoquinovopiranosil unida al grupo fosfato que esterifica la tercera posición de la molécula de glicerol. Este glicolípido se denomina diacilsulfoquinovosilglicerol (DSQG) y representa, aproximadamente, el 5 % de los glicerolípidos presentes en las membranas cloroplásticas.

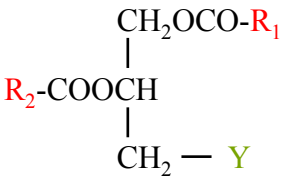

Figura 17. Estructura de los glicolípidos. R = ácido graso, Y = azúcar.

2.3.4. Esfingolípidos

Los esfingolípidos son componentes estructurales de células eucariotas y algunas bacterias. Por otro lado, también pueden jugar el papel segundos mensajeros regulando procesos como el crecimiento celular, diferenciación, apoptosis y defensa contra patógenos (Sperling, 2003).

Estructuralmente, los esfingolípidos son definidos como derivados de bases de cadena larga o LCBs (Long Chain Bases). El primer paso en la síntesis de estas LCBs es la condensación de una serina con palmitil-CoA rindiendo 3-cetodihidroxiesfinganina (KDS). Este paso es catalizado por la enzima serina-palmitil transferasa (Figura 18). A continuación la molécula de KDS es reducida por la 3-ketoesfinganina reductasa generando una molécula de esfinganina (d18:0). Esta sería la primera LCB de la cual derivan el resto tras sufrir varias modificaciones.

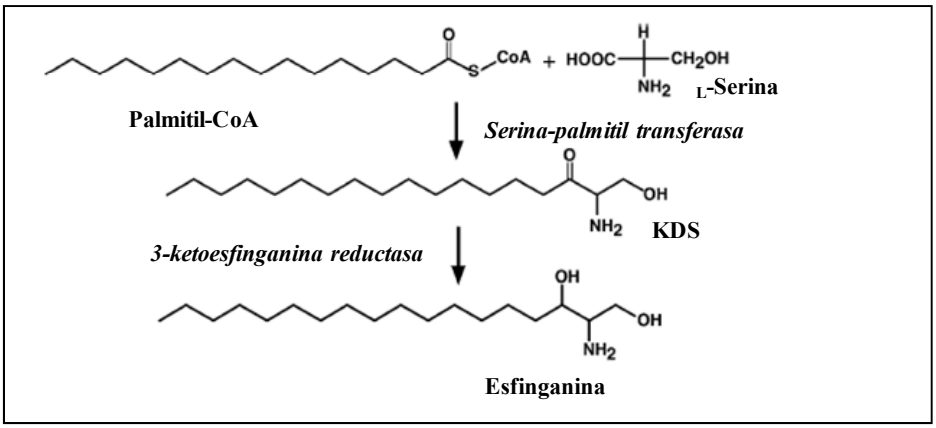

Figura 18: Biosíntesis de esfinganina (d18:0) a partir de palmitil-CoA y serina. Modificada de Hanada (2003).

En mamíferos, la principal LCB es la (*E*)-esfing-4-enina o esfingosina (d18:1^4), mientras que en la levadura *S. cerevisiae*, la LCB predominante es la 4-hidroxiesfinganina o fitoesfingosina (t18:0) formadas por la desaturación o hidroxilación de d18:0 en la posición C-4, respectivamente. A diferencia de lo que ocurre en mamíferos y levaduras, la composición de bases de esfingolípidos en plantas es más compleja ya que además de la Δ4 insaturación pueden sufrir hidroxilación e insaturación en la posición Δ8 (Figura 19). Otras LCBs de diferente longitud de cadena también pueden ser encontradas como componentes minoritarios de los esfingolípidos de plantas.

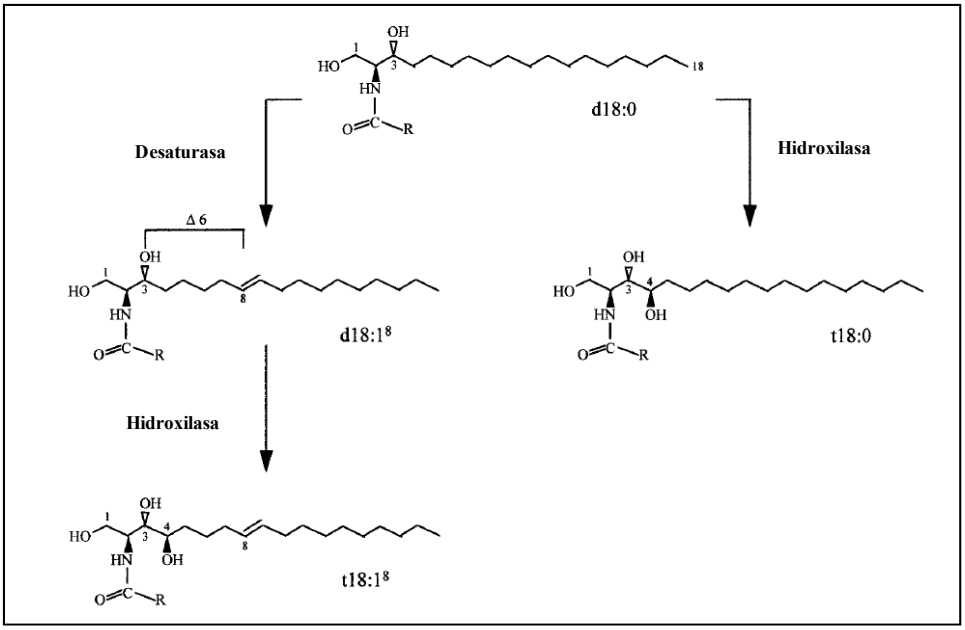

Figura 19: Modificación de LCBs. Acción de la Δ4-hidroxilasa y la Δ8-desaturasa sobre la molecula de esfinganina (d18:0). Modificada de Sperling *et al*. (1998).

Las estructuras de algunas de las diferentes LCBs encontradas en mamíferos, levaduras y plantas se describen en la figura 20.

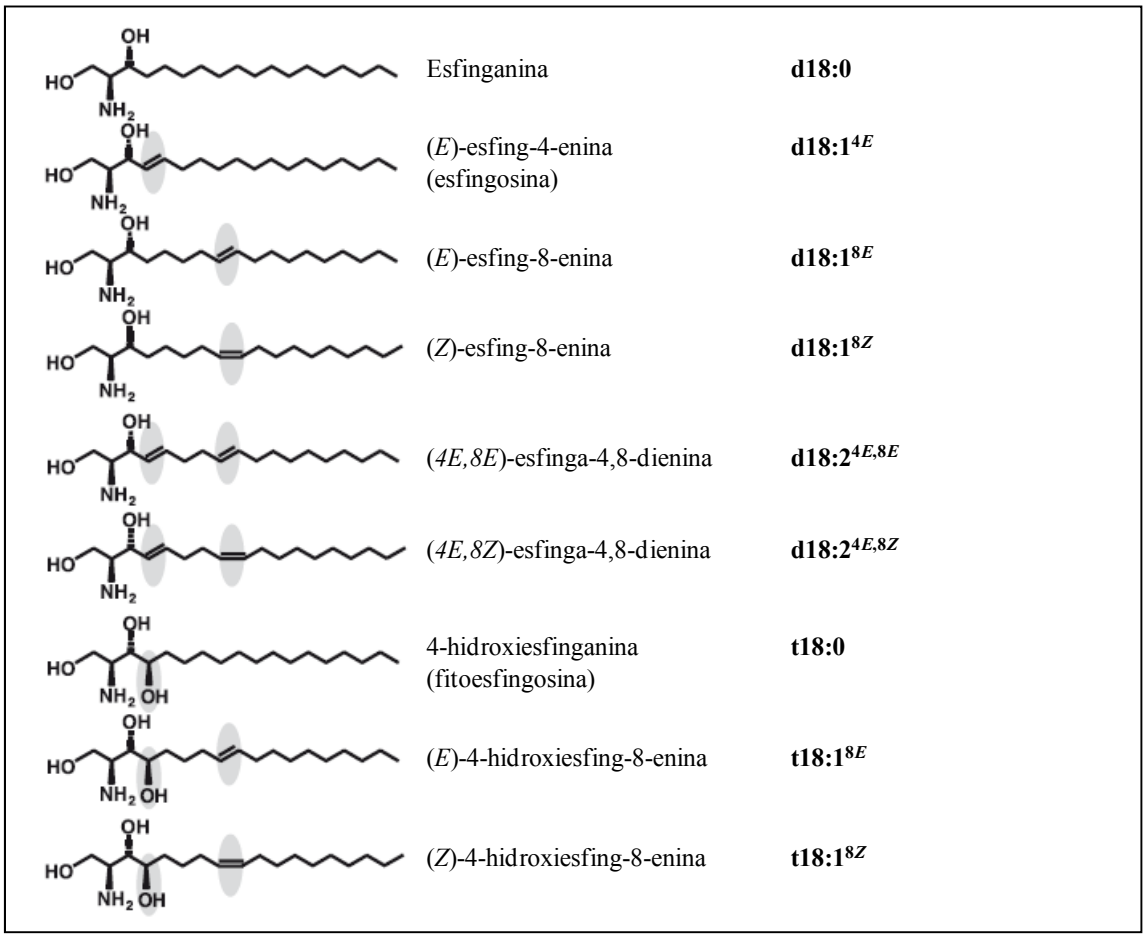

Figura 20: Estructuras de las LCBs más comunes. Dobles enlaces y grupos hidroxi adicionales de las bases derivadas de la esfinganina están marcados con círculos grises. Modificada de Sperling y Heinz (2003).

Las LCBs de plantas se encuentran normalmente esterificadas en el grupo amino con un Δ2-hidroxi-ácido graso y con un grupo polar en la posición 1-hidroxi lo que da lugar a la gran variedad de esfingolípidos que se encuentran en los tejidos de plantas. En el bloque III se detallará la clonación y caracterización de una Δ4-hidroxilasa y una Δ8-desaturasa de esfingolípidos de girasol.

2.3.5. Ceras

Las ceras son esteres de ácidos grasos de cadena larga con alcoholes grasos monohidroxílicos o con esteroles. Son insolubles en agua y forman cubiertas de las hojas y frutos de plantas superiores.

3. BIOSÍNTESIS DE ÁCIDOS GRASOS Y GLICEROLÍPIDOS EN PLANTAS

3.1. Biosíntesis de ácidos grasos

La síntesis de novo de los ácidos grasos constituye una ruta metabólica primaria encontrada en todas las células, siendo esencial para su desarrollo (Ohlrogge y Jaworski, 1997). En plantas tiene lugar en los plastidios de semillas y tejidos no verdes, y en los cloroplastos de los tejidos verdes. Es llevada a cabo mediante la acción combinada de dos sistemas multienzimáticos: la acetil-CoA carboxilasa (ACC) y las sintasas de ácidos grasos (FAS) (Harwood, 2005), y consiste en la extensión de las cadenas de acilos (ácidos grasos) por ciclos de condensación de dos unidades de carbono (Figura 21).

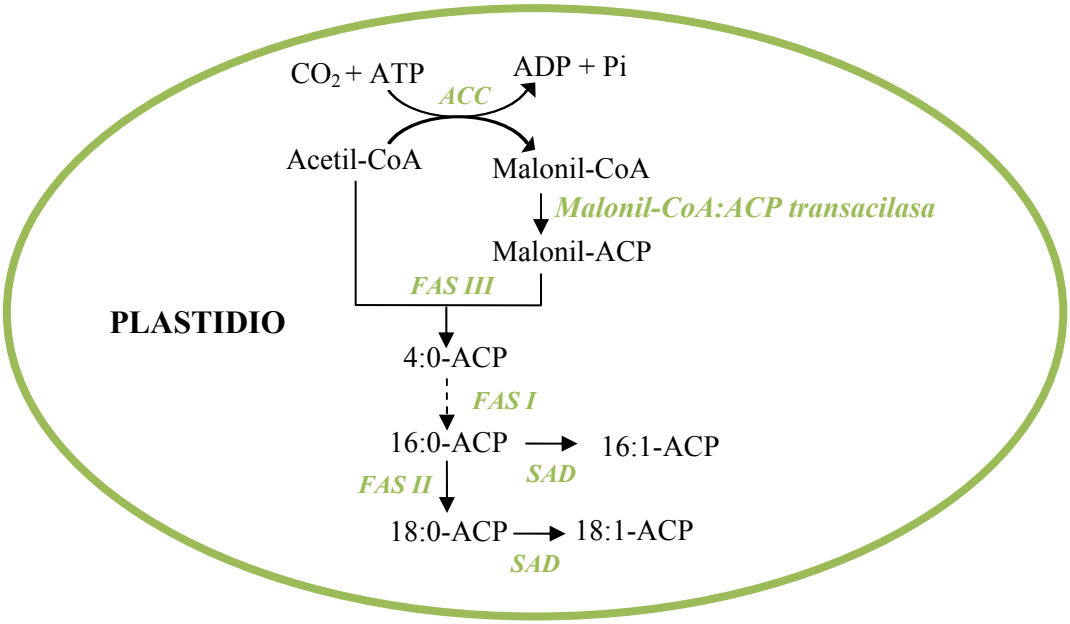

Figura 21 Esquema general de la biosíntesis de ácidos grasos en semillas oleaginosas. ACC, acetil-CoA carboxilasa; FAS I, II, III, complejo ácido graso sintasa I, II, III; SAD, estearato desaturasa.

3.1.1. Síntesis de precursores para la reacción de condensación

La ACC cataliza el primer paso en la síntesis de ácidos grasos, se encarga de la formación de malonil-CoA por medio de una reacción dependiente de ATP a partir de bicarbonato y acetil-CoA (Figura 22). La reacción general de la ACC se encuentra

catalizada en dos pasos principales que necesitan distintos sitios activos (Knowles, 1989). La primera reacción parcial se encuentra catalizada por la biotin carboxilasa y utiliza ATP para llevar a cabo la carboxilación de un grupo prostético de la proteína portadora de biotina carboxilada (BCCP). Generalmente se utiliza un intermediario carboxifosfato junto con bicarbonato como fuente de carbono. La segunda reacción parcial es llevada a cabo por una carboxiltransferasa. El grupo carboxilo es transferido desde BCCP a acetil-CoA para rendir una molécula de malonil-CoA (Harwood, 1996).

El malonil-CoA producido pasa a malonil-ACP mediante la acción de la malonil-CoA:ACP transacilasa. El malonil-ACP es utilizado posteriormente por todas las reacciones de condensación de la síntesis de novo llevadas a cabo en el plastidio.

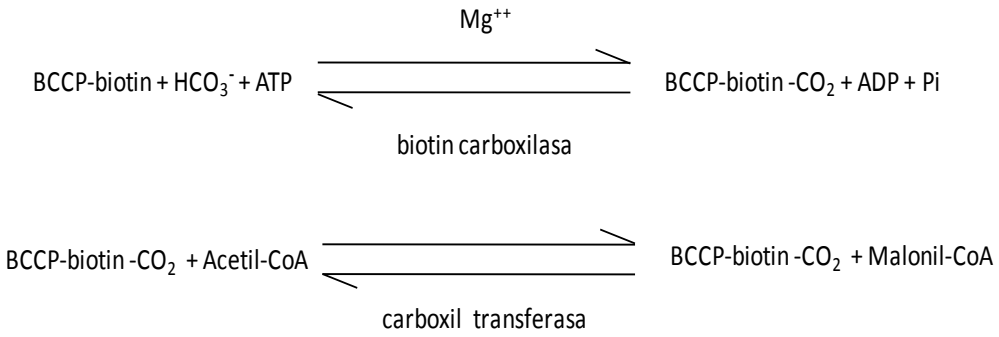

Figura 22. Reacción de la acetil-CoA carboxilasa (ACC) de plantas. Modificado de Harwood (2005).

3.1.2. Enzimas que realizan el paso de condensación

La posterior extensión de las cadenas de acilos viene dada por ciclos de condensación-reducción-deshidratación-reducción de las mismas; reacciones llevadas a cabo por enzimas que residen en los complejos FAS: sintasa de β-cetoacil-ACP (KAS), reductasa de 3-oxoacil-ACP (KR), dehidratasa de hidroaxil-ACP (DH), y reductasa de enoil-ACP (ENR) (Figura 23).

En el caso de las plantas, el complejo FAS es de tipo II. Este tipo de sistema es totalmente disociado donde cada componente es codificado por un gen independiente y cataliza un paso individual de la ruta biosintética.

La condensación inicial tiene lugar entre malonil-ACP y acetil-CoA y está catalizada por la enzima KAS III (Jaworski et al., 1989), enzima que da nombre al

complejo FAS III. Aunque KAS III puede catalizar más reacciones (González-Mellado et al., 2010), se considera que KAS I realiza las reacciones de condensación de ácidos grasos de 4 a 16 carbonos mediante condensaciones sucesivas de 2 unidades de carbono procedentes de acetil-CoA a la cadena saturada del acil-ACP. Posteriormente, el palmitil-ACP (16:0-ACP) generado sirve como substrato de la FAS II (KAS II) que dará lugar al estearil-ACP, de 18 átomos de carbono (18:0-ACP).

La expresión de todos estos genes implicados en la síntesis *de novo* de ácidos grasos parece estar regulada y sincronizada. En semillas de *Brassica napus*, donde se han estudiado los niveles de expresión, se obtienen las mayores acumulaciones de mensajeros de estos genes entre los 20 y 29 días después de floración (DDF), que coinciden con el periodo de mayor síntesis de ácidos grasos (O'Hara et al., 2002).

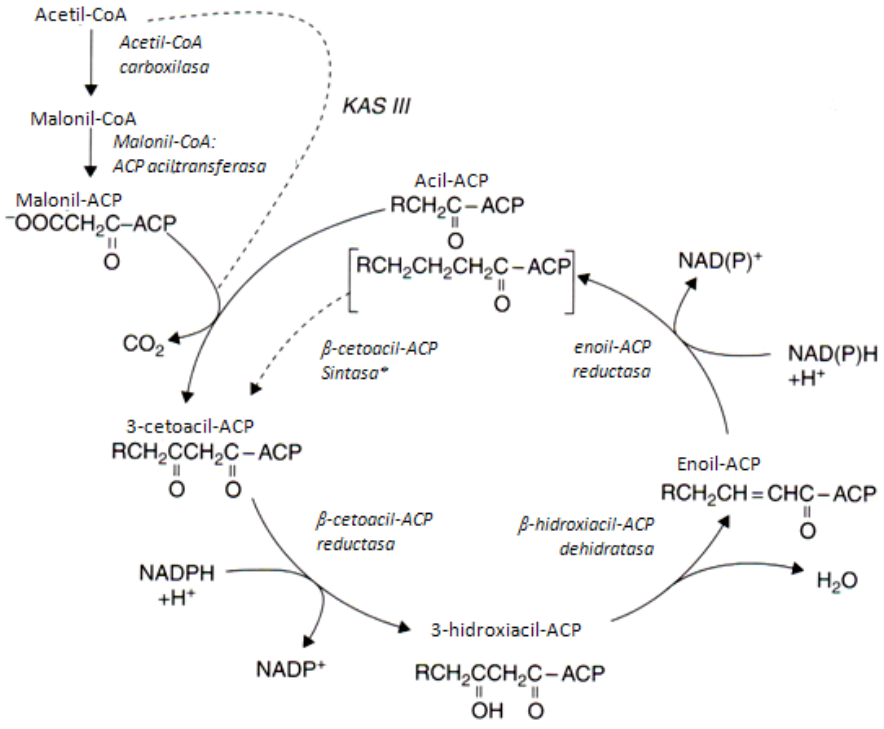

Figura 23. Reacción de la sintasa de ácidos grasos. *La primera reacción de condensación está catalizada por la enzima β-cetoacil-ACP sintasa III (KAS III) que utiliza acetil-CoA y malonil-ACP como substratos. Las siguientes reacciones de condensación hasta la síntesis de palmitil-ACP las cataliza KAS I y para la obtención de estearil-ACP la realiza KAS II. Modificado de Harwood (2005).

3.1.3. Desaturación intraplastidial de ácidos grasos

Una vez que la cadena de acil-ACP llega a 16 ó 18 carbonos, es sustrato para distintas reacciones en el plastidio. El estearil-ACP es el sustrato de la estearil-ACP desaturasa (SAD) que introduce un doble enlace en la posición Δ9 formando oleil-ACP (Figura 21). Es una enzima soluble que se localiza en el estroma del plastidio. Normalmente tiene mayor actividad relativa que la FAS II, lo que explica la menor acumulación de esteárico que de palmítico en plantas (Harwood, 1996). Aunque el estearil-ACP es su sustrato natural la SAD, esta presenta una actividad relativa de un 1% hacia el palmitil-ACP, produciendo en este caso ácido palmitoleico como producto. La k_m para ambos sustratos es similar (McKeon y Stumpf, 1982).

3.1.4. Liberación de ácidos grasos. Acil-ACP tioesterasas

Los grupos acilo se utilizan para la biosíntesis de glicerolípidos siguiendo dos rutas distintas (Ohlrogge y Browse, 1995): (i) la ruta eucariota que se localiza en el retículo endoplásmico (RE) y requiere la actuación de una acil-ACP tioesterasa (TE) que hidroliza el enlace tioéster liberando el ácido graso libre (AGL). Éstos pueden salir de los plastidios, aunque no se sabe con certeza cómo son transportados al citosol y activados a acil-CoA, si bien se ha descrito una actividad acil-CoA sintetasa (ACS) que podría estar implicada. (ii) Por otra parte, la ruta procariota de biosíntesis de glicerolípidos que tiene lugar en el plastidio.

Ya que las TEs determinan los ácidos grasos que salen al citosol para la posterior biosíntesis de lípidos, su especificidad tiene un papel muy importante en la composición final de éstos en los aceites. De ahí el interés despertado por la purificación y caracterización de las mismas en distintas especies vegetales, para así determinar su especificidad, y la posibilidad de ser modificadas y empleadas en la mejora de plantas oleaginosas.

Las acil-ACP tioesterasas son proteínas homodímeras, codificadas por genes nucleares. Se clasifican en dos grupos bien diferenciados en función de su especificidad por los distintos acil-ACPs y sus secuencia génicas: *fatA* y *fatB*. Dichos genes son parálogos, derivan de la duplicación de un gen más antiguo (antes de la separación de las distintas familias de plantas), aparentemente del tipo de las *fatB*. Las tioesterasas del tipo A (FatA), u oleoil-ACP tioesterasas presentan una gran especificidad por 18:1-ACP, y menos por

16:0-ACP y 18:0-ACP, mientras que las del tipo B (FatB) tienen preferencia por ácidos grasos saturados. Dentro de las FatB hay dos grupos funcionales, el primero con especificidad por cadenas de 8 a 14 carbonos, se han encontrado sólo en especies que producen ácidos grasos de cadena media, y el segundo con especificidad por cadenas de 14 a 18 carbonos (Jones *et al*., 1995).

Mientras que los genes *fatA* están muy conservados en todas las plantas superiores, posiblemente porque el oleico es el precursor de la mayoría de los ácidos grasos encontrados en fosfolípidos y triglicéridos, los genes de tioesterasas tipo *fatB* muestran una gran variabilidad, dada la diferencia de afinidad por sustratos entre las distintas tioesterasas de este tipo. Al alinear las secuencias de ambos tipos de tioesterasas podemos distinguir una serie de segmentos con distinto grado de conservación. Ésta estructura se conserva dentro de los dos grupos, existiendo regiones con gran homología entre ambos y regiones más específicas (Facciotti *et al*., 1998). En la Figura 24 se representan esquemáticamente las distintas regiones encontradas en los dos tipos de tioesterasas.

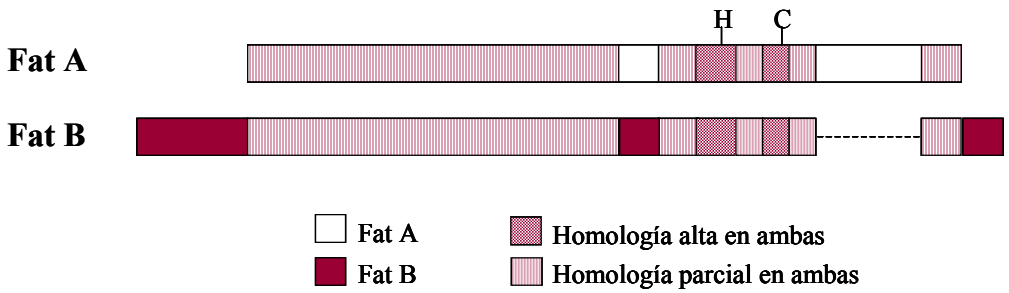

Figura 24. **Esquema de las secuencias de FatAs y FatBs, sin el péptido señal**. Modificada de Facciotti *et al*., 1998.

Ambas tioesterasas presentan un péptido señal, de unos 60 aminoácidos (aa), que facilita su transporte al plastidio, una vez allí es eliminado. En ambos casos el péptido señal es muy variable, dado que su secuencia no afecta a la función. A continuación del péptido señal, las TEs FatB tienen una región conservada entre ellas, altamente hidrofóbica, de unos 35 aa. Este dominio está ausente en las TEs FatA. Tras el péptido señal, ambas tioesterasas presentan una región parcialmente homóloga seguida de una región no homóloga. Posteriormente se localizan 2 cajas muy conservadas entre ambos tipos de proteínas donde encontramos una histidina y una cisteína con papel catalítico (Yuan *et al*., 1996).

El objetivo principal de esta tesis es la caracterización del sistema de TEs de diferentes plantas oleaginosas (girasol, macadamia y ricino). Este tema se abordará en el Bloque I además de otros aspectos como la modificación de dichas enzimas mediante mutagénesis dirigida o la caracterización de mutantes de Arabidopsis para genes codificantes para FatAs.

3.2. Biosíntesis intraplatidial de glicerolípidos

La ruta de biosíntesis intraplastidial de glicerolípidos (Maréchal et al., 1997; Dormän, 2005), también llamada ruta procariota (Figura 25), genera lípidos de membrana y es cuantitativamente poco relevante en semillas oleaginosas, si bien es mucho más importante en tejidos verdes pudiendo alcanzar hasta el 38% en plantas como Arabidopsis (Browse et al. 1986). En esta ruta actúan dos aciltransferasas que transfieren sucesivamente el grupo acilo de los acil-ACPs generados a las posiciones *sn*-1 y *sn*-2 del glicerol-3-fosfato (G3P), dando lugar a una molécula de PA. La primera, denominada G3P aciltransferasa (GPAT), es una enzima soluble y utiliza preferentemente oleil-ACP como sustrato, y la segunda, la lisofosfatidil aciltransferasa (LPAAT), es una enzima de la membrana interna de los plastidios con preferencia por el palmitil-ACP como sustrato.

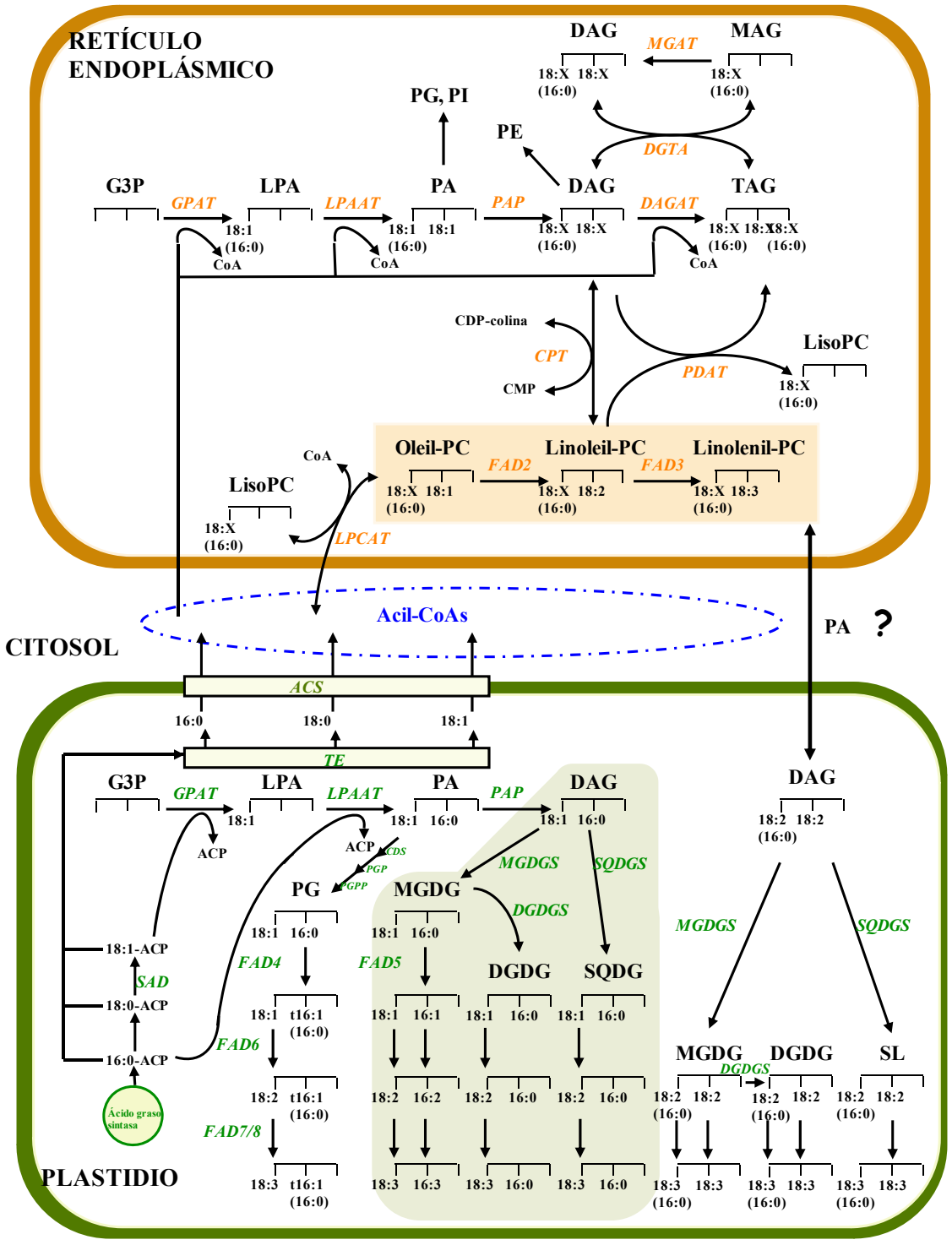

Figura 25. Rutas procariota y eucariota de biosíntesis de glicerolípidos en plantas. Los pasos enzimáticos de la ruta procariota ausentes en plantas 18:3 se encuentran sombreados en verde (Hernández, 2008).

El PA generado por la LPAAT puede ser utilizado para la síntesis de PG o convertirse en DAG mediante la acción de una fosfatidato fosfatasa (PAP). Las

moléculas de DAG actúan como precursoras para la síntesis de otros lípidos de membrana plastidiales, como son el MGDG, DGDG y DSQG (Joyard et al., 1993). El ácido oleico es incorporado principalmente a MGDG, para ser desaturado a linoleico por acción de la oleato desaturasa plastidial (FAD6) y después a α-linolénico, que es el principal ácido graso plastidial, por acción de la linoleato desaturasa plastidial (FAD7/8).

3.3. Modificaciones extraplastidiales de los ácidos grasos

El oleil-CoA exportado al citosol puede ser incorporado a la posición *sn*-2 de la lisofosfatidilcolina (LPC) mediante la acción de la lisofosfatidilcolina aciltransferasa (LPCAT) originando PC (Stymne y Appelqvist, 1978). En plantas, se ha detectado un intercambio de acilos insaturados entre la posición *sn*-2 de la PC microsomal y el conjunto de acil-CoAs citoplasmático, que también está catalizado por la LPCAT y que regeneraría el LPC (Stymne y Stobart, 1984). Una vez que el oleato es incorporado a PC, puede ser desaturado a linoleato por acción de la oleato desaturasa microsomal (FAD2) y después a α-linolenato por acción de la linoleato desaturasa microsomal (FAD3) (Figura 25).

3.4. Biosíntesis extraplastidial de glicerolípidos

La biosíntesis extraplastidial de glicerolípidos (Figura 25), tiene lugar en el RE a través de la denominada ruta eucariota y es la única responsable de la biosíntesis de lípidos de reserva, principalmente TAG (Stobart et al., 1998; Weselake, 2005). Al igual que en el plastidio, la síntesis se realiza a partir de G3P, pero en este caso, las aciltransferasas del RE utilizan acil-CoAs como sustrato, tanto procedentes del plastidio (palmitil-, estearil- y oleil-CoA) como del propio RE (linoleil- y linolenoil-CoA). El núcleo central de esta ruta es una serie de cuatro reacciones que constituyen la ruta de Kennedy y producen TAG como producto final. La primera reacción consiste en la transferencia del grupo acilo a la posición *sn*-1 del G3P para formar ácido lisofosfatídico (LPA) y está catalizada por la GPAT microsomal. Por lo general, esta enzima microsomal muestra preferencia por el palmitil-CoA, aunque puede funcionar bien con oleil-CoA, sobre todo si éste último está presente en gran proporción en el conjunto de acil-CoAs (Ichiara, 1984). En la segunda reacción, el LPA es acilado en

posición *sn*-2 por la acción de la LPAAT, dando lugar a PA, que es precursor de la síntesis de fosfolípidos. Esta enzima muestra una fuerte selectividad por ácidos grasos insaturados, linoleato mejor que oleato, y excluye casi totalmente a los saturados (Griffiths et al., 1985). A continuación, en la tercera reacción de la ruta, el PA es convertido a DAG por la acción de la PAP, la cual tiene preferencia por especies de fosfatidatos con dos ácidos grasos insaturados (Ichiara, 1991). Los DAG también pueden sintetizarse a partir de PC por la acción de la colina fosfotransferasa (CPT), la cual cataliza una reacción reversible, por lo que este paso también puede considerarse como una vía de entrada de oleato a PC para su desaturación (Slack et al., 1983). El último paso de la ruta de Kennedy consiste en la acilación de la posición *sn*-3 del DAG para formar TAG. Esta reacción está catalizada por la diacilglicerol aciltransferasa (DAGAT), única enzima exclusiva de la biosíntesis de TAG y que, normalmente, presenta una escasa especificidad y selectividad por sustrato. Así pues, la cadena acídica esterificada en la posición *sn*-3 del glicerol reflejaría fuertemente la composición del conjunto de acil-CoAs. La actividad DAGAT parece ser limitante para la síntesis de TAG y, por tanto, para la acumulación de aceite en tejidos oleaginosos (Perry y Harwood, 1993a). Recientemente se han descrito dos nuevas actividades, independientes de acil-CoAs, implicadas en la formación de TAG a partir de DAG: la fosfolípido:diacilglicerol aciltransferasa (PDAT) (Dahlqvist et al., 2000) y la diacilglicerol:diacilglicerol transacilasa (DGTA) que cataliza la formación reversible de una molécula de TAG y otra de MAG a partir de dos de DAG (Stobart et al., 1997).

Por otro lado, la ausencia en la posición *sn*-2 de MGDG, DGDG y SQDG de ácido palmitolinolénico (16:3) en las denominadas "plantas 18:3", debida a la ausencia de la actividad PAP cloroplástica (Heinz y Roughan, 1983) y, por tanto, de la ruta procariota excepto para la síntesis de PG, ha puesto de manifiesto que en estas plantas debe existir un mecanismo que transfiera ácidos grasos desde PC, sintetizado en el RE mediante la ruta eucariota, a DAG presente en los plastidios, posiblemente en forma de PA (Benning, 2009). Este DAG genera galactolípidos y sulfolípidos con 18:3 en la posición *sn*-2, aunque no se conoce bien la naturaleza de dicho mecanismo y de los ácidos grasos implicados. Sin embargo, en estudios realizados con mutantes de *Arabidopsis* se ha demostrado que dicha transferencia debe ser reversible (Miquel y Browse, 1992; Browse et al., 1993), y que al menos el ácido linoleico debe participar en ella (Browse et al., 1989).

BIBLIOGRAFÍA

Alba, A., Llanos, M., 1990. El cultivo del girasol. Colección agroguias mundi-prensa.

Atsmon, D., 1989. Castor. En: Oil crops of the world: Their breeding and utilization. Downey, R.K., Ashri A. (eds). Mc. Graw-Hill, New York, EE.UU.

Benning, C., 2009. Mechanisms of lipid transport involved in organelle biogenesis in plant cells. Annu Rev Cell Dev Biol, 25: 71-91.

Block, M.A., Dorne, A.J., Douce, R., 1983. Preparation and characterization of membrane fractions enriched in outer and inner envelope membranes from spinach chloroplasts. II. Biochemical characterization. J Biol Chem, 258: 13281-13286.

Bonjean, A., 1991. Le Ricin. Une culture pour la chimie fine. En: Castor cultivation for chemical applications. Bonjean, A. (ed). Galileo/ONIDOL, Les Lilas, Francia.

Brigham, R.D., 1993. Castor: Return of an old crop. Janick, J., Simon, J.E. (eds) New crops. John Wiley & Sons, New York, EE.UU.

Browse, J., Warwick, N., Somerville, C.R., Slack, C.R., 1986. Fluxes through the prokaryotic and eukaryotic pathways of lipid synthesis in the '16:3' plant *Arabidopsis thaliana.* Biochem J, 235: 25-31.

Browse, J., Kunst, L., Anderson, S., Hugly, S., Somerville, C., 1989. A mutant of *Arabidopsis* deficient in the chloroplast 16:1/18:1 desaturase. Plant Physiol, 90: 522-529.

Browse, J., McConn, M., James, D., Miquel, M., 1993. Mutants of *Arabidopsis* deficient in the synthesis of α-linolenate. J Biol Chem, 268: 16345-16351.

Coultate, T.P., 1996. Lipids. En: Food: the chemistry of its components. Coultate, T.P. (ed.) The Royal Society of Chemistry, Cambridge, pp 54-93.

Dahlqvist, A., Stahl, U., Lenman, M., Banas, A., Lee, M., Sandager, L., Ronne, H., Stymne, S., 2000. Phospholipid:diacylglycerol acyltransferase: An enzyme that catalyzes the acyl-CoA-independent formation of triacylglycerol in yeast and plants. Proc Natl Acad Sci USA, 97: 6487-6492.

Dörmann, P., 2005. Membrane lipids. Biology, utilisation and Manipulation. En: Plant Lipids. Murphy, D.J. (ed.) Blackwell Publishing, Oxford, UK, pp 123-161.

Garcés, R., Martínez-Force, E., Salas, J.J., 2010. Vegetable oil basestocks for lubricants, Grasas y aceites, en prensa.

Garg, M.L., Blake, R.J., Wills, R.B.H., 2003. Macadamia nut consumption lowers plasma total and LDL cholesterol levels in hypercholesterolemic men. J Nutr, 133: 1060-1063.

Gitonga, L., Kahangi, E., Muigai, A., Ngamau, K., Gichuki, S., Cheluget, W., Wepukhulu, S., 2008. Assessment of phenotypic diversity of macadamia (*Macadamia* spp) germplasm in Kenya using leaf and fruit morphology. Afr J Plant Sci, 2: 86-93.

González-Mellado, D., Wettstein-Knowles, P., Garcés R., Martínez-Force, E., 2010. The role of ketoacyl-acyl carrier protein synthase III in the condensation steps of fatty acid biosynthesis in sunflower. Planta, 231: 1277-1289.

Griel, A. E., Cao, Y., Bagshaw, D.D., Cifelli, A.M., Holub, B., Kris-Etherton P.M., 2008. A macadamia nut-rich diet reduces total and LDL-cholesterol in midly hypercholesterolemic man and women. J Nutr, 138: 761-767.

Griffths G., Stobart, A.K., Stymne, S., 1985. The acylation of *sn* glycerol 3-phophate and the metabolism of phosphatidate in microsomal preparations from the developing cotyledons of safflower (*Carthamus tinctoriu*s L.) seed. Biochem J, 230: 379-388.

Gunstone, F.D., Harwood, J.L., Dijkstra, A.J., 2007. The Lipid Handbook. Gunstone, F.D., Harwood, J.L., Dijkstra, A.J. (eds) CRC Press, New York, EEUU.

Hanada, K., 2003. Serine palmitoyltransferase, a key enzyme of sphingolipid metabolism. Biochimica et Biophysica Acta (BBA) - Molecular and Cell Biology of Lipids, 1632: 16-30.

Hanahan, D.J., Chaikoff, I.L., 1947. A new phospholipid-splitting enzyme specific for the ester linkage between the nitrogenous base and the phosphoric acid grouping, J Biol Chem, 169: 699-705.

Harrison, G., Somerset, S., 2004. Macadamia or olive oil enriched diets induce changes in heart structure and function similar to regular exercise in rats. Asia Pac J Clin Nutr, 13: S48.

Harwood, J.L., 1979. The synthesis of acyl lipids in plant tissues. Prog Lipid Res, 18: 55-86.

Harwood, J.L., 1996. Recent advances in the biosynthesis of plant fatty acids. Biochim Biophys Acta, 1031: 7-56.

Harwood, J.L., 2005. Fatty acid biosynthesis. En: Plant Lipids. Murphy, D.J. (ed). Blackwell Publishing, Oxford, UK, pp: 27-101.

Hayatsu, H., Arimoto, S., Negishi, T., 1988. Dietary inhibitors of mutagenesis and carcinogenesis. Mutat Res, 202: 429-446.

Heinz, E., Roughan, G., 1983. Similarities and differences in lipid metabolism of chloroplasts isolated from 18:3 and 16:3 plants. Plant Physiol, 72: 273-279.

Hernández, M.L., 2008. Análisis metabólico y molecular del contenido de ácido linoleico en el fruto del olivo (*Olea europaea*). Tesis doctoral. Universidad de Sevilla.

Ichiara, K., 1984. *sn*-Glycerol-3-phosphate acyltransferase in a particular fraction from maturing safflower seeds. Arch Biochem Biophys, 232: 685-698.

Ichiara, K. 1991. The action of phosphatidate phosphatise on the fatty-acid composition of safflower triacylglycerol and spinach glycerolipids. Planta, 183: 353-358.

Jackson. R.C., Murray, B.G., 1983. Colchicine induced quadrivalent formation in Helianthus: evidence of ancient polyploidy. Theor Appl Genet 64: 219-222.

Jaworski, J.G., Clough, R.C., Barnum S.R., 1989. A cerulenin insensitive short chain 3-ketoacyl-acyl carrier protein synthase in *Spinacia oleracea* leaves. Plant Physiol, 90: 41-44.

Jones, A., Davies, H.M., Voelker, T.A., 1995. Palmitoyl-acyl carrier protein (ACP) thioesterase and the evoluctionary origin of plant acyl-ACP thioesterases. Plant Cell, 7: 359-371.

Joyard, J., Block, M.A., Malherbe, A., Maréchal. E., Douce, R., 1993. Origin and synthesis of galactolipids and sulfolipid head groups. En: Lipid Metabolism in Plants. Moore, T.S. Jr. (ed). CRC Press, Boca Raton, FL, pp: 231-258.

Knowles, J.R., 1989. The mechanism of biotin-dependent enzymes. Annual Rev Biochem, 58: 195-221.

Koo, A.J., Ohlrogge, J.B., Pollard, M., 2004. On the export of fatty acids from the chloroplast. J Biol Chem, 279: 16101-10.

Maguire, L.S., O'Sullivan, S.M., Galvin, K., O'Connor, T.P., O'Brien, N.M., 2004. Fatty acid profile, tocopherol, squalene and phytosterol content of walnuts, almonds, peanuts, hazelnuts and the macadamia nut. Int J Food Sci Nutr, 55: 171-178.

Maréchal, E., Block, M.A., Dome, A.J., Douce, R., Joyard, J., 1997. Lipid synthesis and metabolism in the plastid envelope. Physiol Plant, 100: 65-77.

McHargue, L.T., 1996. Macadamia production in southern California. En: Progress in new crops. Janick, J. (ed), ASHS Press, Arlington, VA. pp. 458-462.

McKeon, T.A., Stumpf, P.K., 1982. Purification and characterization of the stearoyl-acyl carrier protein desaturase and the acyl-acyl carrier protein thioesterase from maturing seeds of safflower. J Biol Chem, 257: 12141-12147.

Miquel, M., Browse, J., 1992. *Arabidopsis* mutants deficient in plyunsaturated fatty acid synthesis. J Biol Chem, 267: 1502-1509.

O'Hara P., Slabas A.R., Fawcett T., 2002. Fatty acid and lipid biosynthesis genes are expressed at constant molar ratios but different absolute levels during embryogenesis. Plant Physiol, 129: 310-320.

Ohlrogge, J.B., Browse, J., 1995. Lipid biosynthesis. Plant Cell, 7: 957-970.

Ohlrogge, J.B., Jaworski, J.G., 1997. Regulation of fatty acid synthesis. Annu Rev Plant Physiol Plant Mol Biol, 48: 109-136.

Perry, H.J., Harwood, J.L., 1993. Radiolabeling studies of acyl lipids in developing seeds of *Brassica napus* - use of [1-C-14]acetate precursor. Phytochem, 33: 329-333.

Rojas-Barros, P.A., de Haro, A., Fernández-Martínez, J.M., 2004. Isolation of natural mutant in castor bean (*Ricinus communis* L.) with high oleic/low ricinoleic acid content. Crop Sci, 44: 76-80.

Rojas-Barros, P.A., de Haro A., Fernández-Martínez, J.M., 2005. Inheritance of high oleic/low ricinoleic acid content in the seed oil of the castor bean mutant OLE-1. Crop Sci, 45: 157-162.

Slack, C.R., Campbell, L.C., Browse, J.A., Roughan, P.G., 1983. Some evidence for the reversibility of the cholinephosphotransferase-catalysed reaction in developing linseed cotyledons in vivo. Biochim Biophys Acta, 754: 10-20.

Sperling, P., Zahringer, U., Heinz, E., 1998. A sphingolipid desaturase from higher plants: identification of a new cytochrome b5 fusion protein. J Biol Chem, 273: 28590-28596.

Sperling, P., Heinz, E., 2003. Plant sphingolipids: structural diversity, biosynthesis, first genes and functions. Biochim Biophys Acta. 1632, 1-15.

Stobart, A.K., Mancha, M., Lenman, M., Dahlqbist, A., Stymne, S., 1997. Triacylglycerols are synthesised and utilized by transacylation reactions in microsomal preparations of developing safflower (*Carthamus tinctorius* L.). Planta, 203: 58-66.

Stobart, A.K., Stymne, S., Shewry, P.R., Napier, J., 1998. Triacylglycerol biosynthesis. En: Plant lipid biosynthesis. Fundamentals and agricultural applications. Harwood JL (ed). Cambridge University Press, Cambridge, UK, pp: 223-245.

Stymne, S., Appelqvist, L.A., 1978. The biosynthesis of linoleate from oleoyl-CoA via oleoyl-phosphatidylcholine in microsomes of developing safflower seeds. Eur J Biochem, 90: 223-229.

Stymne, S., Stobart, A.K., 1984. Evidence for the reversibility of the acyl-CoA:lysophosphatidylcholine acyltransferase in microsomal preparations from developing safflower (*Carthamus tinctorius* L.) cotyledons and rat liver. Biochem J, 223: 305-314.

Wang, X., Xu, L., Zheng, L., 1994. Cloning and expression of phosphatidylcholine-hydrolyzing phospholipase D from *Ricinus communis* L, J Biol Chem, 269: 20312-20317.

Wang, X., 2000. Multiple forms of phospholipase D in plants: the gene family, catalytic and regulatory properties, and cellular functions. Prog Lipid Res, 39:109–49.

Wang, X., 2002. Phospholipase D in hormonal and stress signaling. Curr Opin Plant Biol, 5: 408-414.

Weiss, E.A., 1983. Castor. En: Oilseed crops. Tropical agriculture series. Weiss, E.A. (ed). Longman Inc., New York, EE.UU.

Weselake, R.J., 2005. Storage lipids. En: Plant Lipis. Murphy, D.J. (ed). Blackwell Publishing, Oxford. UK, pp: 162-225.

Yuan, L., Nelson, B.A., Gwyndolyn, C., 1996. The catalytic cysteine and histidine in the plant acyl-acyl carrier protein thioesterases. J Biol Chem, 271: 3417-3419.

OBJETIVOS

El objetivo general de este trabajo es la identificación y caracterización de genes implicados en la síntesis o modificación de lípidos en distintas plantas oleaginosas. Para ello se han abordado los siguientes objetivos específicos:

Bloque I. Caracterización y modificación de las acil-ACP tioesterasas de oleaginosas.

1. Identificación y caracterización de los genes que codifican para las acil-ACP tioesterasas tipo A y B de semillas de ricino.
2. Identificación y caracterización de los genes que codifican para las acil-ACP tioesterasas tipo A y B de nueces de macadamia.
3. Caracterización de una línea de Arabidopsis deficiente en los genes codificantes para acil-ACP tioesteresas tipo A.
4. Modificación de la especificidad de la acil-ACP tioesterasa tipo A de girasol mediante mutagénesis dirigida.

Bloque II. Clonación y caracterización funcional de una fosfolipasa Dα de girasol.

Bloque III. Caracterización de enzimas involucradas en la modificación de bases de esfingolípidos en girasol.

1. Clonación y caracterización de una Δ4-hidroxilasa de girasol.
2. Clonación y caracterización de una Δ8-desaturasa de girasol.

BLOQUE I

Acyl-ACP thioesterases from castor (*Ricinus communis* L.): An enzymatic system appropriate for high rates of oil synthesis and accumulation.

Sánchez-García, A.[a,1], Moreno-Pérez, A.J.[a,1], Alicia M. Muro-Pastor, A.M.[b], Salas, J.J.[a], Garcés, R. [a], Martínez-Force, E.[a]

[a]Instituto de la Grasa (CSIC), Av. Padre García Tejero 4, E-41012 Seville, Spain
[b]Instituto de Bioquímica Vegetal y Fotosíntesis (CSIC -Universidad de Sevilla), Centro de Investigaciones Científicas Isla de la Cartuja, Av. Américo Vespucio 49, E-41092 Seville, Spain

Published in *Phytochemistry*
Phytochem. (2010), 71:860-869

[1] These authors have contributed equally to the studies presented in this manuscript

Abstract

Acyl-acyl carrier protein (ACP) thioesterases are enzymes that terminate the intraplastidial fatty acid synthesis in plants by hydrolyzing the acyl-ACP intermediates and releasing free fatty acids to be incorporated into glycerolipids. These enzymes are classified in two families, FatA and FatB, which differ in amino acid sequence and substrate specificity. In the present work, both FatA and FatB thioesterases were cloned, sequenced and characterized from castor (*Ricinus communis*) seeds, a crop of high interest in oleochemistry. Single copies of *FatA* and *FatB* were found in castor resulting to be closely related with those of *Jatropha curcas*. The corresponding mature proteins were heterologously expressed in *Escherichia coli* for biochemical characterization after purification, resulting in high catalytic efficiency of *Rc*FatA on oleoyl-ACP and palmitoleoyl-ACP and high efficiencies of *Rc*FatB for oleoyl-ACP and palmitoyl-ACP. The expression profile of these genes displayed the highest levels in expanding tissues that typically are very active in lipid biosynthesis such as developing seed endosperm and young expanding leaves. The contribution of these two enzymes to the synthesis of castor oil is discussed.

1. Introduction

Plant fatty acid biosynthesis is a process restricted to plastids, chloroplasts and to a lesser extent to mitochondria (Rawsthorne, 2002). This pathway consists of successive elongations by two carbons units of acyl-acyl carrier protein (acyl-ACP) derivatives by the action of fatty acid synthase complexes III, I and II. In all plants the acyl moieties synthesized by these enzyme complexes must be exported out of the plastids to be incorporated into the extraplastidial pathways of glycerolipid synthesis (Ohlrogge et al., 2000). The acyl export from plastids involves the cleavage of the acyl-ACP derivatives by the action of acyl-ACP thioesterases, enzymes that hydrolyze the thioester bond between ACP and the newly synthesized fatty acid (Voelker, 1996). The products of this reaction are ACP, which is recycled for further synthesis of acyl-ACP, and free fatty acids that are quickly exported to the cytosol via acyl-CoA synthetase (Koo et al., 2004). The existence of free fatty acid intermediates in this pathway has been controversial, because they are present only in trace amounts in plant living tissues. However, labeling experiments using ^{18}O confirmed they were actually produced during plastidial export (Pollard and Ohlrogge, 1999). Nevertheless, acyl-ACP thioesterases are the key enzymes at determining which fatty acids are exported to the cytosol and thus incorporated into glycerolipids synthesized in the endoplasmic reticulum (ER), which include the reserve triacylglycerols (TAG) present in oil seeds (Voelker, 1996). These enzymes can be classified in two groups that have been named FatA and FatB (Jones et al., 1995). FatA enzymes are present in all plants, with high substrate specificity towards oleoyl-ACP (18:1-ACP). FatB are classified in two subclasses, FatB1, which is present in all plants and shows preference towards long-chain acyl-ACPs, especially palmitoyl-ACP (Dörmann et al., 2000), and FatB2, which shows preference towards short/medium chain acyl-ACPs and are only found in certain species of plants accumulating C8-C14 fatty acids in their seed oils (Voelker et al., 1997). FatAs release most fatty acids necessary for plant cells and, on the other hand, FatBs play a role in the export of saturated fatty acid species. The disruption of the *FatB* gene in *Arabidopsis* led to abnormal fatty acid composition of tissues and dwarf phenotype (Bonaventure et al., 2003), which could have been caused by an insufficient rate of synthesis of sphingolipid long-chain bases (Chen et al., 2008).

The fact that these enzymes determine the fatty acids exported from plastids makes them an important target for the manipulation of fatty acid composition of the

seed oil. The expression of FatB1 from *Umbellularia californica* in rapeseed resulted in oil enriched in lauric acid (Voelker et al., 1992). Moreover, the expression of one of the FatAs from *Garcinia mangostana*, displaying high activity towards stearoyl-ACP, increased the levels of the corresponding fatty acid in transgenic *Brassica* seeds (Hawkins and Kridl, 1998). This observation generated a great interest in finding the structural features that determine the substrate specificity of these enzymes. Salas and Ohlrogge (2002) reported that the N-terminal domain was responsible for the enzyme specificity of FatA and FatB. The structure of these two enzymes was later modeled on the basis of their structural similarity towards *Escherichia coli* 4-hydroxybenzoyl-CoA thioesterase. In this regard, the active site of thioesterases displays a hot-dog fold pattern, with a catalytic triad of amino acids similar to that in papain (Mayer and Shanklin, 2005, 2007; Serrano-Vega et al., 2005). The interest of acyl-ACP thioesterases in lipid biotechnology has led to a very active research on their different forms coming from a variety of sources, especially in oil seeds (Mandal et al., 2000; Othman et al., 2000; Serrano-Vega et al., 2005; Ghosh et al., 2007).

Castor plant (*Ricinus communis* L.) is an Euphorbiaceae that accumulates between 40 and 60% oil in its seeds. This oil is very rich in ricinoleic acid (12-hydroxy-9-octadecenoic acid), which accounts for 85-95% of total fatty acids. The hydroxyl group of this fatty acid confers an unusual polarity and viscosity to this oil making it an interesting substrate for oleochemistry. Thus, castor oil derivatives are being used in the manufacture of soaps, lubricants, hydraulic and brake fluids, paints, dyes, coatings, inks, cold resistant plastics, waxes and polishes, nylon, pharmaceuticals and perfumes (Gunstone et al., 2007). Developing castor seeds are very active at synthesizing TAG and exhibit certain interesting aspects from the point of view of lipid biochemistry, such as the mechanism for the channeling of ricinoleic acid towards TAG and its removal from membrane lipids (Bafor et al., 1991).

In the present work, we studied the acyl-ACP thioesterases present in castor plant. Two forms, FatA and FatB, were cloned and expressed in *E. coli* in order to purify and biochemically characterize them. Furthermore, their identification in the castor genome, levels of expression and their relationship with thioesterases from other species were investigated.

2. Results and discussion

2.1. Isolation and sequence analysis of acyl-ACP thioesterases from castor

Conserved regions from known thioesterase amino acid sequences were used to design degenerate primer pairs, FatA1 and FatAB for FatA and FatB-F1 and FatB-R1 for FatB (Table 1). Using these primer pairs and cDNAs from developing castor seeds two fragments of 458 bp and 523 bp, respectively, were amplified. The alignment of the deduced amino acid sequences showed a high degree of identity to internal coding regions of known FatA and FatB thioesterase sequences, respectively. Subsequently, full-length *RcFatA* and *RcFatB* cDNA clones of 1116 bp (accession number EF495065) and 2001 bp (accession number EU000562) respectively, were obtained by RACE using specific primers (see Section 4 for details).

Table 1. Degenerated and non-degenerated oligonucleotides used in this work. [a] Restriction sites introduced are underlined. H: A or C or T; K: G or T; N: A or C or G or T; R: A or G; and Y: C or T.

Primer name	Sequence 5'-3'
FatA1	GARATHTAYARRTAYCCNGC
FatAB	CAYTCNCKNCKRTANTC
FatB-F1	ATYMGRTCHTAYGARATWGG
FatB-R1	TNACRTGYTGRTTRAYRTC
RcFATA-1f	TGCAGGAGGTTGGATGTAATCATGC
RcFATA-2f	GATGGATTTGCCACAACCACCAGC
RcFATA-3r	CAACAATATCATCATGTTGACATTCC
RcFATA-4r	GTGTCAATTATTTCTTGAGGTATGC
RcFATA-5r	CTACTTCAACTACATCGCTCCAGG
RcFATB-1f	CTGCTGCTACTTCCTCTTTCTTTCC
RcFATB-2f	TCTACCTCTTGCTCTCGGGGTTTAC
RcFATB-5f	GGTGAGTAAATCAGGAAAGAATGG
RcFATB-3r	TTCTACTATCACGGACGCACCAATC
RcFATB-9r	CCTAGTCAGTTTATTCATCATCACC
RcFATABamH-6f[a]	TTGGATCCGTGTCTGATATTAGCAGTGT
RcFATAHind-7r	ACACAAGCTTTCATCTCGCAGATTTCTTTC
RcFATBSac-9f	AGAGCTCAGGCGGCCTGACATGC
RcFATBKpn-10r	CGGTACCTTAAGCACTTTCGACTGGAATC
RcActF	TTATGAAGGTTATGCTCTC
RcActR	GAATCCACGAGACTACATACAAC

The identified *RcFatA* and *RcFatB* open reading frames (ORFs) would encode predicted preproteins of 371 and 419 amino acid residues (Fig. 1), which correspond to calculated molecular masses of 42.2 kDa and 46.5 kDa, and pIs of 6.7 and 7.0, respectively. The nucleotides around the methionine start codon in *RcFatA* resemble the consensus sequence for initiation of translation in plants (Lütcke et al., 1987; Joshi et al., 1997). Despite the fact that *Rc*FatB does not present such a sequence, it conserves the purine at -3 and G at +4 positions from ATG, which have been shown to be required for fidelity of translation initiation (Kozak, 1991). All three proposed residues representing the papain-like catalytic triad required for the reaction (Yuan et al., 1996; Mayer and Shanklin, 2005) were conserved in both proteins (Fig. 1).

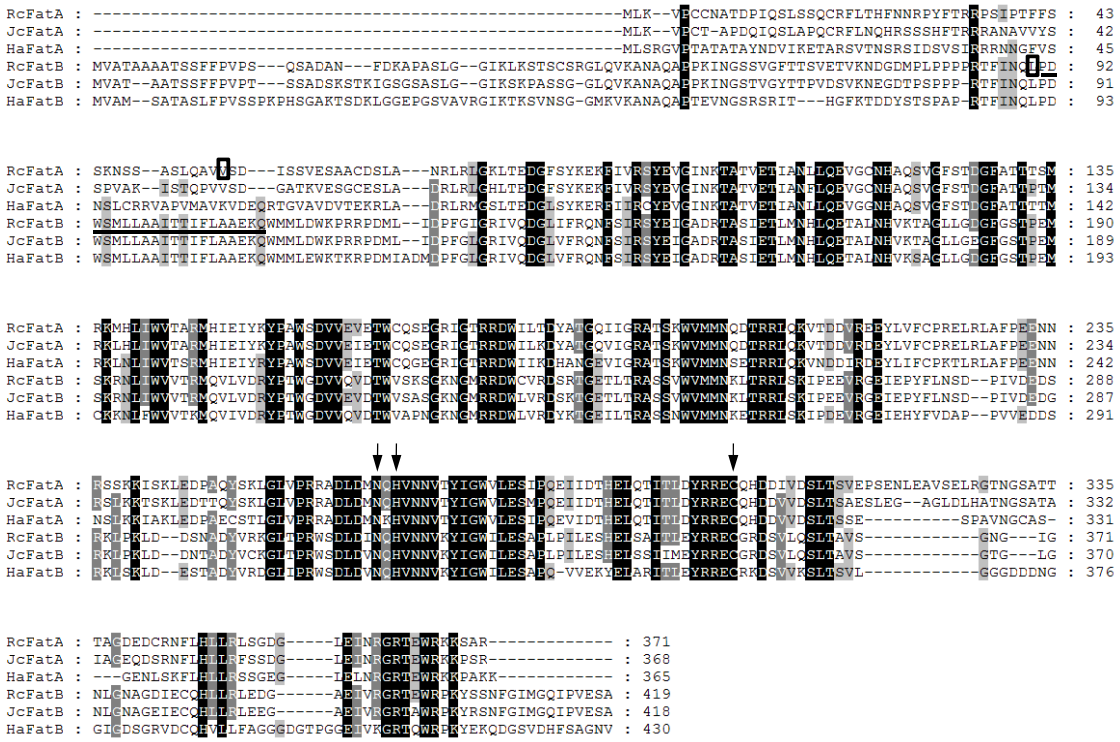

Fig. 1. Alignment of deduced amino acids sequences of *Ricinus communis* (*Rc*FatA, ABS30422; *Rc*FatB, ABV54795), *Jatropha curcas* (*Jc*FatA, ABX82799; *Jc*FatB, ABU96744) and *Helianthus annuus* (*Ha*FatA, AAL79361; *Ha*FatB, AAX19377) thioesterases shown as representatives of FatA and FatB proteins. Identical amino acids are shaded in black, whereas conserved residues are shaded in grey. The amino acids considered to be the start of the mature proteins are boxed and the hydrophobic region in FatB is underlined. The three conserved residues that constitute the catalytic triad are indicated by arrows.

Using a protein subcellular localization prediction program, WoLF PSORT (Horton et al., 2007), we found that the V55 in the castor FatA sequence was the best

candidate to be the N-terminal amino acid of the mature protein. For castor FatB sequence, in order to identify a putative transit peptide cleavage site we compared the *Rc*FatB sequence with other similar thioesterase sequences. We considered L90 the first amino acid of the mature protein of *Rc*FatB as proposed for many other plants (Dörmann et al., 1995; Jones et al., 1995; Voelker et al., 1997; Huynh et al., 2002; Jha et al., 2006; Ghosh et al., 2007). Taking into account the presence of a signal peptide in both proteins, the putative N-terminus of the mature thioesterase proteins would be V55 for *Rc*FatA and L90 for *Rc*FatB (Fig. 1), producing proteins of 317 and 330 amino acid residues, respectively. After the transit peptide, *Rc*FatB exhibits a hydrophobic domain extending from residue L90 to Q109, that is absent in FatA thioesterases and probably involved in the anchorage to the membrane but not related to activity or affinity for different substrates (Jones et al., 1995; Facciotti and Yuan, 1998).

Alignment of the two deduced amino acid sequences (Fig. 1) showed that *Rc*FatA and *Rc*FatB shared 29% identity and 44% similarity between them. *Rc*FatA and *Rc*FatB showed 80% and 88% identity with the corresponding *Jatropha curcas* thioesterases. A phylogenetic tree was generated for the novel thioesterase genes, using their deduced amino acid sequences, in relation to all other known plant thioesterase sequences (Fig. 2). Each castor thioesterase protein was included in a different group, FatA and FatB thioesterases, with elevated conservation inside each group. As mentioned above, thioesterases from castor grouped very closely with those from *J. curcas*, both species belonging to the Euphorbiaceae family. Other closely related sequences were those from genera *Garcinia* and *Populus* classified, as *Ricinus* and *Jatropha*, in the order Malpighiales.

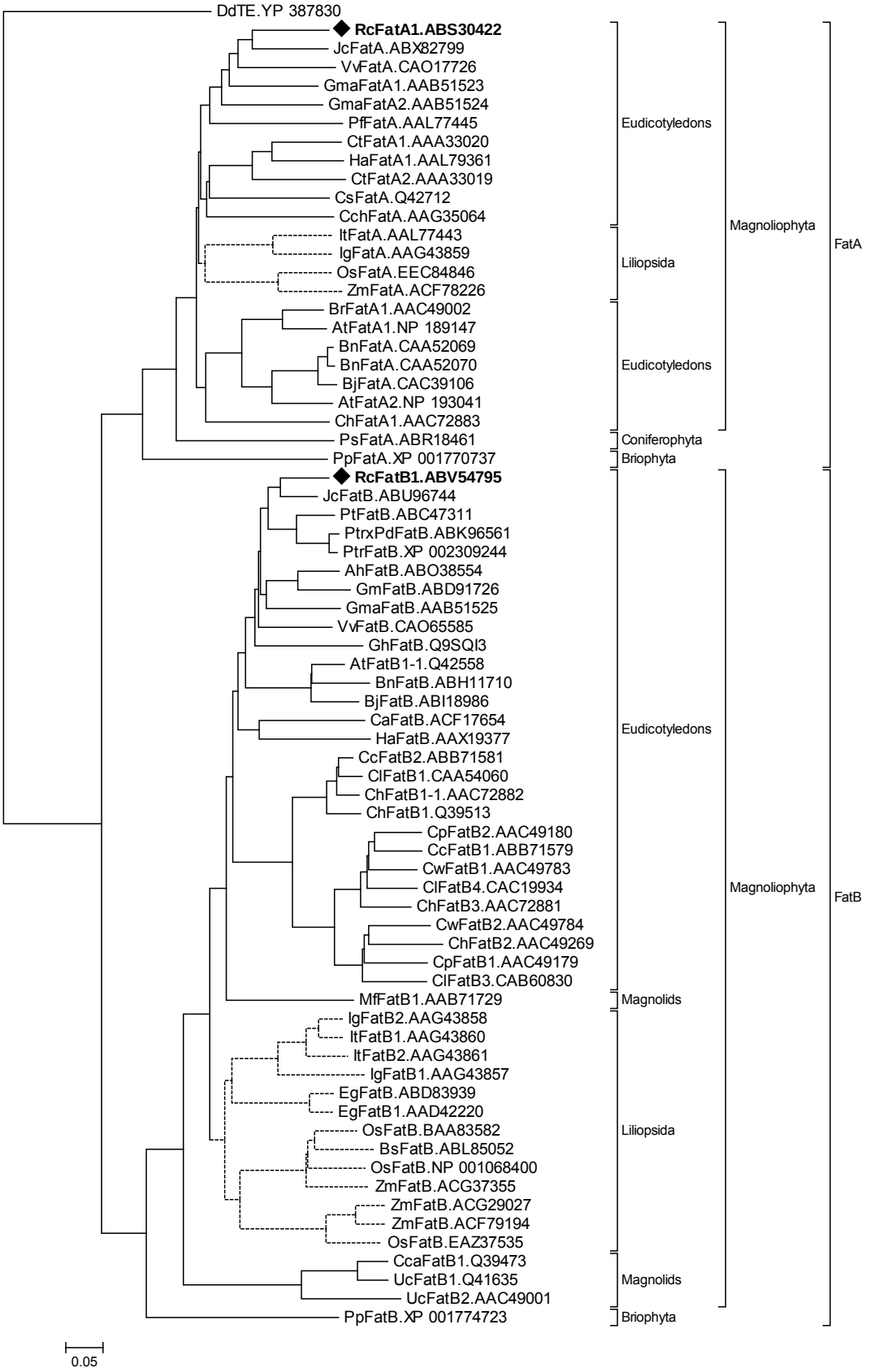

Fig. 2. Phylogenetic comparison of plant acyl-ACP thioesterase enzymes. Plant species included in the phylogenetic tree are: At, *Arabidopsis thaliana*; Ah, *Arachis hypogaea*; Bs, *Brachypodium*

sylvaticum; Bj, *Brassica juncea*; Bn, *Brassica napus*; Br, *Brassica rapa*; Ca, *Capsicum annuum*; Cch, *Capsicum chinense*; Ct, *Carthamus tinctorius*; Cca, *Cinnamomum camphora*; Cs, *Coriandrum sativum*; Cc, *Cuphea calophylla*; Ch, *Cuphea hookeriana*; Cl, *Cuphea lanceolata*; Cp, *Cuphea palustris*; Cw, *Cuphea wrightii*; Db, *Diploknema butyracea*; Eg, *Elaeis guineensis*; Gma, *Garcinia mangostana*; Gm, *Glycine max*; Gh, *Gossypium hirsutum*; Ha, *Helianthus annuus*; Ig, *Iris germanica*; It, *Iris tectorum*; Jc, *Jatropha curcas*; Ml, *Madhuca longifolia*; Mf, *Myristica fragans*; Os, *Oryza sativa*; Pf, *Perilla frutescens*; Pp, *Physcomitrella patens*; Ps, *Picea sitchensis*; Pt, *Populus tomentosa*; Ptr, *Populus trichocarpa*; PtrxPd, *Popuplus trichocarpa x Populus deltoids*; Rc, *Ricinus communis*; Ta, *Triticum aestivum*; Uc, *Umbellularia californica*; Vv, *Vitis vinifera*; Zm, *Zea mays*. *Desulfovibrio desulfuricans* acyl-ACP thioesterase (DdTE, YP_387830.1) was used as outgroup to root the tree.

2.2. Genomic organization of castor acyl-ACP thioesterase genes

Genomic Southern blot analysis using *RcFatA* and *RcFatB* gene-specific probes revealed the presence of distinct single bands in each lane (Fig. 3) suggesting that there are no cleavage sites for the restriction enzymes used to digest the genomic DNA within the regions covered by probe sequences.

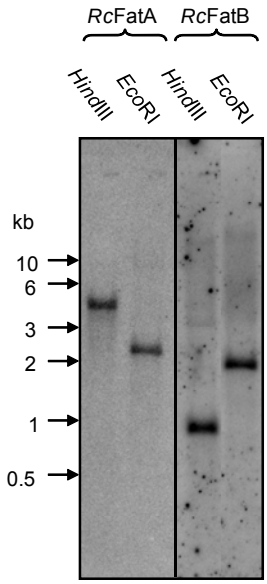

Fig. 3. Southern blot analysis of castor bean genomic DNA digested with the indicated restriction enzymes and probed with *RcFatA* (left) and *RcFatB* (right) gene-specific probes. The position of molecular weight standards in kb is indicated on the left.

This indicates the occurrence of a single copy of each gene in the castor genome and demonstrates that the cloned cDNAs correspond to the genes encoding *Rc*FatA and *Rc*FatB enzyme. FatA thioesterases from *Brassica napus* (Loader et al., 1993) and

Arabidopsis thaliana (Mekhedov et al., 2000) are encoded by more than one gene, while the FatB1 proteins studied so far (Dörmann et al., 1995; Othman et al., 2000; Jha et al., 2006; Ghosh et al., 2007) are encoded by single copy genes, except for *Gossypium hirsutum* in which at least two genes encode FatB1 thioesterases (Pirtle et al., 1999).

2.3. Seed development stage characterization based on ricinoleic acid content

Mature castor seeds synthesize and accumulate TAG and proteins in the endosperm tissue (Roberts and Lord, 1981). The morphological changes of developing castor seeds have been previously characterized and a time-course has been established for assessing the endosperm development (Chen et al., 2004). Castor endosperm development starts with a free-nuclear phase and then progresses into cellularization and maturation. The whole course takes about 54 days after pollination (DAP) (Chen et al., 2007). During the initial phase (stages 1-2, Fig. 4A), castor seeds grow rapidly, with high levels of cell division and low accumulation of oil. The synthesis of most of the TAG takes place in the next phase (stages 2-5, Fig. 4A) and finishes when the seed coat changes its color and starts to dry. The last phase involves the shutdown of synthetic activities and seed drying (stages 5-7, Fig. 4A). During the course of cellular endosperm development and maturation, the seeds gradually lose water and rapidly accumulate lipids to a maximum level of 60% at 54 DAP and maintain the same high level thereafter (Chen et al., 2007).

The ricinoleic acid content was measured in castor seeds at various developmental stages. As shown in Fig. 4B, the ricinoleic acid accumulated progressively during the maturation of the embryo, reaching a plateau when the cellularization of the endosperm finished (Chen et al., 2007) and accounting for 90% of the total fatty acid content. At the same time, unsaturated and saturated fatty acids contents diminished in the seed (Fig. 4B). It has been reported that ricinoleic acid is incorporated almost exclusively into storage TAG rather than membrane lipids in castor seeds (Bafor et al., 1991). Therefore, the content of ricinoleic acid in seed lipids directly correlates with the accumulation of TAG (Fig. 4B).

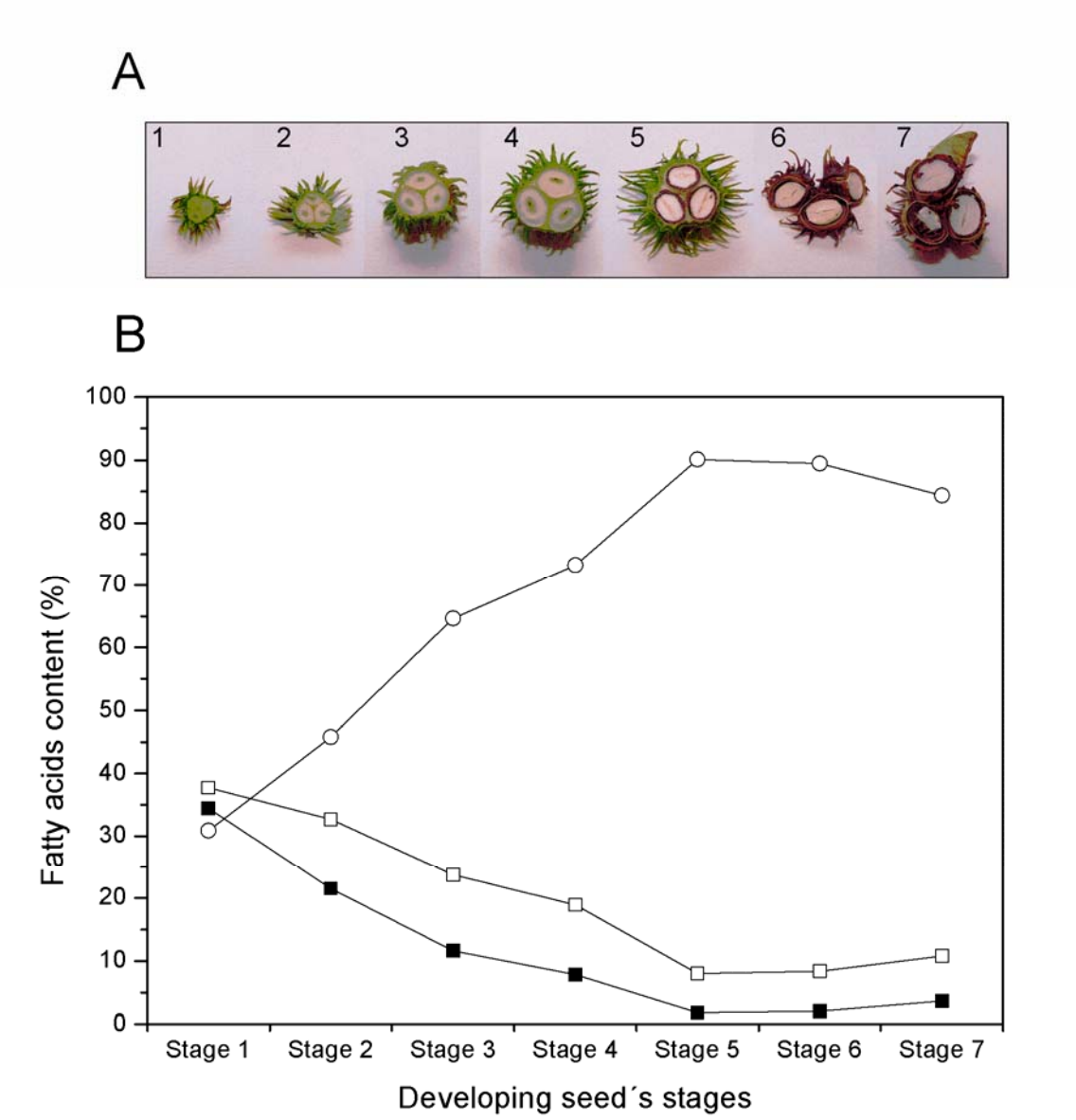

Fig. 4. Changes in morphology (A) and fatty acid composition (B) during castor seed development. Fatty acid composition was determined as indicated in Experimental. (○) ricinoleic acid, (□) unsaturated fatty acids and (■) saturated fatty acids.

2.4. Expression profiles of castor acyl-ACP thioesterases

The expression levels of acyl-ACP thioesterase genes were studied by QRT-PCR in developing seeds and vegetative tissues of castor. Results in Fig. 5A show that the transcript accumulation profile was temporally regulated during embryo development. The highest levels of expression of *RcFatA* and *RcFatB* genes in developing seeds were found in stages 3-5, which correspond to the phase of oil

accumulation (He et al., 2004) and were significantly lower in the rest of the stages. A similar profile has been reported using semi-quantitative RT-PCR data for cotton FatB thioesterase (Pirtle et al., 1999), using Northern blot analysis for *B. napus* FatA thioesterases (Loader et al., 1993; O'Hara et al., 2002) or using both techniques for other castor seed enzymes from the lipid biosynthetic pathway (He et al., 2004; Chen et al., 2007). Furthermore, the expression level of *RcFatB* gene was higher than those from *RcFatA* gene in seeds from stages 1 to 4 and in all vegetative tissues studied. In contrast, in *Arabidopsis*, FatB transcripts maintain constitutive levels in all seed stages while FatA isoenzymes expression follows a profile similar to the one found in castor seeds (Fig. 5B). In castor seeds, transcripts also accumulated at considerable levels in leaves (Fig. 5A) as it has been shown for other acyl-ACP thioesterases genes (Othman et al., 2000; Zhou et al., 2007) but in contrast again with the data obtained from microarrays experiments in *Arabidopsis* (Fig. 5B).

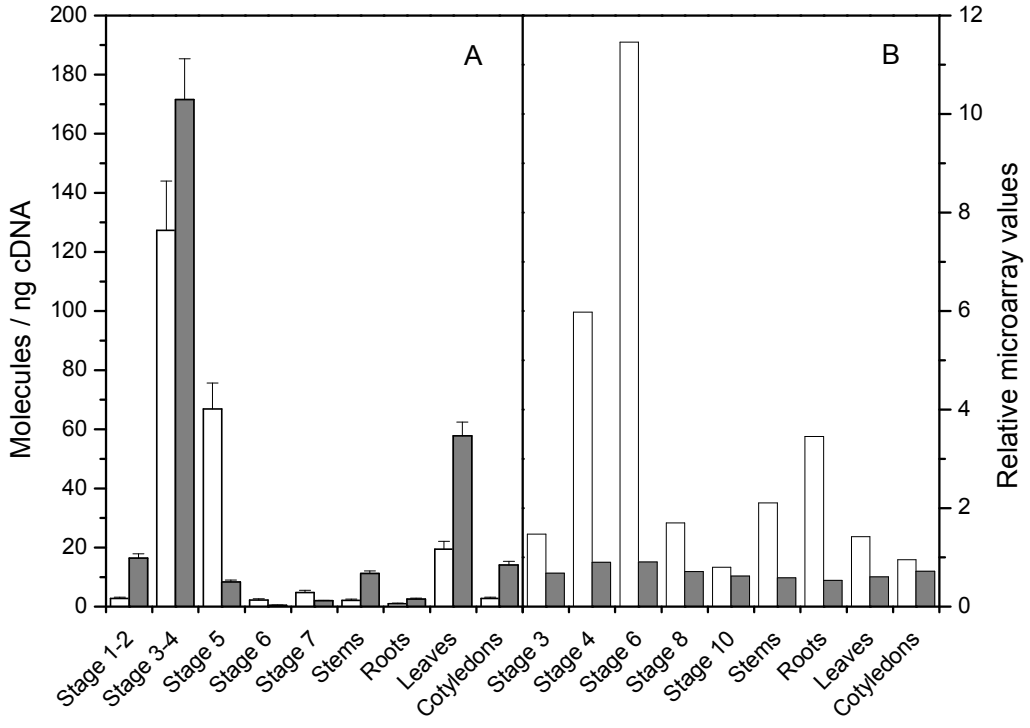

Fig. 5. Expression of *FatA* (white columns) and *FatB* (light grey columns) genes in developing seeds and vegetative tissues of *Ricinus communis* and *Arabidopsis thaliana*. A, *RcFatA* and *RcFatB* expression determined by QRT-PCR; B, *AtFatA* and *AtFatB* expression estimated from microarrays of Schmid et al. (2005). Castor seeds stages as shown in Fig. 4. *Arabidopsis* stages: 3, mid globular to early heart embryos; 4, early to late heart embryos; 6, mid to late torpedo embryos; 8, walking-stick to early curled cotyledons embryos; and 10, green cotyledons embryos. Values in panel A represent mean values ± SD of three independent samples.

The pattern observed in this analysis suggests that castor acyl-ACP thioesterases are important for oil deposition in the seed. Castor oil is rich in ricinoleic acid, a C18 fatty acid that derives from oleate released via FatA. Therefore, the synthesis of castor oil requires of high rates of export of this fatty acid from plastids. This fits well with the high levels of expression of *RcFatA* in stages 3 to 5 shown in Fig. 5. In later stages the expression of this gene is considerably reduced provided the TAG synthesis is switched off. The expression of *RcFatB* was also high during the period of oil accumulation, although it was down-regulated earlier than that corresponding to *RcFatA*. Thioesterases of the FatB type are mainly related to the export of palmitic and stearic acid from plastids (Bonaventure et al., 2004). Castor oil accumulates low levels of saturated fatty acids, so the role of *RcFatB* should be related to the supply of saturated acyl chains destined to keep a correct balance of fatty acids in the plant membranes and serve as substrates for the synthesis of sphingolipid long-chain bases (Chen et al., 2008).

2.5. Fatty acid analysis of E. coli cells expressing castor acyl-ACP thioesterases

In the case of *RcFatB*, the nucleotide sequence of the hydrophobic region in the amino terminal end of the mature protein, not involved in neither the substrate specificity nor the enzyme activity *in vitro* (Jones et al., 1995; Facciotti and Yuan, 1998), was also removed to obtain the recombinant protein from *E. coli* in the soluble fraction. The predicted mature coding regions of castor thioesterases were cloned into pQE-80L vector providing high levels of expression in *E. coli* XL1-Blue.

The fatty acid composition of *E. coli* cells bearing plasmids containing castor acyl-ACP thioesterase genes was analyzed and compared to that of control cells bearing pQE-80L vector (Table 2). The expression of *Rc*FatA produced a decrease in the unsaturated fatty acids, while the expression of *Rc*FatB caused the opposite effect. *Rc*FatA and *Rc*FatB would thus act on unsaturated or saturated fatty acids, respectively, releasing free fatty acids that would be degraded by β-oxidation pathway. The bacteria seem to compensate the decrease of available fatty acids by increasing the metabolic flux to the fatty acid biosynthetic pathway. As a consequence, a substantial change in the total unsaturated to saturated ratio is observed. This experiment reproduced the results reported by Voelker and Davies (1994) using the thioesterase from *U. californica* and confirmed that genes introduced in the prokaryotic host were properly expressed and that their products were in fact active enzymes.

Table 2. Fatty acids composition of *E. coli* cells containing control and recombinant plasmids. Data are the average of three independent samples. SD<5% of mean value. [a]*cis*-9,10-methylen-hexadecanoic acid, cyclopropane derivative from 16:1; [b]*cis*-11,12-methylen-octadecanoic acid, cyclopropane derivative from 18:1; [c]Unsaturated fatty acids; [d]Saturated fatty acids; and [e](18:1+19:0Δ)/(16:1+17:0Δ).

	Fatty acids (mol %)						UFAc/SFAd	18:1/16:1e
Plasmid	**16:0**	**16:1**	**17:0Δa**	**18:0**	**18:1**	**19:0Δb**		
pQE-80L	49.42	23.01	10.65	0.64	14.00	2.29	1.00	0.48
pQERcFatA	54.87	19.84	14.48	0.55	8.65	1.62	0.80	0.30
pQERcFatB	47.03	14.42	22.09	0.52	12.83	3.12	1.11	0.44

2.6. Substrate specificity and kinetic parameters of castor acyl-ACP thioesterases

In vitro assays using crude extracts from *E. coli* expressing recombinant acyl-ACP thioesterases or purified proteins have been shown to be an effective method to characterize these enzymes (Knutzon et al., 1992; Voelker and Davies, 1994; Dehesh et al., 1996a,b). Although toxic effects associated with *FatB* genes overexpression in bacteria have been reported previously (Dörmann et al., 1995; Serrano-Vega et al., 2003), relatively short growth periods after induction allowed us to produce enough recombinant proteins in order to purify them by immobilized metal ion affinity chromatography (IMAC). Therefore, the kinetic parameters of *Rc*FatA and *Rc*FatB were investigated in purified proteins from transgenic *E. coli* in order to evaluate the contribution of these enzymes to castor oil biosynthesis. Histidine-tagged *Rc*FatA and *Rc*FatB were purified from the soluble protein preparations of cells harboring pQE*Rc*FatA and pQE*Rc*FatB, respectively, by IMAC. This method made possible the purification to homogeneity of the recombinant proteins in a single step (Fig. 6). The data obtained from the purification were in agreement with the predicted mass for the recombinant histidine-tagged versions of *Rc*FatA (37.52 kD) and *Rc*FatB (36.80 kD), respectively.

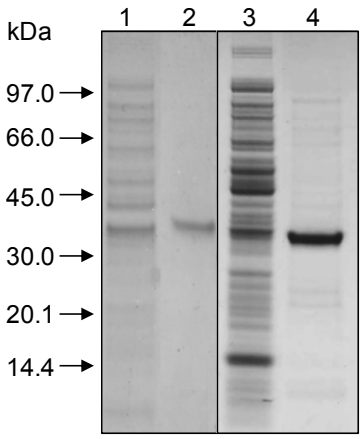

Fig. 6. Comassie blue stained SDS-PAGE showing recombinant castor acyl-ACP thioesterases. Lane 1, soluble fraction of pQE*Rc*FatA lysate; lane 2, purified His-tagged *Rc*FatA protein; lane 3, soluble fraction of pQE*Rc*FatB lysate; lane 4, purified His-tagged *Rc*FatB protein. The position of molecular weight (kDa) markers is shown on the left.

Substrate specificity of castor thioesterases was determined by assaying the activity of both enzymes on different acyl-ACPs at a constant substrate concentration (Fig. 7). *Rc*FatA enzyme displayed low levels of activity on saturated stearoyl- and palmitoyl-ACP derivatives. Moreover, it was 3-fold more active on the monounsaturated palmitoleoyl-ACP than on the saturated substrates, and its maximum activity was displayed towards oleoyl-ACP (Fig. 7, open columns). These results are similar to those previously reported for FatA thioesterases from other plants such as *G. mangostana* (Hawkins and Kridl, 1998), *Carthamus tinctorius* (Knutzon et al., 1992), *Brassica campestris* (Pathak et al., 2004), *A. thaliana* and *Coriandrum sativum* (Salas and Ohlrogge, 2002). The *Rc*FatB enzyme displayed the highest activity towards 18:1-ACP, but also showed significant activity towards 16:0-ACP (Fig. 7, light grey columns). Lower activities were measured for 18:0-ACP and 16:1-ACP. *Rc*FatB specificity was different to the profiles reported for *A. thaliana* (Salas and Ohlrogge, 2002), *G. mangostana* (Hawkins and Kridl, 1998), *Cuphea hookeriana* FatB1 (Jones et al., 1995) and *G. hirsutum* (Huynh et al., 2002) FatB proteins, that showed higher activity on 16:0-ACP. FatB cloned from oil palm (Othman et al., 2000) displayed high activity towards 16:0-ACP, although it differed with castor enzyme in the relatively lower activity level towards 18:1-ACP. The broad acyl chain specificity of the *Rc*FatB markedly contrasts with that of the *Rc*FatA which is highly specific for 18:1-ACP.

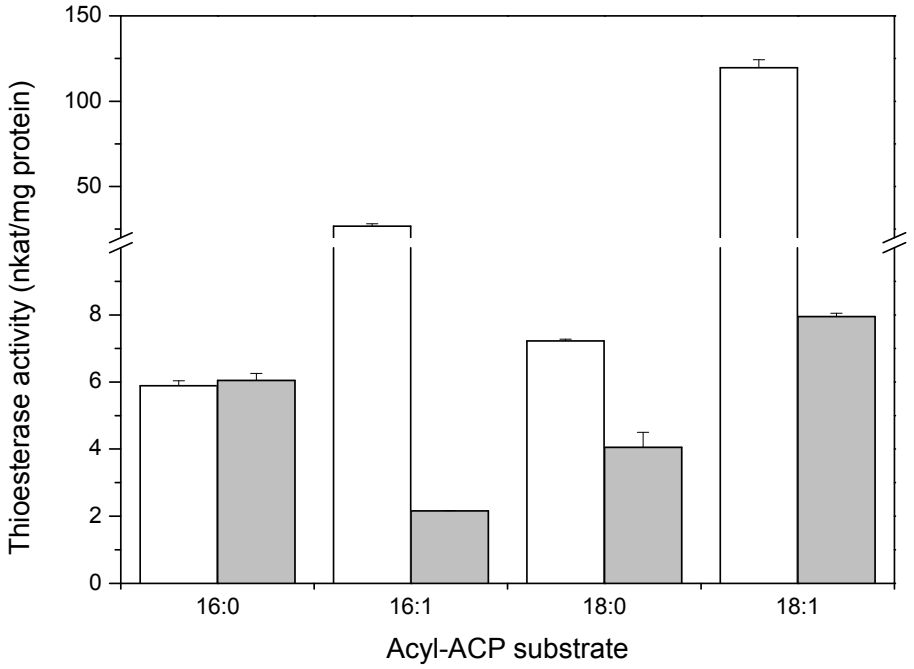

Fig. 7. Substrate specificity of castor acyl-ACP thioesterases expressed in *E. coli*. The activity was measured with purified His-tagged *Rc*FatA (white columns) and His-tagged *Rc*FatB (light grey columns) proteins, testing different acyl-ACP substrates. Data represent the mean (±SD) from three independent experiments.

Although kinetic studies have been previously published for several different acyl-ACP thioesterases, most of them were carried out on crude extracts or with partially purified proteins and characterized only one type of thioesterase. Kinetic characterization of purified thioesterases of both types, FatA and FatB, from one species provides additional information of its fatty acid biosynthetic pathway. In the case of castor when kinetic parameters were calculated for both enzymes, *Rc*FatA and *Rc*FatB, they displayed similar K_m values, in the micromolar order, for all the assayed substrates (Table 3). Those values are lower than those previously reported, being only comparable to those observed for *C. tinctorius* FatA thioesterase (McKeon and Stumpf , 1982), and purified FatA from *Helianthus annuus* (Serrano-Vega et al., 2005).

The major differences between both enzymes relate to V_{max} values: (i) the very high values found for by *Rc*FatA on oleoyl-ACP and palmitoleoyl-ACP, and (ii) the similar activity of both enzymes on saturated fatty acids varying from 10.55 to 15.41 nkat/mg protein (Table 3). *Rc*FatA displayed V_{max} values one order of magnitude higher than *Rc*FatB towards oleoyl-ACP (seven-fold higher in the case of palmitoleoyl-ACP),

which resulted in important differences in both *k*cat and catalytic efficiency (k_{cat}/K_m) values between these enzymes (Table 3). *Rc*FatA displayed k_{cat} and catalytic efficiencies significantly higher than those found in FatAs from other species (Dörmann et al., 1994; Salas and Ohlrogge, 2002; Serrano-Vega et al., 2005), and the presence of this highly efficient enzymatic machinery is in a good correlation with the high levels of oil and content of C18 fatty acids observed in castor seeds. On the contrary, the *Rc*FatB k_{cat} values were lower than those found in other FatB forms like that from *A. thaliana* (Salas and Ohlrogge, 2002), but the lower K_m values of *Rc*FatB made the catalytic efficiency of FatB from both species very similar.

Table 3. Kinetic parameters of purified recombinant *Rc*FatA and *Rc*FatB proteins on different acyl-ACP substrates.

	Substrate	K_m (μM)	V_{max} (nkat/mg protein)	k_{cat} (s^{-1})	k_{cat}/K_m (s^{-1} μM^{-1})
***Rc*FatA**	16:0-ACP	0.56	12.83	0.46	0.83
	16:1-ACP	0.35	44.76	1.62	4.63
	18:0-ACP	0.54	15.41	0.56	1.03
	18:1-ACP	0.42	221.24	7.99	19.03
***Rc*FatB**	16:0-ACP	0.54	11.28	0.41	0.76
	16:1-ACP	0.86	6.00	0.22	0.25
	18:0-ACP	0.88	10.55	0.38	0.44
	18:1-ACP	0.67	18.49	0.67	0.99

2.7. Substrate specificity of the acyl-ACP thioesterase in developing castor seeds

Thioesterase activity was also determined in extracts from developing castor seeds. The assays were carried out with crude homogenates and clarified soluble fractions prepared from seeds of stages 3-4, using different acyl-ACPs as substrates (Fig. 8). The specific activity was higher in the soluble fraction, because all the membrane proteins had been removed by centrifugation. The 16:0-ACP and 18:0-ACP thioesterase activities in castor seeds were around 3.5% of its 18:1-ACP thioesterase activity, whereas the activity towards the 16:1-ACP accounted for 11% of that found for

18:1-ACP (Fig. 8). This profile differed from that obtained for *Rc*FatA purified from bacteria, and indicates that the system in which the enzyme is expressed is able to alter its characteristics.

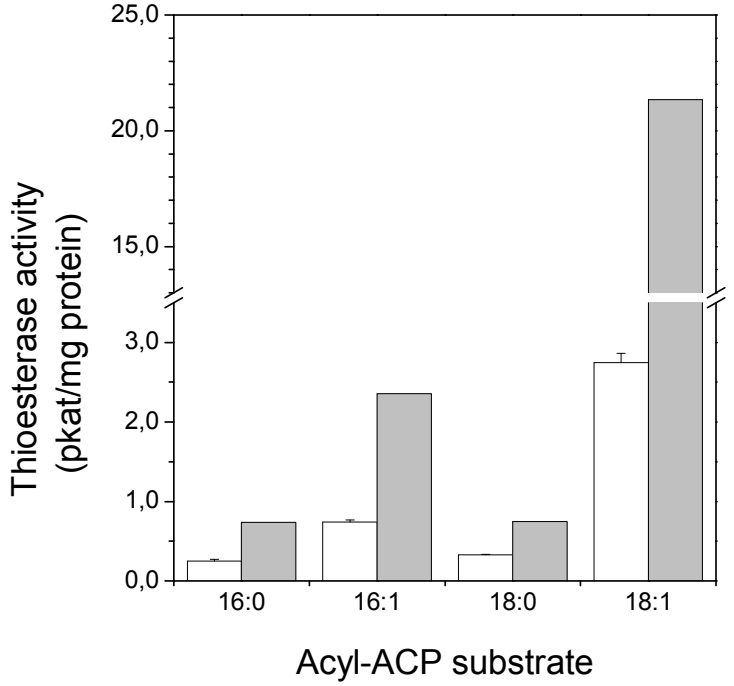

Fig. 8. Thioesterase activity found in castor seed extracts. The activity was measured in crude extract (open bars) and in the soluble fraction (grey bars) from castor seeds, testing different acyl-ACP substrates. Data represent the mean (±SD) from three independent experiments.

3. Conclusions

Acyl-ACP thioesterases are enzymes of great biotechnological interest because they control the length of the fatty acids that are produced in C18 plants. *Fat*A and *Fat*B thioesterases from *R. communis* were cloned, heterologously expressed, purified and characterized. Southern blot analysis indicated that the plant contains single copies for both genes that were transcribed at high levels in seeds during the period of oil synthesis. These thioesterases were expressed in *E. coli*, displaying profiles of substrate specificity similar to those found in thioesterases from other species. *Rc*FatA displayed catalytic efficiencies higher than most reported FatAs, which could be of interest in

order to engineer acyl-ACP thioesterases with higher levels of activity to promote high fatty acid fluxes from plastids to the cytosol for them to be incorporated into glycerolipids. On the other hand, *Rc*FatB showed a very peculiar substrate profile with a higher affinity on oleoyl-ACP that, together with the high catalytic efficiency shown by *Rc*FatA, could explain the high content of C18 derivatives that can be found in castor seeds. The expression profiles of genes encoding these enzymes displayed maximum level of transcription in the period of maximum oil accumulation, again pointing to the involvement of these enzymes in the process of oil accumulation in castor.

4. Experimental

4.1. Biological material and growth conditions

Castor plants were cultivated in growth chambers at 25 ºC/15 ºC (day/night cycles), with a 16 h photoperiod and a photon flux density of 200 μmol m^{-2} s^{-1}. The *E. coli* strain XL1-Blue (Stratagene) was used as host for the expression of *Rc*FatA and *Rc*FatB. The bacteria were grown in LB medium (1% tryptone, 0.5% yeast extract, 1% NaCl, pH 7) and the liquid cultures were shaken vigorously at 37 ºC. For plasmid selection 100 μg/ml of ampicillin were added.

4.2. mRNA preparation and cDNA synthesis

Approximately 0.25 g of developing castor seeds were ground in liquid nitrogen using a precooled sterile mortar and pestle. Total RNA was isolated using the Spectrum Plant Total RNA Kit (Sigma). Subsequently, mRNA was isolated from the total RNA using a GenElute mRNA Miniprep Kit (Sigma). The mRNA pellet was resuspended in 33 μl RNAase-free TE buffer (10 mM Tris-HCl, 1 mM EDTA, pH 8) and cDNA was synthesized using a Ready-To-Go T-Primed First-Strand Kit (Amersham Bioscience).

4.3. Cloning of genes encoding castor thioesterases

FatA and FatB protein sequences from public databases were aligned to identify regions of homology using the ClustalX v1.8 program (Thompson et al., 1997). Using cDNA from developing castor seeds as template, two different PCR fragments, 458 bp

and 523 bp long, were amplified with degenerate primers designed from highly conserved regions of FatA (FatA1 and FatAB, see Table 1), and FatB (FatB-F1 and FatB-R1, see Table 1), respectively. Subsequently, 5'- and 3'-ends of the corresponding cDNAs were obtained using the SMART-RACE cDNA Amplification Kit (Clontech) and specific primers RcFATA-1f, RcFATA-4r and RcFATA-5r for *RcFatA* and RcFATB-2f, RcFATB-5f and RcFATB-3r for *RcFatB* (Table 1). The PCR fragments were cloned into the pMBL-T vector (Dominion MBL), sequenced, and their identities were confirmed using the BLAST software (Altschul et al., 1990).

Primers with internal *Bam*HI and *Hin*dIII restriction sites for *RcFatA* (RcFATABamH-6f and RcFATAHind-7r) or *Sac*I and *Kpn*I for *RcFatB* (RcFATBSac-9f and RcFATBKpn-10r) were designed to amplify the coding region of the mature proteins by PCR (Table 1). The PCR products obtained for *RcFatA* and *RcFatB* were subcloned into the *Bam*HI-*Hin*dIII or *Sac*I-*Kpn*I sites of the pQE-80L expression vector (Quiagen), respectively, to produce the corresponding fusion proteins with a 6xHis tag at the N-terminus. Ligations into the correct reading frames were confirmed by sequencing and the resulting constructs were designated pQE*Rc*FatA and pQE*Rc*FatB, respectively. XL1-Blue cells containing the plasmid pQE-80L were used as a control. All primers were synthesized by Eurofins MWG Operon (Germany).

4.4. Genomic Southern analysis

Genomic DNA was isolated from seeds of *R. communis* by CTAB (*c*etyl*t*rimethyl*a*mmonium *b*romide) method (Murray and Thomson, 1980). Samples of castor genomic DNA (15 µg) were digested with different restriction enzymes and electrophoresed through a 0.8% agarose gel. The gel was soaked in 250 mM HCl for 30 min, then washed three times in distilled water and finally blotted onto a Hybond-N+ nylon transfer membrane (GE Healthcare). The filter was probed with [α-^{32}P]dCTP-labelled *RcFatA* and *RcFatB* gene-specific DNA probes. The gene-specific probes with a size of 594 and 705 bp, respectively, were obtained by PCR amplification with the following pairs of primers: RcFATA-1f and RcFATA-3r for *Rc*FatA and RcFATB-1f and RcFATB-3r for *Rc*FatB. Hybridization was performed in 0.2 mM sodium phosphate buffer (pH 7.2), 250 mM SDS and 1 mM EDTA overnight at 65 ºC. The filter was washed twice in 2 x SSC buffer, 0.1% SDS for 10 min at the same temperature. Images

of radioactive filters were obtained using a Cyclone™ Storage Phosphor System (PerkinElmer) and the Optiquant™ image analysis software (Packard).

4.5. Protein expression and purification

Five hundred milliliter cultures of *E. coli* XL1-Blue cells harboring pQE*Rc*FatA or pQE*Rc*FatB were grown as described above. Expression of *Rc*FatA or *Rc*FatB was induced at OD_{600} 0.6 by adding 1 mM IPTG and growth continued for 4 h. The cells were harvested by centrifugation for 10 min at 2,500*g*, washed with distilled water and resuspended in 5 ml of Binding buffer (20 mM sodium phosphate, 500 mM NaCl, 20 mM imidazole, pH 7.4). Cells were lysed adding 0.5% Triton X-100, 5 mM DTT, 1 mM $MgCl_2$, 1 mM PMSF, 20 µg/ml DNase I (Roche) and 0.2 mg/ml lysozyme (Roche) for 45 min at 4 ºC with shaking. The resulting lysed cell suspension was centrifuged at 25,000*g* for 30 min. The supernatant was filtered through 0.22 µm filters and loaded onto a HisTrap FF 1 ml column (GE Healthcare) interfaced with an Äkta*prime* system (Amersham Bioscience). Histidine-tagged proteins were eluted from the column using an imidazole gradient ranging from 20 to 500 mM. Fractions containing *Rc*FatA or *Rc*FatB were subsequently used for thioesterase activity assays.

4.6. Gel electrophoresis of proteins

Protein samples were combined with SDS-PAGE loading buffer and heated at 95 ºC for 5 min. The samples were separated by electrophoresis on 4–12% NuPAGE Novex Bis-Tris gels in MES buffer (Invitrogen), and the gels were fixed and stained with 0.1% Coomassie R-250 in 40% ethanol, 10% acetic acid. Molecular weight standards used were obtained from GE Healthcare.

4.7. Preparation of acyl-ACP substrates

Labeled acyl-ACP substrates were prepared using a recombinant acyl-ACP synthetase from *E. coli* kindly provided by John Shanklin (Brookhaven National Laboratory, Upton, NY, USA). Acylation reactions contained 50 µg of recombinant ACP from *E. coli* (Sigma), 180 kBq (approx. 0.1 µmol) of [1-^{14}C] fatty acid ammonium salt ([^{3}H] fatty acid in the case of 16:1$^{\Delta 9}$), 5 mM ATP, 2 mM DTT, 400 mM $LiCl_2$, 10

mM $MgCl_2$, 100 mM Tris-HCl pH 8.0 and 10 µg acyl-ACP synthetase, in a final volume of 0.5 ml. Reactions were carried out at room temperature for 3 h and the acyl-ACPs were purified and concentrated by ion exchange chromatography on DEAE-sepharose as described by Rock and Garwin (1979).

4.8. Acyl-ACP thioesterase assays

Seeds were peeled and ground in extraction buffer containing 50 mM Tris-HCl pH 8.0 and 5 mM DTT, 1 g of tissue per 10 ml of buffer (Martínez-Force et al., 2000). The protein concentration in the crude extracts was measured using the Bio-Rad Protein Assay (Hercules, CA, USA) according to the manufacturer's instructions and using BSA as standard.

Thioesterase activity was assayed in 0.1 ml reactions containing 50 mM Tris-HCl pH 8.0, 5 mM DTT, 0.2-12 µg of the protein preparation (crude extracts from seeds or purified *Rc*FatA or *Rc*FatB expressed in *E. coli*) and the amount of acyl-ACP substrate ranging from 0.02 to 0.08 nmol (30-170 Bq approximately). Reactions were carried out at room temperature for 5 min and stopped by the addition of 0.25 ml of 1 M acetic acid in 2-propanol. Unesterified fatty acids were then extracted twice with 0.3 ml hexane, and the radioactivity in the pooled organic phase was determined in a calibrated liquid scintillation counter (Rackbeta II; LKB). The data from thioesterase assays was fitted to the Hill equation by nonlinear least-squares regression analysis using OriginPro 8 software, and correlated at $P<0.005$ as determined by Student's *t*-test. Both the V_{max} and K_m were derived from these curves.

4.9. Fatty acid analysis

Peeled seeds were ground in a glass tube with sand. Total lipids were extracted with hexane:2-propanol (Hara and Radin, 1978). Fatty acid methyl esters were obtained from castor seeds by heating the samples at 80 ºC in 1.8 ml of methanol/toluene/dimethoxipropane/sulphuric acid (33:14:20:10) for 1.5 h. After cooling, 1 ml heptane and 1 ml water were added and mixed. The fatty acid methyl esters were recovered from the upper phase and transferred to a fresh tube. Subsequently, the solvent was evaporated to dryness with nitrogen and the trimethylsilyl ether derivative of ricinoleic acid was prepared adding 100 µl of

hexamethyldisilazane/trimethylchlorosilane/pyridine (3:1:5). After 1 min, the derivatives were extracted with 1.8 ml heptane and analyzed by GLC using a Hewlett-Packard 6890 gas chromatograph (Palo Alto, CA, USA). The column was a Supelco SP-2380 fused-silica capillary column (30 m length, 0.25 mm i.d., 0.20 μm film thickness; Supelco, Bellefonte, PA, USA). Hydrogen was used as the carrier gas at 28 cm/s, the temperature of flame ionization detector and injector was 200 ºC, the oven temperature was 170 ºC and the split ratio was 1:50.

Twenty-five milliliter cultures of *E. coli* XL1-Blue cells harboring pQE-80L or pQE*Rc*FatA or pQE*Rc*FatB were grown and expression of the corresponding thioesterase induced as described above. The cells were harvested by centrifugation for 10 min at 2500*g*, washed with distilled water and the total fatty acid content was determined using the one-step method proposed by Garcés and Mancha (1993). Volumes of 3.3 ml of methanol/toluene/dimethoxipropane/sulphuric acid (39:20:5:2) and 1.7 ml heptane were added to the pellet of bacterial cells, and the mixture was heated at 80 ºC for 1 h. After cooling, the upper phase containing the fatty acid methyl esters was transferred to a fresh tube, washed with 6.7% sodium sulphate and evaporated to dryness with nitrogen. The methyl esters were dissolved in an appropriate volume of heptane and analyzed by GLC. The different methyl esters were identified by comparison with a combination of standards.

4.10. Quantitative real time PCR

The cDNAs were subjected to quantitative real time PCR (QRT-PCR) with specific pairs of primers, RcFATA-2f and RcFATA-5r for *RcFatA* gene and RcFATB-5f and RcFATB-9r for *RcFatB* gene (Table 1), and SYBR Green I (QuantiTect® SYBR® Green PCR Kit, Quiagen, Crawley, UK) using a MiniOpticon system (Bio-Rad). The reaction mixture was heated to 50 ºC for 2 min and then heated to 95 ºC for 15 min before subjecting it to 40 PCR cycles of 94 ºC for 15 s, 60.5 ºC for 30 s, and 72 ºC for 15 s, while monitoring the resulting fluorescence. Calibration curves were drawn up using sequential dilutions of pQE*Rc*FatA and pQE*Rc*FatB. These were used to estimate the transcript content of the calibrator gen. The Livak method (Livak and Schmittgen, 2001) was applied to calculate comparative expression levels between samples. The castor actin gen (accession number AY360221) was used as internal

reference to normalize the relative amount of cDNAs for all samples with the specific pair of primers RcActF and RcActR (Table 1).

Acknowledgements

This work was supported by MICINN (PSS-420000-2008-19) and FEDER.

References

Altschul, S.F., Gish, W., Miller, W., Myers, E.W., Lipman, D.J., 1990. Basic local alignment search tool. J. Mol. Biol. 215, 403-410.

Bafor, M., Smith, M.A., Jonsson, L., Stobart, K., Stymne, S., 1991. Ricinoleic acid biosynthesis and triacylglycerol assembly in microsomal preparations from developing castor-bean (*Ricinus communis*) endosperm. Biochem. J. 280, 507-514.

Bonaventure, G., Salas, J.J., Pollard, M.R., Ohlrogge, J.B., 2003. Disruption of the FATB gene in Arabidopsis demonstrates an essential role of saturated fatty acids in plant growth. Plant Cell 15, 1020-1033.

Bonaventure, G., Ba, X.M., Ohlrogge, J., Pollard, M., 2004. Metabolic responses to the reduction in palmitate caused by disruption of the FATB gene in Arabidopsis. Plant Physiol. 135, 1269-1279.

Chen, G.,Q., He, X., Liao, L.P., McKeon, T.A., 2004. 2S albumin gene expression in castor plant (*Ricinus communis* L.). J. Am. Oil Chem. Soc. 81, 867-872.

Chen, G.Q., Turner, C., He, X., Nguyen, T., McKeon, T.A., Laudencia-Chingcuanco, D., 2007. Expression profiles of genes involved in fatty acid and triacylglycerol synthesis in castor bean (*Ricinus communis* L.). Lipids 42, 263-274.

Chen, M., Markham, J.E., Dietrich, C.R., Jaworski, J.G., Cahoon, E.B., 2008. Sphingolipid long-chain base hydroxylation is important for growth and regulation of sphingolipid content and composition in Arabidopsis. Plant Cell 20, 1862-1878.

Dehesh, K., Edwards, P., Hayes, T., Cranmer, A.M., Fillatti, J., 1996a. Two novel thioesterases are key determinants of the bimodal distribution of acyl chain length of *Cuphea palustris* seed oil. Plant Physiol. 110, 203-210.

Dehesh, K., Jones, A., Knutzon, D.S., Voelker, T.A., 1996b. Production of high levels of 8:0 and 10:0 fatty acids in transgenic canola by overexpression of *Ch FatB2*, a thioesterase cDNA from *Cuphea hookeriana*. Plant J. 9, 167-172.

Dörmann, P., Kridl, J.C., Ohlrogge, J.B., 1994. Cloning and expression in *Escherichia coli* of a cDNA coding for the oleoyl-acyl carrier protein thioesterase form coriander (*Coriandrum sativum* L.). Biochim. Biophys. Acta 1212, 134-136.

Dörmann, P., Voelker, T.A., Ohlrogge, J.B., 1995. Cloning and expression in *Escherichia coli* of a novel thioesterase from *Arabidopsis thaliana* specific for long-chain acyl-acyl carrier proteins. Arch. Biochem. Biophys. 316, 612-618.

Dörmann, P., Voelker, T.A., Ohlrogge, J.B., 2000. Accumulation of palmitate in Arabidopsis mediated by the acyl-acyl carrier protein thioesterase FATB1. Plant Physiol. 123, 637-644.

Facciotti, M.T., Yuan, L., 1998. Molecular dissection of the plant acyl-acyl carrier protein thioesterases. Fett Lipid 100, 167-172.

Garcés, R., Mancha, M., 1993. One-step lipid extraction and fatty acid methyl esters preparation from fresh plant tissues. Anal. Biochem. 211, 139-143.

Ghosh, S.K., Bhattacharjee, A., Jha, I.K., Mondal, A.K., Maiti, M.K., Basu, A., Ghosh, D., Ghosh, S., Sen, S.K., 2007. Characterization and cloning of a stearoyl/oleoyl specific fatty acyl-acyl carrier protein thioesterase from the seeds of *Madhuca longifolia* (*latifolia*). Plant Physiol. Biochem. 45, 887-897.

Gunstone, F.D., Harwood, J.L., Dijkstra, A.J., 2007. The Lipid Handbook, third ed. CRC Press, Boca Raton.

Hara, A., Radin, N.S., 1978. Lipid extraction of tissues with a low-toxicity solvent. Anal. Biochem. 90, 420-426.

Hawkins, D.J., Kridl, J.C., 1998. Characterization of acyl-ACP thioesterases of mangosteen (*Garcinia mangostana*) seed and high levels of stearate production in transgenic canola. Plant J. 13, 743-752.

He, X., Chen, G.Q., Lin, J.T., McKeon, T.A., 2004. Regulation of diacylglycerol acyltransferase in developing seeds of castor. Lipids 39, 865-871.

Horton, P., Park, K.J., Obayashi, T., Fujita, N., Harada, H., Adams-Collier, C.J., Nakai, K., 2007. WoLF PSORT: protein localization predictor. Nucleic Acids Res. 35, W585-W587

Huynh, T.T., Pirtle, R.M., Chapman, K.D., 2002. Expression of a *Gossypium hirsutum* cDNA encoding a FatB palmitoyl-acyl carrier protein thioesterase in *Escherichia coli*. Plant Physiol. Biochem. 40, 1-9.

Jha, J.K., Maiti, M.K., Bhattacharjee, A., Basu, A., Sen, P.C., Sen, S.K., 2006. Cloning and functional expression of an acyl-ACP thioesterase FatB type from *Diploknema* (*Madhuca*) *butyracea* seeds in *Escherichia coli*. Plant Physiol. Biochem. 44, 645-655.

Jones, A., Davies, H.M., Voelker, T.A., 1995. Palmitoyl-acyl carrier protein (ACP) thioesterase and the evolutionary origin of plant acyl-ACP thioesterases. Plant Cell 7, 359-371.

Joshi, C.P., Zhou, H., Huang, X., Chiang, V.L., 1997. Context sequences of translation initiation codon in plants. Plant Mol. Biol. 35, 993-1001.

Knutzon, D.S., Bleibaum, J.L., Nelsen, J., Kridl, J.C., Thompson, G.A., 1992. Isolation and characterization of two safflower oleoyl-acyl carrier protein thioesterase cDNA clones. Plant Physiol. 100, 1751-1758.

Koo, A.J., Ohlrogge, J.B., Pollard, M., 2004. On the export of fatty acids from the chloroplast. J. Biol. Chem. 279, 16101-10.

Kozak, M., 1991. An analysis of vertebrate mRNA sequences: intimations of translational control. J. Cell Biol. 115, 887-903.

Livak, K.J., Schmittgen, T.D., 2001. Analysis of relative gene expression data using real-time quantitative PCR and the $2^{-\Delta\Delta CT}$ method. Methods 25, 402-408.

Loader, N.M., Woolner, E.M., Hellyer, A., Slabas, A.R., Safford, R., 1993. Isolation and characterization of two *Brassica napus* embryo acyl-ACP thioesterase cDNA clones. Plant Mol. Biol. 23, 769-778.

Lütcke, H.A., Chow, K.C., Mickel, F.S., Moss, K.A., Kern, H.F., Scheele, G.A., 1987. Selection of AUG initiation codons differs in plants and animals. EMBO J. 6, 43-48.

Mandal, M.N., Santha, I.M., Lodha, M.L., Mehta, S.L. 2000. Cloning of acyl-acyl carrier protein (ACP) thioesterase gene from *Brassica juncea*. Biochem. Soc. Trans. 28:967-969.

Martínez-Force, E., Cantisán, S., Serrano-Vega, M.J., Garcés, R., 2000. Acyl-acyl carrier protein thioesterase activity from sunflower (*Helianthus annuus* L.) seeds. Planta 211, 673-678.

Mayer, K.M., Shanklin, J., 2005. A structural model of the plant acyl-acyl carrier protein thioesterase FatB comprises two helix/4-stranded sheet domains, the N-terminal domain containing residues that affect specificity and the C-terminal domain containing catalytic residues. J. Biol. Chem. 280, 3621-3627.

Mayer, K.M., Shanklin, J., 2007. Identification of amino acid residues involved in substrate specificity of plant acyl-ACP thioesterases using a bioinformatics-guided approach. BMC Plant Biol. 7, 1.

McKeon, T.A., Stumpf, P.K., 1982. Purification and characterization of the stearoyl-acyl carrier protein desaturase and the acyl-acyl carrier protein thioesterase from maturing seeds of safflower. J. Biol. Chem. 257, 12141-12147.

Mekhedov, S., Ilárduya, O.M., Ohlrogge, J., 2000. Toward a functional catalog of the plant genome. A survey of genes for lipid biosynthesis. Plant Physiol. 122, 389-401.

Murray, M.G., Thompson, W.F., 1980. Rapid isolation of high molecular weight plant DNA. Nucleic Acids Res. 8, 4321-4325.

O'Hara, P., Slabas, A.R., Fawcett, T., 2002. Fatty acid and lipid biosynthetic genes are expressed at constant molar ratios but different absolute levels during embryogenesis. Plant Physiol. 129, 310-320.

Ohlrogge, J., Pollard, M., Bao, X., Focke, M., Girke, T., Ruuska, S., Mekhedov, S., Benning, C., 2000. Fatty acid synthesis: from CO_2 to functional genomics. Biochem. Soc. Trans. 28, 567-73.

Othman, A., Lazarus, C., Fraser, T., Stobart, K., 2000. Cloning of a palmitoyl-acyl carrier protein thioesterase from oil palm. Biochem. Soc. Trans. 28, 619-622.

Pathak, M.K., Bhattacharjee, A., Ghosh, D., Ghosh, S., 2004. Acyl-Acyl carrier protein (ACP)-thioesterase from developing seeds of *Brassica campestris* cv. B-54 (Agrani). Plant Sci. 166, 191-198.

Pirtle, R.M., Yoder, D.W., Huynh, T.T., Nampaisansuk, M., Pirtle, I.L., Chapman, K.D., 1999. Characterization of a palmitoyl-acyl carrier protein thioesterase (FatB1) in cotton. Plant Cell Physiol. 40, 155-163.

Pollard, M., Ohlrogge, J., 1999. Testing models of fatty acid transfer and lipid synthesis in spinach leaf using *in vivo* oxygen-18 labeling. Plant Physiol. 121, 1217-1226.

Rawsthorne, S., 2002. Carbon flux and fatty acid synthesis in plants. Prog. Lipid Res. 41, 182-196.

Roberts, L.M., Lord, J.M., 1981. Protein biosynthetic capacity in the endosperm tissue of ripening castor bean seeds. Planta 152, 420-427.

Rock, C.O., Garwin, J.L., 1979. Preparative enzymatic synthesis and hydrophobic chromatography of acyl-acyl carrier protein. J. Biol. Chem. 254, 7123-7128.

Salas, J.J., Ohlrogge, J.B., 2002. Characterization of substrate specificity of plant FatA and FatB acyl-ACP thioesterases. Arch. Biochem. Biophys. 403, 25-34.

Schmid, M., Davison, T.S., Henz, S.R., Pape, U.J., Demar, M., Vingron, M., Schölkopf, B., Weigel, D., Lohmann, J.U., 2005. A gene expression map of *Arabidopsis thaliana* development. Nat. Genet. 37, 501-506.

Serrano-Vega, M.J., Venegas-Calerón, M., Garcés, R., Martínez-Force, E., 2003. Cloning and expression of fatty acids biosynthesis key enzymes from sunflower (*Helianthus annuus* L.) in *Escherichia coli*. J. Chromatogr. B. 786, 221-228.

Serrano-Vega, M.J., Garcés, R., Martínez-Force, E., 2005. Cloning, characterization and structural model of a FatA-type thioesterase from sunflower seeds (*Helianthus annuus* L.). Planta 221, 868-880.

Thompson, J.D., Gibson, T.J., Plewniak, F., Jeanmougin, F., Higgins, D.G., 1997. The CLUSTAL_X windows interface: flexible strategies for multiple sequence alignment aided by quality analysis tools. Nucleic Acids Res. 25, 4876-4882.

Voelker, T., 1996. Plant acyl-ACP thioesterases: chain-length determining enzymes in plant fatty acid biosynthesis. Genet. Eng. 18, 111-133.

Voelker, T.A., Davies, H.M., 1994. Alteration of the specificity and regulation of fatty acid synthesis of *Escherichia coli* by expression of a plant medium-chain acyl-acyl carrier protein thioesterase. J. Bacteriol. 176, 7320-7327.

Voelker, T.A., Jones, A., Cranmer, A.M., Davies, H.M., Knutzon, D.S., 1997. Broad-range and binary-range acyl-acyl-carrier-protein thioesterases suggest an alternative mechanism for medium-chain production in seeds. Plant Physiol. 114, 669-677.

Voelker, T.A., Worrell, A.C., Anderson, L., Bleibaum, J., Fan, C., Hawkins, D.J., Radke, S.E., Davies, H.M., 1992. Fatty acid biosynthesis redirected to medium chains in transgenic oilseed plants. Science 257, 72-74.

Yuan, L., Nelson, B.A., Caryl, G., 1996. The catalytic cysteine and histidine in the plant acyl-acyl carrier protein thioesterases. J. Biol. Chem. 271, 3417-3419.

Zhou, Z., Zhang, D., Lu, M., 2007. Cloning and expression analysis of *PtFATB* gene encoding the acyl-acyl carrier protein thioesterase in *Populus tomentosa* Carr. J. Gen. Genomics 34, 267-274.

Acyl-ACP thioesterases from macadamia (*Macadamia tetraphylla*) nuts: cloning, characterization and impact on macadamia oil composition.

Moreno-Pérez, A. J.[1], Sánchez-García, A.[1], Salas, J. J., Garcés, R., Martínez-Force, E.[a]

Instituto de la Grasa (CSIC), Av. Padre García Tejero 4, E-41012 Sevilla, Spain

Submitted to *Plant Physiology and Biochemistry*

[1] These authors have contributed equally to the studies presented in this manuscript

Abstract

The mechanisms by which macadamia nuts accumulate the unusual palmitoleic and asclepic acyl moieties, up to 20%, are still unknown. Acyl-acyl carrier protein (ACP) thioesterases (EC 3.1.2.14) are intraplastidial enzymes that terminate the synthesis of fatty acids in plants and make possible the export of the acyl moieties to the endoplasmic reticulum to be used in the production of glycerolipids. In the present work, we investigated the possible role of acyl-ACP thioesterase activity in the composition of macadamia kernel oil. In this regard, two acyl-ACP thioesterases, one of the FatA type and other of the FatB type, were cloned from developing macadamia kernel and heterologously expressed in *Escherichia coli*. Recombinant thioesterase enzymes were purified, kinetically characterized and assayed with a variety of substrates, resulting in high specificity of macadamia FatA towards 16:1-ACP. Furthermore, acyl-ACP thioesterase activity was also characterized in crude extracts from two different varieties of macadamia, Cate and Beaumont, accumulating different amounts of n-7 fatty acids. The impact of acyl-ACP thioesterase activities in the oil composition of these kernels is discussed in function of the results.

1. Introduction

Macadamia is a genus that belongs to the family of *Proteaceae* comprising nine species of tree naturally occurring in Australia, New Caledonia and Indonesia [1]. From those nine species only two are of commercial importance, *Macadamia integrifolia* Maiden & Betche and *Macadamia tetraphylla* L. Johnson. Edible macadamia nuts are a valuable food rich in oil, protein and minerals. In this regard, macadamia oil is of special interest because it contains some unusual n-7 monounsaturated fatty acids, such as palmitoleic ($16:1^{\Delta 9}$) and asclepic ($18:1^{\Delta 11}$) acids, which make it a healthy oil [2]. Macadamia oil is an interesting basestock for some industrial oil applications, such as for lubricant industry. The stability of monounsaturated fatty acids plus the low melting point of palmitoleic acid could make this oil interesting for lubricant applications [3].

The mechanisms by which macadamia nuts accumulate these unusual fatty acids are still unknown. Intraplastidial *de novo* fatty acid synthesis consists of successive elongations of acyl-ACP derivatives by the action of fatty acid synthase (FAS) enzymatic complexes. The final product of these elongations is stearoyl-ACP that is usually desaturated by very active intraplastidial stearoyl-ACP desaturase [4] to produce oleoyl-ACP, the ending product of the intraplastidial fatty acid biosynthesis. Acyl-ACP thioesterases are the enzymes that terminate the intraplastidial synthesis of fatty acids by hydrolyzing the acyl-ACP complexes [5]. There are two gene families of acyl-ACP thioesterases named *FatA*, which displays high specificity towards oleoyl-ACP and is responsible for most of the acyl-ACP hydrolysis in plants, and *FatB*, specialized in the release of saturated or shorter saturated acyl-ACP [6]. The 3D structure of these enzymes have been modeled by establishing analogy with some bacterial acyl-CoA thioesterases [7, 8], but they have not yet been confirmed by crystallographic data. It has been proposed that unusual monoenes such as palmitoleic acid are produced during intraplastidial fatty acid synthesis by the action of diverged acyl-ACP desaturases that act on substrates different than stearoyl-ACP [9, 10, 11], or even standard stearoyl-ACP desaturases acting on palmitoyl-ACP because it was found in higher concentration than expected [12]. Some species, as *Doxantha unguis-cati*, which also produces oil enriched in n-7 fatty acids, possesses an acyl-ACP desaturase with higher specificity towards palmitoyl-ACP [13], supporting a high *de novo* synthesis of palmitoleic acid that is exported out of the plastids and later incorporated into glycerolipids. Regarding macadamia nuts, no diverged desaturases have been described to date. Thus, a previous

study reported by [14], pointed that extracts from developing macadamia nuts displayed higher desaturase activity towards palmitoyl-ACP than other seeds that did not contain such high levels of n-7 fatty acids, but still stearoyl-ACP desaturase was the highest activity found. However, the desaturase cloned from that species did not show unusual substrate specificity. Furthermore, the sunflower (*Helianthus annuus)* mutant CAS-37 has been reported to accumulate n-7 fatty acids in seeds at similar levels to those found in macadamia nuts [12, 15]. As stated above, biochemical characterization of this mutant did not show altered substrate specificity in endogenous acyl-ACP desaturase activity, but the high n-7 phenotype was due to reduced activity of the FAS II complex, which is the responsible for most palmitoyl-ACP elongation [16]. Theoretically, to accumulate palmitoleic acid it is necessary to have high levels of intraplastidial palmitoyl-ACP and/or desaturation of it, together with a relatively high acyl-ACP thioesterase activity towards palmitoleoyl-ACP, making possible the export of palmitoleic acid out of the plastids for its incorporation into glycerolipids. In so doing, we hypothesize in this work that acyl-ACP thioesterases are in part responsible for the accumulation of n-7 fatty acids observed in macadamia nuts, both *FatA* and *FatB* thioesterase genes were cloned from *M. tetraphylla* and heterologously expressed in *E. coli*. The corresponding enzymes, purified by affinity chromatography, were kinetically characterized and assayed for a variety of substrates. Their role on the accumulation of n-7 fatty acids that takes place in the kernel was discussed. Moreover, acyl-ACP thioesterase activity was measured and characterized in crude extracts of two cultivars of macadamia, Cate and Beaumont. The possible involvement of acyl-ACP thioesterase activity in the accumulation of n-7 fatty acids in these two cultivars was discussed.

2. Results

2.1. Oil content and fatty acid composition of two macadamia cultivars.

Macadamia nuts of two different cultivars, Cate and Beaumont, displayed similar oil content ranging over 50% of the kernel dry weight (Table 1), but different fatty acid composition, the Cate variety accumulated more n-7 fatty acids, with contents of palmitoleic and asclepic acids of 16.9% and 4.8%, respectively, which contrasted with the 9.8 and 3.7% that are found in the Beaumont cultivar. The increment of the n-7

fatty acids in the Cate cultivar takes place at the expense of oleic (18:1), arachidic (20:0), behenic (22:0) and eicosenoic (20:1) acids.

Table 1. Fatty acid composition of two different varieties of macadamia kernels, Cate and Beaumont. Data are the average of three independent samples. SD <5% of mean value. [a] Sum of 16:1 and 18:1A n-7 fatty acids. 14:0, myristic acid; 16:0, palmitic acid; 16:1, palmitoleic acid; 18:0, stearic acid; 18:1, oleic acid; 18:1A, asclepic acid; 18:2, linoleic acid; 20:0, behenic acid; 22:0, arachidic acid; 22:1, erucic acid.

Fatty acids (mol %)												
Variety	**14:0**	**16:0**	**16:1**	**18:0**	**18:1**	**18:1A**	**18:2**	**20:0**	**22:0**	**20:1**	**∑n-7[a]**	**% Fat**
Cate	0.5	10.2	16.9	4.5	56.3	4.8	1.9	2.8	0.6	1.5	21.7	50.9
Beaumont	0.4	9.5	9.8	4.5	62.6	3.7	1.8	4.0	1.0	2.7	13.7	49.4

2.2. Acyl-ACP thioesterase activity in macadamia kernels.

To check if the variability in the n-7 fatty acid content in the kernels is caused by different acyl-ACP hydrolyzing activities, acyl-ACP thioesterase activity was measured in crude extracts of the two cultivars investigated in this work. Furthermore, activity was assayed with acyl-ACP substrates including saturated, palmitoyl- and stearoyl-ACP, and Δ9 unsaturated acyl moieties, palmitoleoyl- and oleoyl-ACP. The observed total thioesterase activity levels were different in both kernels, so the relative activities towards different substrates were compared. Substrate specificity found in the kernels of both cultivars was quite similar (Fig. 1). The substrate hydrolyzed at a higher rate was oleoyl-ACP followed of palmitoleoyl-ACP and the saturated derivatives. In this regard, slightly higher specificity of the Cate cultivar to hydrolyze acyl-ACP substrates different from 18:1-ACP was observed.

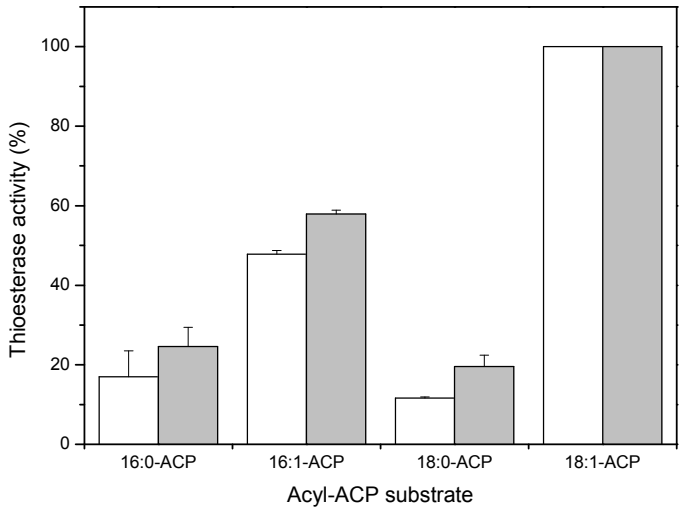

Fig. 1. Thioesterase activity measured in macadamia kernels of var. Beaumont (open bars) or var. Cate (grey bars). Percent of activity respect to oleoyl-ACP as substrate. Error bars represent the standard deviation of the data obtained from three independent experiments.

2.3. MtFatA and MtFatB sequences from M. tetraphylla.

To confirm the substrate specificity of the thioesterase activity found in kernels, specifically from Cate variety, conserved regions from known plant thioesterase amino acid sequences were used to design degenerated primer pairs, FatA1 and FatAB for FatA and MtFatB-F1 and MtFatB-R1 for FatB (Table 2). Using these primer pairs and cDNA from developing *M. tetraphylla* kernels, two fragments of 460 and 522 bp, respectively, were amplified. Subsequently, full-length *MtFatA* and *MtFatB* cDNA clones of 1146 bp (GenBank accession number EU383030) and 1251 bp (GenBank accession number FJ936170), respectively, were obtained by RACE using specific primers (Table 2). The full-length cDNA clones revealed ORFs that generate predicted preproteins of 381 and 416 amino acids (Fig. 2), with calculated molecular mass of 46.2 kDa and pI of 7.1 for *Mt*FatA and 45.9 kDa and pI of 6.2 for *Mt*FatB.

Table 2. Degenerated and non-degenerated oligonucleotides used in this work. [a] Restriction sites introduced are underlined. H: A or C or T; K: G or T; N: A or C or G or T; R: A or G; and Y: C or T.

Primer name	Sequence 5'-3'
FatA1	GARATHTAYARRTAYCCNGC
FatAB	CAYTCNCKNCKRTANTC
MtFatB-F1	ATYMGRTCHTAYGARATWGG
MtFatB-R1	TNACRTGYTGRTTRAYRTC
MtFatA-1f	GGGAGAGCCACCAGCAAATG
MtFatA-2f	GAGCTTGCCTCAGGAAATTATTG
MtFatA-3r	CTCAAGAAGCCATCCAATGTAGG
MtFatA-4r	CGTCTGGTCCCAACTCGTCC
F1MtFatB	CCATGTTAGAAGTGCGGGG
F2MtFatB	TTAGAGGGGAAATAGAACC
R4MtFatB	TTGACATCCAAATCATTCCACCGAGG
R5MtFatB	GAGTTTCACCAGTCTTGGAGTCACG
MtFatA-SacIb[a]	GCCGAGCTCGTATCGGAACGGACGAATGG
MtFatA-KpnI	GGCGGTACCCTATCTCGTTGATTTTCTTCTCC
MtFatB_PEP_F	ATCGAGCTCAGGCGCCCTGACATGCTTGTTG
MtFatB_ORF_R	GATGGTACCTTACGCAGCCTCTGCTGG

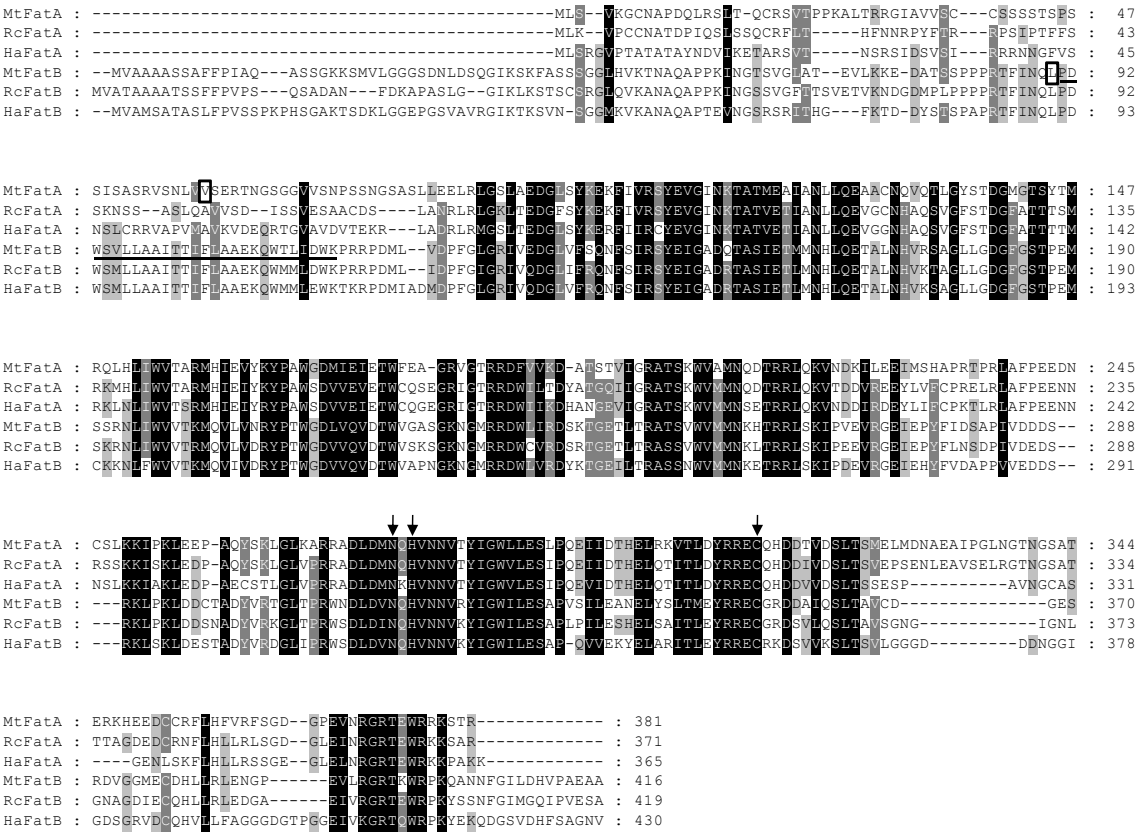

Fig. 2. Alignment of deduced amino acids sequences of *M. tetraphylla* (*Mt*FatA, GenBank accession number ACB29661; *Mt*FatB, GenBank accession number ADA79524), *R. communis* (*Rc*FatA, GenBank accession number ABS30422; *Rc*FatB, GenBank accession number ABV54795) and *H. annuus* (*Ha*FatA, GenBank accession number AAL79361; *Ha*FatB, GenBank accession number AAX19377) thioesterases shown as representatives of FatA and FatB proteins. Identical amino acids are shaded in black, whereas conserved residues are shaded in grey. The amino acids considered to be the start of the mature proteins are boxed and the hydrophobic region in FatB is underlined. The three conserved residues that constitute the catalytic triad are indicated by arrows.

2.4. Purification and characterization of macadamia FatA and FatB

Both *Mt*FatA and *Mt*FatB were expressed at high level in *E. coli* using the constructs described in the experimental section. These enzymes were endowed with a 6x-His tag at the N-terminus allowing their purification by immobilized metal ion affinity chromatography (IMAC) to homogeneity from the soluble protein preparations of cells harboring pQE*Mt*FatA and pQE*Mt*FatB (Fig. 3).

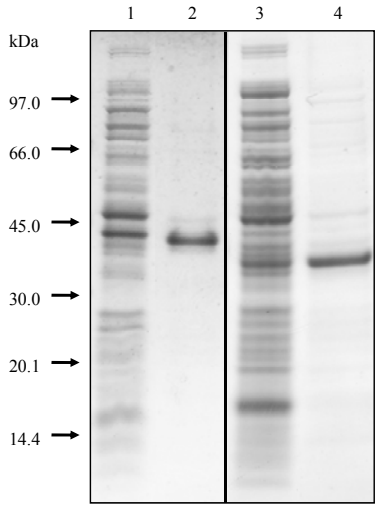

Fig. 3. Comassie blue stained SDS-PAGE showing recombinant castor acyl-ACP thioesterases. Lane 1, soluble fraction of pQE*Mt*FatA lysate; lane 2, purified His-tagged *Mt*FatA protein; lane 3, soluble fraction of pQE*Mt*FatB lysate; lane 4, purified His-tagged *Mt*FatB protein. The position of molecular weight (kDa) markers is shown on the left.

Substrate specificities of purified enzymes were determined using the palmitoleoyl-, oleoyl- and saturated acyl-ACP derivatives (Fig. 4). Purified *Mt*FatA displayed a higher activity towards 18:1-ACP than to16:1-ACP. The purified *Mt*FatB showed lower specific activity levels but higher specificity towards 16:0-ACP comparing to *Mt*FatA.

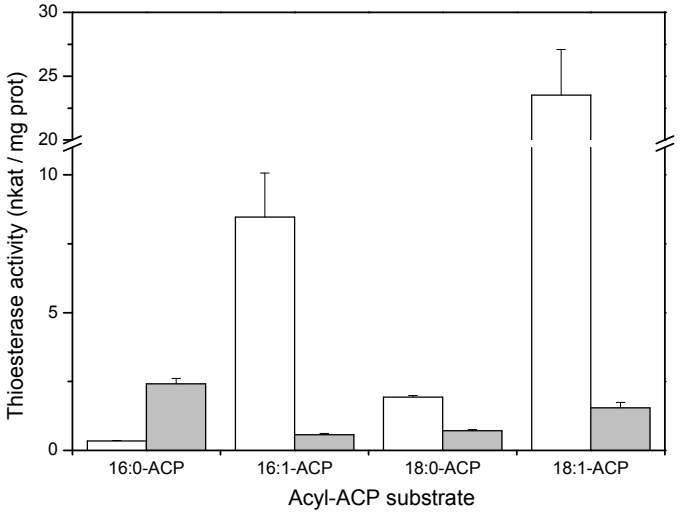

Fig. 4. Substrate specificity of macadamia acyl-ACP thioesterases expressed in *E. coli*. The activity was measured with purified His-tagged *Mt*FatA (open bars) and His-tagged *Mt*FatB (grey bars) proteins, testing different acyl-ACP substrates. Data represent the mean (±SD) from three independent experiments.

Moreover these enzymes were kinetically characterized for the same substrates (Table 3). The $K_m$values of *Mt*FatA were submicromolar for all the substrates out of 18:0-ACP. This enzyme displayed not only a remarkable high affinity towards 18:1-ACP, with a K_m value of 0.08 µM, but also the maximum V_{max} and catalytic efficiency (k_{cat}/K_m) were towards 18:1-ACP. It also exhibited a relatively high catalytic efficiency for the hydrolysis of 16:1-ACP with respect to saturated substrates. On the other hand, the enzyme *Mt*FatB displayed K_m values in the µM order. There were no important differences in affinity for the substrates assayed, although the maximum catalytic efficiency was recorded towards 16:0-ACP.

Table 3. Kinetic parameters of purified recombinant *Mt*FatA and *Mt*FatB proteins on different acyl-ACP substrates.

	Substrate	K_m	V_{max}	k_{cat}	k_{cat}/K_m
		(µM)	**(nkat/mg protein)**	**(s^{-1})**	**(s^{-1} $µM^{-1}$)**
***Mt*FatA**	16:0-ACP	0.96	0.71	0.03	0.03
	16:1-ACP	0.35	12.40	0.45	1.30
	18:0-ACP	9.54	24.09	0.88	0.09
	18:1-ACP	0.08	26.81	0.98	12.91
***Mt*FatB**	16:0-ACP	3.60	12.96	0.44	0.12
	16:1-ACP	5.51	4.36	0.15	0.03
	18:0-ACP	5.63	5.40	0.18	0.03
	18:1-ACP	2.97	7.29	0.25	0.08

3. Discussion

Macadamia nuts are a good source of oil rich in monounsaturated fatty acids (Table 1). Unlike other species of oils, macadamia showed important differences in the oil composition found in different cultivars (Table 1). Interestingly, this variability, regarding the unusual n-7 fatty acids in the cultivars studied in this work, pointed out that there were important differences in the activity or the expression of the enzymes

responsible for that phenotype. At this point, it is important to notice the changes in other fatty acids of the oil because these will provide important information about the enzymatic steps involved in n-7 fatty acid accumulation. The differences in n-7 fatty acids between both cultivars took place at the expense of oleic and longer fatty acids. This means that the variations between the fatty acid compositions of Cate and Beaumont cultivars should be due to differences on the activity of 16:0-ACP elongation catalyzed by the FAS II complex, on the activity in the acyl-ACP desaturase or in the export of 16:1 from plastids catalyzed by acyl-ACP thioesterases [12]. In this regard, a possible role of acyl-ACP thioesterases on the distinct macadamia phenotypes reported in this work was also investigated. We attended more to the substrate specificity than to the absolute thioesterase activity level to compare both cultivars, because the latter could be influence by differences in the developing stage that we harvested the nuts. Results in Fig. 1 depicted a typical activity profile obtained from FatA thioesterase, with the highest level of activity towards 18:1-ACP. Interestingly, the activity level towards 16:1-ACP was remarkably high in both cultivars, indicating that macadamia thioesterases can support a high rate of synthesis of palmitoleic acid by breaking the ACP derivatives and releasing these acyl moieties to be exported to the cytosol. However, the differences on substrate specificity between both cultivars were low and did not justify the differences in the content of n-7 fatty acids reported in Table 1. These results seemed to indicate that an acyl-ACP thioesterase with high specificity towards 16:1-ACP is a condition necessary but not sufficient to produce oils with a high content of palmitoleic acid.

Using the available sequences for acyl-ACP thioesterases we were able to obtain the genes responsible for this activity from Cate variety nuts, *MtFatA* and *MtFatB*. The three proposed residues involved in the active-site [17, 18] were conserved in both proteins (Fig. 2). A signal peptide for targeting the proteins to the plastid/chloroplast was also identified, using a protein subcellular localization prediction software, WolF PSORT [19] in the case of *Mt*FatA and a comparison between FatB sequences in the case of *Mt*FatB. The putative N-terminus of the mature thioesterase proteins would be V59 for *Mt*FatA and L90 for *Mt*FatB (Fig. 2), generating proteins 323 and 327 amino acid residues, respectively. The signal peptide in *Mt*FatB is followed by a hydrophobic domain extending from residue L90 to K116, probably involved in the anchorage to the membrane but not related to activity or affinity for different substrates [6, 20, 21]. *MtFatA* ORF from Beaumont variety was also cloned (data not shown) and no

differences between *FatA* genes from the two cultivars was found, indicating that the variability in the accumulation of n-7 fatty acids was not due to different substrate specificity of FatA enzyme. Alignment of the two deduced amino acid sequences (Fig. 2) showed that *Mt*FatA and *Mt*FatB shared 36% identity and 48% similarity. Both *Mt*FatA and *Mt*FatB showed high identity with thioesterases from sunflower (62% and 63% respectively) and castor (68% and 65% respectively), pointing that thioesterases are conserved proteins in plants.

The thioesterases cloned from macadamia kernels were expressed in *E. coli* using the pQE-80L vector, which provide high levels of expression. Both enzymes accumulated in the soluble fraction, which allowed their purification to homogeneity (Fig. 3). The removal of the membrane domain in the N-terminal region in *Mt*FatB facilitated its purification, otherwise the enzyme would have been targeted to the membrane fraction making difficult its purification and assay. Special attention was paid to the purified enzyme substrate specificity (Fig. 4). *Mt*FatA displayed the typical FatA-type thioesterase specificity profile with the maximum activity towards 18:1-ACP. Furthermore, this form of FatA exhibited very high activity towards 16:1-ACP, which was in good agreement with the fatty acid composition found in macadamia kernels (Table 1) and the substrate specificity of the crude extracts (Fig. 1). This form of FatA displayed specifically the highest specificity towards 16:1-ACP measured from the enzymes purified and characterized to date, including species like sunflower [8], castor [21], *Arabidopsis thaliana* or *Coriandrum sativum* [22] and really supports a role of this enzyme on the high content of n-7 fatty acids found in macadamia kernels. On the contrary, *Mt*FatB displayed much less specific activity than *Mt*FatA (Fig. 4) and showed high substrate specificity towards saturated acyl-ACPs as it was found for the FatB-type thioesterase enzymes in other species [23, 24, 6]. More complete information can be retrieved from the kinetic parameters in Table 3. In the case of *Mt*FatA the maximum V_{max} were found towards 18:1-ACP and 18:0-ACP, with lower values for 16:1-ACP and 16:0-ACP. The K_m values for *Mt*FatA were under the micromolar range out of that from 18:0-ACP, which almost reaches a value of 10μM. Thus, the highest catalytic efficiencies were for 18:1-ACP and 16:1-ACP. The k_{cat} of this enzyme for 18:1-ACP ranged to 1 s^{-1}, a similar value than k_{cat} of Arabidopsis FatA [22] and one magnitude order lower than k_{cat} calculated for sunflower FatA [8]. Moreover, *Mt*FatB displayed lower affinity for their acyl-ACP substrates, which were all in the micromolar range. The highest V_{max} values corresponded to 16:0-ACP and 18:1-ACP. The catalytic

efficiencies and k_{cat}s of FatB for the different substrates were in general below than those found for FatA, which indicates that this enzyme has probably a more secondary implication than FatA on the accumulation of lipids in macadamia kernels.

4. Materials and methods

4.1. Biological material and growth conditions

Macadamia nuts from the Experimental Station La Mayora (CSIC, Málaga, Spain) were collected from two different varieties, Cate (*M. tetraphylla*) and Beaumont (*M. integrifolia/M. tetraphylla* hybrid), frozen in liquid nitrogen and stored at -80ºC until use. Nuts were collected at a stage of high rate of lipid synthesis, before they started to dry out, nuts were dehusked and kernel used for experiments. The *E. coli* strain XL1-Blue (Stratagene) was used as host for the expression of *Mt*FatA and *Mt*FatB. The bacteria were grown in LB medium (1% tryptone, 0.5% yeast extract, 1% NaCl, pH 7) and the liquid cultures were shaken vigorously at 37 ºC. For plasmid selection 100 μg/ml of ampicillin were added.

4.2. mRNA preparation and cDNA synthesis

Approximately 0.25 g of developing macadamia kernels were ground in liquid nitrogen using a precooled sterile mortar and pestle. Total RNA was isolated using the Spectrum Plant Total RNA Kit (Sigma). Subsequently, mRNA was isolated from the total RNA using a GenElute mRNA Miniprep Kit (Sigma). The mRNA pellet was resuspended in 33 μl RNAase-free TE buffer (10 mM Tris-HCl, 1 mM EDTA, pH 8) and cDNA was synthesized using a Ready-To-Go T-Primed First-Strand Kit (Amersham Bioscience).

4.3. Cloning of genes coding for macadamia thioesterases

FatA and FatB protein sequences from public databases were aligned to identify regions of homology using the ClustalX v1.8 program [25]. Using cDNA from developing macadamia kernels as template, two different PCR fragments, were

amplified with degenerate primers designed from highly conserved regions of FatA (FatA1 and FatAB, see Table 2), and FatB (MtFatB-F1 and MtFatB-R1, see Table 2), respectively. Subsequently, 5'- and 3'-ends of the corresponding cDNAs were obtained using the SMART-RACE cDNA Amplification Kit (Clontech) and specific primers MtFatA-1f, MtFatA-2f, MtFatA-3r and MtFatA-4r for *MtFatA* and F1MtFatB, F2MtFatB, R4MtFatB and R5MtFatB for *MtFatB* (Table 2). The PCR fragments were cloned into the pMBL-T vector (Dominion MBL), sequenced, and their identities were confirmed using the BLAST software [26].

Primers with internal *Sac*I and *Kpn*I restriction sites for *MtFatA* (MtFatA-SacIb and MtFatA-KpnI) and *MtFatB* (MtFatB_PEP_F and MtFatB_ORF_R) were designed to amplify the coding regions of the mature proteins by PCR (Table 2). The PCR products obtained for *MtFatA* and *MtFatB* were subcloned into the *Sac*I-*Kpn*I sites of the pQE-80L expression vector (Quiagen) to produce the corresponding fusion proteins with a 6xHis tag at the N-terminus. Ligations into the correct open reading frames (ORFs) were confirmed by sequencing and the resulting constructs were designated pQE*Mt*FatA and pQE*Mt*FatB, respectively. XL1-Blue cells containing the plasmid pQE-80L were used as a control. All primers were synthesized by Eurofins MWG Operon (Germany).

4.4. Protein expression and purification

Five hundred milliliter cultures of *E. coli* XL1-Blue cells harboring pQE*Mt*FatA or pQE*Mt*FatB were grown as described above. Expression of *Mt*FatA or *Mt*FatB was induced at OD_{600} 0.6 by adding 1 mM IPTG and growth continued for 4 h. The cells were harvested by centrifugation for 10 min at 2500*g*, washed with distilled water and resuspended in 5 ml of Binding buffer (20 mM sodium phosphate, 500 mM NaCl, 20 mM imidazole, pH 7.4). Cells were lysed adding 0.5% Triton X-100, 5 mM DTT, 1 mM $MgCl_2$, 1 mM PMSF, 20 µg/ml DNase I (Roche) and 0.2 mg/ml lysozyme (Roche) for 45 min at 4 ºC with shaking. The resulting lysed cell suspension was centrifuged at 25000*g* for 30 min. The supernatant was filtered through 0.22 µm filters and loaded onto a His SpinTrap column (GE Healthcare). Histidine-tagged proteins were eluted from the column using a 500mM imidazole solution. Fractions containing *Mt*FatA or *Mt*FatB were subsequently used for thioesterase activity assays.

4.5. Gel electrophoresis of proteins

Protein samples were combined with SDS-PAGE loading buffer and heated at 95 ºC for 5 min. The samples were separated by electrophoresis on 4–12% NuPAGE Novex Bis-Tris gels (Invitrogen) in MES buffer, and the gels were fixed and stained with 0.1% Coomassie R-250 in 40% ethanol, 10% acetic acid. Molecular weight standards used were obtained from GE Healthcare.

4.6. Preparation of acyl-ACP substrates

Labeled acyl-ACP substrates were prepared using a recombinant acyl-ACP synthetase from *E. coli*. Acylation reactions contained 50 µg of recombinant ACP form *E. coli* (Sigma), 180 kBq (approx. 0.1 µmol) of [1-^{14}C] fatty acid ammonium salt ([^{3}H] fatty acid in the case of 16:1$^{\Delta 9}$), 5 mM ATP, 2 mM DTT, 400 mM $LiCl_2$, 10 mM $MgCl_2$, 100 mM Tris-HCl pH 8.0 and 10 µg acyl-ACP synthetase, in a final volume of 0.5 ml. Reactions were carried out at room temperature for 3 h and the acyl-ACPs were purified and concentrated by ion exchange chromatography on DEAE-sepharose as described by [27].

4.7. Acyl-ACP thioesterase assays

Macadamia kernels were ground in extraction buffer containing 50 mM Tris-HCl pH 8.0 and 5 mM DTT, 1 g of tissue per 10 ml of buffer [28]. The protein concentration in the crude extracts was measured using the Bio-Rad Protein Assay (Hercules, CA, USA) according to the manufacturer's instructions and using BSA as standard.

Thioesterase activity was assayed in 0.1 ml reactions containing 50 mM Tris-HCl pH 8.0, 5 mM DTT, 0.2-12 µg of the protein preparation (crude extracts from kernels or purified *Mt*FatA or *Mt*FatB expressed in *E. coli*) and the amount of acyl-ACP substrate ranging from 0.02 to 0.08 nmol (30-170 Bq approx.). Reactions were carried out at room temperature for 5 min and stopped by the addition of 0.25 ml of 1 M acetic acid in 2-propanol. Unesterified fatty acids were then extracted twice with 0.3 ml hexane, and the radioactivity in the pooled organic phase was determined in a calibrated liquid scintillation counter (Rackbeta II; LKB). The data from thioesterase assays was

fitted to the Hill equation by nonlinear least-squares regression analysis using OriginPro 8 software, and correlated at $P<0.005$ as determined by Student's *t*-test. Both the V_{max} and K_m were derived from these curves.

4.8. Oil content and fatty acid analysis

Kernels were dried and then ground in a glass tube with sand and the total lipids were extracted with hexane:2-propanol [29]. To quantify the total oil content, the lipids were weighed after the extraction and referred to dry weight. Fatty acid methyl esters were obtained by heating the samples at 80 ºC in 1.8 ml of methanol/toluene/dimethoxipropane/sulphuric acid (33:14:2:1) for 1.5 h. After cooling, 1 ml heptane and 1 ml water were added and mixed. The fatty acid methyl esters were recovered from the upper phase and transferred to a fresh tube. The methyl esters were analyzed by GLC using a Hewlett-Packard 6890 gas chromatograph (Palo Alto, CA, USA). The column was a Supelco SP-2380 fused-silica capillary column (30 m length, 0.25 mm i.d., 0.20 µm film thickness; Supelco, Bellefonte, PA, USA). Hydrogen was used as the carrier gas at 28 cm/s, the temperature of flame ionization detector and injector was 200 ºC, the oven temperature was 170 ºC and the split ratio was 1:50. The different methyl esters were identified by comparison with a combination of standards.

Acknowledgements

We are thankful to Arantxa González and Barbara López for their technical assistance. This work was supported by the MICINN and FEDER (Project AGL2008-01086/ALI).

References

[1] C.G. Cavaletto, Macadamia nuts, in: H.T. Chan Jr. (Ed.), Handbook of Tropical Foods, Marcel Dekker Inc., New York, 1983, pp. 361-396.

[2] L.S. Maguire, S.M. O'Sullivan, K. Galvin, T.P. O'Connor, N.M. O'Brien, Fatty acid profile, tocopherol, squalene and phytosterol content of walnuts, almonds,

peanuts, hazelnuts and the macadamia nut, Int. J. Food Sci. Nutr. 55 (2004) 171-178.

[3] R. Garcés, E. Martínez-Force, J.J. Salas, Vegetable oil basestocks for lubricants, Grasas y aceites (2010) in press.

[4] J. Shanklin, E.B. Cahoon, Desaturation and related modifications of fatty acids, Annu. Rev. Plant Physiol. Plant Mol. Biol. 49 (1998) 611-641.

[5] T.A. Voelker, Plant acyl-ACP thioesterases: chain-length determining enzymes in plant fatty acid biosynthesis, Genet. Eng. 18 (1996) 111-133.

[6] A. Jones, H.M. Davies, T.A.Voelker, Palmitoyl-acyl carrier protein (ACP) thioesterase and the evolutionary origin of plant acyl-ACP thioesterases, Plant Cell. 7 (1995) 359-371.

[7] K.M. Mayer, J. Shanklin, A structural model of the plant acyl-acyl carrier protein thioesterase FatB comprises two helix/4-stranded sheet domains, the N-terminal domain containing residues that affect specificity and the C-terminal domain containing catalytic residues, J. Biol. Chem. 280 (2005) 3621–3627.

[8] M.J. Serrano-Vega, R. Garcés, E. Martínez-Force, Cloning, characterization and structural model of a FatA-type thioesterase from sunflower seeds (Helianthus annuus L.), Planta 221 (2005) 868-880.

[9] E.B. Cahoon, A.M. Cranmer, J. Shanklin, J.B. Ohlrogge, Δ^6 Hexadecenoic acid is synthesized by the activity of a soluble Δ^6 palmitoyl-acyl carrier protein desaturase in Thunbergia alata endosperm, J. Biol. Chem. 269 (1994) 27519-27526.

[10] E.B. Cahoon, J.B. Ohlrogge, Metabolic evidence for the involvement of a Δ^4-palmitoyl-acyl carrier protein desaturase in petroselinic acid synthesis in coriander endosperm and transgenic tobacco cells, Plant Physiol. 104 (1994) 827-837.

[11] E.B. Cahoon, S.J. Coughlan, J. Shanklin, Characterization of a structurally and functionally diverged acyl-acyl carrier protein desaturase from milkweed seed, Plant Mol. Biol. 33 (1997) 1105-1110.

[12] J.J. Salas, E. Martínez-Force, R. Garcés, Biochemical characterization of a high-palmitoleic acid Helianthus annuus mutant, Plant Physiol. Biochem. 42 (2004) 373-381.

[13] E.B. Cahoon, S. Shah, J. Shanklin, J. Browse, A determinant of substrate specificity predicted from the acyl–acyl carrier protein desaturase of developing cat's claw seed, Plant Physiol. 117 (1998) 593-598.

[14] P.O. Gummeson, M. Lenman, M. Lee, S. Singh, S. Stymne, Characterisation of acyl-ACP desaturases from Macadamia integrifolia Maiden & Betche and Nerium oleander L., Plant Sci. 154 (2000) 53-60.

[15] J.J. Salas, A.J. Moreno-Pérez, E. Martínez-Force, R. Garcés, Characterization of the glycerolipid composition of a high-palmitoleic acid sunflower mutant, Eur. J. Lipid Sci. Technol. 109 (2007) 591-599.

[16] J. Ohlrogge, J. Browse, Lipid biosynthesis, Plant Cell 7 (1995) 957-970.

[17] L. Yuan, B.A. Nelson, G. Caryl, The catalytic cysteine and histidine in the plant acyl-acyl carrier protein thioesterases, J. Biol. Chem. 271 (1996) 3417-3419.

[18] K.M. Mayer, J. Shanklin, Identification of amino acid residues involved in substrate specificity of plant acyl-ACP thioesterases using a bioinformatics-guided approach, BMC Plant Biol. 7 (2007) 1.

[19] P. Horton, K.J. Park, T. Obayashi, N. Fujita, H. Harada, C.J. Adams-Collier, K. Nakai, WoLF PSORT: protein localization predictor, Nucleic Acids Res. 35 (2007) W585-W587.

[20] M.T. Facciotti, L. Yuan, Molecular dissection of the plant acyl–acyl carrier protein thioesterases, Fett Lipid 100 (1998) 167-172.

[21] A. Sánchez-García, A.J.; Moreno-Pérez, A.M. Muro-Pastor, J.J. Salas, R. Garcés, E. Martínez-Force, Acyl-ACP thioesterases from castor (Ricinus communis L.): an enzymatic system appropriate for high rates of oil synthesis and accumulation, Phytochemistry 71 (2010) 860-869.

[22] J.J. Salas, J.B. Ohlrogge, Characterization of substrate specificity of plant FatA and FatB acyl-ACP thioesterases, Arch. Biochem. Biophys. 403 (2002) 25-34.

[23] P. Dörmann, T.A. Voelker, J.B. Ohlrogge, Accumulation of Palmitate in Arabidopsis Mediated by the Acyl-Acyl Carrier Protein Thioesterase FATB1, Plant Physiol. 123 (2000) 637-644.

[24] T.T. Huynh, R.M. Pirtle, K.D. Chapman, Expression of a Gossypium hirsutum cDNA encoding a FatB palmitoyl-acyl carrier protein thioesterase in Escherichia coli, Plant Physiol. Biochem. 40 (2002) 1-9.

[25] J.D. Thompson, T.J. Gibson, F. Plewniak, F. Jeanmougin, D.G. Higgins, The CLUSTAL_X windows interface: flexible strategies for multiple sequence

alignment aided by quality analysis tools, Nucleic Acids Res. 25 (1997), 4876-4882.

[26] S.F. Altschul, W. Gish, W. Miller, E.W. Myers, D.J. Lipman, Basic local alignment search tool, J. Mol. Biol. 215 (1990) 403-410.

[27] C.O. Rock, J.L. Garwin, Preparative enzymatic synthesis and hydrophobic chromatography of acyl-acyl carrier protein, J. Biol. Chem. 254 (1979) 7123-7128.

[28] E. Martínez-Force, S. Cantisán, M.J. Serrano-Vega, R. Garcés, Acyl-acyl carrier protein thioesterase activity from sunflower (Helianthus annuus L.) seeds, Planta, 211 (2000) 673-678.

[29] A. Hara, N.S. Radin, Lipid extraction of tissues with a low-toxicity solvent, Anal. Biochem. 90 (1978) 420-426.

Arabidopsis mutant showing a reduction in expression levels of both FatA thioesterase genes produces low-oil seeds and fatty acid composition similar to *wri1* mutant.

Moreno-Pérez, A.J.[a], Venegas-Calerón, M.[a], Vaistij, F.E.[b], Salas, J.J.[a], Larson, T.R.[b], Garcés, R.[a], Graham, I.A. [b], Martínez-Force, E.[a]

[a]Instituto de la Grasa, CSIC, Av. Padre García Tejero, 4, 41012, Seville, Spain.
[b]Centre for Novel Agricultural Products, Department of Biology, University of York, PO Box 373, York YO10 5YW, UK.

Manuscript in preparation

Abstract

Acyl-acyl carrier protein (ACP) thioesterases are enzymes specific of plants that have the important role of terminate the intraplastidial fatty acid synthesis by hydrolyzing the acyl-ACP complexes that are intermediate metabolites in the fatty acid condensation and desaturation reactions. Amongst different thioesterases gene families found in plants the *FatA*-type plays a principal role in the export of the C18 fatty acid moieties that will be used for the synthesis of most of plant glycerolipids. The present work is aimed to further investigate the role of *FatA* thioesterase in plant metabolism and especially in the oil accumulation in oil seeds. Thus, a reverse genomic approach was considered and different mutant collections were screened for *FatA* knockouts of *Arabidopsis thaliana*. Two mutants, with T-DNA insertions in the promoter region of each of the two copies of *FatA* present in Arabidopsis genome, were identified, from which a double *FatA* Arabidopsis mutant was raised. This double mutant (*fata1/fata2)* displayed reduced expression of both forms of *FatA* thioesterases and reduced FatA activity. This decrease did not cause any evident morphological changes in the mutant plants, but the partial reduction of this activity affected the oil content and fatty acid composition of the Arabidopsis seeds. Thus, mutant dry seeds displayed reduced contents of triacylglycerols, but not affected other neutral lipids like diacylglycerols. Furthermore, the amounts and composition of the different glycerolipids species of developing seeds at different stages of development were analyzed, which demonstrated a significant reduction of the metabolic flow into seed oil in the *fata1/fata2* line. The decrease of metabolic flow induced increases in the proportion of linolenic and erucic fatty acids in oil seed, which had been previously reported for the *wri1* Arabidopsis mutant deficient in oil accumulation. The similarities between these two mutants and the origin of their phenotype were discussed in function of the results.

1. Introduction

Plant *de novo* fatty acid synthesis is catalyzed by a fully dissociated type-2 fatty acids synthase (FAS) complex (Ohlrogge and Jaworski, 1997). This process is compartmented and it mostly takes place in the stroma of plastids or chloroplasts. Thus, this pathway consisted in sequential elongations of acyl intermediates esterified to the acidic protein called acyl carrier protein (ACP) by the action of the above mentioned FAS complex (Figure 1).

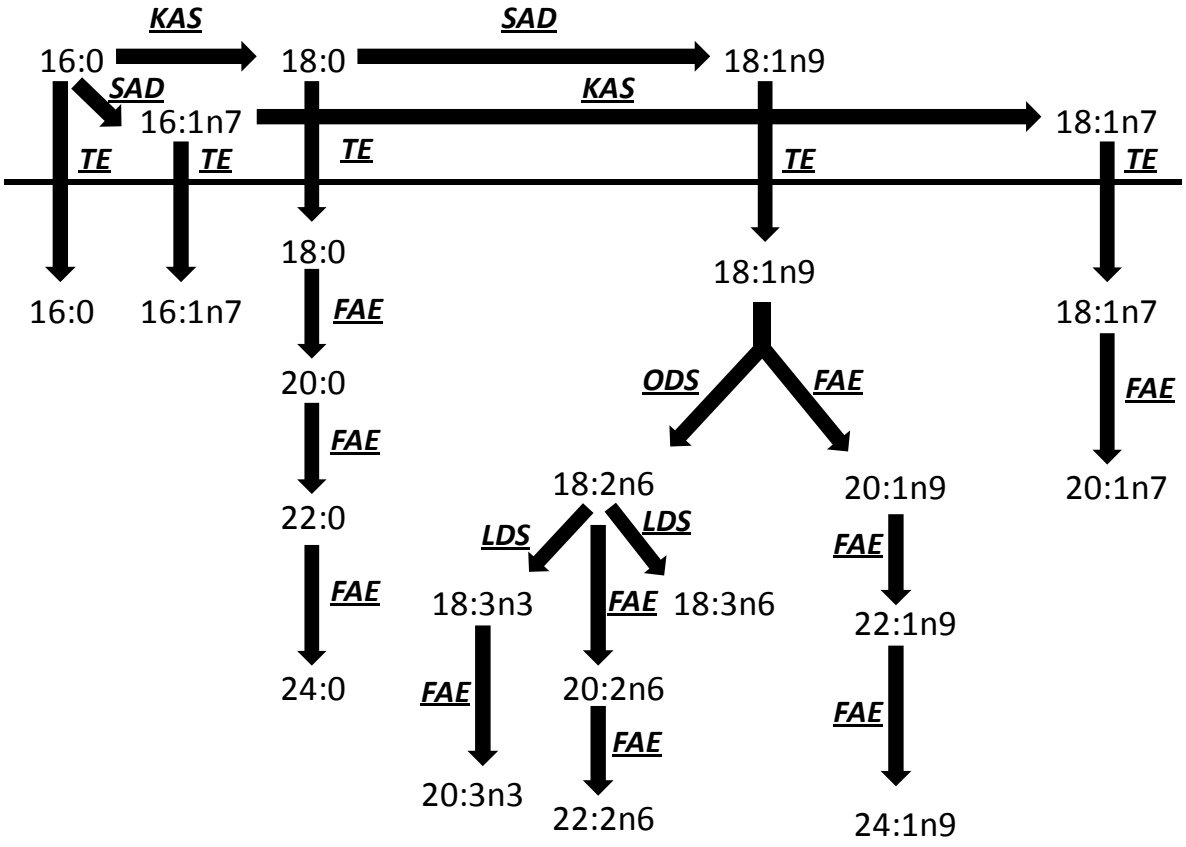

Figure 1. Fatty acid biosynthesis pathway. KAS: β-Ketoacyl-ACP synthase II; SAD: Stearoyl-ACP desaturase; TE: Acyl-ACP thioesterase; ODS: Oleate desaturase; LDS: Linoleate desaturase and FAE: Fatty acid elongase.

Inside the plastid, the newly synthesized acyl chains can be transferred to glycerol-3-P by a plastidial glycerol-3-P acyltransferase, feeding the prokaryotic pathway of lipid synthesis (Roughan and Slack, 1982). However, glycerolipids in most plant seeds are synthesized through eukaryotic pathway that takes place in the endoplasmic reticulum. This makes necessary a mechanism of export of the newly synthesized acyl moieties to the cytoplasm. This mechanism involves the hydrolysis of

the acyl-ACP complexes by the action of acyl-ACP thioesterases, to release free reduced ACP and free fatty acids (Browse and Somerville, 1991). Recent evidences indicated that free fatty acids are quickly transported to the cytosol in the form of acyl-CoAs by the action of an acyl-CoA synthetase located in the outer plastidial membrane (Koo et al., 2004). The model of export involving free fatty acid intermediates created certain controversy when it was hypothesized, and alternative models suggesting export via acyl-CoA or acyl-carnitine derivatives were proposed (Joyard and Stumpf, 1980; Thomas et al., 1983; McLaren et al., 1985). However, ^{18}O labeling experiments carried out by Pollard and Ohlrogge (1999) demonstrated that unesterified acyl moieties were released during the fatty acid biosynthesis in plants.

Acyl-ACP thioesterases are enzymes encoded by nuclear genes that are imported into the plastids via maturation by hydrolysis of an N-terminal transit peptide. These enzymes were classified in two gene families called *FatA* and *FatB* by Jones et al. (1995). The *FatA*-type thioesterases, also called oleoyl-thioesterases, are ubiquitous in plants, displaying high specificity for the substrate oleoyl-ACP (Hellyer et al., 1992; Dörmann et al., 1994; Salas and Ohlrogge, 2002; Sánchez-Garcia et al., 2010). These enzymes displayed a high degree of similarity between different plant species and there is a consensus about their role as the general housekeeping thioesterase responsible for the export of most C18 fatty acids from plastids. The other members of the family were thioesterases of the *FatB* type. This family exhibited higher variability and they can be classified in two subfamilies: *FatB*1 and *FatB*2. *FatB*1 thioesterases displayed high specificity towards palmitoyl-ACP and oleoyl-ACP and are widespread along the plant kingdom (Jones et al., 1995; Dörmann et al., 2000). In Arabidopsis, there is a single copy of the *FatB* gene. When it was knocked out the plant showed reduced amounts of saturated fatty acids in all tissues. On the basis of the composition of the different tissues it was concluded that one half of the flux of saturated fatty acids in this plant was exported via *FatB* (Bonaventure et al., 2003). Examining the lipid composition of all the tissues of this mutant it is difficult to find what causes the dwarf phenotype of the plant. In a later work this defective growth was attributed to a shortage of the supply of palmitoyl-CoA for sphingolipid synthesis (Chen et al., 2006). The enzymes classified in the other *FatB* subfamily, *FatB*2, are much less common. They are found in species accumulating high levels of short chained fatty acids in their seed oils and exposes high activity towards saturated C8 to C14 acyl-ACPs of saturated fatty acids (Dehesh et al., 1996; Voelker et al., 1997). The enzymes with an unusual specificity have been of

special importance in plant lipid biotechnology. Thus, when *Cuphea californica FatB*2 was expressed at high levels in rapeseed it was able to interrupt the pathway of fatty acid and induced the accumulation of medium chain fatty acids in this crop (Voelker et al., 1992).

Acyl-ACP thioesterases have not been crystallized yet. However, the structure of these enzymes have been modeled on the basis of their structural similarity towards *Escherichia coli* 4-hydroxybenzoyl-CoA thioesterase and so it was hypothesized that the active site of these enzymes displays a hot-dog fold pattern, with a catalytic triad of amino acids similar to that in papain (Mayer and Shanklin, 2005; Serrano-Vega et al., 2005).

Amongst all thioesterases, the *FatA* is probably essential for plant viability. Moreover, its role at diverging acyl chains to the extraplastidial glycerolipids synthesis makes them quite important at the time of determining the metabolic flux into triacylglycerols in oil seeds. *Arabidopsis thaliana* contain two copies of *FatA* in its genome (At3g25110 or *FatA1* and At4g13050 or *FatA2*). These forms of thioesterase display similar expression profile and seemed to be ubiquitously expressed in all tissues (Beisson et al., 2003). In the preset work the effect of a reduction of FatA activity in Arabidopsis was studied. Thus two lines with T-DNA insertions in the promoter regions of the two copies of *FatA* were identified and crossed to obtain a double mutant. This double mutant displayed changes in the amount and composition of the seed oil in a similar way as reported for the Arabidopsis *wri1* mutant (Focks and Benning, 1998). Arabidopsis *wri1* mutant exhibited a deficiency in glucose metabolism in seeds that produced a reduction of oil accumulation. The reasons for these similarities were discussed in this work in function of the data.

2. Results

2.1. Generation of the fata1/fata2 double mutant line. Phenotyping.

All available sequenced knockout libraries of Arabidopsis were screened for insertions in the loci At3g25110 (*FatA1*) and At4g13050 (*FatA2*), and mutants having T-DNA insertions in the 5´unstranlated regions were acquired from the European Arabidopsis Stock Center. The T-DNA insertions were located 100 bp upstream from the start of coding sequences (Figure 2) and the homozygous lines for the insertions

obtained. Both homozygous lines were crossed and the resulting offspring was screened for double mutants, which were identified by PCR techniques as described in the experimental section.

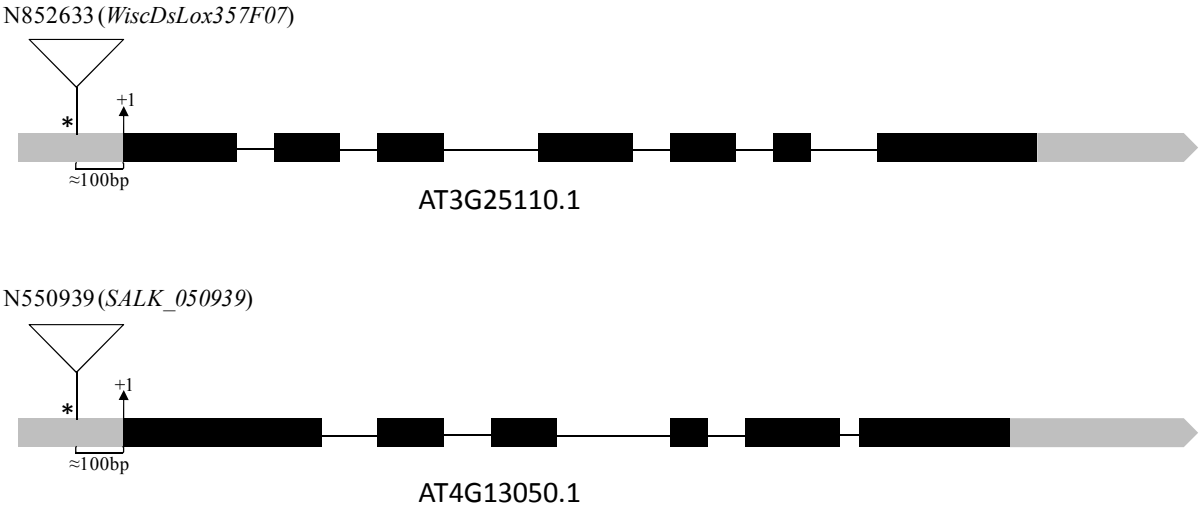

Figure 2. **Model of AT3G25110 and AT4G13050 loci.** In grey, untranslated regions (UTR); in black, coding sequence (CDS) where blocks mean exons and lines mean introns. The start codons are marked with +1 and the T-DNA insertions with *.

Double mutant line (*fata1/fata2*) was fixed in the third generation. *fata1/fata2* plants were grown in parallel with wild type (Col-0) plants and no significant differences were found between them (Figure 3, Table 1). Thus, both plants displayed equivalent number of rosette diameter and number of leaves at 3 weeks after sowing and no differences were found either in older plants.

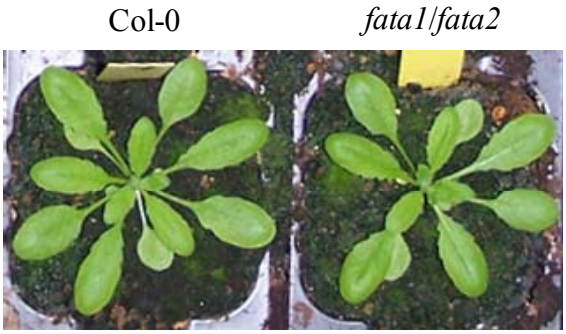

Figure 3. Col-0 and *fata1/fata2* plants. Photographs corresponding to 3 weeks old plants.

Table 1. **Phenotype data of Arabidopsis Col-0 and *fata1/fata2* plants.** Data are the average of 20 different plants.

	Wild type		Double mutant	
	Average	**SD**	**Average**	**SD**
Nº rosette leaves	11,1	2,2	10,9	2,2
Rosette diameter	4,2	1,9	4,1	2,3

2.2. Expression levels of FatA genes and acyl-ACP thioesterase activity.

The highest expression levels for *FatA1* and *FatA2* genes in Arabidopsis are reached in late torpedo to early walking stick embryos (Schmid et al., 2005). Siliques containing embryos at those stages of Col-0 and *fata1*/*fata2* lines were harvested and the mRNA was extracted. Subsequently the cDNA was synthesized and used in RT-quantitative PCR (RT-Q-PCR).

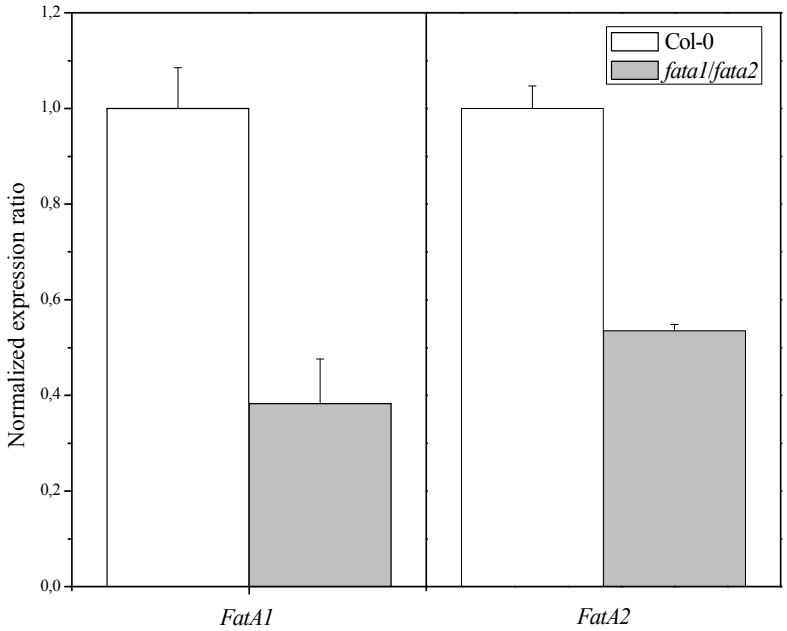

Figure 4. **Expression levels corresponding to the genes *FatA*1 (AT3G25110) and *FatA*2 (AT4G13050) from Col-0 and *fata1/fata2* plants.** Data corresponded to green developing siliques and showed the average and standard deviations of three independent determinations.

As Figure 4 shows, T-DNA insertions in the gene promoter regions in the double mutant reduced the expression levels of both genes about 50% respect to Col-0 line. This reduction in the number of transcripts of *FatA* genes induced an important decrease

in the acyl-ACP thioesterase activity measured in crude extracts from developing Siliques (Figure 5). Thus, the substrate 18:1-ACP was hydrolyzed in *fata1/fata2 mutant line* at a rate that was 40% of that found in Col-0. The decrease of activity was not significant in the case of the other assayed acyl-ACP species.

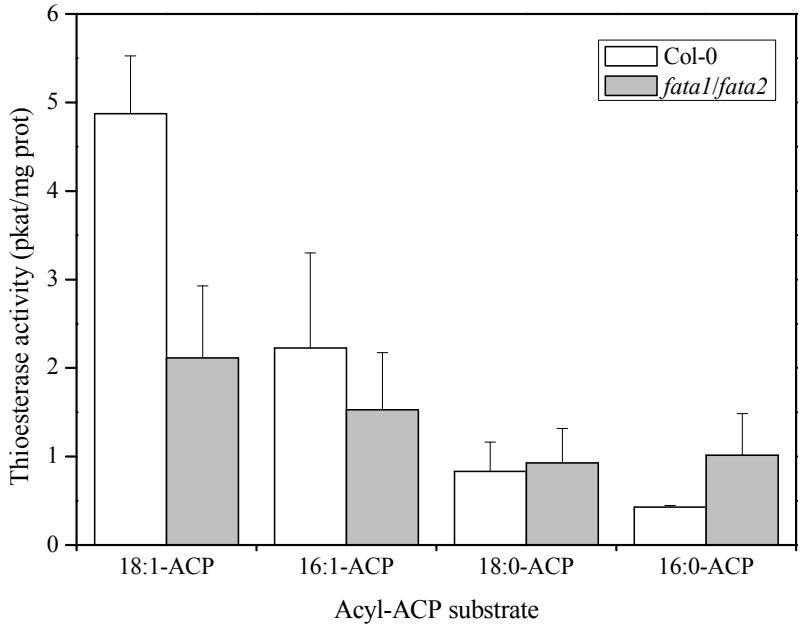

Figure 5. **Acyl-ACP thioesterase activity assays in crude silique extracts from Col-0 and *fata1/fata2* lines.** Green siliques containing developing seeds were used in this preps. Results are the average and standard deviation of three independent determinations.

2.3. Seed lipid content and composition

The content of storage lipids in seeds was carefully analyzed in Col-0 and *fata1/fata2* plants in order to find the impact of the FatA activity decrease in the metabolic flux into oil. Total fatty acids, triacylglycerols (TAGs) and diacylglycerols (DAGs) content in seeds at different stages of development and seedlings are shown in Figure 6. The study embraced lipid content in different embryo stages (walking stick, green cotyledon, mature seed and dry seed) and seedlings at 12h and 5 days after imbibition. It was remarkable that the average amount of the studied neutral lipid species and total fatty acids were always lower in the double mutant in all cases analyzed, although these differences were highly significant only in some cases (Figure 6, Table 2).

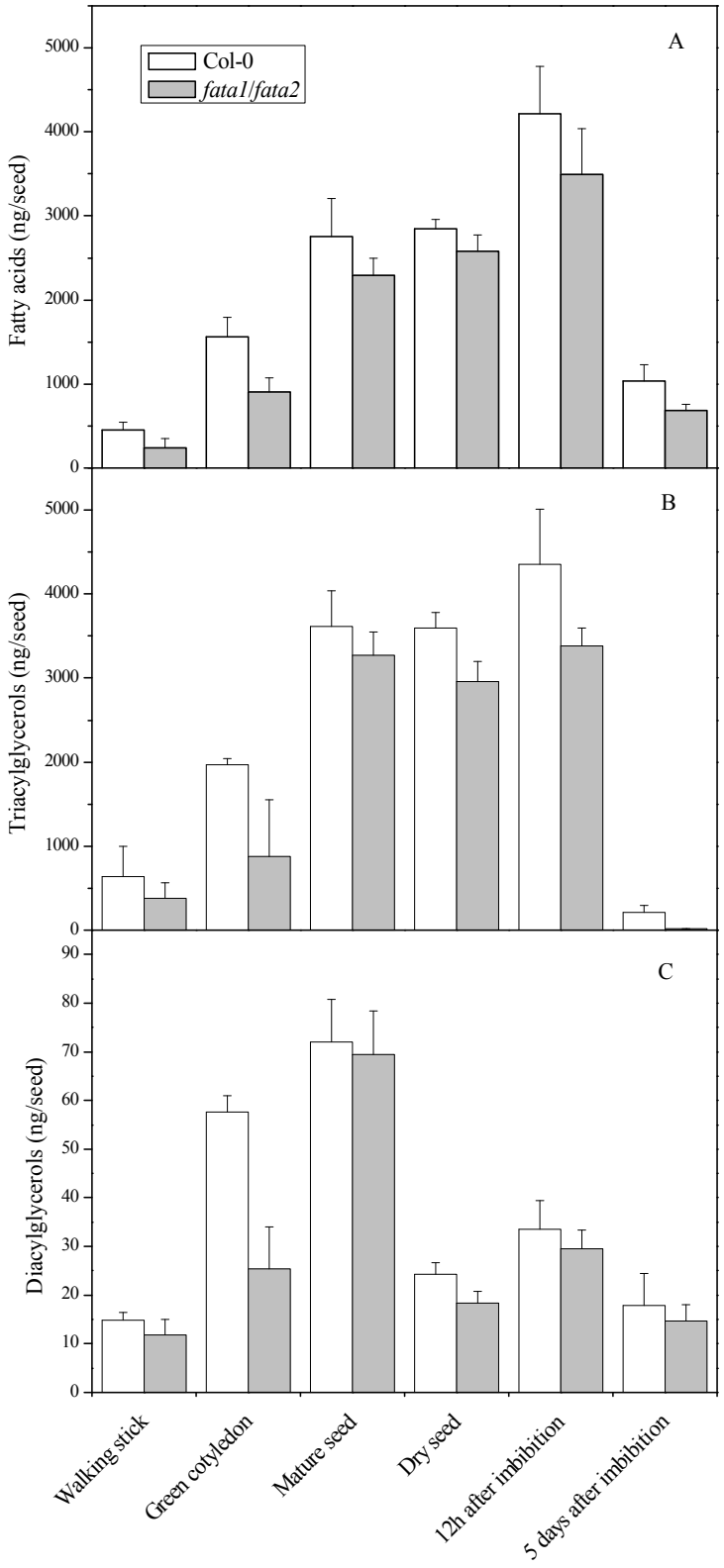

Figure 6. **Lipids in developing seeds from Arabidopsis Col-0 and *fata1/fata2* lines at different seed developmental stages and seedlings.** A:Total fatty acids; B: Total triacylglycerols; C: Total diacylglycerols. Results are the average and standard deviation of five independent determinations.

The most evident stage where this happened was green cotyledon, which accumulated significantly less amounts of the three lipids analyzed in all cases. With differences that ranged around 40% between Col-0 and *fata1/fata2*. There were significantly less TAGs in *fata1/fata2* dry seeds, although the differences were lower than in green cotyledons (around 10%).

Table 2. **Fatty acid content of seeds from wild type, Col-0, and double *FatA* mutant at different stages of development.** Data are the average of five independent samples.

	Fatty acids (ng/seed)																			
		16:0	16:1n9	16:1n7	18:0	18:1n9c	18:1n7c	18:2n6c	18:3n6	18:3n3	20:0	20:1n9	20:1n7	20:2n6	20:3n3	22:0	22:1n9	22:2n6	24:0	24:1n9
Walking stick	Col-0	56,4	1,1	3,4	26,5	83,2	18,5	156,2	0,0	58,1	6,3	23,9	5,1	3,3	0,0	1,6	2,5	0,0	2,7	0,0
	fata1/fata2	38,9	2,8	3,0	14,2	38,3	8,6	67,8	0,0	38,2	2,6	8,7	4,1	2,4	0,0	0,0	8,4	0,0	1,9	0,0
Green cotyledon	Col-0	143,7	3,2	8,2	55,8	159,2	37,4	465,8	0,5	310,3	34,9	241,8	2,8	38,2	10,1	7,8	29,7	2,5	6,4	3,7
	fata1/fata2	105,1	2,4	0,4	28,1	89,2	21,6	290,3	0,4	172,0	14,7	109,1	21,2	21,3	5,8	3,8	16,7	0,5	2,8	2,4
Mature seed	Col-0	214,0	4,4	9,2	78,0	298,3	41,6	721,1	0,0	608,0	61,8	459,5	71,2	66,3	21,2	11,4	67,2	6,9	6,1	8,4
	fata1/fata2	195,4	4,5	3,2	46,7	123,0	22,1	459,1	0,0	686,2	53,7	383,9	48,3	79,9	44,3	9,8	102,7	9,7	8,4	7,3
Dry seed	Col-0	221,4	3,9	10,8	84,5	316,2	38,7	762,5	2,2	612,8	64,2	469,9	61,3	70,2	21,0	11,2	70,4	8,4	7,9	9,0
	fata1/fata2	219,9	4,1	5,6	56,7	167,8	25,6	531,5	3,5	738,0	57,7	423,5	50,7	87,9	45,6	12,0	117,0	12,1	8,6	8,2
12h after imbibition	Col-0	309,7	6,0	12,9	126,1	493,7	55,7	1125,0	3,9	888,8	95,1	759,1	77,5	93,0	29,4	15,6	95,9	5,7	9,4	11,5
	fata1/fata2	274,3	4,6	4,7	66,2	217,5	33,4	761,2	4,2	984,0	75,8	642,6	62,0	118,1	59,5	14,5	144,2	9,4	9,5	10,9
5 days after imbibition	Col-0	121,3	29,1	3,0	48,3	61,6	9,7	221,1	1,7	432,1	9,6	39,4	3,1	16,7	17,7	7,3	5,0	0,0	11,9	0,0
	fata1/fata2	83,4	16,7	2,2	32,2	39,5	5,8	131,6	0,0	274,0	4,8	32,8	15,6	12,4	15,6	5,1	6,2	0,0	7,7	1,6

Furthermore, seeds from *fata1/fata2* line displayed altered fatty acid composition. These alterations were even more important that those found in the total amount of lipids. The most remarkable difference along the development of the seeds was the higher accumulation of linolenic acid in all stages of development excepting the green cotyledon one. This increase took place at expenses of C18 fatty acids with a lower degree of unsaturation, oleic and linoleic acids, either considering absolute amounts of fatty acids (Table 2) or relative composition of the developing seeds (Figure 7). Moreover, there were also alterations in the content of very long chain fatty acids (C20 to C24) in the *fata1/fata2* line. They concerned mainly to erucic acid that was accumulated in a higher proportion (30 to 40% higher) in the mutant plants.

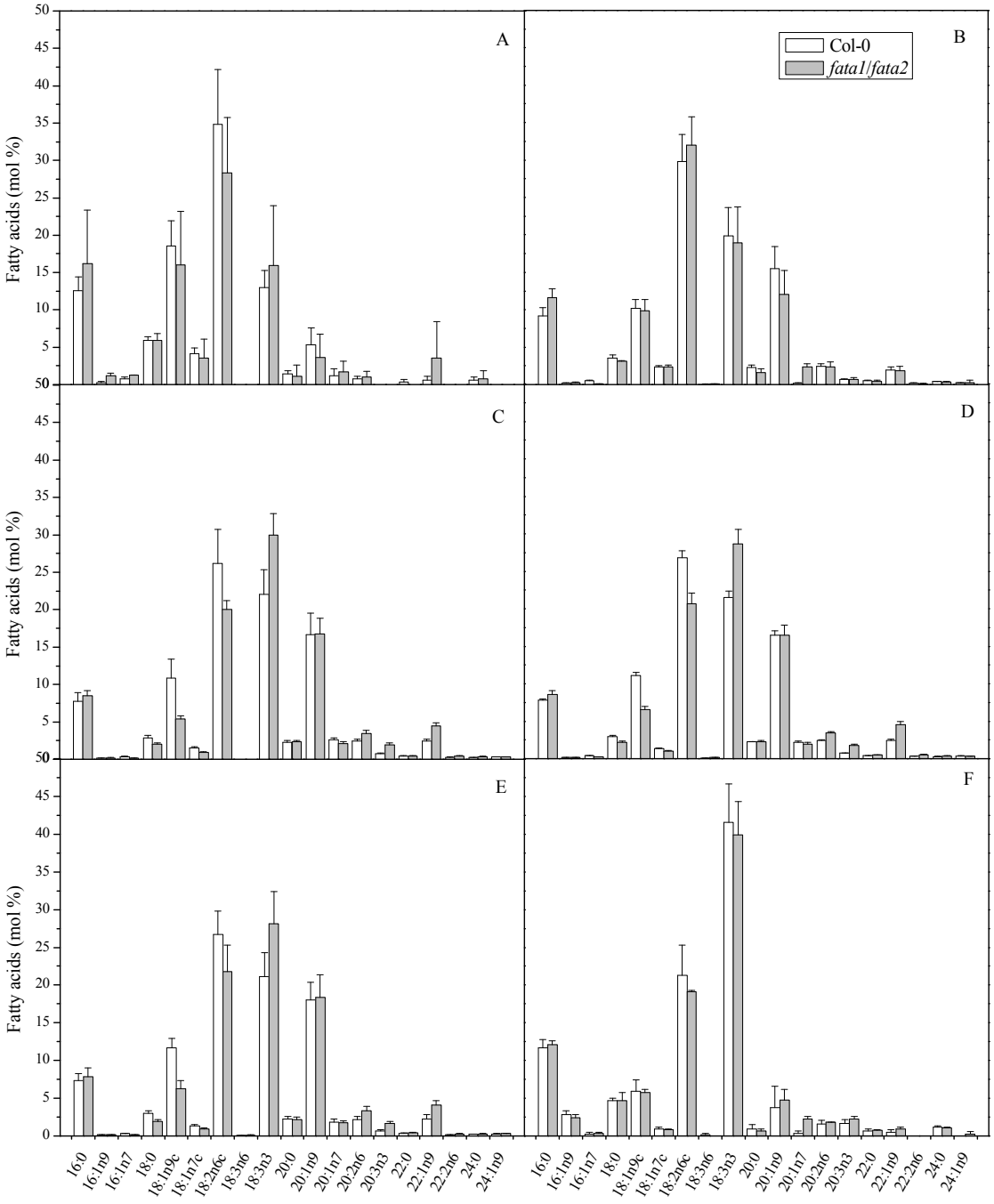

Figure 7. **Fatty acid composition of seeds from Arabidopsis Col-0 and *fata1/fata2* lines at different stages of seed development and in seedlings.** Data corresponded to the average and standard deviation of five determinations. A: Walking stick; B: Green cotyledon; C: Mature seed; D: Dry seed; E: 12h after imbibition and F: 5 days after imbibition.

2.4. Composition of the Acyl-CoA pool

The changes observed in the fatty acid composition in developing seeds from lines studied also appeared in the acyl-CoA pool composition of dry seeds (Figure 8). Thus, there was an increase of the 18:3-CoA at expenses of their precursors having a lower degree of unsaturation 18:2-CoA and 18:1-CoA. The increment was in a lower range than that found in seed TAGs. The C22 acyl CoA derivatives were also more abundant in the pools from the double mutant, which displayed lower contents of C20 CoAs. The increase was especially important in the case of erucic acid that increased two-fold in *fata1/fata2* line.

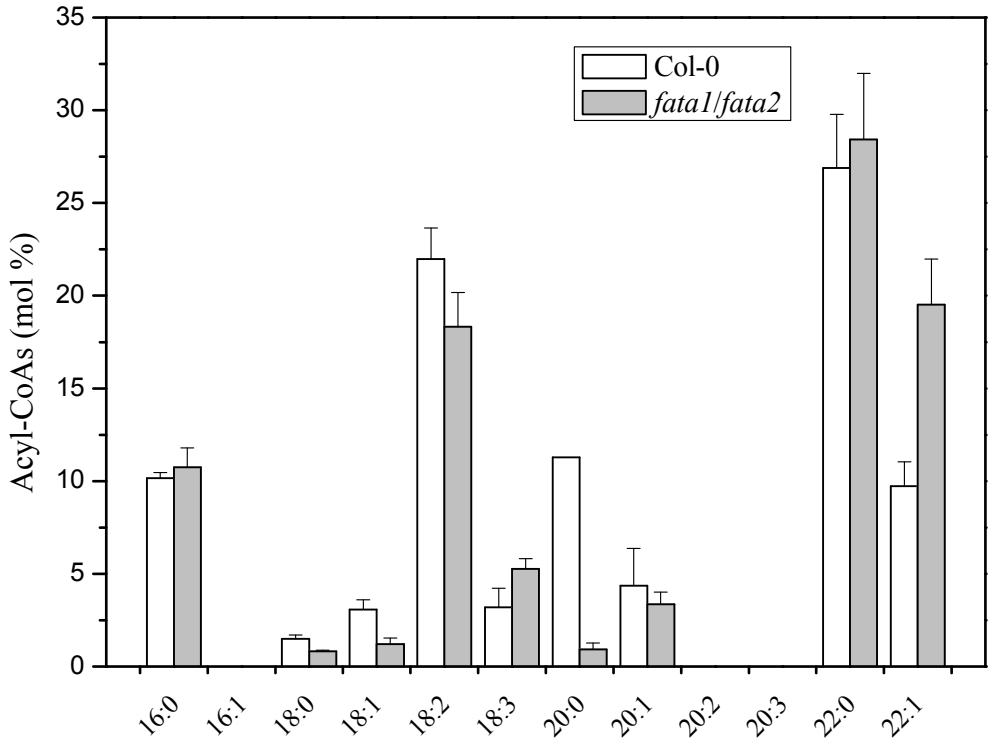

Figure 8. Fatty acid composition of the acyl-CoA pool of dry seeds from Col-0 and *fata1/fata2* lines. Data corresponded to the average and standard deviation of three independent determinations.

2.5. TAG and DAG molecular species

The TAG species in dry seeds of *fata1/fata2* line were altered, as expected, when compared with those from Col-0 line (Figure 9). The differences in TAGs species between the two lines concerned mainly those containing linolenic acid. Thus 13 species of TAGs were in a higher proportion in the seeds of the double mutant and all of them contained one, two or three 18:3 residues. On the contrary, TAGs species

containing 18:1 and 18:2 acyl moieties were in a lower proportion in *fata1/fata2* line. There was not such a clear tendency in the case of very long chain fatty acids between the two studied lines.

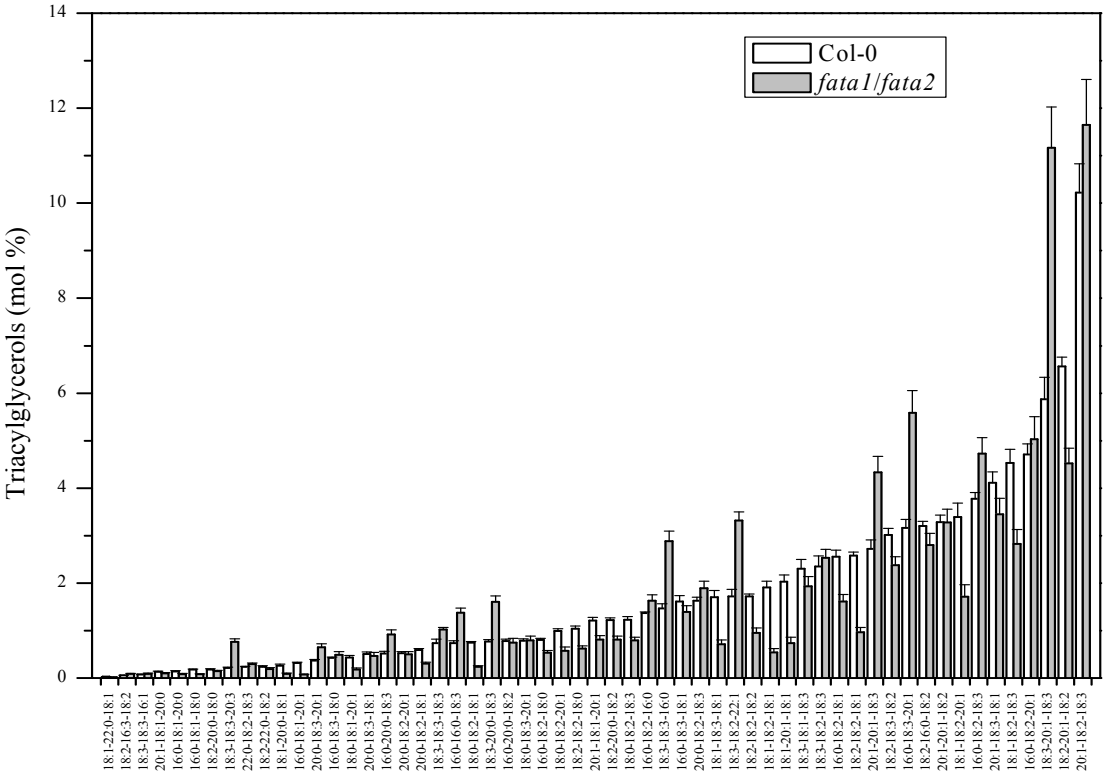

Figure 9. **Triacylglycerols species composition of dry seeds from Col-0 and *fata1/fata2* lines.** Data corresponded to the average of three independent determinations.

The same tendency was found in DAGs in dry seeds (Figure 10), again, species carrying esterified linolenic acid were in a higher proportion in *fata1/fata2*, whereas DAGs containing 18:2 and 18:1 were down-represented when compared with the above mentioned ones. In general, DAGs showed much lower content of very long chain fatty acids than TAG species.

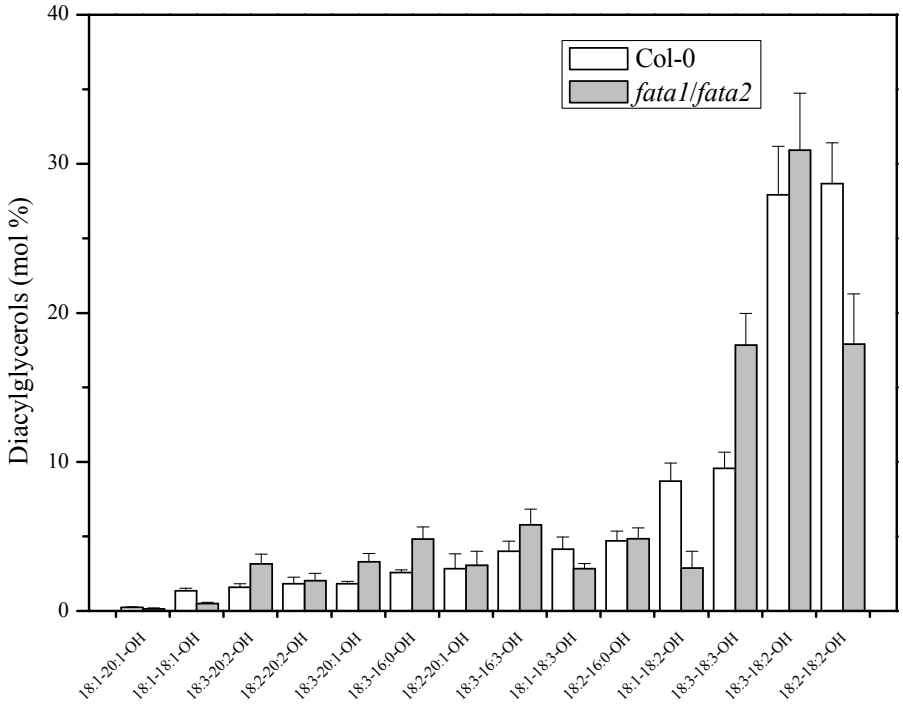

Figure 10. **Diacylglycerols species composition of dry seeds from Col-0 and *fata1/fata2* lines.** Data corresponded to the average of three independent determinations.

3. Discussion

Acyl-ACP thioesterases, FatA- and FatB-types, are important enzymes within the *de novo* fatty acid synthesis pathway in plants due to they are responsible of the termination of the intraplastidial elongation pathway previous to the exportation of acyl moieties towards extraplastidial glycerolipids synthesis in the endoplasmic reticulum. Unlike FatB, there was no previous study on the depletion of FatA thioesterases, which are the main contributors to the acyl metabolic flux out of the plastids attending to their activity level, specificity and level of expression (Jones et al., 1995). Arabidopsis plants contain two copies of the *FatA* gene in their genome and so we screened all available KO sequenced mutant databases in order to find insertional *FatA* mutants. The result of this screening was two mutants displaying insertions in the promoter that kept intact their coding regions (Figure 2). The absence of mutants having insertions in either exons or introns may be due to they provoked lethality. Nevertheless, there is no direct evidence supporting this hypothesis in data reported in this paper. Lethality of the silencing of *FatA* could be tested in the future by studies of repression by techniques of RNA interaction on these genes. Once a homozygous line containing the two insertions

was isolate it was studied to find any external phenotype. Both Col-0 and *fata1/fata2* lines exhibited no differences in number of leaves, rates of growth or number and viability of the seeds, which indicated that the insertions did not interfere with the synthesis of lipids that were necessary for the vegetative development of the plant (Figure 3 and Table 1). In this regard, most of the present study was focussed to oil-accumulating developing seeds due to this tissue was the most active at synthesizing lipids in the plant and any change in its metabolic flux should have an impact in the amount and composition of the fatty acids accumulated in this organ in the form of TAGs. Therefore, the expression levels of both *FatA1* and *FatA2* genes were studied by techniques of Q-RT-PCR to investigate the impact of the insertions on the regulation of these genes. Results in Figure 4 are clear regarding to the significant decrease of the expression of both genes in developing siliques, which in the case of the double insertional mutant displayed half number of transcripts than the control line. This level of reduction of *FatA* expression was far from those found for other insertional mutants of thioesterases. Thus, the *FatB* knockout mutant described by Bonaventure et al. (2003) showed expression levels that were 150-fold lower than those in control plants. Consequently, the mutant described in this work should be considered a mutant deficient in *FatA* expression but no a knockout *FatA* mutant. The reduction of the expression of both *FatA* genes significantly affected the levels of acyl-ACP thioesterase activity in crude extracts from developing siliques (Figure 5). So, a reduction of the rates of oleoyl-ACP hydrolysis was found in the mutant lines, which was in a good agreement with the reduction of the expression of both *FatA* genes. The reduction of activity was not significant for the other substrates assayed, which could be affected by other hydrolyzing activities like FatB or unspecific ones. Although there was no impact on the plant growth, the rates of lipid accumulation in seeds were affected by the double mutation. The profiles of accumulation of TAGs, DAGs and total fatty acids were investigated along the development of the seeds from both control and mutant plants. In all cases the content of all the lipids analyzed were lower in the *FatA* deficient mutant (Figure 6 and Table 2). However, these differences were low and often no significant out of the case of green cotyledons, where in all cases the differences were significant and lipids accumulated in the mutant were in all cases around the 50% of those found in the control plants. In later stages of development the accumulation of TAGs, DAGs and total fatty acids reached similar levels, although in some cases significant differences were actually found, like in the case of TAGs in dry seeds. The

levels of lipid in seedlings were also examined, resulting data similar to those obtained during the period of accumulation with higher amounts of lipids in the Col-0 line. This profile of lipid accumulation is compatible with a reduced flux of lipid synthesis in *fata1/fata2* line. Therefore, at the beginning of the oil accumulation period there was important differences between the lines. The Col-0 line having a higher flux accumulated more lipids than the double mutant. At later stages the lipids amounts accumulated become more even, although with slight differences favouring Col-0 plants. Hence, the reduction in FatA activity in developing seeds induced a decrease of the flux of lipid synthesis that was more apparent in the green cotyledon stage and was compensated by later lipid deposition.

The reduction of *FatA* expression caused changes in the fatty acid composition (Figure 7). Taking in consideration the profiles of specificity of FatA and FatB from Arabidopsis the expectable changes in fatty acids composition in a *FatA* deficient mutant would concern to the ratio between C16 and longer fatty acids. Thus, a decrease of FatA keeping constant the activity levels of FatB would increase the relative amount of palmitic acid incorporated to glycerolipids at expenses of C18 or longer fatty acids that mostly derived from oleate moieties exported via FatA. However, there was no important increase of C16 fatty acids at any stage of development of Arabidopsis seeds (Figure 7). So, the proportion of palmitic acid was only slightly higher and did not exhibit significant differences in the samples analyzed. This contrasted with the Arabidopsis *FatB* mutant where there was important decrease of palmitic acid in all tissues, which altered the relative C16 fatty acid content in the accumulated oil (Bonaventure et al., 2003). This difference between these two mutants was probably caused by the differences in expression of the repressed thioesterase genes described above. The differences of fatty acid composition between the two mutants mainly concerned to the level of unsaturation of C18 fatty acids. These differences were especially high in mature and dry seeds where there were significant differences in the content of linolenic acid that was more abundant in *fata1/fata2* at expenses of oleic and linoleic acid. Furthermore, a similar tendency was observed with C22 fatty acids, which were in a higher proportion in *fata1/fata2* than in Col-0 plants. Interestingly, the changes in the fatty acid composition did not regard to the *de novo* synthesis but to the later steps of fatty acid modification (see Figure 1). This means that the changes were not direct consequence of the reduction of FatA activity but to a metabolic response of the plant to the alteration caused by the insertions. The changes in seed fatty acid

content affected also to the acyl-CoA pool (Figure 8). In that case the increase in the C22 fatty acids was much more important than in the total fatty acid determination, probably due to elongation of to C20 and C22 fatty acids takes place on acyl-CoA substrates. Thus, almost all the 20:0-CoA was converted to C22 derivatives in *fata1/fata2*, which displayed double amounts of 22:1-CoA than control dry seeds. The increased accumulation of linolenic acid in the seeds of *fata1/fata2* affected the TAG composition of the seed and species containing multiple residues of linolenic acid were in a higher proportion in the double mutant at expenses of those containing oleic or linoleic acid (Figure 9). In the case of DAGs, the last precursor of TAGs, all species containing 18:3 were more abundant in the mutant (Figure 10). It was also remarkable that DAGs displayed low proportion of 22:1 and in general of all very long chain fatty acids present in Arabidopsis, which means that most of their incorporation into TAGs takes place in the last step of synthesis, via DAG-acyl-CoA acyltransferase (DAGAT).

All these modifications of the fatty acid composition were unexpected and were not caused directly by the decrease of the *FatA* activity, which would affect to the relative amount of the C16 fatty acids, but to metabolic responses of the plant to the shortage of fatty acid flux caused by the reduction in FatA activity. The response of plant metabolism to depletion of *FatB* thioesterase was studied by Bonaventure et al. (2004), resulting that plants tried to compensate the lack of saturated fatty acids by increasing at the time the rates of synthesis and degradation of fatty acids. However, that mutant displayed alterations that regarded mainly to saturated fatty acids exported by FatB, with substrate specificity different to *FatA*.

Thus, it seemed that the regulatory pathways activated by depletion of *FatA* were essentially different to those activated in the *FatB* knockout mutant. The alterations found in the double *FatA* mutant were probably induced by the decrease of the metabolic flux into fatty acids, and so it kept more similarities with Arabidopsis mutants deficient in oil accumulation such as *wri1*. This mutant was described by Focks and Benning (1998) and displayed a reduction in the oil content caused by a deficiency of the embryos to convert sucrose into precursors of TAG biosynthesis. This mutation affected to the AP2/EREB domain, encoding for a transcription factor involved in the control of storage compound biosynthesis (Cernac and Benning, 2004). Interestingly, *wri1* plants displayed changes in the fatty acid composition similar to those reported in this work, with increases in the linolenic and erucic acid content.

Fatty acid synthesis in Arabidopsis involves the export of saturated and monounsaturated fatty acids via intraplastidial thioesterases followed by the desaturation by reticular oleate and linoleate desaturases, which act on fatty acids esterified to the *sn*-2 position of phosphatidylcholine. Acyl-CoAs derivatives can also be elongated by fatty acid elongases to C20 or C22 fatty acids typically found in the seeds of this plant. Each enzymatic step could be associated with given fatty acids and so it would be possible to establish the relative flux of each enzyme and compare the values obtained in the control and the mutant lines as it is shown in the Table 3.

		A					B				
		Estimation of fatty acid out put (TE)					KAS	SAD	ODS	LDS	FAE
		16:0	∑16:1	∑18:0	∑18:1n9	∑18:1n7					
	Col-0	12,6	1,0	8,3	72,9	5,3	86,4	21,0	48,49	13,0	12,2
Walking stick	***fata1/fata2***	16,2	2,4	7,8	68,3	5,3	81,4	22,2	45,21	15,9	16,7
	Col-0	9,2	0,7	6,7	80,8	2,6	90,1	15,6	52,94	20,5	28,0
Green cotyledon	***fata1/fata2***	11,6	0,3	5,4	78,0	4,7	88,1	17,3	53,96	19,6	25,3
	Col-0	7,8	0,5	5,7	81,9	4,1	91,7	19,3	51,68	22,8	32,5
Mature seed	***fata1/fata2***	8,5	0,3	5,2	82,9	3,1	91,1	17,7	55,91	31,9	39,4
	Col-0	7,8	0,5	5,9	82,3	3,5	91,7	19,3	51,82	22,3	32,2
Dry seed	***fata1/fata2***	8,5	0,4	5,2	82,9	3,0	91,1	18,5	54,93	30,6	38,7
	Col-0	7,3	0,4	5,8	83,2	3,2	92,2	19,0	50,83	21,9	32,1
12h after imbibition	***fata1/fata2***	7,8	0,3	4,7	84,4	2,7	91,9	17,5	55,26	30,0	38,8
	Col-0	11,7	3,1	7,4	76,6	1,2	85,2	10,0	66,19	43,5	14,1
5 days after imbibition	***fata1/fata2***	12,1	2,7	7,2	74,8	3,1	85,1	13,2	63,11	42,2	19,1

TE	16:0	16:0
	∑16:1	16:1n9+16:1n7
	∑18:0	18:0+20:0+22:0+24:0
	∑18:1n9	18:1n9+18:2n6+18:3n6+18:3n3+20:1n9+22:1n9+24:1n9+20:2n6+20:3n3+22:2n6
	∑18:1n7	18:1n7+20:1n7
KAS		18:0+20:0+22:0+24:0+18:1n9+18:2n6+18:3n6+18:3n3+20:1n9+22:1n9+24:1n9+20:2n6+20:3n3+22:2n6+18:1n7+20:1n7
SAD		18:1n9+20:1n7+22:1n9+24:1n9+20:2n6+20:3n3
ODS		18:2n6+18:3n3+20:2n6+20:3n3+22:2n6
LDS		18:3n3+18:3n6+20:3n3
FAE		(20:0+20:1n9+20:1n7+20:2n6+20:3n3)+2*(22:0+22:1n9+22:2n6)+3*(24:0+24:1n9)

Table 3. **Estimation of fatty acids coming out from the plastid and enzymatic activities in Col-0 and *fata1/fata2* seeds from their total fatty acid composition.**

Table 3 showed that the relative activities of the β-ketoacyl-ACP synthase II (KASII) complex and stearoyl-ACP desaturase (SAD) were similar in both lines, whereas linoleate desaturase (LDS) and fatty acid elongase (FAE) were higher in the double mutant. This data involved that the decrease in metabolic flux caused by *FatA* genes depletion involve a general down regulation of some genes involved in fatty acid synthesis like KAS and SAD, whereas other genes were not down regulated (ODS, LDS and FAE) in the same way and stayed at the same level than in the control plants (or higher), which caused the increase of linolenic and erucic acid at expenses of their

direct precursors. These facts were also demonstrated for *wri1* mutant by studies of gene expression by techniques of microarrays (Ruuska et al., 2002), and seemed to be the same that take place in *fata1/fata2* mutant. That work showed that during Arabidopsis seed development there were genes following different patterns of expression, which pointed to different mechanism of regulation for them. When the expression pattern of these genes in WT plant were compared with those in *wri1* mutant less than 1% displayed important differences in their expression levels. Amongst these genes were some encoding for central fatty acid synthesis enzymes, like KAS and SAD, which indicated that they were regulated according the metabolic flux and that a reduction in the glycolysis rate induced a down-regulation of fatty acid synthesis pathway. Nevertheless, there were genes also involved in lipid synthesis and modification that were not altered in the mutant. These were typically abscisic-acid regulated ones like FAE1 and LDS, which displayed similar expression levels in both wild type and mutant. That provoked that the products of these enzymes (linolenic acid and C22 fatty acids) were in a higher proportion in the oil of mutant plants as an indirect consequence of the changes in metabolic flux. This phenotype was quite similar to that found in the double *FatA* mutant reported in this work, which indicated that the decrease in the expression of the two *FatA* forms induced a reduction of the metabolic flux into TAGs involving the down-regulation of most of the enzymes of this pathway (Table 3), but not FAE or LDS enzymes that were not concerned by this modulation of the metabolic flux and involved increases in linolenic and erucic fatty acids in agreement with results obtained for the *wri1* mutant. Therefore, this result showed that there are mechanisms regulating the flux of fatty acid synthesis in Arabidopsis in function of external stimuli. The reduction of FatA activity activated this mechanism with the consequence of a slightly lower rate of lipid accumulation and changes in the fatty acid composition of the seeds involving increases in the products resulting from enzymes encoded by the genes that did not have their expression altered. The resulting phenotype was similar to that reported to the *wri1* mutant showing that this mechanism was also related with the phenotype of that plant. The way in which this mechanism is activated and controlled has not been yet well described but it would be of great interest to explain how the metabolic flux in seeds is diverged to carbohydrates or oil and could be an important tool to alter the oil content of seeds to obtain improved crops.

4. Experimental

4.1. Biological material and growth condition

The *Arabidopsis thaliana* homozygous *fat1* and *fata2* mutant lines, WiscDsLox357F07 and SALK_050939 respectively, from the European Arabidopsis Stock Center, were crossed. The *fata1/fata2* double mutant plants were genotyped and the homozygous line was selected. *A. thaliana fata1/fata2* line and Columbia-0 (Col-0) ecotype were used in this study. Arabidopsis seeds were surface sterilized, cold-treated at 4ºC and imbibed in the dark for 4 days on 1% phytoagar plates containing 1% sucrose and 0.5 MS media. The seeds were then germinated and grown in soil at 20ºC under a 16h day/8h night photoperiod.

4.2. Genotyping

PCR reactions using genomic DNA were used for detecting homozygosity of T-DNA insertions in mutant line *fata1* and *fata2*. T-DNA-specific primers (p745 for At3g25110 or LBb1.3 for At4g13050) and At3g25110 or At4g13050 gene-specific RP primers (N852633RP or N550939RP, respectively) were used to detect the existence of T-DNA (Table 4). The T-DNA signal is present only in the mutant lines; then the LP (N852633LP for At3g25110 and N550939LP for At4g13050) and RP primers specific for the gene sequences near the left and right borders of T-DNA insertion were used to amplify the intact gene (Table 4). The mutant lines lack the signal, indicating their homozygosity.

4.3.Phenotyping

Three weeks Arabidopsis plants for both lines were analyzed; the rosette diameter, the number of rosette leaves and the viability of the seeds were measured.

4.4. RNA preparation and cDNA synthesis

Approximately 0.25 g of Arabidopsis siliques containing embryos at walking-stick stage were ground in liquid nitrogen using a precooled sterile mortar and pestle. Total RNA was isolated using the RNeasy Mini Kit (Quiagen). RNA samples were

treated with DNAseI (Promega) and this DNA-free RNA (1µg) was retrotranscribed with oligo (dT) primer and SuperScript II RT (Invitrogen).

4.5. Quantitative real time PCR

Samples of the first strand cDNA were used in quantitative real time PCR (QRT-PCR) reactions using the following gene-specific primers: At*FatA*1-F and At*FatA*1-R2 for FatA1, At*FatA*2 and FAt*FatA*2-R2 for FatA2, AtActin-F and AtActin-R for the Arabidopsis actin gene (Table 4). The method of Livak and Schmittgen (2001) was applied to calculate comparative expression levels between samples. Actin gen was used as internal reference to normalize the relative amount of cDNAs for all samples.

Table 4. Sequences of PCR primers used in this work.

Primer name	Sequence
N852633LP	5'-CCAACTCGAACAAAAGAAACG-3'
N852633RP	5'-CAATGGTTTCAACAGTAGCGG-3'
p745	5'-AACGTCCGCAATGTGTTATTAAGTTGTC-3'
N550939LP	5'-TCTTCCATCAATCGACCAAAC-3'
N550939RP	5'-ATTTTGCCGATTTCGGAAC-3'
LBb1.3	5'- CGGGTACCATGGAGGTTAAGATATCGG -3'
At*FatA*1-F	5'-GGAAGTGTGGTTCAAGG-3'
At*FatA*1-R2	5'-ACTACCCACTTCGTAAGATC-3'
At*FatA*2-F	5'-ACAGCAGCGTCCGTGTTGC-3'
At*FatA*2-R2	5'-AATCCCAACTTCATAGCTTC-3'
AtActin-F	5'-GGAAGGATCTGTACGGTAAC-3'
AtActin-R	5'-TGTGAACGATTCCTGGACCT-3'

4.6. Preparation of acyl-ACP substrates

Labeled acyl-ACP substrates were prepared using a recombinant acyl-ACP synthetase from *E. coli*. Acylation reactions contained 50 µg of recombinant ACP form *E. coli* (Sigma-Aldrich), 180 kBq (approx. 0.1 µmol) of [1-^{14}C] fatty acid ammonium salt ([^{3}H] fatty acid in the case of 16:1$^{\Delta 9}$), 5 mM ATP, 2 mM DTT, 400 mM $LiCl_2$, 10

mM $MgCl_2$, 100 mM Tris-ClH pH 8.0 and 10 µg acyl-ACP synthetase, in a final volume of 0.5 ml. Reactions were carried out at room temperature for 3 h and the acyl-ACPs were purified and concentrated by ion exchange chromatography on DEAE-sepharose as described by Rock and Garwin (1979).

4.7. Acyl-ACP thioesterase assays

Siliques with walking-stick embryos were harvested and ground in extraction buffer containing 50 mM Tris-HCl pH 8.0 and 5 mM DTT, 1 g of tissue per 10 ml of buffer (Martínez-Force et al., 2000). The protein concentration in the crude extracts was measured using the Bio-Rad Protein Assay (Hercules, CA, USA) according to the manufacturer's instructions and using BSA as standard. Thioesterase activity was assayed in 0.1 ml reactions containing 50 mM Tris-HCl pH 8.0, 5 mM DTT, 2-6 µg of the protein preparation and 0.07 nmol (150 Bq approx.) of acyl-ACP substrate. Reactions were carried out at room temperature for 5 min and stopped by the addition of 0.25 ml of 1 M acetic acid in 2-propanol. Unesterified fatty acids were then extracted twice with 0.3 ml hexane, and the radioactivity in the pooled organic phase was determined in a calibrated liquid scintillation counter (Rackbeta II; LKB).

4.8.Lipid analysis

Developing seeds or whole young plants leaves were harvested for lipid analysis. The samples were ground and fatty acid composition was determined via acid-catalysed transmethylation and analysed by gas-chromatography with flame ionization detection (GC8000 Top, Thermoquest Separation Products, Manchester, UK), fitted with a 30 m long 0.25 mm ID SGE BPX70 column (SGE, Milton Keynes, UK). Helio was used as a carrier gas at 1 ml min^{-1} with a 30:1 split ratio. The oven was run isothermally at 110ºC for 1 min, then ramped to 180ºC at 20ºC min^{-1} then to 221ºC at 2.5ºC min^{-1} (Larson and Graham, 2001). The pool of acyl-CoAs was determined by HPLC using the method of Larson and Graham (2001) with modifications (Larson et al., 2002), and neutral lipids were analyzed by LC/MS/MS according to Burgal et al. (2008).

Acknowledgements

We are thankful to Rosario Sánchez and Valeria Gazda for their technical assistance. We also thank Dr. Luisa Hernández for help with experimental approach. This work was supported by the Spanish MICINN and FEDER, Project AGL2008-01086/ALI.

References

Beisson, F., Koo, A.J.K., Ruuska, S., Schwender, J., Pollard, M., Thelen, J.J., Paddock, T., Salas, J.J., Savage, L., Milcamps, A., Mhaske, V.B., Cho, Y. and Ohlrogge, J.B. (2003) Arabidopsis genes involved in acyl lipid metabolism. A 2003 census of the candidates, a study of the distribution of expressed sequence tags in organs, and a Web-based database. Plant Physiol. 132: 681-697.

Bonaventure, G., Bao, X., Ohlrogge, J. and Pollard, M. (2004) Metabolic responses to the reduction in palmitate caused by disruption of the FATB gene in Arabidopsis. Plant Physiol. 135: 1269-1279.

Bonaventure, G., Salas, J.J., Pollard, M.R. and Ohlrogge, J.B. (2003) Disruption of the FATB gene in Arabidopsis demonstrates an essential role of saturated fatty acids in plant growth. Plant Cell 15: 1020-1033.

Browse, J. and Somerville, C.R. (1991) Glycerolipid synthesis: biochemistry and regulation. Annu. Rev. Plant Physiol. Plant Mol. Biol. 42, 467-506.

Burgal, J., Shockey, J., Lu, C., Dyer, J., Larson, T., Graham, I. and Browse, J. (2008) Metabolic engineering of hydroxy fatty acid production in plants: RcDGAT2 drives dramatic increases in ricinoleate levels in seed oil. Plant Biotechnol. J. 8: 819-831.

Cernac, A. and Benning, C. (2004) WRINKLED1 encodes an AP2/EREB domain protein involved in the control of storage compound biosynthesis in Arabidopsis. Plant J. 40: 575-585.

Chen, M., Han, G., Dietrich, C.R., Dunn, T.M. and Cahoon E.B. (2006) The essential nature of sphingolipids in plants as revealed by the functional identification and

characterization of the Arabidopsis LCB1 subunit of serine palmitoyltransferase. Plant Cell 18:3576-3593.

Dehesh, K., Jones, A., Knutzon, D.S. and Voelker, T.A. (1996) Production of high levels of 8:0 and 10:0 fatty acids in transgenic canola by overexpression of Ch FatB2, a thioesterase cDNA from *Cuphea hookeriana*. Plant J. 9: 167-172.

Dörmann, P., Kridl, J.C. and Ohlrogge, J.B. (1994) Cloning and expression in *Escherichia coli* of a cDNA coding for the oleoyl-acyl carrier protein thioesterase from coriander (*Coriandrum sativum* L.). Biochim. Biophys. Acta - Lipids and Lipid Metabolism 1212: 134-136.

Dörmann, P., Voelker, T.A. and Ohlrogge, J.B. (2000) Accumulation of palmitate in Arabidopsis mediated by the acyl-acyl carrier protein thioesterase FATB1. Plant Physiol. 123: 637-644.

Focks, N. and Benning, C. (1998) Wrinkled1: a novel, low-seed-oil mutant of Arabidopsis with a deficiency in the seed-specific regulation of carbohydrate metabolism. Plant Physiol. 118: 91-101.

Hellyer, A., Leadlay P.F. and Slabas, A.R. (1992) Induction, purification and characterisation of acyl-ACP thioesterase from developing seeds of oil seed rape (*Brassica napus*). Plant Mol. Biol. 20: 1573-5028.

Jones, A., Davies H.M. and Voelker, T.A. (1995) Palmitoyl-acyl carrier protein (ACP) thioesterase and the evolutidnary-origin of plant acyl-ACP thioesterases. Plant Cell, 7: 359-371.

Joyard, J. and Stumpf, P.K. (1980) Characterization of an acyl-coenzyme A thioesterase associated with the envelope of spinach chloroplasts. Plant Physiol. 65: 1039-1043.

Koo, A.J.K., Ohlrogge, J.B. and Pollard, M. (2004) On the export of fatty acids from the chloroplast. J. Biol. Chem. 279: 16101-16110.

Larson, T.R., Edgell, T., Byrne, J., Dehesh, K. and Graham, I.A. (2002) Acyl CoA profiles of transgenic plants that accumulate medium-chain fatty acids indicate inefficient storage lipid synthesis in developing oilseeds. Plant J. 32: 519-527.

Larson, T.R., Graham, I.A. (2001) A novel technique for the sensitive quantification of acyl CoA esters from plant tissues. Plant J. 25: 115-125.

Livak K.J. and Schmittgen T.D. (2001) Analysis of relative gene expression data using real-time quantitative PCR and the $2^{-\Delta\Delta CT}$ method. Methods 25: 402-408.

Martínez-Force, E., Cantisán, S., Serrano-Vega, M.J. and Garcés, R. (2000) Acyl-acyl carrier protein thioesterase activity from sunflower (*Helianthus annuus* L.) seeds. Planta 211: 673-678.

Mayer, K.M. and Shanklin, J. (2005) A structural model of the plant acyl-acyl carrier protein thioesterase FatB comprises two helix/4-stranded sheet domains, the N-terminal domain containing residues that affect specificity and the C-terminal domain containing catalytic residues. J. Biol. Chem. 280: 3621-3627.

McLaren, I., Wood, C., Jalil, M.N.H., Yong, B.C.S. and Thomas, D.R. (1985) Carnitine acyltransferases in chloroplasts of *Pisum sativum* L. Planta 163: 197-200.

Ohlrogge, J.B. and Jaworski, J.G. (1997). Regulation of fatty acid synthesis. Annual Rev. of Plant Physiol. and Plant Mol. Biol. 48: 109-136.

Pollard, M. and Ohlrogge, J. (1999) Testing models of fatty acid transfer and lipid synthesis in spinach leaf using in vivo oxygen-18 labeling. Plant Physiol. 121: 1217-1226.

Rock, C.O. and Garwin, J.L. (1979) Preparative enzymatic synthesis and hydrophobic chromatography of acyl-acyl carrier protein. Journal of Biological Chemistry. 254: 7123-7128.

Roughan, P.G. and Slack, C.R. (1982) Cellular organization of glycerolipid metabolism. Annu Rev Plant Physiol 33: 97-132.

Ruuska, S.A., Girke, T., Benning, C. and Ohlrogge, J.B. (2002) Contrapuntal networks of gene expression during Arabidopsis seed filling. Plant Cell, 14: 1191-1206.

Salas, J.J. and Ohlrogge, J.B. (2002) Characterization of substrate specificity of plant FatA and FatB acyl-ACP thioesterases. Arch. Biochem. Biophys. 403: 25-34.

Sánchez-García, A., Moreno-Pérez, A.J., Muro-Pastor, A.M., Salas, J.J., Garcés, R. and Martínez-Force, E. (2010) Acyl-ACP thioesterases from castor (*Ricinus communis* L.): An enzymatic system appropriate for high rates of oil synthesis and accumulation. Phytochemistry 71: 860-869.

Schmid, M., Davison, T.S., Henz, S.R., Pape, U.J., Demar, M., Vingron, M., Schölkopf, B., Weigel, D. and Lohmann, J.U. (2005) A gene expression map of *Arabidopsis thaliana* development. Nat. Genet. 37: 501-506.

Serrano-Vega, M.J., Garcés, R. and Martínez-Force, E. (2005) Cloning, characterization and structural model of a FatA-type thioesterase from sunflower seeds (*Helianthus annuus* L.). Planta 221: 868-880.

Thomas, D.R., Jalil, M.N.H., Ariffin, A., Cooke, R.J., McLaren, I., Yong, B.C.S. and Wood, C. (1983) The synthesis of short- and long-chain acylcarnitine by etioplasts of greening barley leaves. Planta 158: 259–263.

Voelker, T.A., Jones, A., Cranmer, A.M., Davies, H.M. and Knutzon, D.S. (1997) Broad-range and binary-range acyl-acyl-carrier-protein thioesterases suggest an alternative mechanism for medium-chain production in seeds. Plant Physiol. 114: 669-677.

Voelker, T.A., Worrell, A.C., Anderson, L., Bleibaum, J., Fan, C., Hawkins, D.J., Radke, S.E. and Davies, H.M. (1992) Fatty acid biosynthesis redirected to medium chains in transgenic oilseed plants. Science 257: 72-74.

Obtention of improved acyl-ACP thioesterase allele from sunflower by site-directed mutagenesis and effect of its transient expression in tobacco cells.

Moreno-Pérez, A.J.[a], Venegas-Calerón, M. [a], Vaistij, F.E. [b], Salas, J.J. [a], Larson, T.R. [b], Garcés, R. [a], Graham, I.A. [b], Martínez-Force, E. [a]

[a]Instituto de la Grasa, CSIC, Av. Padre García Tejero, 4, 41012, Seville, Spain.
[b]Centre for Novel Agricultural Products, Department of Biology, University of York, PO Box 373, York YO10 5YW, UK.

Manuscript in preparation

Abstract

Substrate specificity of the acyl- acyl carrier protein (ACP) thioesterases (FAT) determines the type of fatty acids that are exported from plastids and incorporated into acyl-CoA pool. Thus, designing acyl-ACP thioesterases with different substrate specificity or kinetic properties would be of interest for plant lipid biotechnology to produce oils enriched in specialty fatty acids. In the present work, FatA thioesterase from *Helianthus annuus* was used to test the impact of changes in the amino acids present in the binding pocket, found after the protein was modeled by comparison with other enzymes catalyzing similar reactions, on substrate specificity and catalytic efficiency. Amongst all the mutated enzymes the one carrying the change Q215W was especially interesting for its higher specificity towards saturated acyl-ACP substrates and for having higher catalytic efficiency than wild type *H. annuus* FatA. Normal, null (T182W) and high-efficient (Q215W) alleles were transiently expressed in tobacco leaves to check their effect on lipid biosynthesis. Expression of active FatA thioesterases altered the level and composition of leaf triacylglycerols but did not alter total lipid content. Moreover, studies on subcellular localization of the exogenous enzymes showed the chloroplast localization of FasA. The role and influence of acyl-ACP thioesterases in plants metabolism and their possible applications in lipid biotechnology were discussed in function of the results.

1. Introduction

Plant *de novo* fatty acid biosynthesis takes place in chloroplast and in non green plastids. This process demands carbon chains, which are imported from cytosolic glycolitic pathway, and reducing equivalents in the form of NADPH (Rawsthorne, 2002). This process consists of successive elongations of acyl-ACP derivatives by the action of the fatty acid synthase fully dissociated enzyme complexes (Ohlrogge and Jaworski, 1997). In oilseeds accumulating triacylglycerols (TAGs), the process of acyl-acyl-carrier-protein (ACP) elongation is terminated by acyl-ACP thioesterases that are enzymes that hydrolyze the thioester bond of those derivatives releasing a free fatty acid and free ACP moieties (Browse and Somerville, 1991). Fatty acids are then transported / activated to the cytosol in the form of acyl-CoAs by an acyl-CoA synthetase complex present in the external membrane of plastids (Koo et al., 2004) and incorporated into glycerolipids via the Kennedy pathway. In this regard, there is evidence indicating that the substrate specificity of acyl-ACP thioesterases broadly determines the fatty acids that are exported from plastids to glycolipids synthesis and so they have an important contribution to the fatty acid composition of the oil accumulated by the seeds. Thus, the thioesterases most commonly found in plants are of the FatA and FatB1 types (Jones et al., 1995). The former one displays high specificity towards oleoyl-ACP, the precursor of most C18 to C22 fatty acids found in oilseeds (Dörmann et al., 1994; Salas and Ohlrogge, 2002). The second one displays high specificity for the hydrolysis of palmitoyl-ACP and contributes significantly to the accumulation of saturated fatty acids (Jones et al., 1995; Bonaventure et al., 2003). Furthermore, species accumulating oils with unusual fatty acids often express acyl-ACP thioesterases with altered specificity. Thus, tropical species accumulating fats containing high levels of short and medium chained fatty acids (C8 to C14) possesses thioesterases of the FatB2 type specialized in the hydrolysis of short and medium chain acyl-ACP derivatives (Dehesh et al., 1996; Voelker et al., 1997). Moreover, *Coriandrum sativum* accumulating the unusual monoene petroselinic acid in their seeds also express a specific acyl-ACP thioesterase to maintain high rates of synthesis of that fatty acid (Dörmann et al., 1994). This fact has made acyl-ACP thioesterases enzymes of a great interest in the field of plant lipid biotechnology. In so doing, the expression of a thioesterase of the FatB2 type in *Brassica* gave place to the high laurate canola, the first oil crop with genetically modified oil (Voelker et al., 1992). Moreover expression of modified *FatA*s to increase

their activity towards saturated fatty acid also increased the content of stearic acid in *Brassica* transformants (Facciotti et al., 1999).

Oilseed genetic engineering has been interested in the production of speciality oils containing unusual fatty acids to be used in food or oleochemical industries (Ohlrogge, 1994). Thus, designing and engineering new enzymes with new substrate specificities would be of a great interest in this field. The most important advances reached on enzymes involved in lipid synthesis regarded to acyl-ACP desaturases. A form of this enzyme, cloned from castor seeds, was crystallized and its structure studied by RX diffraction (Lindqvist et al., 1996). In function of these data it was possible to find which amino acids were involved in the hydrophobic pocket determining specificity and so it was possible to produce new engineered forms with altered substrate specificity without losing catalytic efficiency (Cahoon et al., 2000). In the case of thioesterases there are not crystallographic data, although it was possible to fulfill a model of the tertiary structure based on the *Escherichia coli* 4-hydroxybenzoyl-CoA thioesterase. This model was coherent with previous research on the specificity of these enzymes, involving changes in different protein residues and domain swapping (Yuan et al., 1995, 1996; Salas and Ohlrogge, 2002). Thus, it was hypothesized that the active site of these enzymes displays a hot-dog fold pattern, with a catalytic triad of amino acids similar to that in papain (Mayer and Shanklin, 2005; Serrano-Vega et al., 2005). Furthermore, the regions interacting with the substrate were identified, including a hydrophobic pocket that was a clear candidate to determine the substrate specificity (Mayer and Shanklin, 2007).

In the present work the acyl-ACP thioesterase FatA from sunflower (*Ha*FatA) was used to test the effect of different amino acid changes in its hydrophobic pocket. FatA are dimeric enzymes coded by nuclear genes that are imported into plastids mediating maturation involving hydrolysis of an N-terminal transit peptide. *Ha*FatA is expressed at high levels in sunflower seeds displaying catalytic efficiencies higher than other FatAs previously described (Serrano-Vega et al., 2005). Changes in the binding pocket involved the change of some amino acids residues by the aromatic tryptophan, which interfered in the pocket size and shape. Among the different mutations assayed the change Q215W provoked a general increase of the catalytic efficiency of the enzyme and T182W the loss of activity. The effect of this enzyme on lipid metabolism was studied by transient expression of wild type (WT) *Ha*FatA, T182W null mutant and Q215W mutant in tobacco leaves. The impact of the expression of these thioesterases

on lipid metabolism of tobacco was discussed in function of the results. Moreover, it was possible to study the location of these enzymes in tobacco cells by techniques of fluorescence labeling. The implications of this result were also discussed in this paper.

2. Results and Discussion

2.1. HaFatA site-directed mutagenesis

Sunflower acyl-ACP thioesterase cDNA (*HaFatA*) has been previously cloned and characterized (Serrano-Vega et al., 2005). On the basis of acyl-ACP thioesterase structural models (Mayer and Shanklin, 2005; Serrano-Vega et al., 2005) and the use of bioinformatic tools it has been possible to indentify amino acid residues candidates to be involved in substrate specificity of these proteins. In the case of *Ha*FatA it was identified a region from amino acid 80 to 228 that generates a hydrophobic pocket including residues that have been demonstrated to be involved in substrate specificity of FatA1 from *Garcinia mangostana* (Facciotti et al., 1999), FatB from *Umbellaria californica* (Yuan et al., 1995) and FatB from *Arabidopsis thaliana* (Mayer and Shanklin, 2007). Moreover, this region has also been identified in experiments with chimeric constructs as being involved in substrate specificity (Facciotti and Yuan, 1998; Salas and Olhrogge, 2002). The position and orientation into the hydrophobic pocket were the criteria selected to choose the amino acids Leu 118 (L118), Thr 172 (T172), Thr 182 (T182), Arg 184 (R184), Met 206 (M206) and Gln 215 (Q215). All of them having the lateral residues orientated inwards of the pocket. T182 and R184 are situated in the deepest region; L118, T172 and M206 are in the intermediate region; and Q215 is in the most exterior zone of the pocket. These amino acids were mutated to tryptophan which is an aromatic amino acid with a big volume that could modify the interaction of the enzyme with the acyl-ACP substrates. Figure 1 shows the structural model of the region described above with the wild type residue or the mutated one.

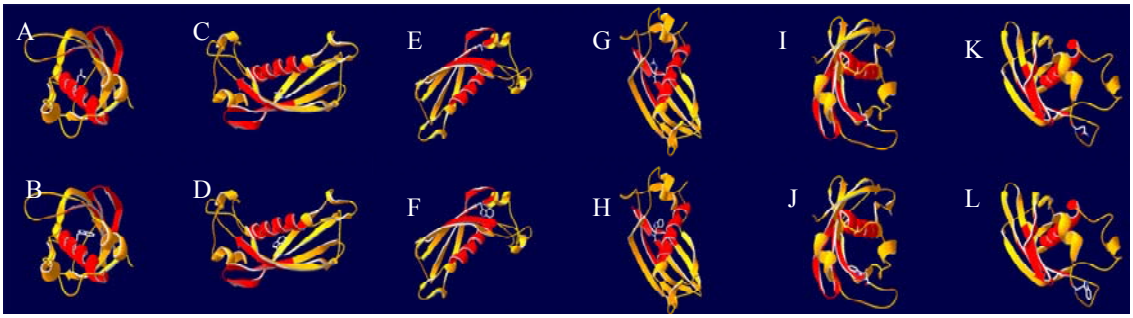

Figure 1. Structural models of *Ha*FatA mutants. A. Leu 118 wt, B. Leu 118 Trp, C. Thr 172 wt, D. Thr 172 Trp, E. Thr 182 wt, F. Thr 182 Trp, G. Arg 184 wt, H. Arg 184 Trp, I. Met 206 wt, J. Met 206 Trp, K. Gln 215 wt, L. Gln 215 Trp. The upper row shows the models corresponding to wild type HaFatA and the last row shows the mutant alleles. Each residue changed is modeled in the corresponding mutant.

2.2. Heterologous expression in E. coli and biochemical characterization

*Ha*FatAs are expressed at a high level in the soluble fraction of recombinant *Escherichia coli*, so it can be efficiently recovered in the supernatant resulting from broken cells and purified by immobilized metal affinity chromatography (IMAC) (Serrano-Vega et al., 2005). When the WT *Ha*FatA was modified by site-directed mutagenesis the pattern of expression of the different alleles in *E. coli* also changed. Thus, out of the WT, only the mutant alleles L118W, T182W, M206W and Q215W were purified using the above mentioned protocol. The other ones produced toxic effects or were targeted to inclusion bodies (data not shown). Figure 2 shows a SDS-PAGE with an example of the FatA purification. A single-protein band of about 37 kDa, corresponding to the mature protein without the signal peptide (His-FatA), was detected. These data were in agreement with predicted mass and previous purification data (Serrano-Vega et al., 2005).

Kinetic studies were carried out with the IMAC-purified proteins. Studies of substrate specificity were fulfilled by assaying the different enzymes with the substrates 16:0-ACP, 18:0-ACP, 16:1-ACP and 18:1-ACP (Table 1).

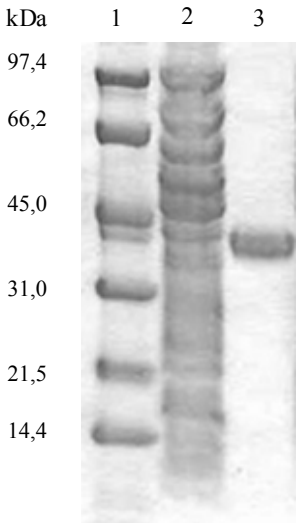

Figure 2. Comassie blue stained SDS-PAGE showing recombiant sunflower acyl-ACP thioesterase. Lane 1, marker; lane 2, soluble fraction of pQE-80L:*Ha*FatA lysate; lane 3, purified His- FatA protein. The position of molecular weight (kDa) markers is shown on the left.

Table 1: Kinetic parameters of purified recombinant *Ha*FatA proteins on different acyl-ACP substrates whose lengths and degree of saturation varied.

	Substrate	K_m	V_{max}	k_{cat}	k_{cat}/K_m
		(µM)	**(nkat/mg protein)**	**(s^{-1})**	**(s^{-1} μM^{-1})**
FatA wt	**18:1-ACP**	0,9	1008,6	35,6	39,1
	16:1-ACP	0,3	225,9	8,0	23,4
	18:0-ACP	0,7	22,7	0,8	1,2
	16:0-ACP	1,0	30,0	1,1	1,1
L118W	**18:1-ACP**	0,6	61,3	2,2	3,7
	16:1-ACP	0,3	16,3	0,6	1,8
	18:0-ACP	1,0	5,6	0,2	0,2
	16:0-ACP	0,7	4,8	0,2	0,3
T182W	**18:1-ACP**	0,6	0,9	0,032	0,050
	16:1-ACP	0,6	0,5	0,016	0,028
	18:0-ACP	1,5	0,1	0,003	0,002
	16:0-ACP	0,9	0,1	0,002	0,003

M206W	**18:1-ACP**	21,2	3567,0	125,8	5,9
	16:1-ACP	0,2	44,6	1,6	6,6
	18:0-ACP	0,4	5,4	0,2	0,5
	16:0-ACP	1,2	13,6	0,5	0,4
Q215W	**18:1-ACP**	2,2	2420,0	85,4	39,3
	16:1-ACP	0,1	177,0	6,2	48,0
	18:0-ACP	2,5	115,2	4,1	1,6
	16:0-ACP	0,9	67,1	2,4	2,8

These studies showed that modified *Ha*FatA forms displayed high catalytic efficiency (k_{cat}/K_m) towards unsaturated substrates similarly to WT *Ha*FatA. In absolute terms all mutants displayed catalytic activities lower than WT *Ha*FatA excepting Q215W, which kept high levels of activity towards C-18 substrates and increasing its activity for the C-16 ones, being 2-fold more active for the palmitoleoyl-ACP and 2.6-fold for saturated palmitoyl-ACP than for the same substrates in WT *Ha*FatA. Furthermore, the T182W mutant displayed catalytic activity values that were three magnitude orders lower than those of WT *Ha*FatA. As a general rule the K_m values of the mutants assayed remained similar to those of WT form, differing in the V_{max} values that were much lower in the new FatA alleles. Q215W and T182W were selected for further studies as improved and deficient alleles of *Ha*FatA respectively.

2.3. Transient expression in tobacco leaves

Methods for stable transformation of plants are time-consuming and expensive, although they are necessary for the production of transgenic crops. However, the transient expression is a more immediate way to obtain rapid information about the functionality of genes. The transient expression of transgenes in leaves was first introduced by Kapila et al. (1997). With this technique, nuclei of permissive cells (Zipfel et al., 2006) are transformed via infiltration of abaxial air-spaces with *Agrobacterium* cultures harbouring expression constructs within T-DNA borders. Expression of transgenes in leaves is significantly enhanced by the co-infiltration of the

viral suppression proteins P19 which prevents host transgene silencing (Voinnet et al. 2003). WT *Ha*FatA, T182W and Q125W complete cDNAs were transferred for their overexpression to Gateway-compatible binary vector pB2GW7where inserted sequences are transcribed to the outside of the T-DNA. Single T-DNA inserts will then usually result in the overexpression of the transgene (Karimi et al., 2002). These constructs were agroinfiltrated into *Nicotiana benthamiana* leaves in the presence of the P19 viral suppressor protein and the *HaFatA* expression analysis was carried out four days later (Figure 3). For all the constructs a specific-single band was observed corresponding to *HaFatA* gen in the treated leaves, pointing to the overexpression was successful.

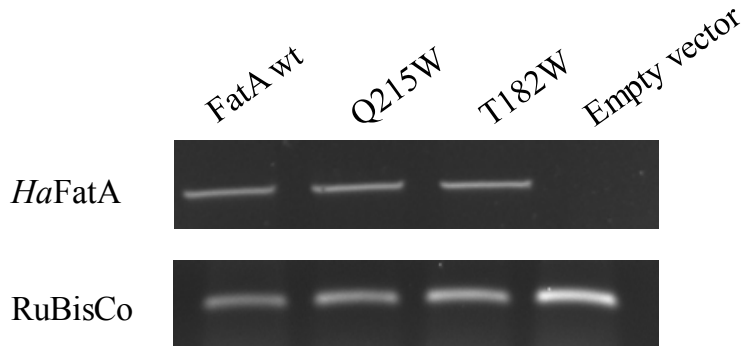

Figure 3. Expression analysis of *Ha*FatA alleles on tobacco leaves. RuBisCo gen was used as positive control.

2.4. Lipid analysis

Nicotiana benthamiana leaves are very active at synthesizing lipids, so they are a good model to test alterations in fatty acid metabolism. The expression of sunflower functional FatAs (*Ha*FatA and Q215W) in tobacco leaves did not increase the absolute amount of fatty acids respect to the controls (leaves transformed with the empty vector or T182W) (Figure 4A). However, it altered the total content of leaf triacylglycerols (TAGs) by 2-fold and 4-fold respectively when WT FatA and Q215W were expressed (Figure 4B). The amount of TAGs represents a small part of the leaf lipids, which

amount was regulated differently than the most abundant chloroplastic or membrane lipids. The first logical consequence of overexpression of a functional thioesterase in plant cells is an increment of the flux of acyl moieties that are transported out of the plastid and a restriction of substrates fated to the synthesis of prokaryotic lipids. These changes in metabolic flux did not affect to polar lipids component of the cell membrane and photosynthetic machinery (data not shown), which indicated that the content of functional and structural lipids is strongly regulated in leaves and that there are mechanisms that control the amount of these lipids in plant cells. Thus, when FatB from Arabidopsis was knocked-out there was an increase of both the rates of synthesis and degradation of lipids in order to equilibrate the deficiency of saturated fatty acids in the eukaryotic lipid pathway (Bonaventure et al., 2004). Nevertheless it seemed that leaf TAGs were not affected by this regulatory mechanism, so their amount on a fresh weight basis was affected by the expression of exogenous thioesterases and by their activity level. In this regards, the increase in TAG content was almost doubled when leaves were transformed with the construct Q215W. This result is in agreement with the kinetic characterization of Q215W thioesterase, which displayed the higher catalytic efficiency for most substrates (Table 1). The transient expression of other enzymes involved in TAG biosynthesis produced an effect similar to that described in these results. Thus, transient expression of acyl-CoA-diacylglycerol acyltransferase 1 gene from Arabidopsis also increased the tobacco leaf TAG fraction (Wood et al., 2009).

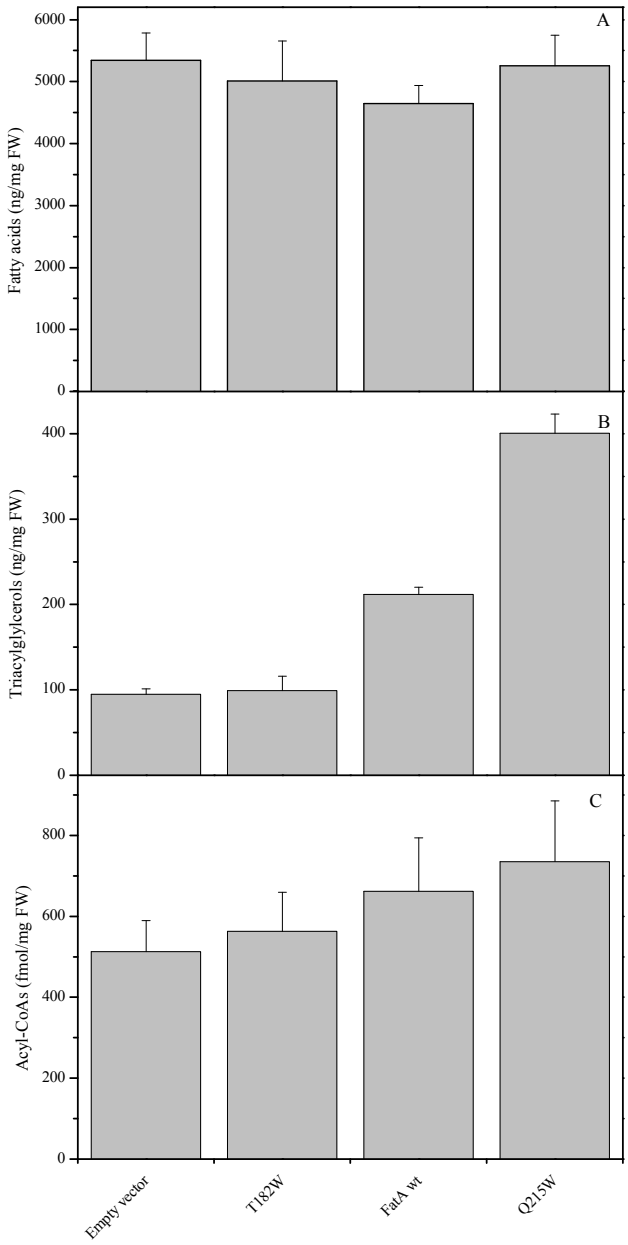

Figure 4. Total amount of fatty acids (A), triacylglycerols (B) and acyl-CoA esters (C). Data are the average of five independent samples.

Increases in the flux of fatty acid and glycerolipids synthesis should also affect the pool size of intermediate metabolites like acyl-CoAs, which are the ones connecting fatty acid and glycerolipids synthesis. The amount of the acyl-CoA pool was measured in control and transformed plants and not highly significant differences were observed in their absolute amount, although there was a higher average values in leaf expressing WT *Ha*FatA and Q215W (Figure 4C). The composition of the acyl-CoA pools were

also investigated, resulting a significant decrease of the short chained 8:0-CoA intermediate and a significant increase of 16:0-CoA and 18:0-CoA in lines expressing functional thioesterases (Figure 5).

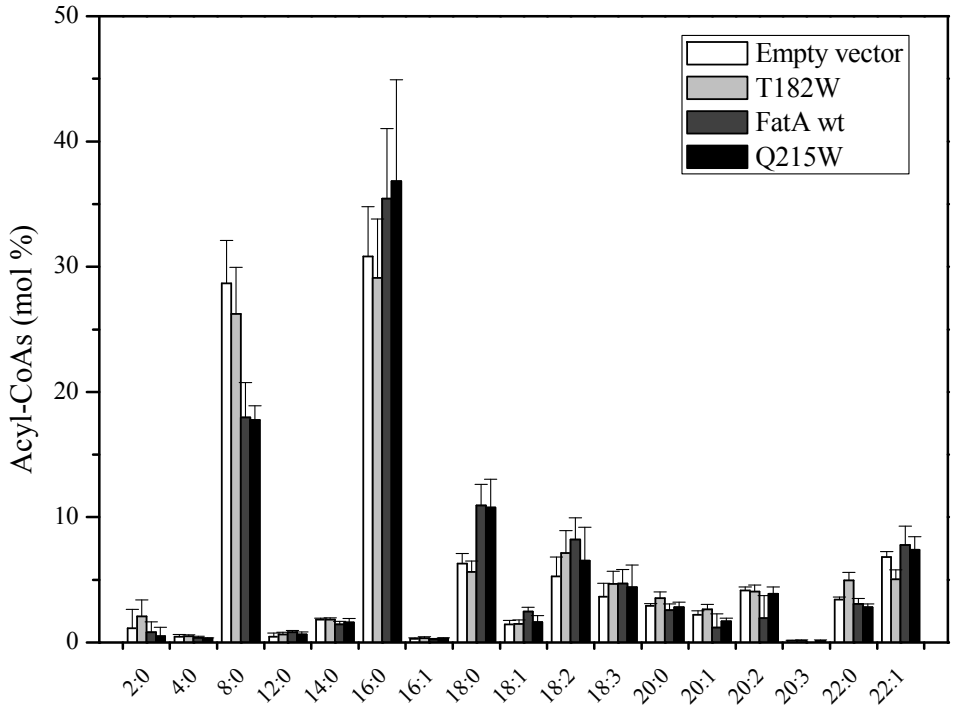

Figure 5. Acyl-CoA esters composition (mol%). Data are the average of five independent samples.

So it seems that recombinant thioesterases increased the export of saturated fatty acid moieties from the plastids. However, these results are maybe somewhat difficult to interpret because acyl-CoA is a very dynamic pool involved with many other synthetic and degradative pathways and punctual determinations only allow a fixed picture of the pool that usually not provide with enough information to explain all metabolic responses of the plant. The total fatty acid composition of the leaf tissue was determined and no significant differences where found neither in the total amount (Figure 4A) nor in the relative amount of each fatty acid (Figure 6A). These results differed from those observed in the triacylglycerol composition. The tissues agroinfiltrated with WT *Ha*FatA or Q215W displayed an increase in the relative fatty acid composition of saturated acyl moieties and a decrease of unsaturated ones (Figure 6B), which agreed with the acyl-CoA pool determinations.

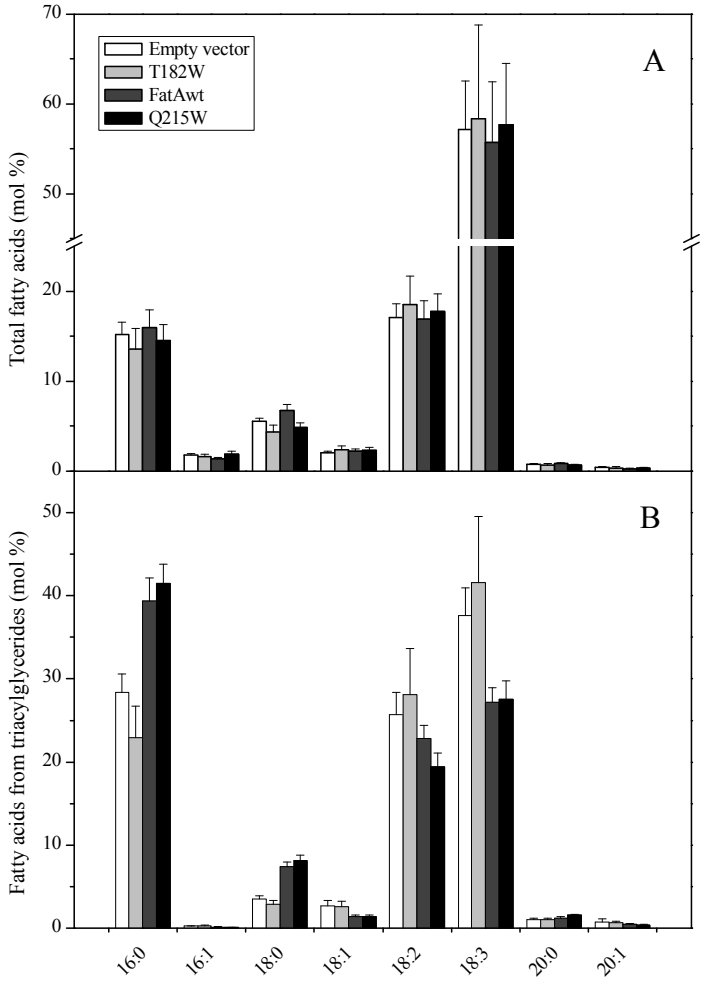

Figure 6. Fatty acid composition (mol %). Data are the average of five independent samples.

The composition of the fatty acids exported from plastids depends of the affinity of the enzymes that compete for the acyl-ACP substrates. The primary product of fatty acid synthesis, 16:0-ACP, can undergo one of three competing reactions: hydrolysis by acyl-ACP thioesterase, transfer to plastidial lysophosphatidic acid or elongation to 18:0-ACP which is mostly desaturated to form 18:1-ACP. The 18:1-ACP can be incorporated into the "prokaryotic" pathway by the action of glycerol-3-phosphate acyltransferase (GPAT) or hydrolyzed by acyl-ACP thioesterase. On the contrary, the 18:0-ACP is not incorporated into the prokaryotic pathway and only can be desaturated to form 18:1-ACP or directly hydrolyzed and exported out of the plastid. In leaves the de novo synthesized lipids flux going into the prokaryotic pathway is quantitatively higher than that synthesized by the same pathway in seeds. Although the acyl-ACP thioesterases that have been expressed corresponded to type A thioesterases, which displays high specificity towards 18:1-ACP, the 18:1-ACP is probably well hydrolyzed at high rates

by endogenous *N. benthamiana* thioestherases and its flux was probably not altered by the expression of the exogenous thioesterases. Saturated acyl-ACPs are exported in a high proportion by thioesterases of the B type (Bonaventure et al., 2003) and their export was more limited when the extra functional thioesterases were introduced. This explains why the relative amount of unsaturated fatty acids in TAGs decrease respect to saturated ones. Figure 7 shows the relative triacylglycerol species composition. TAG species containing two saturated fatty acids increased in tissues agroinfiltrated with WT *Ha*FatA and Q215W at expenses of species containing unsaturated acyl moieties, in good agreement with results in Figure 6B.

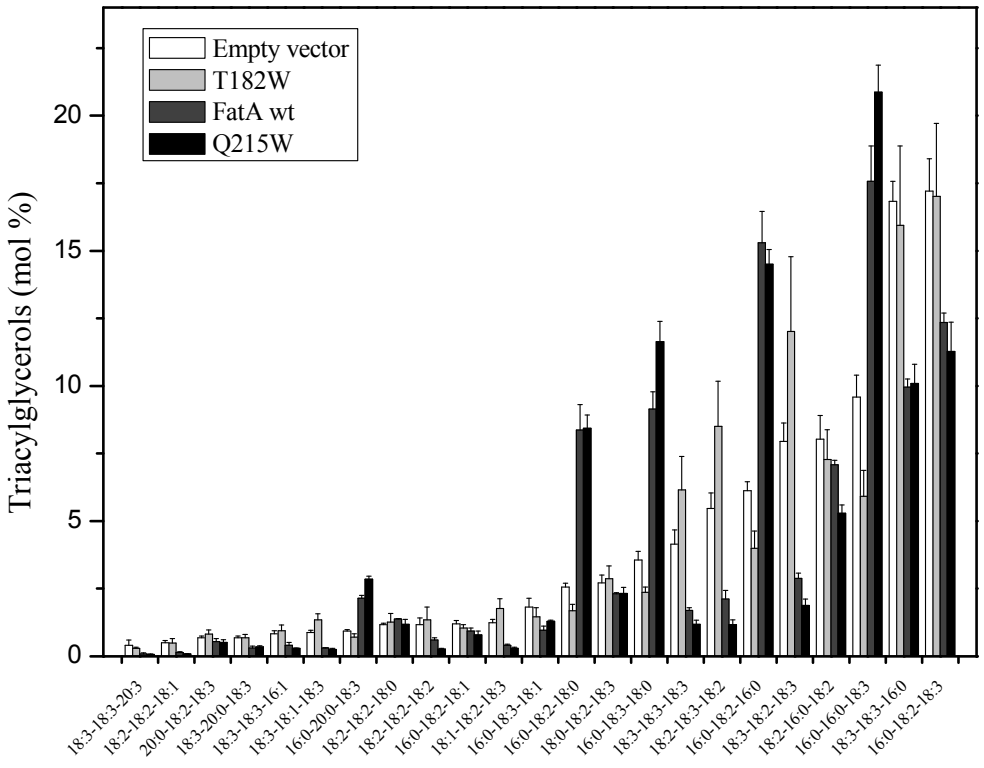

Figure 7. Triacylglycerols composition (mol%). Data are the average of five independent samples. Triacylglycerols species lower than 0.25% are not showed in the figure.

The diacylglicerol (DAG) pool was also analyzed (Figure 8) and no significant differences were displayed. This pool is also very variable due to it depends on the equilibrium of several metabolic reactions were DAG are involved.

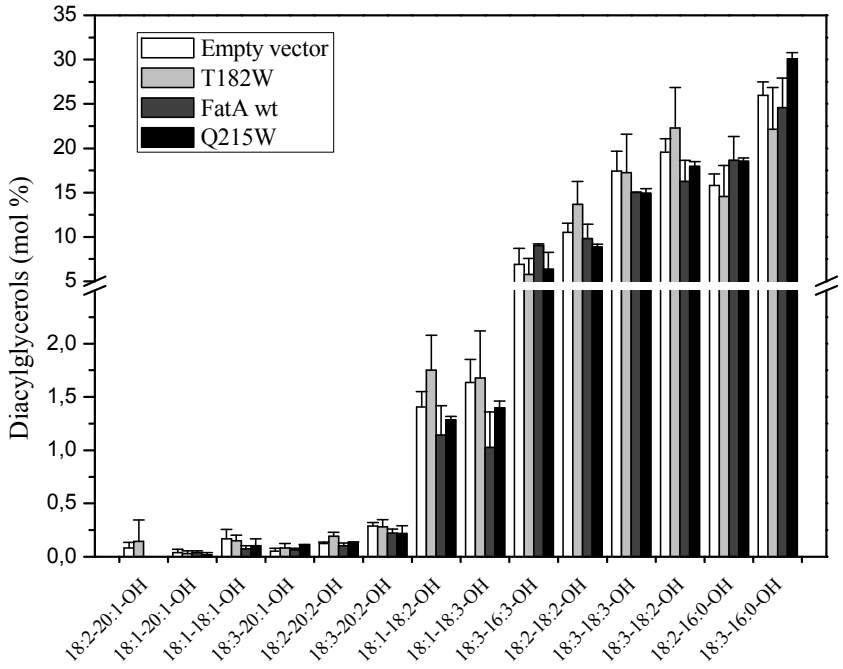

Figure 8. Diacylglycerols composition (mol %). Data are the average of five independent samples.

2.5. HaFatA-GFP fusion protein localization

Using a neural network based method for identify chloroplast transit peptides, ChloroP (Emanuelsson et al., 1999), was determined that *Ha*FatA preprotein exhibit a chloroplastic transit peptide that corresponded to the first 55 amino acids (Serrano-Vega et al., 2005). Unlike thioesterase type B, type A does not present any hydrophobic N-terminal domain involved in the anchorage to plastid membranes (Jones et al., 1995; Facciotti and Yuan, 1998; Sánchez-García et al., 2010). Thus, FatA protein is a soluble protein located in the plastid stroma. To detect the localization in vivo, full length *Ha*FatA cDNA was cloned into a vector that fuses Green Fluorescence Protein (GFP) in the C-terminal protein extreme. *Ha*FatA-GFP fusion protein transiently expressed in tobacco leaves was punctually localized in chloroplast (Figure 9A) although a weak fluorescent background appears around the studied organelles. Chloroplasts were visualized by chlorophyll autofluorescence and appear in red (Figure 9B). Moreover, the overlay is showed in Figure 9C where the co-localization was confirmed. These results indicate that effectively the transit peptide of the preprotein is sufficient for it to be imported into plastids.

Plant de novo fatty acid biosynthesis is catalyzed by a fully dissociated type-2 fatty acids synthase (FAS) complex (Ohlrogge and Jaworski, 1997). This process is

compartmented and it mostly takes place in the stroma of plastids or chloroplasts. Some components of the machinery for fatty acid biosynthesis like the plastidial isoform of acetil-CoA carboxilase or the ACP, which is a cofactor of acyl-ACP:glycerol-3-P acyltransferase, are preferentially bound to the thylakoid membranes (Kannangara and Jensen, 1975; Slabas and Smith, 1988). Furthermore, plastid ω3 fatty acid desaturase FAD7, which is responsible for the synthesis of trienoic fatty acid, is also majority localized in thylakoid membranes (Andreu et al., 2007), suggesting that thylakoids could also be sites of fatty acid biosynthesis and desaturation in plants. The fluorescence pattern of *Ha*FatA-GFP fusion protein proved a specific localization into the plastid, pointing to the acyl moieties are transported out of the plastid by a unique point in each organelle.

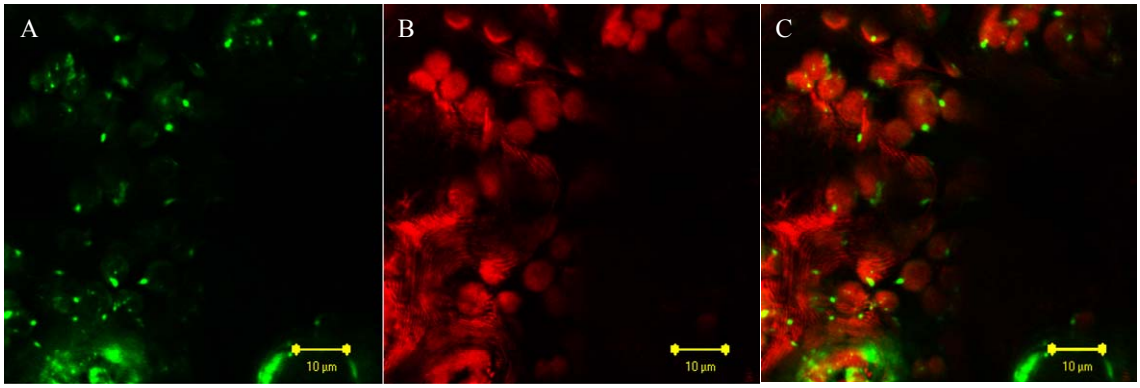

Figure 9. Chloroplast localization of *Ha*FatA-GFP fusion after transient expression in leaves of *N. benthamiana.* A: GFP fluorescence; B: Chlorophyll autofluorescence (in red); C: Overlay.

3. Experimental

3.1. Biological material

Helianthus annuus and *Nicotiana benthamiana* plants were cultivated in growth chambers at 25 ºC/15 ºC (day/night cycles), with a 16 h photoperiod and a photon flux density of 300 µmol m^{-2} s^{-1}. The *E. coli* strain XL1-Blue (Stratagene) was used as host for the expression of *Ha*FatA alleles and the *Agrobacterium tumefaciens* strain GV 3101 was used for agroinfiltration. Bacteria were grown at 37ºC in LB medium (1% tryptone, 0.5% yeast extract, 1% NaCl, pH 7) with the appropriate antibiotic addition. All liquid cultures were growth with vigorous shaking.

3.2. FatA site-directed mutagenesis

The *HaFatA* coding sequence (Accession number: AY078350; Serrano-Vega et al., 2005) without signal peptide, was cloned into pQE-80L expression vector (Quiagen) using primers with internal *Sac*I and *Kpn*I restriction sites (SacI-FatA: 5'- GAGCTCA-TGGCGGTGAAGGTTGATGAGCAGC-3'; KpnI-FatA: 5'- GGTACCTTTTTTTGC-GGGTTTTTTCCTCCATTCAGTGCG-3'). The construct was designated pQE-FatA. Several point mutations in the *FatA* gene were carried out, pQE-FatA construct and the QuickChange Site-Directed Mutagenesis Kit (Stratagene) were used for this objective. The amino acids mutated were: L118, T172, T182, R184, M206 and Q215. All of them were mutated to tryptophan using the following primers in the mutagenesis: L118W, 5'-GAGACGATTGCGAATCTGTGGCAGCAGGAGGTAGGAGGAAATCATGC -3'; T172W, 5' -GCGATGTGGTGGAAATTGAGTGGTGGTGTCAAGGTGAAGGG- 3'; T182W, 5'-GTTGAAGGGAGAATCGGGTGGAGACGTGATTGGATTATC-3'; R184W, 5'-GGGAGAATCGGGACTAGATGGGATTGGATTATCAAAGATC-3'; M206W, 5'-GCTACAAGCAAGTGGGTGTGGATGAACTCAGAAACTAGAAGAC-3'; Q215W, 5'-CTCAGAAACTAGAAGACTCTGGAAAGTCAATGACGATATAA-GAG-3. The mutated nucleotides are underlined.

3.3. Protein expression in E.coli and purification

Five hundred milliliter cultures of *E. coli* XL1-Blue cells harboring pQE-FatA were grown as described above. Expression of *Ha*FatA alleles were induced at OD600 0.6 by adding 1 mM IPTG and growth for 4 h. The cells were harvested by centrifugation for 10 min at 2500g, washed with distilled water and resuspended in 5 ml of Binding buffer (20 mM sodium phosphate, 500 mM NaCl, 20 mM imidazole, pH 7.4). Cells were lysed adding 0.5% Triton X-100, 5 mM DTT, 1 mM MgCl2, 1 mM PMSF, 20 µg/ml DNase I (Roche) and 0.2 mg/ml lysozyme (Roche) for 45 min at 4 ºC with shaking. The resulting lysed cell suspension was centrifuged at 25000g for 30 min. The supernatant was filtered through 0.22 µm filters and loaded onto a HisTrap FF 1 ml column (GE Healthcare) interfaced with an Äktaprime system (Amersham Bioscience). Histidine-tagged proteins were eluted from the column using an imidazole gradient

ranging from 20 to 500 mM. Fractions containing *Ha*FatA were subsequently used for thioesterase activity assays.

3.4. Gel electrophoresis of proteins

Protein samples were combined with SDS-PAGE loading buffer and heated at 95 ºC for 5 min. The samples were separated by electrophoresis on 4–12% NuPAGE Novex Bis-Tris gels in MES buffer (Invitrogen), and the gels were fixed and stained with 0.1% Coomassie R-250 in 40% ethanol, 10% acetic acid. Molecular weight standards used were obtained from GE Healthcare.

3.5. Preparation of acyl-ACP substrates

Labeled acyl-ACP substrates were prepared using a recombinant acyl-ACP synthetase from E. coli. Acylation reactions contained 50 µg of recombinant ACP form E. coli (Sigma), 180 kBq (approx. 0.1 µmol) of [1-14C] fatty acid ammonium salt ([3H] fatty acid in the case of 16:1Δ9), 5 mM ATP, 2 mM DTT, 400 mM LiCl2, 10 mM MgCl2, 100 mM Tris-ClH pH 8.0 and 10 µg acyl-ACP synthetase, in a final volume of 0.5 ml. Reactions were carried out at room temperature for 3 h and the acyl-ACPs were purified and concentrated by ion exchange chromatography on DEAE-sepharose as described by Rock and Garwin (1979).

3.6. Acyl-ACP thioesterase assays

Thioesterase activity was assayed in 0.1 ml reactions containing 50 mM Tris-HCl pH 8.0, 5 mM DTT, 0.2-12 µg of the purified protein and the amount of acyl-ACP substrate ranging from 0.02 to 0.08 nmol (30-170 Bq approx.). Reactions were carried out at room temperature for 5 min and stopped by the addition of 0.25 ml of 1 M acetic acid in 2-propanol. Unesterified fatty acids were then extracted twice with 0.3 ml hexane, and the radioactivity in the pooled organic phase was determined in a calibrated liquid scintillation counter (Rackbeta II; LKB). The data from thioesterase assays was fitted to the Hill equation by nonlinear least-squares regression analysis using OriginPro

8 software, and correlated at P<0.005 as determined by Student's t-test. Both the V_{max} and K_m were derived from these curves.

3.7. Transient expression in Tobacco

For *Agrobacterium*-transient expression, HaFatA complete cDNAs corresponding to wild type allele and both T182W and Q215W mutants were amplified by PCR and cloned into pENTR Gateway vector (Invitrogen). Then, were transferred into the Gateway-compatible binary vector pB2GW7 (*Ha*FatA wt, T182W and Q125W cDNAs) or pK7FWG2 (HaFatA wt cDNA) (Karimi et al., 2002). The 35S:p19 viral suppressor construct and the agroinfiltration procedure were carried out according to Voinnet et al. (2003). Disk were punched from tobacco leaves 4 days after *Agrobacterium* infiltration and analyzed.

3.8. RNA preparation and cDNA synthesis

Approximately 0.25 g of tobacco leaves were ground in liquid nitrogen using a precooled sterile mortar and pestle. Total RNA was isolated using the RNeasy Mini Kit (Quiagen). RNA samples were treated with DNAseI (Promega) and this DNA-free RNA (1µg) was retrotranscribed with oligo(dT) primer and SuperScript II RT (Invitrogen).

3.9. Checking of transient expression

PCR techniques were used to check the expression of *HaFatA* using specific pair of primers FatA-F (5'-CACCATGCTCTCCAGAGGTGTTCCGACCG-3') and FatA-R (5'-TTATTTTTTTGCGGGTTTTTTCCTCC-3'). RuBisCo gen from tobacco was used as reference and the specific pair of primers Rub-F (5'-TGGCTTCCTCAGTTCTTCC-3') and Rub-R (5'-AAAAGGTACTCAACTTCACTA-3') were used.

3.10.Lipid analysis

Agroinfiltrated-tobacco leaves were harvested four days after infiltration for lipid analysis. The samples were ground and fatty acid composition was determined via

acid-catalysed transmethylation and analysed by gas-chromatography with flame ionization detection (GC8000 Top, Thermoquest Separation Products, Manchester, UK), fitted with a 30 m long 0.25 mm ID SGE BPX70 column (SGE, Milton Keynes, UK). Helio was used as a carrier gas at 1 ml min^{-1} with a 30:1 split ratio. The oven was run isothermally at 110ºC for 1 min, then ramped to 180ºC at 20ºC min^{-1} then to 221ºC at 2.5ºC min^{-1} (Larson and Graham, 2001). The pool of acyl-CoAs was determined by HPLC using the method of Larson and Graham (2001) with modifications (Larson et al., 2002), and neutral lipids were analyzed by LC/MS/MS according to Burgal et al. (2008).

3.11. GFP-fusion protein imaging

Sample leaves imaging was carried out on a Zeiss LSM 510 META laser scanning confocal equipped with a Zeiss Axioplan 2 microscope (Carl Zeiss Ltd, Welwyn Garden City, UK). Images were acquired using a Plan-Neofluar 20x/0.5 or a Plan-Apochromat 63x/1.4 Oil immersion DIC objective. Imaging of GFP and chlorophyll emission was performed by sequential scanning. GFP was excited with the 488nm line of a 30mW argon laser and the emission collected through a 505-530bp emission filter. Chlorophyll was excited with a 1mW 543nm Helium Neon laser and the emission collected through a 560 long pass emission filter. Images were taken at Nyquist resolution with 8 line averaging.

Acknowledgements

We are thankful to Rosario Sánchez and Valeria Gazda for their technical assistance. We also thank Joanne Marrison (Technology Facility Department of Biology, University of York) for help with the confocal microscope. This work was supported by the MICINN and FEDER (Project AGL2008-01086/ALI).

References

Andreu, V., Collados, R., Testillano, P.S., Risueño, M.C., Picorel, R. and Alfonso, M. (2007) In situ molecular identification of the plastid ω3 fatty acid desaturase FAD7 from soybean: evidence of thylakoid membrane localization. Plant Physiol. 145, 1336-1344.

Bonaventure, G., Bao, X., Ohlrogge, J. and Pollard, M. (2004) Metabolic responses to the reduction in palmitate caused by disruption of the FATB gene in Arabidopsis. Plant Physiol. 135, 1269-1279.

Bonaventure, G., Salas, J.J., Pollard, M.R. and Ohlrogge, J.B. (2003) Disruption of the FATB gene in Arabidopsis demonstrates an essential role of saturated fatty acids in plant growth. Plant Cell 15, 1020-1033.

Burgal, J., Shockey, J., Lu, C., Dyer, J., Larson, T., Graham, I. and Browse J. (2008) Metabolic engineering of hydroxy fatty acid production in plants: RcDGAT2 drives dramatic increases in ricinoleate levels in seed oil. Plant Biotechnol. J. 8, 819-831.

Cahoon, E.B. and Shanklin, J. (2000) Substrate-dependent mutant complementation to select fatty acid desaturase variants for metabolic engineering of plant seed oils, Proc. Natl. Acad. Sci. USA 97, 12350-12355.

Dehesh, K., Jones, A., Knutzon, D.S. and Voelker, T.A. (1996) Production of high levels of 8:0 and 10:0 fatty acids in transgenic canola by overexpression of ChFatB2, a thioesterase cDNA from *Cuphea hookeriana*. Plant J. 9, 167-172.

Dörmann, P., Kridl, J.C. and Ohlrogge, J.B. (1994) Cloning and expression in *Escherichia coli* of a cDNA coding for the oleoyl-acyl carrier protein thioesterase from coriander (*Coriandrum sativum* L.). Biochim. Biophys. Acta - Lipids and Lipid Metabolism 1212, 134-136.

Emanuelsson, O., Nielsen, H. and Von Heijne, G. (1999) ChloroP a neural network-based method for predicting chloroplast transit peptides and their cleavage sites. Protein Sci. 8, 978-984.

Facciotti, M.T. and Yuan, L. (1998) Molecular dissection of the plant acyl-acyl carrier protein thioesterases. Fett Lipid 100, 167-172.

Facciotti, M.T., Bertain, P.B. and Yuan, L. (1999) Improved stearate phenotype in transgenic canola expressing a modified acyl-acyl carrier protein thioesterase. Nature Biotech. 17, 593-597.

Jones, A., Davies, H.M. and Voelker, T.A. (1995) Palmitoyl-acyl carrier protein (ACP) thioesterase and the evolutionary origin of plant acyl-ACP thioesterases. Plant Cell 7, 359-371.

Kannangara, C.G. and Jensen, C.J. (1975) Biotin carboxyl proteinin barley chloroplast membranes. Eur. J. Biochem. 54, 25-30.

Kapila, J., DeRycke, R., VanMontagu, M. and Angenon, G. (1997) An Agrobacterium-mediated transient gene expression system for intact leaves. Plant Sci. 122, 101-108.

Karimi, M., Inzé, D. and Depicker, A. (2002) GATEWAY vectors for Agrobacterium-mediated plant transformation. Trends Plant Sci. 7, 193-195.

Koo, A.J.K., Ohlrogge, J.B. and Pollard, M. (2004) On the export of fatty acids from the chloroplast. J. Biol. Chem. 279, 16101-16110.

Larson, T.R. and Graham, I.A. (2001) A novel technique for the sensitive quantification of acyl CoA esters from plant tissues. Plant J. 25, 115-125.

Larson, T.R., Edgell, T., Byrne, J., Dehesh, K. and Graham, I.A. (2002) Acyl CoA profiles of transgenic plants that accumulate medium-chain fatty acids indicate inefficient storage lipid synthesis in developing oilseeds. Plant J. 32, 519-527.

Lindqvist, Y., Huang, W., Schneider, G. and Shanklin, J. (1996) Crystal structure of delta9 stearoyl-acyl carrier protein desaturase from castor seed and its relationship to other di-iron proteins. EMBO J. 15, 4081-4092.

Mayer, K.M. and Shanklin, J. (2005) A structural model of the plant acyl-acyl carrier protein thioesterase FatB comprises two helix/4-stranded sheet domains, the N-terminal domain containing residues that affect specificity and the C-terminal domain containing catalytic residues. J. Biol. Chem. 280, 3621-3627.

Mayer, K.M. and Shanklin, J. (2007) Identification of amino acid residues involved in substrate specificity of plant acyl-ACP thioesterases using a bioinformatics-guided approach. BMC Plant Biol. 7, 1.

Ohlrogge, J.B. (1994) Design of new plant products: engineering of fatty acid metabolism. Plant Physiol. 104, 821-826.

Ohlrogge, J.B. and Jaworski, J.G. (1997) Regulation of fatty acid synthesis. Annu. Rev. of Plant Physiol. Plant Mol. Biol. 48, 109-136.

Rawsthorne, S. (2002) Carbon flux and fatty acid synthesis in plants. Prog. Lipid Res. 41, 182-196.

Rock, C.O. and Garwin, J.L. (1979) Preparative enzymatic synthesis and hydrophobic chromatography of acyl-acyl carrier protein. J. Biol. Chem. 254, 7123-7128.

Salas, J.J. and Ohlrogge, J.B. (2002) Characterization of substrate specificity of plant FatA and FatB acyl-ACP thioesterases. Arch. Biochem. Biophys. 403, 25-34.

Sánchez-García, A., Moreno-Pérez, A.J., Muro-Pastor, A.M., Salas, J.J., Garcés, R. and Martínez-Force, E. (2010) Acyl-ACP thioesterases from castor (*Ricinus communis* L.): an enzymatic system appropriate for high rates of oil synthesis and accumulation. Phytochem. 71, 860-869.

Serrano-Vega, M.J., Garcés, R. and Martínez-Force, E. (2005) Cloning, characterization and structural model of a FatA-type thioesterase from sunflower seeds (*Helianthus annuus* L.). Planta 221, 868-880.

Slabas, A.R. and Smith, C.G. (1988) Immunogold localization of acyl carrier protein in plants and *Escherichia coli* evidence of membrane association in plants. Planta 175, 145-152.

Voelker, T.A., Jones, A., Cranmer, A.M., Davies, H.M. and Knutzon D.S. (1997) Broad-range and binary-range acyl-acyl-carrier-protein thioesterases suggest an alternative mechanism for medium-chain production in seeds. Plant Physiol. 114, 669-677.

Voelker, T.A., Worrell, A.C., Anderson, L., Bleibaum, J., Fan, C., Hawkins, D.J., Radke, S.E. and Davies, H.M. (1992) Fatty acid biosynthesis redirected to medium chains in transgenic oilseed plants. Science 257, 72-74.

Voinnet, O., Rivas, S., Mestre, P. and Baulcombe, D. (2003) An enhanced transient expression system in plants based on suppression of gene silencing by the p19 protein of tomato bushy stunt virus. Plant J. 33, 949-956.

Wood, C.C., Petrie, J.R., Shrestha, P., Mansour, M.P., Nichols, P.D., Green, A.G. and Singh, S.P. (2009) A leaf-based assay using interchangeable design principles to rapidly assemble multistep recombinant pathways. Plant Biotechnol. J. 7, 914-924.

Yuan, L., Nelson, B.A. and Caryl, G. (1996) The catalytic cysteine and histidine in the plant acyl-acyl carrier protein thioesterases. J. Biol. Chem. 271, 3417-3419.

Yuan, L., Voelker, T.A. and Hawkins, D.J. (1995) Modification of the substrate specificity of an acyl-acyl carrier protein thioesterase by protein engineering. Proc. Natl. Acad. Sci. USA 92, 10639-10643.

Zipfel, C., Kunze, G., Chinchilla, D., Caniard, A., Jones, J.D.G., Boller, T. and Felix, G. (2006) Perception of the bacterial PAMP EF-Tu by the receptor EFR restricts Agrobacterium-mediated transformation. Cell 125, 749-760.

BLOQUE II

Phospholipase Dα from sunflower (*Helianthus annuus*): cloning and functional characterization.

Moreno-Pérez, A.J., Martínez-Force, E., Garcés, R., Salas, J.J.

Instituto de la Grasa (CSIC), Av. Padre García Tejero, 4 41012, Seville, Spain.

Published in *Journal of Plant Physiology*
J. Plant Physiol. (2010), 167:503-511

Abstract

D type phospholipases (PLD) are enzymes that hydrolyze the head group of phospholipids to produce phosphatidic acid. This activity is ubiquitous in plant tissues, and it has been isolated and characterized from different species and organs. On the basis of their gene sequences several families of these proteins have been described in plants (PLD α, β, γ, δ, ζ and ε), and they have been shown to be involved in many metabolic events, such as the response to abiotic stress, signal transduction, and membrane lipid turnover and degradation. In the present study, PLD activity was measured in the soluble fractions isolated from different organs of this plant. A PLD of α type was cloned from leaf cDNA that was responsible for most of this activity. The gene encoding this 810 aa protein was heterologously expressed in *E. coli*. This protein was not lethal for the eukaryotic host, although it altered its profile of phospholipids. PLDα was purified to almost homogeneity by His-tag affinity chromatography, displaying an optimum pH of 6.5 and strong dependence on the presence of Ca^{2+} and SDS in the assay medium. The enzyme was active towards phosphatidyl choline, phosphatidyl ethanolamine and phosphatidyl glycerol. Furthermore, *HaPLDα* gene was found to be expressed at high levels in leaf and stem tissues.

1. **Introduction**

The type D Phospholipases (PLD; E.C. 3.1.4.4) are enzymes that are widely distributed in plants and that catalyze the hydrolysis of esterified polar moieties of the phosphate group of the most common phospholipids, such as phosphatidylcholine (PC) or phosphatidylethanolamine (PE; Pappan and Wang, 1999a). This reaction releases a polar compound such as choline or ethanolamine, and a phosphatidic acid (PA) molecule and in the presence of organic alcohol, it also can occur as alcoholysis. From a molecular point of view, plant PLDs can be classified into six gene families that have been denominated with the initial letters of the greek alphabet on the basis of the order in which they were discovered: PLDα, β, γ, δ, ζ and ε (Wang, 2000 and 2005). All these forms of the enzyme, except PLDζ, share the Ca^{2+} binding domain (C2 domain) and two catalytic HxKxxxD motifs that are typical of phospholipid metabolizing enzymes from plants, yeast and mammals. PLDζ does not carry the C2 domain but rather the so-called PH (phox homology) and PX (pleckstrin homology) domains, sites of interaction with phosphoinositides. PLDβ and γ also have phosphatidylinositol biphosphate (PIP2) binding domains, as well as a myristoylation site in the case of PLDγ (Wang, 1997). Furthermore, PLDβ and γ depend on the presence of PE to achieve maximum activity, whereas PLDζ depends on the presence of free fatty acids (Zhang et al., 2003).

In plant tissues, PLDα is the most active enzyme of this family (Zhang et al., 2004), and it has been associated with the catabolism and turnover of membrane lipids (Wang, 2002 and 2005). Furthermore, there is clear evidence that it participates in signal transduction during plant metabolism. In this regard, PLDα is inhibited by Gα proteins that produce important secondary messengers in plant abscisic acid (ABA) phytohormone signal transduction pathways. Suppression of PLDα in Arabidopsis increases the time during which ABA promotes leaf senescence (Fan et al., 1997) and similar studies also demonstrated a role for this enzyme in plant responses to abiotic stress. Thus, a reduction of PLDα in leaves hampers stomatal closure induced either by ABA or water loss, reducing the plants resistance to osmotic stress. By contrast, overexpression of this enzyme induces the response to ABA and stomatal closure to avoid water loss (Sang et al, 2001; Wang, 2005). An increase in freezing tolerance is also caused by the suppression of PLDα in *Arabidopsis thaliana* leaves, indicating that the enzyme contributes to the destruction of cell membranes characteristic of freezing

damage (Welti et al., 2002; Rajashekar et al., 2006). This result contrasted with the increase in susceptibility to freezing due to the suppression of PLDγ (Li et al., 2004), indicating that this enzyme was possibly involved in the transduction of the response to freezing or other abiotic stresses in Arabidopsis. An analysis of the lipid profile in the PLDα-knockout mutant provided further evidence that PLDα is involved in glycerolipid degradation, since lower levels of phosphatidic acid (PA) and lysophosphatidic acid (LPA) were evident in the flowers, seeds and roots (Devaiah et al., 2006). PLDα is located in the cytoplasm and vacuoles, and it is usually associated with the plasma membrane or endoplasmic reticulum (Xu et al., 1996; Young et al., 1996).

PLDα enzymes have been characterized from a wide number of species like castor, tomato, cabbage, grapes and oilseed rape (Wan et al., 2007; Kim et al., 1999; Novotna et al., 2000; Xu et al., 1996; Whitaker et al., 2001). In sunflower, PLDα has been examined in seedling extracts to assess the influence of the acyl chain composition of PC on enzyme activity (Abousalham et al., 1997). The highest activity was found on PC containing short chained fatty acids (C6 to C8). Thus, PLDα could be an important enzyme for stress responses in sunflower. Furthermore, we cloned a PLDα from sunflower leaves that was expressed at high levels in other tissues. This enzyme presented the typical amino acid domains of the alpha type phospholipases, an acidic optimum pH value and maximum activity in the millimolar range of Ca^{2+}, with high activity towards PC and PE and no activity for phosphatidylinositol (PI) degradation. The study was completed by assaying total PLD in different organs and comparing these results with the expression of the gene.

2. Materials and methods

2.1. Biological material.

Sunflower (*Helianthus annuus* L.) plants were cultivated on soil in growth chambers at 25ºC/15ºC (day/night cycles), with a 16 h photoperiod and a photon flux density of 200 µmol $m^{-2}s^{-1}$. The *E. coli* strain XL1-Blue (Stratagene) was used as the plasmid host for *Ha*PLDα protein expression and production. The bacteria were grown in LB medium (1% Bacto Tryptone, 0.5% Bacto Yeast Extract, 1% NaCl, pH 7) at 37ºC with shaking, and plasmid selection was performed in the presence of ampicillin (100 µg).

2.2. Enzyme extracts preparation.

Enzyme extracts were prepared by grinding 0.25 g of tissue in 2.5 mL of ice cooled 50 mM Tris pH 8.0, 5 mM DTT using a glass homogenator. Homogenates were centrifuged for 15 min at 12,000g in a centrifuge at 5ºC. Enzyme activity was assayed in the resulting supernatant. Vegetative tissues were dissected from young plants that were approximately 1 month old.

2.3. Enzyme assay.

The standard PLD assay involved incubating radiolabelled PC with the active enzyme extract followed by thin layer chromatography fractionation of the lipid products to determine the relative conversion into PA. Typical assay mixtures contained 100mM MES pH 6.5, 10 mM $CaCl_2$, 0.5 mM SDS, 0.4 mM PC (from soybean, Sigma-Aldrich), 0.46 KBeq 1-[^{14}C] dipalmitoyl-PC (4.11 GBeq/mmol) and sufficient enzyme to produce the transformation of 5 to 10% of the initial substrate (10 to 50 μg of protein in the case of leaf extracts in a final volume of 0.1 mL). All phospholipids were dissolved in acetonitrile. The reactions were stopped by adding 50 μL of glacial acetic acid and the lipids were extracted by adding 2 mL of hexane/2-propanol 3:2 plus 0.85 mL of aqueous Na_2SO_4 6.7%. The upper organic phase was transferred to a clean tube and evaporated under nitrogen. The residue was resuspended in 0.1 mL of chloroform and fractionated on a silica gel G60 TLC plate (Merck) using chloroform/methanol/acetic acid/water (85:15:10:3.5) as the solvent. The relative incorporation of radioactivity in the bands corresponding to PA and PC was quantified in a betascope Instant Imager (Packard). The studies of substrate specificity were carried out using a HPLC-based assay. In this case the final volume of the reaction mixture was scaled up ten-fold and no radiolabelled substrate was included. Once reactions were stopped with 0.1 mL of glacial acetic acid, the lipids were extracted with 5 mL of hexane/2-propanol 3:2 plus 1.5 mL of aqueous Na_2SO_4 6.7%. The organic phase was evaporated under nitrogen, resuspended in 0.25 mL of the same solvent and analyzed by HPLC on the same system described above but applying a rapid analysis involving the isocratic elution of the column with hexane/2-PrOH/water/acetic/triethyl amine (50:45:5:1:0.08). Activity was calculated based on the quantification of the PA formed from the phospholipid substrate supplied to the reaction.

2.4. mRNA preparation and cDNA synthesis.

Sunflower leaf tissue (0.25 g, young expanding leaves 5-8 cm) was ground in liquid nitrogen in a precooled sterile mortar. Total RNA was extracted using a Spectrum Plant Total RNA Kit (Sigma) and mRNA was isolated from the total RNA using the GenElute mRNA Miniprep Kit (Sigma). The mRNA pellet was resuspended in 33 µl RNAase free TE buffer (10 mM Tris-HCl, 1 mM EDTA [pH 8]) and the corresponding cDNA was synthesized using the Ready-To-Go T-Primed First-Strand Kit (Amersham Biosciences).

2.5. Sunflower PLDα cloning.

PLDα protein sequences from the public database were aligned to identify regions of homology using the ClustalX v2.0.5 program (Thompson et al., 1997). A PCR fragment was amplified with a forward degenerate primer and a specific reverse primer, both designed from highly conserved regions of PLDαl peptides: FPLD1 (5'-GGCGGNCCCCGCGAACCGTGG-3') and RPLD1 (5'-TGGTTGGTAGGCGCCCAT-TGC-3'). Both the 5' and 3' ends of the cDNA were obtained using the Smart-RACE cDNA amplification kit (Clontech) and the internal oligonucleotides: F1PLDa, 5'-GATTGATGGTGGGGCCGC-3'; F2PLDa, 5'-CCGATGTGGCCCGAAGGG-3'; R1PLDa, 5'-GTCAGGCCGTTCAGATGG-3'; R2PLDa, 5'-CCATGCGTACGAGCT-TCC-3'; and R3PLDa 5'-CGGTTCGCGGGGTCCGCC-3'. The PCR fragments were cloned into the pMBL-T vector (MBL), sequenced by Secugen (Madrid, Spain) and their identities were confirmed using the BLAST software (Altschul et al., 1990). Primers with internal *Sac*I and *Kpn*I restriction sites were designed to amplify the coding region of the mature protein by PCR: PLDa-SacI (5'-GCCGAGCTCGCTCAG-AAGACACATCTCC-3') and PLDa-KpnI (5'-GGCGGTACCCTATGAGGTAAGAA-TTGG-3'). The PCR product obtained was subcloned into the *Sac*I-*Kpn*I sites of pQE-80L (Quiagen, Hilden, Germany) to produce a fusion protein with a six His amino acid tag at the N terminus. Ligation into the correct reading frame was confirmed by sequencing and the resulting construct was designated pQEPLDa. The recombinant plasmids were introduced and expressed in the XL1-Blue *E. coli* strain.

2.6. Preparation of E. coli lysates.

E.coli XL1-Blue cells carrying pQEPLDa were grown in LB medium containing ampicillin (100 μg/ml) at 37ºC with agitation. When an OD_{600} of 0.6 was reached, the cells were induced with 1mM isopropyl-*β*-D-thiogalactopyranoside (IPTG) and the cells were grown for an additional 4 hours. The cells from 100 ml of cultures were harvested by centrifugation for 15 min at 4,000g and resuspended in 5 ml of 20 mM sodium phosphate, 0.5 M NaCl, 30 mM imidazole, pH 7.4 (binding buffer). The cells were lysed in 0.5% Triton X-100, 5 mM DTT, 40 U/ml DNAse I, 0.2 mg/ml lysozyme, 1 mM PMSF and 1 mM $MgCl_2$ (lysis buffer), and incubated for 45 min at 4ºC with shaking. The resulting suspension was centrifuged at 39,000g for 30 min at 4ºC and the supernatant was filtered through 0.20 μm filters before it was transferred to a fresh tube. Polar lipids from *E. coli* were extracted as reported by Blight and Dyer (1959).

2.7. Polar lipid analysis.

Polar lipids from *E. coli* membranes were analyzed by HPLC (Salas et al., 2006). Lipid fractions were evaporated to dryness under nitrogen, dissolved in 0.25 mL hexane/2-PrOH 3:2 and submitted to analysis. The HPLC system used was a Waters separation module 2695, with a Waters ELSD 2420 detector. The separation of lipid classes was performed in a Lichrocart Diol column (Merk) that was initially equilibrated with Solvent A (hexane/2-PrOH/acetic acid/triethyl amine: 87/12/2/0.08) before a 25 mL gradient of solvent B (2-PrOH/water/acetic acid/triethyl amine: 85/15/2/0.08) was introduced to reach a misture of 60 % solvent A and 40 % solvent B. This proportion was maintained for 5 min and the column was then equilibrated again in solvent A for the next analysis. Temperature and flow were kept at 30ºC and 1mL/min throughout the analysis. The detector response was calibrated for quantification by injecting known amounts of standards of each lipid class.

2.8. Purification of HaPLDα.

The filtered soluble fraction was loaded onto Ni^{2+}-charged HisTrap FF columns (GE Healthcare) and the histidine-tagged proteins were purified according to the manufacturer's instructions.

2.9. Gel electrophoresis of proteins.

SDS-PAGE loading buffer was added to the protein samples, which were then heated at 95ºC for 5 min. The samples were separated by electrophoresis on 4-12% NU-PAGE gels in MES buffer (Invitrogen), and the gels were fixed and stained in 0.1% Coomassie R-250/40% ethanol/10% acetic acid. The broad range molecular weight standards used were obtained from GE Healthcare.

2.10. Western blotting.

The proteins previously separated by SDS-PAGE were transferred to nitrocellulose membranes of 0.45 µm pore size (Sigma-Aldrich) in Tris-Glycine buffer (12 mM Tris base, 96 mM glycine, 20% ethanol) using a XCell II mini-Cell system (Novex) run at 25 volts for 2 hours. The membrane was stained with Ponceau solution (Sigma-Aldrich) for 15 min and it was then washed with PBS (1.3 mM NaCl, 0.07 M Na_2HPO_4, 0.03 M NaH_2PO_4, [pH 7.6]) + Tween 20 (0.1%, PBST). The membrane was blocked using a solution of 5% non-fat dry milk in PBS for 1 hour and after washing three times for 5 min each in PBST, the membrane was incubated for two hours with a peroxidase conjugated monoclonal anti-polyHistidine antibody (Sigma-Aldrich) diluted 1/2000 in PBST containing 1% bovine serum albumin (BSA). The membrane was washed three times for 5 min each in PBST and antibody binding was visualized with the Pierce ECL Western Blotting Substrate kit according to manufacturer's instructions.

2.11. Genomic Southern blot analysis.

Genomic DNA was isolated from sunflower leaf tissue by the CTAB method (Murray and Thompson, 1980). Samples of genomic sunflower DNA (15 µg) were digested with restriction enzymes and resolved on a 0.8% agarose gel. The gel was soaked in 250 mM HCl for 30 min, washed three times in distilled water and finally, the gel was blotted onto a Hybond-N+ nylon transfer membrane (Amersham). The filter was probed with a 513 bp [α-^{32}P]dCTP-labelled *HaPLDα* gene-specific DNA fragment obtained by PCR amplification. Hybridization was performed in 0.2 mM potassium buffer, 250 mM SDS and 1 mM EDTA overnight at 65ºC and the filter was then washed

twice in 2xSSC buffer, 0.1% SDS for 20 min at the same temperature. Images of radioactive filters were obtained and quantified using a Cyclone TM Storage Phosphor System (PerkinElmer) and the Optiquant TM image analysis software (Packard).

2.12. Quantitative real-time PCR.

The cDNAs obtained as described above were subjected to quantitative real-time PCR with primer pairs specific to the *HaPLDα* gene (F2PLDa and R1PLDa described above), and SYBR Green I (QuantiteTect™ SYBR® Green PCR Kit, Quiagen, Crawley, UK) using an Opticon system (Bio-Rad). The reaction mixture was heated to 50ºC for 2 min and then to 95ºC for 15 min before subjecting it to 40 PCR cycles of: 94ºC for 15 s, 60.5ºC for 30 s, and 72ºC for 15 s, while monitoring the resulting fluorescence. A calibration curve was drawn up using sequential dilutions of pQEPLDa and this was used to estimate the transcript content of the calibrator gene. The Livak method (Livak and Schmittgen, 2001) was applied to calculate the comparative level of expression between samples. The sunflower actin gene (GenBank FJ487620) was used as the internal reference to normalize the relative amount of cDNAs for all samples.

3. Results

3.1. In vitro PLD activity in sunflower leaf extracts

PLDα displayed high levels of activity in leaf, stems and developing seeds (Fig. 1), and lower in roots and seedling cotyledons. These results indicated that this enzyme was very active in expanding tissues with high biosynthetic rates. When crude leaf homogenates were fractionated by differential centrifugation most of the activity remained in the soluble phase while 20% of the activity stayed bound to membrane fractions, mainly to high density ones (see supplementary material). The total activity accounted for 39 nkat/gFW, which would correspond to PLDα due to the assay was carried out at an acidic pH, and in the absence of free fatty acids and PIP2. As such, the total absence of PLD activity at Ca^{2+} concentrations below millimolar was confirmed in these conditions (data not shown). No membrane bound-PLDα has been reported to date, although this enzyme is usually weakly bound to membranes of different organs, mainly in the cytoplasm and the vacuole (Pappan and Wang, 1999a).

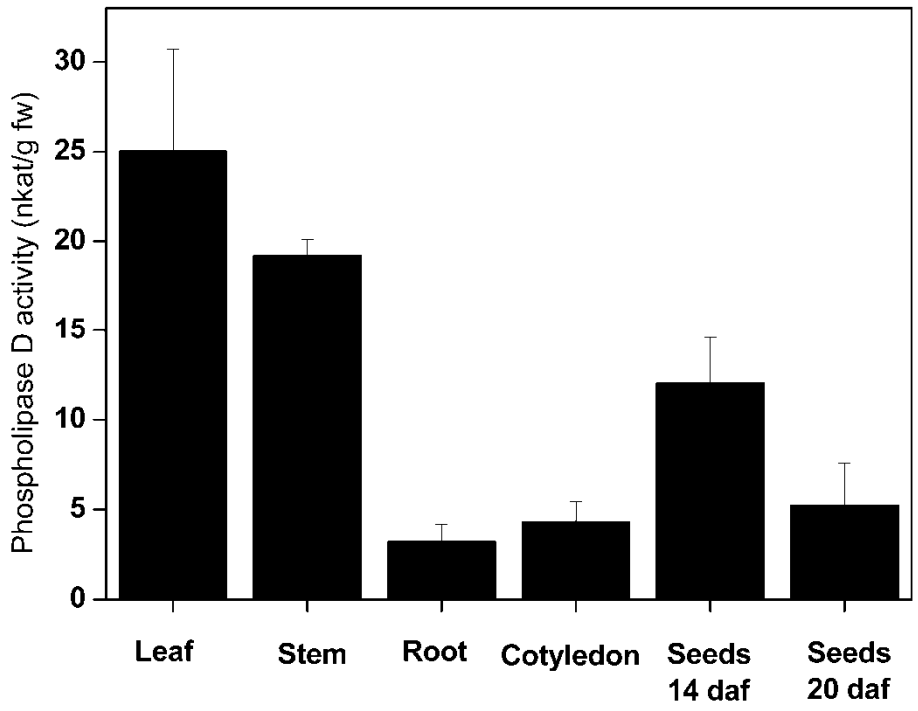

Fig. 1. Phospholipase Dα activity in crude homogenates from different sunflower organs. The data corresponds to the means of 3 independent measurements plus/minus standard deviation. Young plants that were approximately 1 month old were used; daf, days after flowering.

3.2. Isolation and sequence analysis of sunflower phospholipase Dα

Conserved regions different from known plant phospholipases of the Dα type were used to design the oligonucleotide primers FPLD1 and RPLD1 (see Material and Methods). Using these primers, a 903 bp fragment was amplified from sunflower leaf cDNA by PCR, corresponding to an internal fragment of phospholipase Dα. Subsequently, the full-length *HaPLDα* cDNA clone of 2653bp was obtained by RACE using the F1PLDa, F2PLDa, R1PLDa, R2PLDa and R3PLDa primers. This PCR fragment was cloned and sequenced, and its identity as a phospholipase Dα was confirmed using the Blast software (Altschul et al., 1990). The full-length cDNA was predicted to generate a protein of 810 amino acids (Fig. 2), with a molecular mass of 91.91 kDa and a pI of 5.26.

Fig. 2. Alignment of the deduced amino acid sequences of sunflower phospholipase Dα (*Ha*PLDα) with the closely related sequence from *Arabidopsis thaliana* (*At*PLDα, gi841689) and the more phylogenetically distant sequence from *Lolium temulentum* (*Lt*PLDα, gi162286122). The two HKD motifs (HXKX4DX6GSXN) are shaded in black, aspartic residues that are also involved in phospholipase activity are shaded in grey, and the residues involved in the metal binding pocket of the C2 domain are underlined and shaded in grey. The secondary structure prediction is shown under the alignments and the conservation of the residues. *, identical residues; :, conservative changes; and ., weakly-conservative changes between the sequences. H, α-helix; E, β-sheet.

Using our data and other known phospholipase Dα sequences from Viridiplantae, we generated a phylogenetic tree using phospholipase Dα from the moss *Physcomitrella patens* as the outgroup (Fig. 3). This comparison indicated that the protein encoded by *HaPLDα* is homologous to other type D phospholipases and that it is most closely related to those of the Asteraceae family, like *Cynara cardunculus* (Simões et al., 2005) or other Asterids species like *Pimpinella brachycarpa*.

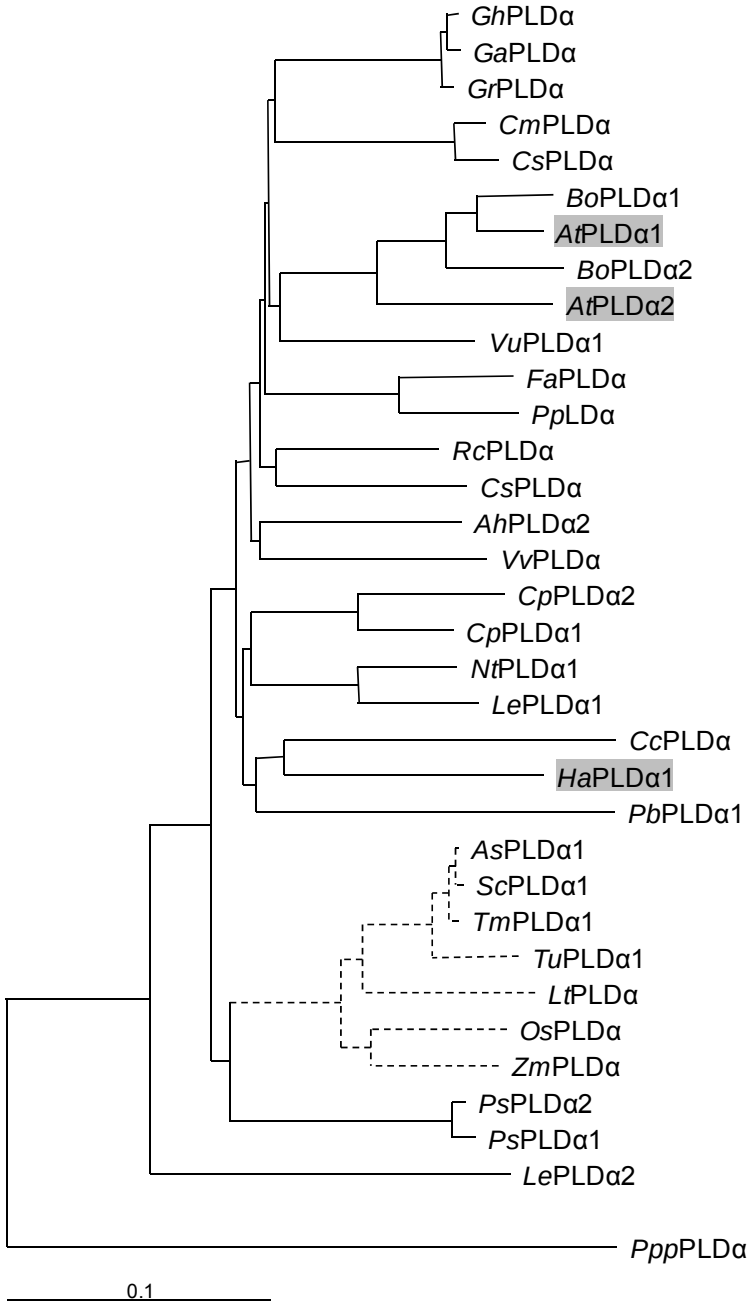

Fig. 3. Phylogenetic comparison of plant phospholipase Dα proteins. The tree was rooted using the PLDα sequence from the bryophyte *Physcomitrella patens* (PppPLDα, gi168029940). Poaceae branches are shown as dashed lines, and the *Helianthus* and *Arabidopsis* sequences are shaded in grey. Accession numbers of the different phospholipase included are as follows: Poaceae: *Oryza sativa* (*Os*PLDα,

gi1020415), *Zea mays* (*Zm*PLDα, gi162459688), *Lolium temulentum* (*Lt*PLDα, gi162286123), *Triticum monococcum* (*Tm*PLDα1, gi209944121), *Triticum urartu* (*Tu*PLDα1, gi209944123), *Aegilops speltoides* (*As*PLDα1, gi209944125), *Secale cereale* (*Sc*PLDα1, gi209944127); Eudicotyledons: *Arabidopsis thaliana* (*At*PLDα1, gi15232671; *At*PLDα2, gi15219031), *Arachis hypogaea* (*Ah*PLDα2, gi88193697), *Brassica oleracea* (*Bo*PLDα1, gi13124444; *Bo*PLDα2, gi13124446), *Citrus sinensis* (*Cs*PLDα, gi169160465), *Craterostigma plantagineum* (*Cp*PLDα1, gi4867805; *Cp*PLDα2, gi4867803), *Cucumis melo* (*Cm*PLDα, gi82547874), *Cucumis sativus* (*Cs*PLDα, gi145974671), *Cynara cardunculus* (*Cc*PLDα, gi66346964), *Fragaria x ananassa* (*Fa*PLDα, gi58891689), *Gossypium arboretum* (*Ga*PLDα, gi195984443), *Gossypium hirsutum* (*Gh*PLDα, gi125711079), *Gossypium raimondii* (*Gr*PLDα, gi195984445), *Helianthus annuus* (*Ha*PLDα1, gi156153085), *Lycopersicon esculentum* (*Le*PLDα1, gi13111657; *Le*PLDα2 gi13111655), *Nicotiana tabacum* (*Nt*PLDα1, gi3914361), *Papaver somniferum* (*Ps*PLDα1, gi46906215; *Ps*PLDα2, gi46906217), *Pimpinella brachycarpa* (*Pb*PLDα1, gi3914360), *Prunus persica* (*Pp*PLDα, gi196886176), *Ricinus communis* (*Rc*PLDα, gi1698844), *Vigna unguiculata* (*Vu*PLDα1, gi3914359) and *Vitis vinífera* (*Vv*PLDα, gi84620126).

3.3. Expression of PLDα in E. coli

The *Ha*PLDα protein was expressed in *E. coli* using the vector pQE-80L, in which genes are expressed under the regulation of the T7 promoter and the control of the galactose operon. This system often produces high levels of protein expression, although no clear band of the exogenous enzyme was observed in lysates of induced bacteria in regular coomasie-dyed gels (Fig. 4A). Therefore, the His-tag proteins were purified from the total extract using a Ni-sepharose affinity column. When the resulting eluates were probed in western blots with an antibody against poly-His, the recombinant *Ha*PLDα protein could be detected. Hence, a 92 KDa band (the expected molecular weight) was clearly detected in the 0.5M imidazole fractions (Fig. 4B), which confirmed the protein was expressed in the prokaryotic host. Recombinant *Ha*PLDα was not lethal to *E. coli* as reported for other PLDαs but it diminished bacterial growth (Kim et al., 1999).

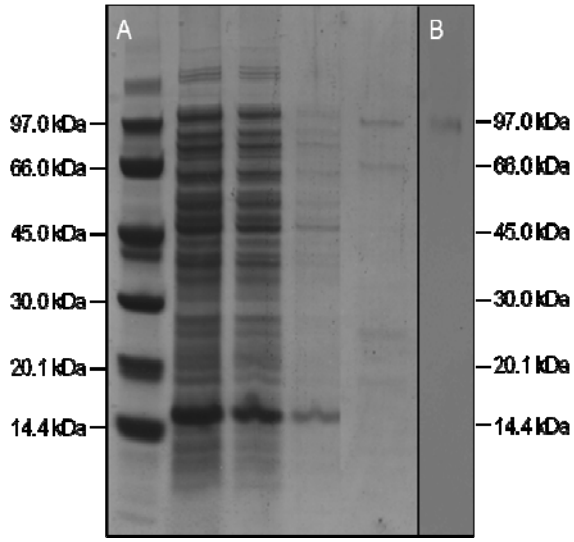

Fig. 4. SDS-PAGE separation of different fractions from *E. coli* expressing phospholipase D*α*. (A) lane 1 corresponds to the crude homogenate, lane 2 to the soluble protein fraction, lane 3 to the Ni-sepharose affinity column flow through, and lane 4 to the fraction eluted with 0.5M imidazole. (B) lane B corresponds to the western blot of the purified protein.

Furthermore, recombinant *E. coli* did not show any differences in fatty acid composition (data not shown), although there were differences in their glycerolipid species. Control cells carrying empty pQE-80L plasmid displays 85.8 % PE and 11.0 % PG, whereas PA and PS accounted for 1.0 % and 2.2 % respectively, the same glycerolipid composition found in uninduced cells carrying the recombinant plasmid under similar growth conditions and cell density (Table 1). However, cells induced with 1mM IPTG displayed more PA and PS, similar amounts of PG and lower contents of PE than uninduced cells, indicating that PLDα from sunflower is able to modify the phospholipid composition of *E. coli.*

Table 1. Glycerolipid composition of *E. coli* expressing the *Ha*PLDα gene. The two controls corresponded to cells carrying the empty plasmid and the uninduced recombinant bacteria. The data corresponded to two independent determinations. SD, standard deviation.

	PG		PE		PS		PA	
	%	SD	%	SD	%	SD	%	SD
Empty plasmid	11.0	1.4	85.8	1.6	2.2	0.1	1.0	0.1
Uninduced	11.2	0.1	86.2	0.2	1.9	0.2	0.8	0.2
Induced (1mM IPTG)	12.2	0.5	83.8	0.5	2.5	0.0	1.5	0.0

3.4. Characterization of recombinant HaPLDα

The recombinant *Ha*PLDα was purified on Ni-sepharose columns and biochemically characterized, examining its dependence on the Ca^{2+}. The enzyme was assayed using a broad range of Ca^{2+} concentrations and it displayed a dependence typical of an α-type phospholipase, with no activity at submicromolar concentrations and a sharp peak of activity at 10 mM, The enzymes activity decayed at higher Ca^{2+} concentrations and reached a plateau of around 600 nkat/mg prot (Fig. 5A). We investigated the impact of the SDS concentration on the activity of the recombinant *Ha*PLDα and we found the enzyme displayed a sharp peak with an optimum concentration of 0.9 mM (Fig. 5B). The activity measured in the absence of SDS was about 7-fold lower than that measured at the optimum concentration. Activity dropped stepwise at concentrations higher than the optimum and there was virtually no activity at 2.0 mM, indicating that the enzyme structure was probably affected by the surfactant.

Furthermore, the pH curve of the enzyme was assayed within pH value range from 4 to 10 using Tris, MES and sodium acetate as the buffers (Fig. 5C). *Ha*PLDα activity was optimal at slightly acid pH values and there was a clear decrease in activity associated with the change from MES to acetate buffer. These results agree well with the optimal pH values displayed by other forms of PLDα (Wang et al., 1993; Kim et al, 1999).

Nevertheless, *Ha*PLDα was assayed with different phospholipids at a constant concentration and the enzyme displayed the usual broad substrate specificity for PLDα. Indeed, it was similarly active on PC, PE and PG (Fig. 5D), although it could not hydrolyze PI.

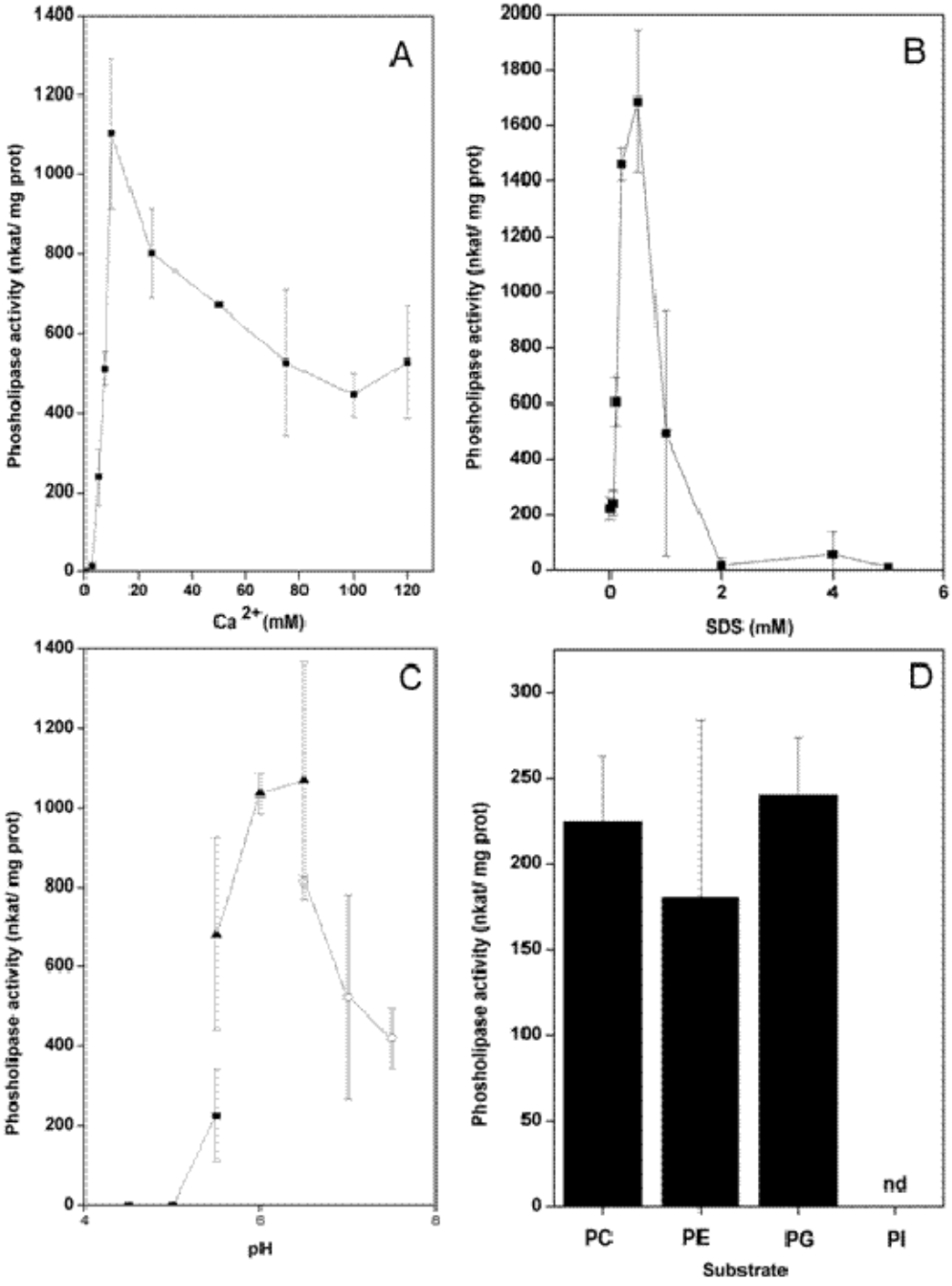

Fig. 5. Characterization of the recombinant phospholipase Dα from sunflower. The effect of the Ca^{2+} (A) and SDS concentration (B), and of pH (C), as well as the substrate specificity (D). Data corresponded to the mean of three measurements plus/minus standard deviation.

3.5. Copies and expression of the HaPLDα gene

HaPLDα gene expression was studied by quantitative real-time PCR in different tissues using actin gene expression to normalize the results (Fig. 6). The *HaPLDα* gene encoding the enzyme was ubiquitously expressed in all the tissues assayed, with the highest number of transcripts in leaves and stems.

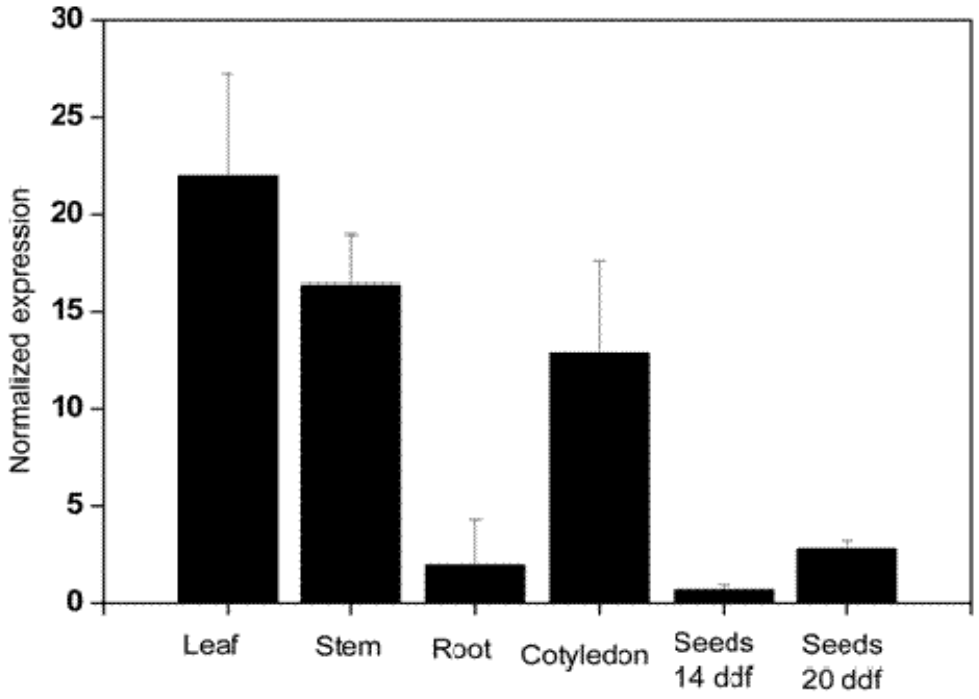

Fig. 6. Expression of phospholipase *HaPLDα* gene in different sunflower tissues (daf: days after flowering). The expression was determined by normalized QRT-PCR and the data correspond to the average of three reactions carried with the same template plus/minus standard deviation.

On the other hand, DNA blots carried out by treating genomic DNA with 4 different restriction enzymes yielded single bands in all cases, suggesting a single copy of this gene in sunflower genome (Fig 7.).

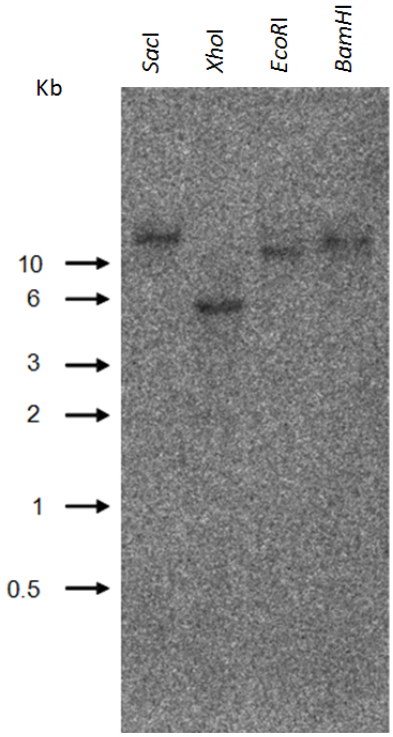

Fig. 7. Southern blot analysis of sunflower genomic DNA digested with restriction enzymes and probed with a *HaPLDα* probe: lane 1, *Sac*I; lane 2, *Xho*I; lane 3, *EcoR*I and lane 4, *BamH*I.

4. Discussion

D type Phospholipases have been the object of much research in the field of plant physiology in recent years. In general, all the enzymes of this class are involved in signal transduction and they are often regulated by phytohormones such as ABA or jasmonic acid. Amongst the different types of PLD, those of the α type are especially remarkable since they are soluble proteins that are not dependent on PIP_2 and they respond to millimolar concentrations of calcium. Here we characterized the PLDα activity from sunflower tissues both *in vivo* and *in vitro*. PLDs are ubiquitous enzymes that can usually be assayed *in vitro* and indeed, cell-free crude sunflower extracts were very active in hydrolyzing PC to PA in the presence of Ca^{2+}. PLDα from sunflower seedlings was purified previously and characterized by applying the kinetic model of Verger et al. (1973) for lipase enzymes (Abousalham et al., 1997). This enzyme proved to be very dependent on the presence of Triton X-100 and SDS in the assay, and when it was fed with different molecular species of PC it displayed high catalytic efficiency towards those containing medium and short chained fatty acid moieties. This specificity

could be a mechanism to exclude these types of fatty acids from cell membranes, as demonstrated in transgenic rape plants (Eccleston and Ohlrogge, 1998). Here, we extended the study of this enzyme to other plant tissues, studying both its expression and activity. The activity PLDα was high in expanding tissues with high biosynthetic activity (young leaves and stems), supporting its possible role in either lipid biosynthesis or the regulation of signals necessary for the formation of new tissues (Fig 1). In this regard, PLD activity was previously reported to be responsible for an artefact destroying phospholipids in developing sunflower seeds, which was not evident in dry fully developed kernels (Salas et al., 2006). Most of PLDα from sunflower was found in the soluble fraction of leaf tissue, and only a part of it remained bound to the particulate phase, the nature of the interaction of this enzyme with the particulate fraction is still unknown.

The alignment of the sunflower *Ha*PLDα protein (Eudicotyledon subclass Asterids family Asteraceae) with other phylogenetically distant plant phospholipases, like that from *Arabidopsis thaliana* (Eudicotyledon subclass Rosids family Brassicaceae) or *Lolium temulentum* (Monocotyledon subclass Commelinids family Poacea), highlighted the high degree of identity, 77% and 74% identity, respectively (Fig. 2). Interestingly, among the residues implicated in the enzyme activity there was a higher degree of conservation in those associated with the HKD motifs, related to the phospholipase activity (shaded in black), than for those associated with the metal binding pocket (underlined and shaded in grey). The species distribution was essentially consistent with conventional species trees, differentiating Monocotyledon (Poaceae species) from Dicotyledon species (Fig. 3). When compared with phospholipases from other phyla (tree not shown), the topology obtained also indicated that the plant phospholipases D (α, β, γ, δ, ε and ζ) originated in the prokaryotic lineage before the appearance of green plants, and that there was a later speciation of the plant PLD subclasses.

The main glycerolipids present in *E. coli* membranes are phosphatidyl glycerol (PG) and PE, with a minor contribution of phosphatidyl serine (PS) and PA. Heterologous expression of *Ha*PLDα significantly increased the levels of PA and PS at expenses of PE (Table 1), indicating that the protein was sufficiently active to change the bacteria lipid composition without affecting viability. There were no significant differences in the level of PG between cells carrying the plasmid and recombinant cells even though they were induced with IPTG. In the case of PE, significant differences were only found between induced and uninduced cells carrying the PLDα insert. Nevertheless, results

pointed that the main lipid hydrolyzed by PLDα in *E. coli* was PE. The PA resulting from this reaction seemed to be quickly recycled to PS, which is synthesized from PA by the successive action of the enzymes CDP-diacylglycerol synthase and PS-synthase (Vance, 2003), increasing the levels of this phospholipid in induced cells. The PLDα protein expressed in *E. coli* was purified and characterized (Fig. 4 and Fig. 5). This enzyme displayed maximum activity at calcium concentrations lower than that reported for castor or cabbage PLDα (Kim et al., 1999; Wang et al., 1993). The high levels of Ca^{2+} necessary for PLD activity has been a topic of discussion, provided *in vivo* concentrations of this cation are in the micromolar range. However, it has been demonstrated that in certain conditions of pH and in the presence of PIP2, the enzyme may be activated at submicromolar concentrations of Ca^{2+} (Pappan and Wang, 1999b). Another requirement for PLDs to achieve maximum activity was the addition of a surfactant to the assay mixture. The most commonly used surfactants are SDS, Triton X-100 or mixtures of both. This element was necessary to produce lipid vesicles of an appropriate size for the enzyme to bind to and hydrolyze the phospholipids that form them. *Ha*PLDα displayed a maximum of activity at 0.5 mM SDS followed of a quick decrease of activity. This rapid inactivation was not observed in PLDα from castor seedlings (Wang et al., 1993), which retained as much as 50 % of its activity at 1.5 mM SDS, and indicated that this enzyme was especially affected by excess of surfactants. In this regard, we tried to investigate the kinetics of *Ha*PLDα towards PC substrate, although it was not possible to adjust the kinetics to any model since no saturation kinetics was observed. This was also reported in assays with the purified sunflower enzyme in the absence of surfactants (Abousalham et al., 1997). However, including 0.8 mM SDS and Triton X-100 changed the kinetics and they closely fitted the model of Verger et al. (1973) for lipases. When the recombinant *Ha*PLDα was assayed at similar surfactant concentrations it displayed strong inactivation (Fig. 5B), making it difficult to determine the catalytic efficiency of this enzyme. Furthermore, *Ha*PLDα displayed broad substrate specificity and it was equally efficient for the hydrolysis of PC, PE and PC but it was not active towards PI, which means that this compound requires a different enzyme for its hydrolysis and metaboslism. This profile was similar to that reported for others PLDα‘s such as that from developing castor bean leaves that was also reported unable for PI hydrolysis (Dyer et al., 1994).

Gene expression of HaPLDα generally correlated well with the activity of the enzyme we detected (Figs. 1 and 6) and again confirms the presence of this PLD in

sunflower vegetative plant tissues. The exceptions to this rule were seeds 14 days after flowering and seedling cotyledons where there was a low correlation between gene expression and activity, indicating that its expression was possibly regulated at the level of messenger translation or enzyme activity. These results confirm that *Ha*PLDα is an enzyme widely expressed, above all in aerial vegetative tissues. A complete study of PLD expression in *Arabidopsis thaliana* highlighted the high levels of PLDα expression and activity in stems and roots, but not that in seeds or leaves (Fan et al., 1999). Moreover, PLDs dependent on PIP2 were expressed more strongly in leaves, above all in old senescent leaves, although this expression was very sensitive to ABA exposure. The results we obtained seem to indicate that sunflower PLDα has a different pattern of expression to that found in *Arabidopsis thaliana*, indicating that this feature is very dependent on the species being studied. Additionally, our DNA blot analysis (Fig. 7) indicated that only a single-copy of the *HaPLDα* gene exists in the *Helianthus annuus* genome.

Acknowledgements

We thank Alicia M. Muro-Pastor for help with southern blot analysis. This work was supported by the MICINN and FEDER, project AGL2008-0186/ALI.

References

Abousalham A, Nari J, Teissère M, Ferté N, Noat G, Verger R. Study of fatty acid specificity of sunflower phospholipase D using detergent/phospholipid micelles. Eur J Biochem 1997; 248: 374-379.

Altschul SF, Gish W, Miller W, Myers EW, Lipman DJ. Basic local alignment search tool. J Mol Biol 1990; 215:403-410.

Blight EG, Dyer WJ. A rapid method of total lipid extraction and purification. Can J Bioch Physiol 1959; 37: 911-917.

Devaiah SP, Roth MR, Baughman E, Li M, Tamura P, Jeannotte R, Welti R, Wang X. Quantitative profiling of polar glycerolipid species from organs of wild-type Arabidopsis and a phospholipase Dalpha1 knockout mutant. Phytochem 2006; 67:1907-1924.

Dyer JH, Ryu SB, Wang X. Multiple forms of phospholipase D following germination and during leaf development of castor bean. Plant Physiol. 1994; 105: 715-724.

Eccleston VS, Ohlrogge JB. Expression of lauroyl-acyl carrier protein thioesterase in *brassica Brassica napus* seeds induces pathways for both fatty acid oxidation and biosynthesis and implies a set point for triacylglycerol accumulation. Plant Cell 1998; 10: 613-622.

Fan L, Zheng S, Wang X. Antisense suppression of phospholipase *Dα* retards abscisic acid- and ethylene-promoted senescence of posthawest Arabidopsis leaves. Plant Cell 1997; 9: 2183-2196.

Fan L, Zheng S, Cui D, Wang X. Subcellular distribution and tissue expression of phospholipase Dalpha, Dbeta, and Dgamma in Arabidopsis. Plant Physiol 1999; 119: 1371-1378.

Kim DU, Roh TY, Lee J, Noh JY, Jang YJ, Hoe KL, Yoo HS, Choi MU. Molecular cloning and functional expression of a phospholipase D from cabbage (*Brassica oleracea* var. capitata). Biochim Biophys Acta 1999; 1437: 409-414.

Li W, Li M, Zhang W, Welti R, Wang X. The plasma membrane-bound phospholipase Ddelta enhances freezing tolerance in *Arabidopsis thaliana*. Nat Biotechnol 2004; 22: 427-33.

Livak KJ, Schmittgen TD. Analysis of relative gene expression data using real-time quantitative PCR and the 2-ΔΔCT method. Methods 2001; 25: 402-408.

Murray MG, Thompson WF. Rapid isolation of high molecular weight plant DNA. Nucleic Acids Res 1980; 8: 4321-4325.

Novotna Z, Valentova O, Martinec J, Feltl T, Nokhrina K. Study of phospholipases D and C in maturing and germinating seeds of *Brassica napus*. Biochem Soc Trans 2000; 28: 817-818.

Pappan K, Wang X. Molecular and biochemical properties and physiological roles of plant phospholipase D. Biochim. Biophys. Acta-Mol. Cell Biol. Lipids 1999a; 1439: 151-166.

Pappan K, Wang X. Plant phospholipase Dα is an acidic phospholipase active at near-physiological Ca^{2+} concentrations. Arch Biochem Biophys 1999b; 368: 347–353.

Rajashekar CB, Zhoua HE, Zhang Y, Li W, Wang X. Suppression of phospholipase Dα1 induces freezing tolerance in Arabidopsis: Response of cold responsive genes and osmolyte accumulation. J Plant Physiol 2006; 163: 916-926.

Salas JJ, Martínez-Force E, Garcés R. Accumulation of phospholipids and glycolipids in seed kernels of different sunflower mutants (*Helianthus annuus*). J Am Oil Chem Soc 2006; 83: 539-545.

Sang Y, Zheng S, Li W, Huang B, Wang X. Regulation of plant water loss by manipulating the expression of phospholipase Dα. Plant J 2001; 28:135-144.

Simões I, Mueller EC, Otto A, Bur D, Cheung AY, Faro C, Pires E. Molecular analysis of the interaction between cardosin A and phospholipase D(alpha). Identification of RGD/KGE sequences as binding motifs for C2 domains. FEBS J 2005; 272: 5786-5798.

Thompson JD, Gibson TJ, Plewniak F, Jeanmougin F and Higgins DG. The CLUSTAL_X windows interface: flexible strategies for multiple sequence alignment aided by quality analysis tools. Nucleic Acids Res 1997; 25: 4876-4882.

Vance JE. Molecular and cell biology of phosphatidylserine and phosphatidylethanolamine metabolism. Prog Nucleic Acid Res Mol Biol. 2003; 75:69-111.

Verger R, Mieras MCE, de Haas GH. Action of phospholipase A at interfaces. J Biol Chem 1973; 248: 4023-4034.

Wan SB, Wang W, Wen PF, Chen JY, Kong WF, Pan QH, Zhan JC, Tian L, Liu HT, Huang WD. Cloning of phospholipase D from grape berry and its expression under heat acclimation. J Biochem Mol Biol 2007; 40: 595-603.

Wang X. Regulatory functions of phospholipase D and phosphatidic acid in plant growth, development, and stress responses. Plant Physiol 2005; 139: 566-573.

Wang X. Molecular analysis of phospholipase D. Trends Plant Sci 1997; 2: 261-266.

Wang X. Multiple forms of phospholipase D in plants: the gene family, catalytic and regulatory properties, and cellular functions. Prog Lipid Res 2000; 39: 109-149.

Wang X. Phospholipase D in hormonal and stress signaling. Curr Opin Plant Biol 2002; 5: 408–414.

Wang XM, Dyer JH, Zheng L. Purification and immunological analysis of phospholipase D from castor bean endosperm. Arch Biolchem Biophys 1993; 306: 386-394.

Welti R, Li W, Li M, Sang Y, Biesiada H, Zhou HE, Rajashekar CB, Williams TD, Wang X. Profiling membrane lipids in plant stress responses. Role of

phospholipase D in freezing-induced lipid changes in *Arabidopsis.* J Biol Chem 2002; 277: 31994-32002.

Whitaker BD, Smith DL, Green KC. Cloning, characterization and functional expression of a phospholipase Dalpha cDNA from tomato fruit. Physiol Plant 2001; 112:87-94.

Xu L, Paulsen AQ, Ryu SB, Wang X. Intracellular localization of phospholipase D in leaves and seedling tissues of castor bean. Plant Physiol 1996; 111: 101-107.

Young SA, Wang X, Leach JE. Changes in the plasma membrane distribution of rice phospholipase D during resistant interactions with *Xanthomonas oryzae* Pv oryzae. Plant Cell 1996; 8: 1079-1090.

Zhang W, Qin C, Zhao J, Wang X. Phospholipase Dalpha1-derived phosphatidic acid interacts with ABI1 phosphatase 2C and regulates abscisic acid signaling. Proc Natl Acad Sci USA 2004; 101: 9508–9513.

Zhang W, Wang C, Qin C, Wood T, Olafsdottir G, Welti R, Wang X. The oleate-stimulated phospholipase D, PLDdelta, and phosphatidic acid decrease H_2O_2-induced cell death in Arabidopsis. Plant Cell 2003; 15: 2285-2295.

BLOQUE III

Sphingolipid base Modifying Enzymes in Sunflower (*Helianthus annuus*): Expression of the Δ4-Hydroxylase Gene and of a new Δ8-Desaturase

Moreno-Pérez, A.J., Martínez-Force, E., Garcés, R., Salas, J.J.

Instituto de la Grasa (CSIC), Av. Padre García Tejero, 4 41012, Seville, Spain.

Submitted to *Journal of Plant Physiology*

Abstract

Sphingolipids are components of plant cell membranes that participate in the regulation of important physiological processes. Unlike their animal counterparts, plant sphingolipids are characterized by high levels of base Δ4-hydroxylation. Moreover, desaturation at the Δ8 position predominates over the Δ4 desaturation typically found in animal sphingolipids. These modifications are due to the action of Δ4-hydroxylases and Δ8-long chain base desaturases, and they are important for complex sphingolipids finally becoming functional. The long base chains of sunflower sphingolipids have high levels of hydroxylated and unsaturated moieties. Here, a Δ4-long chain base hydroxylase was functionally characterized in sunflower plant, an enzyme that could complement the *sur2*Δ mutation when heterologously expressed in a yeast mutant deficient in hydroxylation. This hydroxylase was ubiquitously expressed in sunflower, with the highest levels found in the developing cotyledons. In addition, we identified a new Δ8-long base chain desaturase gene that displays strong homology to a previously reported desaturase gene. This desaturase was also expressed in yeast and was able to change the long chain base composition of the transformed host. We studied the expression of this desaturase and compared it with that of the other isoform described in sunflower. In vegetative tissues, this newly described sphingolipid desaturase was more weakly expressed than the previously encountered isoform, although it was expressed at higher levels in developing seeds.

1. Introduction

Amongst the different classes of plant lipids, sphingolipids have received special attention in the recent years (Sperling and Heinz, 2003) having been demonstrated to be important structural components of plant membranes (Lynch and Phinney, 1995) and lipid rafts (Mongrand et al., 2004; Borner et al., 2005). Moreover, sphingolipid-derived molecules are involved in important regulatory processes, like abscisic acid signalling (Coursol et al., 2003, 2005) and programmed cell death (Liang et al., 2003).

Structurally, sphingolipids are derivatives of long chain bases (LCBs) produced by the condensation of serine with palmitoyl-CoA, an intial step that is catalyzed by the enzyme serine-palmitoyl-CoA transferase (Hanada, 2003). The product of this condensation requires two successive steps of dehydration and reduction to generate a C18 sphinganine (d18:0) with two hydroxyl groups in the α and γ positions, and an amino group in the β position. This is the primary long chain base from which other derivatives can be generated through further modifications. Thus, in mammals and other animals, d18:0 is usually desaturated at the Δ4 position to yield sphingosine (d18:$1^{\Delta 4t}$: Ternes et al., 2002). By contrast, d18:0 is mainly hydroxylated at the Δ4-position in yeast to produce hydroxysphinganine or phytosphinganine (t18:0), the predominant sphingoid base found in these organisms (Obeid et al., 2002). In plants, d18:0 is found in small amounts because it is often hydroxylated and/or desaturated to yield Δ8-sphinganine or Δ4-hydroxy-Δ8-phytosphinganine derivatives (Lynch and Dunn, 2004).

Plant LCBs are usually esterified with a Δ2-hydroxy-fatty acid at the amino group. These fatty acids range in length from C16 to C26, and they may include monounsaturated fatty acids. Furthermore, the α-hydroxy group of the LCBs can be esterified to a polar group (glucose, phosphoinositides or phosphooligosugars), which give rise to a large variety of sphingolipid compounds in plant tissues (up to 300 species: Kaul et al., 1978; Chen et al., 2006; Markham et al., 2006). C4-LCB Hydroxylation in plant and yeast is catalyzed by a diiron-oxo type hydroxylase (Haak et al., 1997; Grilley et al., 1998; Sperling, 2001), depending on oxygen and pyridine nucleotide equivalents (Wright et al., 2003). Yeast deficient in C4-hydroxylation do not display any apparent phenotype, although the mutation confers resistance to syringomicine. Hence, it was hypothesized that LCB hydroxylation is related to the physical properties of the plasma membrane. Indeed, the suppression of sphingolipid hydroxylation causes clearer effects on plant development as rice mutants deficient in

sphingolipid hydroxylase grow more slowly, suggesting that this enzyme is implicated in plant growth (Imamura et al., 2007). However, there is no decrease in the hydroxylated LCBs in the tissues of these mutants. Nevertheless, when the genes encoding sphingolipid hydroxylases were suppressed in *Arabidospsis* (At1g69640 and At1g14290), the resulting plants were not viable. Indeed, the dwarf phenotype of plants displaying an important decrease of hydroxylated sphingoid bases, as well as the severe infertility observed, confirms the role of hydroxylation in plant development (Chen et al., 2008).

LCB Δ8-desturases are enzymes typical of plants and they have histidine box motifs characteristic of membrane-bound desaturases, as well as a N-terminal desaturase domain fused to cytochrome b5 (Sperling et al., 1998). The exact function of Δ8-desaturation of sphingoid bases remains unclear, although studies where these desaturases have been suppressed demonstrate that they participate in plant tolerance to aluminium (Ryan et al., 2007). Indeed, the first desaturase of this class was cloned and characterized from sunflower (Sperling et al., 1995).

In the present work we described the cloning and functional characterization in yeast of a sphingolipid hydroxylase (*HaSC4H*) and of a new sphingolipid desaturase from sunflower, *HaSLD2*. The role of the enzymes encoded by these genes in sunflower sphingolipid biosynthesis is discussed in function of the results.

2. Results

2.1. LCB composition of different sunflower tissues

Control sunflower tissues contained similar LCB compositions (Table 1) in which the most abundant LCB was Δ8-phytosphingenine, for which both geometrical isomers were detected (8E and 8Z). Furthermore, Δ8-sphingenines, sphinganine and phytosphinganine were also present in somewhat smaller amounts. Developing seeds clearly accumulated the highest content of sphingoid bases, with LCB contents in the μmole/g FW range. By contrast, vegetative tissues contained higher proportions of trihydroxylated bases, especially in the aerial organs and green cotyledons. In general, saturated sphinganines or phytoesphinganines were poorly represented in all tissues, ranging from 3 to 8% of the total bases of the samples analyzed. Finally, Δ4,8 diunsaturated sphingolipid bases were not found in any tissue.

Table 1. Typical composition of sphingolipid long chain bases of different tissues from sunflower plants.

	Seeds 15 DAF	Seeds 20 DAF	Roots	Stems	Leaf	Cotyledons
Composition			**%**			
t18:1D8Z	4.0	7.7	4.7	8.7	9.4	13.1
t18:1D8E	31.5	59.9	46.2	48.3	70.3	52.6
t18:0	2.9	2.2	5.2	5.7	6.7	8.4
d18:1D8Z	3.0	2.3	3.8	9.1	2.0	9.1
d18:1D8E	56.7	26.1	39.9	28.0	11.6	16.5
d18:0	1.9	1.8	0.1	0.3	0.1	0.3
Trihydroxylated	38.4	69.8	56.2	62.6	86.3	74.2
Dihydroxylated	61.6	30.2	43.8	37.4	13.7	25.8
			nmole/g FW			
Total content	987.9	1127.3	75.3	47.4	67.0	53.7

2.2. Isolation and sequence analysis of a sunflower Δ4-long chain base hydroxylase cDNA

Conserved regions identified in the available plant sphingolipids hydroxylase sequences were used to design degenerate oligonucleotide primers corresponding to the second conserved histidine box (see Materials and methods): *HaSC4H*-1f (GALYNHP, 64-fold degenerate) and *HaSC4H*-1r (HHQLYG, 192-fold degenerate). Using these primers, a 227 bp fragment was amplified by PCR from developing sunflower seeds cDNA, which corresponded to an internal region of the sphingolipid hydroxylase mRNA. Subsequently, the full-length cDNA clone of *Ha*SC4H (777 bp) was obtained by RACE, using the primers described in Materials and methods. This cDNA was cloned and sequenced, and its identity as a Δ4-long chain base hydroxylase was confirmed using the Blast software (Altschul et al. 1990). The full-length cDNA was predicted to generate a protein of 258 residues (Figure 1), with a theoretical molecular mass of 29.67 kDa and an expected pI of 7.92. The *Ha*SC4H protein from *H. annuus*

(Eudicotyledon subclass Asterids, family Asteraceae) was aligned with other sphingolipid hydroxylases from phylogenetically distant plants like *Ricinus communis* (Eudicotyledon subclass Rosids, family Euphorbiaceae), *Arabidopsis thaliana* (Eudicotyledon subclass Rosids, family Brassicaceae), *Zea mays* (Monocotyledon subclass Commelinids, family Poacea) and yeast *Saccharomyces cerevisiae* (Ascomycota subclass Saccharomycotina, family Saccharomycetaceae), and it displayed 77.5%, 77.4%, 65.5% and 32.0% identity, respectively (Figure 1).

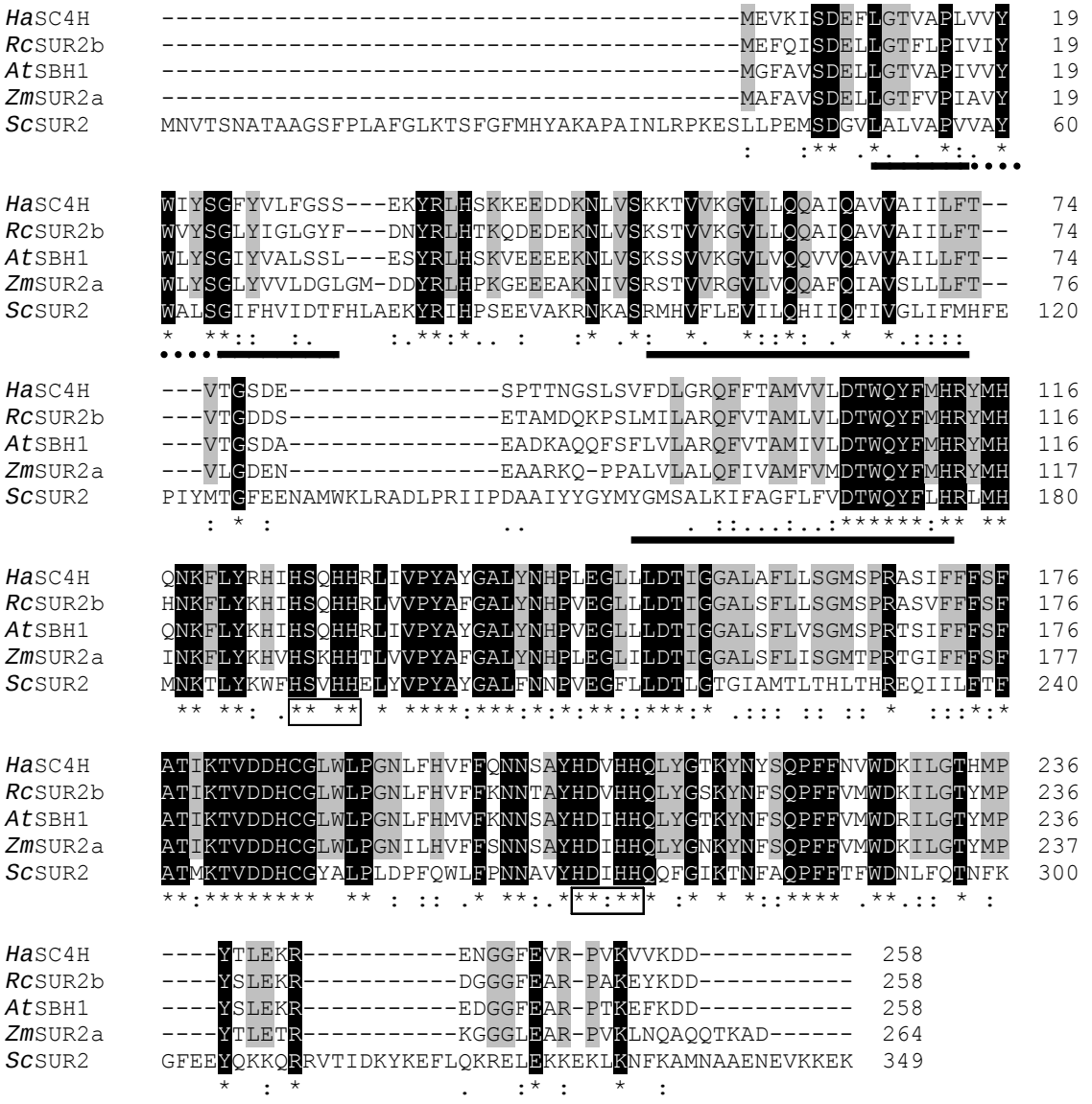

Figure 1. Alignment of the deduced amino acid sequences for sunflower Δ4-long chain base hydroxylase, HaSC4H, with the closely related sequences from *Ricinus communis* (RcSUR2b, gi255562836) and *Arabidopsis thaliana* (*At*SBH1, gi22330531), and with the more phylogenetically distant sequences from *Zea mays* (*Zm*SUR2a, gi226508892) and *Saccharomyces cerevisiae* (*Sc*SUR2, gi6320503). The predicted transmembrane regions are underlined with continuous and dashed black lines, the residues conserved between these plants are highlighted in grey, and the highly conserved residues are

highlighted in black. *, identical residues; :, conservative changes; and ., weakly-conserved changes between the sequences. The two conserved histidine clusters involved in the catalytic centre of the sphingolipid hydroxylases are shown as boxes.

2.3. Expression of HaSC4H in hydroxylation deficient yeast

The mutant Y03656 *S. cerevisiae* strain (Zink et al., 2005) is deficient in LCB hydroxylation and it only displayed dihydroxylated bases when carrying the empty pYES2 vector (Table 2), principally d18:0 bases and to a lesser extent d20:0. When this yeast strain was transformed with the recombinant pYES-*HaSC4H* plasmid its LCB composition changed significantly. Thus, the hydroxylated t18:0 base was evident in considerable proportions (9.6 %), even in uninduced recombinant cells (which probably reflected some basal/leaky expression), whereas its content increased to 58.5 % of the total sphingolipid bases when the cultures were induced. Indeed, a small proportion of t20:0 also appeared following induction (Table 2). The total content of LCBs was around 1 μmole/g FW, while these levels remained slightly lower in the uninduced cells than in control or induced cells.

Table 2. Sphingolipid base composition of sur2Δmutant yeast expressing HaSC4H. Results are the average of three independent biological replicates.

	Empty plasmid	**Induced**	**Uninduced**
	%	**%**	**%**
t18:0	0.0 ± 0.0	58.5 ± 5.9	9.6 ± 1.8
t20:0	0.0 ± 0.0	10.6 ± 0.7	2.1 ± 0.9
d18:0	77.7 ± 1.7	22.8 ± 4.2	70.3 ± 3.2
d20:0	22.3 ± 1.7	8.0 ± 2.4	18.0 ± 0.5
	(nmole/g FW)		
Total	1149.9 ± 16.9	1101.1 ± 381.1	958.2 ± 9.9

2.4. Expression of HaSC4H in different sunflower tissues

The expression of *HaSC4H* gene was studied by Q-PCR in different sunflower tissues (Figure 2) and the presence of its transcripts in all the tissues studied indicated

that it was expressed quite ubiquitously. The strongest expression was found in germinating cotyledons, followed by vegetative tissues like leaves, stems and roots. Finally, the weakest expression was found in developing seeds, which displayed 4 to 5-fold fewer transcripts than the tissues from the aerial organs or roots.

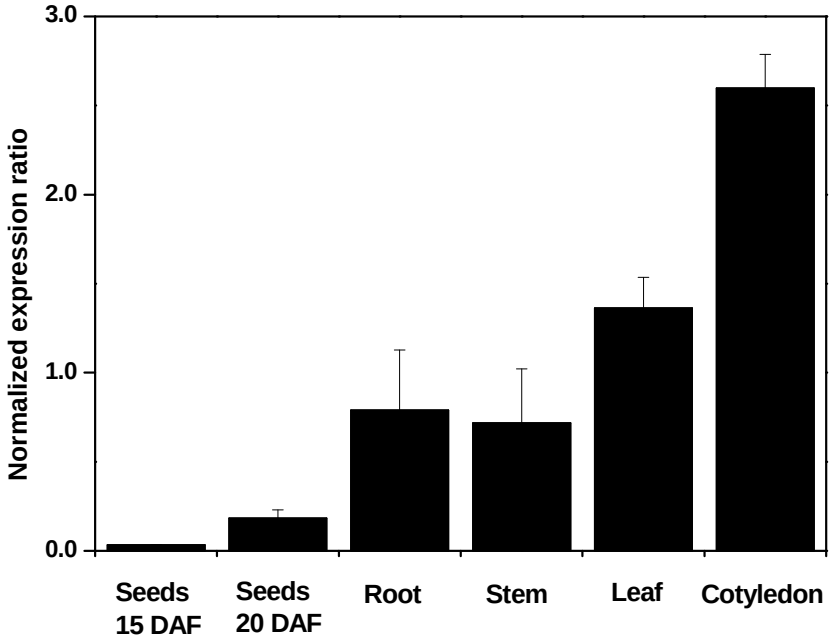

Figure 2. Expression profile of the *HaSC4H* hydroxylase in different tissues from sunflower. The data corresponded to 3 independent replicates.

2.5. Isolation and sequence analysis of a new sunflower Δ8-long chain base desaturase cDNA

As for the *Δ4-long chain base hydroxylase*, conserved regions from the available long chain base desaturase sequences were used to design degenerate oligonucleotide primers to ampliy such sequences from sunflower tissues (see Materials and methods): *HaSLD2*-1f (VTGIQHVQ, 768-fold degenerate) and *HaSLD2*-1r (WEAFNTHG, 64-fold degenerate). Using these primers, a 389 bp fragment was amplified from developing sunflower seed cDNA, which corresponded to an internal region of a Δ8-long chain base desaturase mRNA. The full-length cDNA clone of *HaSLD2* (1401 bp) was obtained by RACE using the primers described in the Materials and methods. This cDNA was cloned, sequenced and its identity as a Δ8-long chain base desaturase was confirmed using the Blast software (Altschul et al., 1990). The full-length cDNA was predicted to generate a protein of 466 residues (Figure 3), with a theoretical molecular

mass of 52.92 kDa and an expected pI of 8.61. The alignment of *Ha*SLD2 protein from sunflower with the already described *Ha*SLD1 isoenzyme (Sperling et al., 1995) and Δ8-long chain base desaturases from *R. communis*, *A. thaliana* and *Z. mays*, demonstrated strong identity of 86%, 71.8%, 66.5% and 55.2%, respectively (Figure 3).

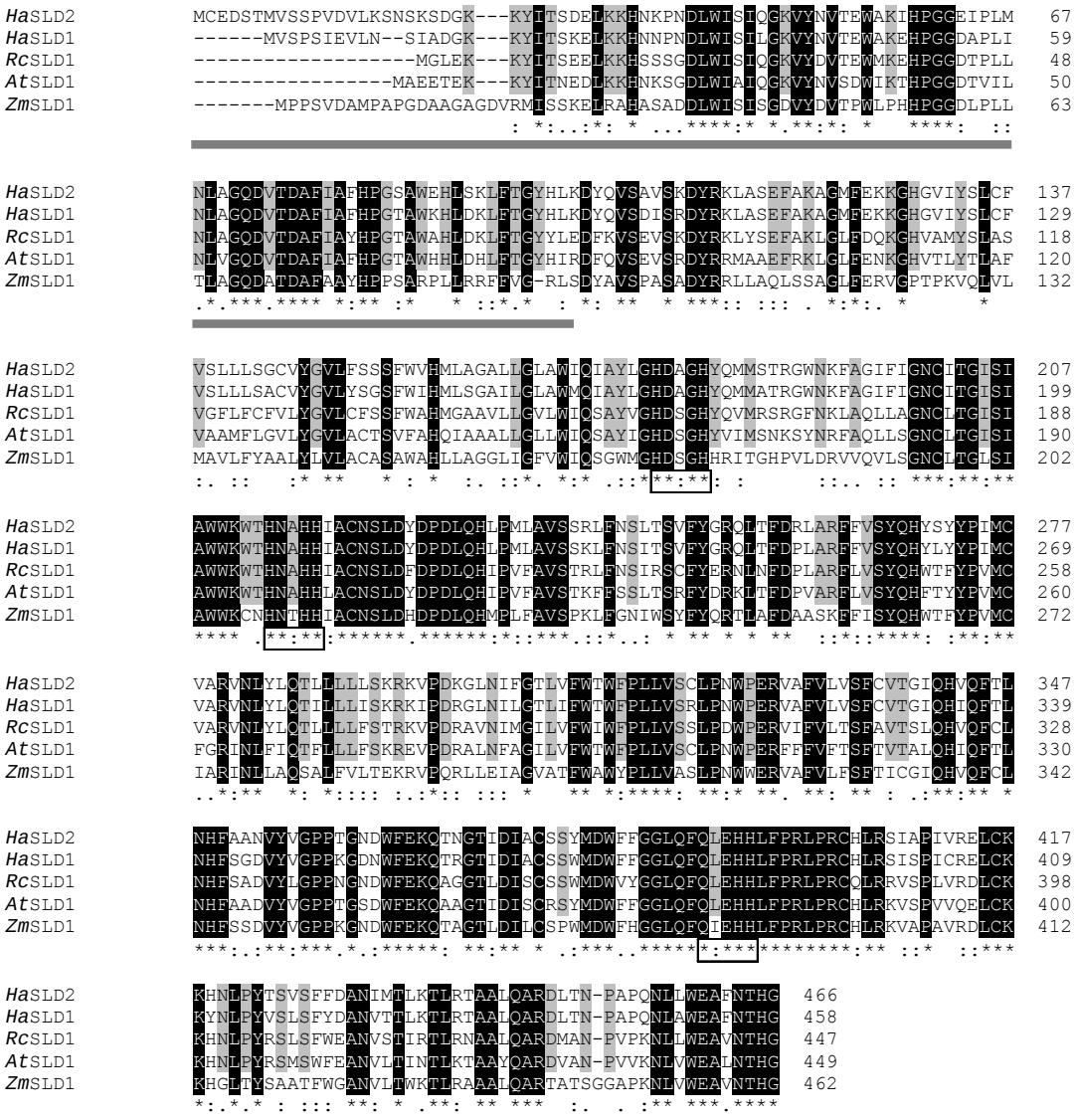

Figure 3. Alignment of the deduced amino acid sequences of the sunflower Δ8-long chain base desaturase, *Ha*SLD2, with the closely related sequence from sunflower *Ha*SLD1 (gi1040729) and the more phylogenetically distant sequences from *Ricinus communis* (*Rc*SLD1, gi255541744), *Arabidopsis thaliana* (*At*SLD1, gi15233152) and *Zea mays* (*Zm*SLD1, gi212274953). The cytochrome b5-like domain is underlined with continuous grey lines, the residues conserved between dicotyledonous plants are highlighted in grey, and the residues highly conserved between plants are highlighted in black. *, identical residues; :, conservative changes; and ., weakly-conservative changes between the sequences. The three conserved histidine clusters involved in the catalytic centre of the sphingolipids desaturases are boxed.

2.6. Expression of HaSLD2 in Saccharomyces cerevisiae

Control *Saccharomyces* cells only produced saturated sphinganines and phytosphinganines of 18 and 20 carbon atoms. In the W303-1A strain, up to 95% of the bases contained 18 carbon atoms with a prevalence of hydroxylated ones. Importantly, the expression of *HaSLD2* desaturase changed the LCB composition of the eukaryotic host both in induced and in uninduced cultures (Table 3). Thus, significant amounts of unsaturated sphingenines appeared in both cases, although the relative conversion into sphingenines was higher in induced cells. These bases were identified as D8 sphingenines in function of their retention times. Desaturation only affected trihydroxylated bases as dihydroxylated bases did not serve as a substrate for this enzyme in the yeast host. Moreover, the total amount of sphingolipids was not altered by the expression of the desaturase.

Table 3. Sphingolipid base composition of yeast W303-1A expressing *HaSLD2*. Results are the average of three independent biological replicates.

	Empty plasmid	**Induced**	**Uninduced**
	%	**%**	**%**
t18:1D8Z	0.0 ± 0.0	2.9 ± 0.3	0.9 ± 0.0
t18:1D8E	0.0 ± 0.0	26.3 ± 1.8	8.9 ± 0.6
t18:0	66.1 ± 6.1	37.0 ± 2.0	48.9 ± 2.1
t20:1D8E	0.0 ± 0.0	12.8 ± 1.0	7.0 ± 0.3
d18:0	29.4 ± 6.5	17.3 ± 2.3	30.6 ± 3.3
t20:0	4.0 ± 0.6	3.3 ± 1.3	3.1 ± 0.7
d20:0	0.5 ± 0.3	0.5 ± 0.2	0.5 ± 0.2
		(nmol/g FW)	
Total	610.6 ± 152.8	641.0 ± 134.8	812.7 ± 164.0

2.7. Expression of HaSLD1 and HaSLD2 in different sunflower tissues

When the expression of the two sphingolipid desaturases found in sunflower was examined, the transcripts that accumulated in the tissues studied varied significantly from one desaturase to other (Figure 4). The expression of the desaturase characterized by Sperling et al. (1995) was stronger in expanding tissues like stems, roots and leaves

than in germinating cotyledons and developing seeds. By contrast, the other desaturase was hardly detected in cotyledons and roots, and it was only weakly expressed in aerial organs, with the maximal expression seen in developing seeds.

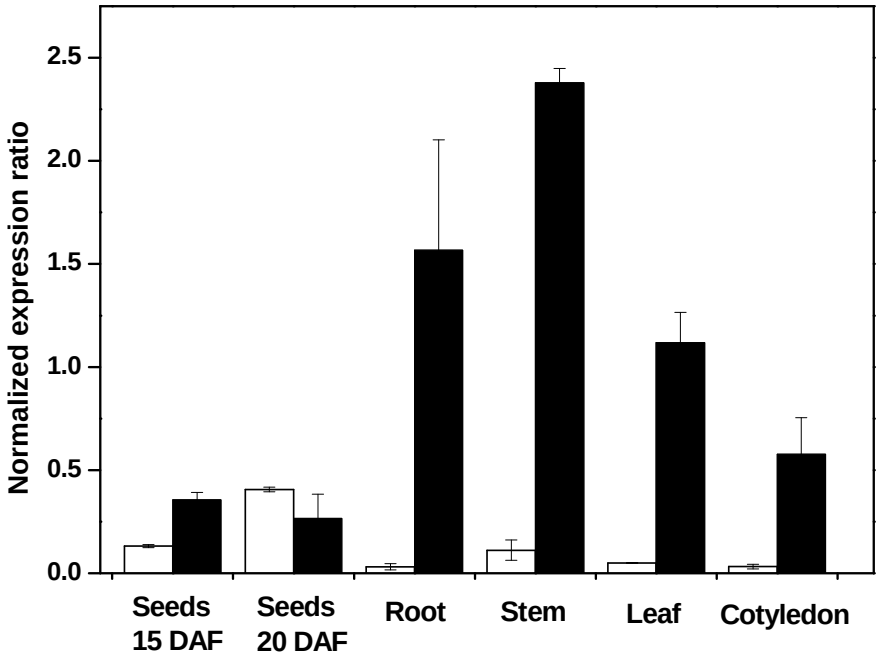

Figure 4. Expression of the *HaSLD1* (black columns) and *HaSLD2* (white columns) desaturases in different sunflower tissues. The data corresponded to 3 independent replicates.

3. Discussion

In plants, C18 sphinganines are desaturated and/or hydroxylated, producing a variety of LCBs. These LCBs can be esterified with regular or α-hydroxyl fatty acids, generating a wide variety of compounds that can be studied by modern sphingolipidomics (Markham et al., 2006; Markham and Jaworski, 2007). Plant sphingolipid desaturases can insert double bonds in the Δ4 or Δ8 positions of LCBs and thus, most plant species have unsaturated sphingoid bases like Arabidopsis, tomato or soybean. Moreover, bases can be hydroxylated to trihydroxylated or even tetrahydroxylated derivatives in some species (Sperling and Heinz, 2003). Hitherto, each plant species displays a characteristic LCB composition, which was simpler in the case of sunflower since Δ4t desaturation does and hence, Δ4-unsaturated and diunsaturated bases species are lacking. The LCBs from sunflower are mostly Δ8-

desaturated, containing only 3 to 8% of saturated bases. Moreover, most LCBs are hydroxylated, especially in green aerial organs like leaves and green cotyledons. The lowest level of hydroxylation is evident in seeds at the beginning of development, which increases at 20 DAF when oil accumulation commences. Furthermore, the total LCB content was similar in vegetative tissues and it was much higher in developing seeds, which reached LCB levels that were 2 orders of magnitude higher than those in roots and green tissues. In this regard, previous works indicated that seeds were rich in glucosyl-ceramides that usually carry d18:1, in close agreement with the lower levels of hydroxylated bases in developing sunflower seeds (Lynch and Dunn, 2004). The enzymes responsible for hydroxylation and desaturation of LCBs are sphingolipid hydroxylases and desaturases, respectively. Here, we have cloned the genes encoding these enzymes in sunflower tissues, *HaSC4H* and *HaSLD2*.

The alignment of *HaSC4H* with other from plant and yeast hydroxylases indicates that the homology between plant sequences is lower than that observed for proteins involved in primary processes like glycolysis, suggesting possible differences in terms of substrate recognition and catalysis. In this respect, the histidine boxes involved in catalysis are well conserved, with the greatest divergence appearing in the amino terminal region that mainly involves the transmembrane expanding regions. Furthermore, we investigated whether the *Ha*SC4H protein encoded by the gene was functional by expressing *HaSC4H* in yeast deficient in LCB hydroxylation. The phytosphingosine defective (*sur2*Δ) strain of *S. cerevisiae* was first described as being resistant to syringomycin E (Grilley et al., 1998) when it was shown that the gene necessary for inhibition by that lipodepsipeptide was also responsible for sphingolipid hydroxylation. The growth of the *sur2*Δ mutant is unaltered, although it totally lacks phytosphinganines in its LCB profile. Nevertheless, this mutant was transformed with the construct pYES:*HaSC4H* that can express the *HaSC4H* under the control of *GAL1*promoter. This gene could complement the mutation, even though its expression was not specifically induced. While *sur2*Δ cells carrying the empty plasmid only displayed d18:0 and d20:0 saturated sphinganines in their LCB profile, trihydroxylated bases appear in the cells transformed with the recombinant plasmid, which augmented from a proportion of approximately 10% to above 70% following induction. Hence, the protein encoded by the *HaSC4H* gene was functional and could complement the *sur2*Δ mutation in *Saccharomyces* as occurred with the *Arabidopsis* hydroxylase (Sperling et al., 2001).

The sunflower hydroxylase enzyme was able to C-4 hydroxylate both C18 and C20 sphinganines to a similar extent and thus, it did not seem showing any clear substrate specificity. Moreover, the expression of the gene did not alter the total LCB content, only their composition. The expression of this gene was studied by Q-PCR in different sunflower tissues, identifying its transcripts in all the tissues assayed, although with important differences in quantitative terms. This gene was expressed less in developing seeds and maximally in germinating cotyledons, with intermediate levels of expression in aerial organs and roots. This expression profile is compatible with a form of LCB hydroxylase activated in association with the development of vegetative tissues and seed germination. There is currently no data as to the number of copies of this gene in sunflower, although the Arabidopsis genome contains two copies of the sphingolipid hydroxylase gene with similar characteristics. The suppression of both of them induced male infertility, which means that sphingolipid hydroxylation was essential for correct plant development (Chen et al., 2008). These genes displayed different expression profiles, whereby one is ubiquitously expressed in different plant tissues while the other is more strongly expressed in roots and flowers. Moreover, the rates of C-4 hydroxylation in seeds in the initial stages of development is lower than in the rest of the plant, which is compatible with the profile of *HaSC4H* expression. Indeed, seeds of 20 DAF have very high sphingolipid contents with a similar degree of C-4 hydroxylation to those found in other tissues and thus, other forms of LCB hydroxylases with different expression profiles are likely to be present, which would account for the hydroxylation of LCBs in developing seeds.

The other gene described here is a sphingolipid desaturase that is similar in sequence to that already described in sunflower (Sperling et al., 1998), the first sphingolipid desaturase described in plants. Many sphingolipid Δ8 desaturases have since been described in different plants, some of which were included in the alignment used here. Indeed, *HaSLD2* displays strong homology with a previously reported in sunflower desaturase, *HaSLD1*. Sphingolipid desaturases from plant species have higher levels of divergence than the hydroxylase genes, with well conserved cytochrome b5-like domains and regions surrounding the catalytic histidine boxes. In addition, when the *HaSLD1* gene was expressed in *Saccharomyces cerevisiae*, it encoded a functional desaturase, producing important changes in the LCB composition of this yeast. Indeed, the expression of the *HaSLD1* in yeast induced the production of Δ8 unsaturated sphingenines and phytosphingenines (Sperling et al., 1998, 2000). A similar effect was

observed in the case of *HaSLD2* whereby yeast cells transformed with the recombinant plasmid displayed unsaturated C18 and C20 phytosphingenines, unlike the saturated sphinganines and phytosphinganines with 18 and 20 carbon atoms observed in the absence of this gene. Indeed, such effects were observed even though the cultures were not induced, probably due to basal/leaky expression from the vector. These compounds appeared as new pairs of peaks corresponding to the Z and E isomer of the LCB. When cultures were induced the relative amount of unsaturated LCB increased by 2.5 fold in the case of C18 bases and less than 2-fold for C20 ones. The new peaks were recognized as Δ8 phytosphingenines, which indicated that this newly reported desaturase displayed similar specificity to the previously reported enzyme in sunflower that only desaturated C-4 hydroxylated sphinganines when expressed in yeast (Sperling, 2000).

In plants, the desaturation/hydroxylation mechanism works in a different way since unsaturated sphingenines are common components of their LCB profiles, indicating that the desaturation of dihydroxylated bases does actually take place in plants. This result demonstrated that the *HaSLD2* gene encodes an active sphingolipid desaturase with similar properties to *HaSLD1*, in agreement with the high degree of homology between both genes. Studies of the expression of these two desaturase genes highlight their complementary distribution. The *HaSLD1* gene was strongly expressed in vegetative tissues, leaves, stems and roots, whereas a fewer transcripts were detected in seeds and cotyledons. By contrast, the *HaSLD2* gene was found at very low levels in cotyledons and vegetative tissues but it was most strongly expressed in developing seeds harvested at 20 DAF, the moment at which oil synthesis reaches its maximum. Thus, *HaSLD2* seemed to be a seed-specific LCB desaturase. The biochemical characterization of plant Δ8-LCB desaturases has been studied extensively but there is still little data about their differential expression in different tissues. The results published here demonstrate that there is a degree of specialization among the distinct LCB desaturases found in sunflower plants.

4. Conclusions

Sunflower sphingolipids contain LCBs with considerable C-4 hydroxylation and Δ8-desaturation. No Δ4 *trans* LCBs are found in the sphingoid base profile of sunflower tissues, which indicates that this species lacks Δ4-LCB desaturases as occurs in

Arabidopsis thaliana. Thus, the enzymes modifying LCBs in sunflower are essentially C-4 LCB hydroxylases and Δ8-LCB desaturases. The *HaSC4H* gene was cloned from sunflower and it encodes a C-4 sphingolipid desaturase. When expressed heterologously in yeast deficient in hydroxylation, this gene complements the *SUR2* mutation and thus, it encodes an active form of this enzyme. The *Ha*SC4H gene was expressed at high levels in cotyledons and vegetative tissues and to a lesser extent in developing seeds. Furthermore, a sphingolipid Δ8-desaturase was also cloned from sunflower that is highly homologous to a previously reported desaturase called *Ha*SLD1. The *Ha*SLD2 cloned was functional in *Saccharomyces cerevisiae*, where the enzyme desaturated endogenous phytosphinganines to Δ8-unsaturated derivatives. The expression profiles of these genes indicated that *Ha*SLD1 was expressed at high levels in all vegetative tissues while the newly described *Ha*SLD2 was a seed-specific enzyme.

5. Experimental Procedures

5.1. Biological material and growth conditions

The wild-type Sunflower (*Helianthus annuus* L.) CAS-6 line (Sunflower Collection of Instituto de la Grasa, CSIC, Sevilla, Spain) was grown as described elsewhere (Álvarez-Ortega et al., 1997). Plants were cultivated in growth chambers at 25 ºC/15 ºC (day/night cycles), with a 16 h photoperiod and a photon flux density of 200 µmol $m^{-2}s^{-1}$. The seeds used for cDNA synthesis were collected at 15 and 20 days after flowering (DAF), while samples of vegetative tissues (stem, leaf, root and seedling cotyledons) were collected from plants 20 days after germination. All the samples were frozen and stored at -80 ºC.

The *E. coli* strain XL1-Blue (Stratagene, La Jolla, CA, USA) was used as the plasmid host for cloning. These bacteria were grown in LB medium [pH 7] (1 % Bacto Tryptone, 0.5 % Bacto Yeast Extract, 1 % NaCl) at 37 °C with shaking, and the plasmids were selected in the presence of ampicillin (50 µg mL^{-1}).

The *S. cerevisiae* strains Y03656 (*MAT***a** *his3Δ1 leu2Δ0 met15Δ0 ura3Δ0 sur2*Δ::*kanMX4*) and W303-1A (MAT**a** *leu2-3,112 trp1-1 can1-100 ura3-1 ade2-1 his3-11,15*) were used here.

5.2. mRNA preparation and cDNA synthesis.

Sunflower leaf tissue (0.25 g) was ground in liquid nitrogen in a precooled sterile mortar. Total RNA was extracted using a Spectrum Plant Total RNA Kit (Sigma-Aldrich) and mRNA was isolated from the total RNA using the GenElute mRNA Miniprep Kit (Sigma-Aldrich). The mRNA pellet was resuspended in 33 µl RNAase free TE buffer (10 mM Tris-HCl, 1 mM EDTA pH 8) and the corresponding cDNA was synthesized using the Ready-To-Go T-Primed First-Strand Kit (Amersham Biosciences).

5.3. Sunflower HaSC4H and HaSLD2 cloning.

Sphingolipid hydroxylase and desaturase protein sequences from the public database were aligned to identify strongly homologous regions using the ClustalX v2.0.5 programme (Thompson et al., 1997). Two PCR fragments were amplified with pairs of degenerate primers designed from the highly conserved regions for both proteins (Table 1): *HaSC4H*-1f and *HaSC4H*-1r for *HaSC4H,* and *HaSLD2*-1f and *HaSLD2*-1r for *HaSLD2*. These fragments were cloned into the pMBL-T vector (MBL) and several clones were sequenced on both strands by SECUGEN (Madrid, Spain), confirming their identity using the BLAST software (Altschul et al., 1990). Both the 5' and 3' ends of the cDNAs were obtained using the Smart-RACE cDNA amplification kit (Clontech) and the following internal oligonucleotides (Table 4): *HaSC4H*-2f, *HaSC4H*-3f, *HaSC4H*-2r, and *HaSC4H*-3r for *HaSC4H,* and *HaSLD2*-2f, *HaSLD2*-2r, and *HaSLD2*-3r for *HaSLD2*. Additional primers with internal *Kpn*I-*Sph*I restriction sites for *HaSC4H*, *HaSC4H*-kpnI-F and *HaSC4H*-sphI-R, and *Kpn*I-*Sac*I for *Ha*SLD2, *Ha*SLD2-kpnI-F and HaSLD2-sacI-R, were designed to amplify the coding regions of the mature proteins by PCR. The PCR products obtained were subcloned into the pYES2 vector (Invitrogen), the correct reading frames were confirmed in these new constructs by sequencing. The resulting constructs were designated as pYES:*HaSC4H* and pYES:*HaSLD2*.

Table 4. Sequence of PCR primers used in this work. *Restriction sites are indicated in bold.

Primer name	Sequence*
***HaSC4H*-1f**	5'-GGRGCWCTWTAYAACCAYCCW-3'
***HaSC4H*-1r**	5'- DCCRTARAGYTGRTGRTG -3'
***HaSC4H*-2f**	5'- GGCCTTCTTCTCGATACAATCG -3'
***HaSC4H*-3f**	5'- TCGATCTTCTTCTTCTCATTTGC -3'
***HaSC4H*-2r**	5'- TGAAAGAGATTTCCAGGAAGCC -3'
***HaSC4H*-3r**	5'- CTGAAAGAAGAAAAGCGAGAGCC -3'
***HaSC4H*-kpnI-F**	5'- CG**GGTACC**ATGGAGGTTAAGATATCGG -3'
***HaSC4H*-sphI-R**	5'- CG**GCATGC**TCAATCATCCTTGACAAC -3'
***HaSC4H*-QPCR-F**	5'-CTTTACAACCATCCATTAGAAGGC-3'
***HaSC4H*-QPCR-R**	5'-GATTTCCAGGAAGCCATAATCCGC-3'
***HaSLD1*-QPCR-F**	5'-CCCGCCAAAAGGAGACAATTGG-3'
***HaSLD1*-QPCR-R**	5'-CGACCTCAAGTGACACCGTGG-3'
***HaSLD2*-1f**	5'-GTNACNGSGHTNCAACATRTTCAG-3'
***HaSLD2*-1r**	5'-CCATGRRTRTKRRAAGCTTCCC-3'
***HaSLD2*-2f**	5'-GGATTGGTTCTTCGGCGGTCTAC-3'
***HaSLD2*-2r**	5'-GCATCAAAGAACGATACGCTGG-3'
***HaSLD2*-3r**	5'-GGAGCTATGGACCTTAAATGGCAC-3'
HaSLD2-kpnI-F	5'-CG**GGTACC**ATGGGTGAAGATTCAACG-3'
HaSLD2-sacI-R	5'-CG**GAGCTC**TCAACCATGGGTGTTGAAAGC-3'
***HaSLD2*-QPCR-F**	5'-CCACCAACGGGAAACGACTG-3'
***HaSLD2*-QPCR-R**	5'-GGACCTTAAATGGCACCGAGG-3'

5.4. Quantitative real time PCR.

The cDNAs were subjected to quantitative real time PCR (QRT-PCR) with specific primer pairs (Table 1; *HaSC4H*-QPCR-F and *HaSC4H*-QPCR-R for *HaSC4H*; *HaSLD1*-QPCR-F and *HaSLD1*-QPCR-R for *HaSLD1*; and *HaSLD2*-QPCR-F and *HaSLD2*-QPCR-R for *HaSLD2*) and using SYBR Green I (QuantiTect® SYBR® Green PCR Kit, Quiagen, Crawley, UK) in a MiniOpticon system to monitor the resulting fluorescence (Bio-Rad). The reaction mixture was heated to 50 °C for 2 min and then to 95 °C for 15 min before subjecting it to 40 PCR cycles of: 94 °C for 15 s; 60.5 °C for 30 s; and 72 °C for 15 s. Calibration curves were drawn up using sequential dilutions of cDNA. The Livak method (Livak and Schmittgen, 2001) was applied to calculate comparative expression levels between samples and the sunflower actin gen *Ha*ACT1 (GenBank accession number FJ487620).

5.5 Expression of HaSC4H and HaSLD2 in yeast.

The pYES:*HaSC4H* and pYES:*HaSLD2* constructs were introduced, into the Y03656 and W303-1A *Saccharomyces cerevisiae* strains, respectively by the lithium acetate method. The cultures were grown at 30 ºC in the presence of 2% (w/v) raffinose, and the expression of the transgene was induced by adding galactose 2% (w/v) and raffinose 1% (w/v), whereas it was inhibited by the addition of glucose 1% (w/v).

5.6. Long chain base analysis.

Fresh sunflower tissue (0.5 g approx) was homogenised in 3 mL of 1,4-dioxane plus 2 mL 10% of $Ba(OH)_2$ after adding 35 nmole of d17:1$^{\Delta 4t}$ as an internal standard. This mixture was digested at 110°C for 24h by a modified version of the method described previously (Sperling et al., 1998). Once the tissue had been digested, 2 mL of 2M $(NH_4)_2SO_4$ was added to precipitate barium as $BaSO_4$ before the lipids were extracted twice with 5 mL of ethyl ether. The organic phase, containing LCBs was evaporated under nitrogen at 40°C and resuspended in 0.1 mL of ethanol. LCBs were then transformed into their orthophthalaldehyde (OPA) derivatives by reaction with 100 µL of the OPA reagent for 15 min. at room temperature (25 mg OPA and 25 µL 2-mercaptoethanol dissolved in 0.5 mL of ethanol and made up to 50 mL with aqueous Na_2BO_3 pH 10.5). The resulting OPA derivatives were made up to a volume of 1ml with methanol and cleared by centrifugation, before analysing the cleared supernatants by HPLC-fluorescence. In yeast, an analogous procedure was used to analyse LCBs, and the digestion mixture and internal standards were applied to the cell pellets resulting from the centrifugation of the liquid yeast culture.

5.7. HPLC system.

The HPLC system used here was a Waters 2695 separation module coupled to a Waters X-Bridge 4.6 x 250 mm reverse-phase column and a Waters 2475 fluorescence detector. The OPA derivatives were separated in a isocratic methanol/phosphate buffer (90:10 v/v) as the mobile phase at a flow rate of 1 mL/min. The excitation and emission wavelengths in the detector were set at 340/455, and the peaks were identified using commercial standards and on the basis of prior separations (Markham et al., 2006).

Furthermore, assignation was later validated by HPLC-MS. Quantification was carried out by comparing the relative areas corresponding to each peak with that of the internal standard d17:1$^{\Delta 4t}$.

Acknowledgments

We would like to thank Dr Frederic Beaudoin (Rothamsted Research, UK) for providing us with the Y03656 *Saccharomyces cerevisiae* strain. This work was supported by the Ministerio de Ciencia e Innovación and FEDER, project AGL2008-01086/ALI.

References

Altschul, S.F., Gish, W., Miller, W., Myers, E.W., Lipman, D.J., 1990. Basic local alignment search tool. J. Mol. Biol. 215, 403-410.

Álvarez-Ortega, R., Cantisán, S., Martínez-Force, E., Garcés, R., 1997. Characterization of polar and non polar seed lipid classes from highly saturated fatty acid sunflower mutants. Lipids. 32, 833-837.

Borner, G.H., Sherrier, D.J., Weimar, T., Michaelson, L.V., Hawkins, N.D., Macaskill, A., Napier, J.A., Beale, M.H., Lilley, K.S., Dupree, P., 2005. Analysis of detergent-resistant membranes in Arabidopsis. Evidence for plasma membrane lipid rafts. Plant Physiol. 137, 104–116.

Chen M., Han G., Dietrich C.R., Dunn T.M., Cahoon, E.B., 2006. The essential nature of sphingolipids in plants as revealed by the functional identification and characterization of the Arabidopsis LCB1 subunit of serine palmitoyltransferase. Plant Cell. 12, 3576–3593.

Chen M., Markham J.E., Dietrich C.R., Jaworski J.G., Cahoon E.B., 2008. Sphingolipid long-chain base hydroxylation is important for growth and regulation of sphingolipid content and composition in Arabidopsis. Plant Cell. 20, 1862–1878.

Coursol, S., Fan, L.M., Le Stunff, H., Spiegel, S., Gilroy, S., Assman, S.M., 2003. Sphingolipid signaling in Arabidopsis guard cells involves heterotrimeric G proteins. Nature. 423, 651–654.

Coursol, S., Le Stunff, H., Lynch, D.V., Gilroy, S., Assmann, S.M., Spiegel, S., 2005. Arabidopsis sphingosine kinase and the effects of phytosphingosine-1-phosphate on stomatal aperture. Plant Physiol. 137, 724-737.

Grilley, M.M., Stock, S.D., Dickson, R.C., Lester, R.L., Takemoto, J.Y., 1998. Syringomycin action gene SYR2 is essential for sphingolipid 4-hydroxylation in Saccharomyces cerevisiae. J. Biol. Chem. 273, 11062-11068.

Haak D., Gable K., Beeler T., Dunn T., 1997. Hydroxylation of Saccharomyces cerevisiae Ceramides Requires Sur2p and Scs7p. J. Biol. Chem. 272, 29704-29710.

Hanada K., 2003. Serine palmitoyltransferase, a key enzyme of sphingolipid metabolism. Biochimica et Biophysica Acta (BBA) - Molecular and Cell Biology of Lipids. 1632, 16-30.

Imamura T., Kusano H., Kajigaya Y., Ichikawa M., Shimada H., 2007. A rice dihydrosphingosine C4 hydroxylase (DSH1) gene, which is abundantly expressed in stigmas, vascular cells and apical meristem, may be involved in fertility. Plant Cell Physiol. 48, 1108-1120.

Kaul, K., Lester, R.L., 1978. Isolation of six novel phosphoinositol containing sphingolipids from tobacco leaves. Biochemistry. 17, 3569-3575.

Liang H., Yao N., Song J.T., Luo S., Lu H., Greenberg J.T., 2003. Ceramide phosphorylation modulates programmed cell death in plants. Genes Dev. 17, 2636-2641.

Livak, K.J., Schmittgen, T.D., 2001. Analysis of relative gene expression data using real time quantitative PCR and the 2-ΔΔCT method. Methods. 25, 402-408.

Lynch D.V., Phinney A.J., 1995. The transbilayer distribution of glucosylceramide in plant plasma membrane, in: Kader, J.C., Mazliak, P. (Eds.), Plant Lipid Metabolism. Kluwer Academic Publishing, Dordrecht, pp. 239-241.

Lynch, D.V., Dunn, T.M., 2004. An introduction to plant sphingolipids and a review of recent advances in understanding their metabolism and function. New Phytol. 161, 677-702.

Markham J.E., Li J., Cahoon E.B., Jaworski J.G., 2006. Separation and identification of major plant sphingolipid classes from leaves. J. Biol. Chem. 281, 22684-22694.

Markham, J.E., Jaworski, J.G., 2007. Rapid measurement of sphingolipids from Arabidopsis thaliana by reversed-phase high-performance liquid chromatography coupled to electrospray ionization tandem mass spectrometry. Rapid Commun. Mass Spectrom. 21, 1304-1314.

Mongrand S., Morel J., Laroche J., Claverol S., Carde J.P., Hartmann M.A., Bonneu M., Simon-Plas F., Lessire R., Bessoule J.J., 2004. Lipid Rafts in Higher Plant Cells Purification and characterization of triton x-100-insoluble microdomains from tobacco plasma membrane. J. Biol. Chem. 279, 36277-36286.

Obeid L.M., Okamotoc Y., Maob C., 2002. Yeast sphingolipids: metabolism and biology. Biochimica et Biophysica Acta - Molecular and Cell Biology of Lipids. 1585, 163-171.

Ryan, P.R., Liu, Q., Sperling, P., Dong, B., Franke, S., Delhaize, E., 2007. A higher plant D8 sphingolipid desaturase with a preference for (Z)-isomer formation confers aluminum tolerance to yeast and plants. Plant Physiol. 144, 1968-1977.

Sperling P., Schmidt H., Heinz E., 1995. A Cytochrome-b5-Containing Fusion Protein Similar to Plant Acyl Lipid Desaturases. Eur. J. Biochem. 232, 798-805.

Sperling P., Zahringer U., Heinz E., 1998. A sphingolipid desaturase from higher plants: identification of a new cytochrome b5 fusion protein. J. Biol. Chem. 273, 28590-28596.

Sperling P., Blume A., Zahringer U., Heinz E., 2000. Further characterization of D8-sphingolipid desaturases from higher plants. Biochem. Soc. Trans. 28, 638-641.

Sperling P., Ternes P., Moll H., Franke S., Zahringer U., Heinz E., 2001. Functional characterization of sphingolipid C4-hydroxylase genes from Arabidopsis thaliana. FEBS Lett. 494, 90-94.

Sperling, P., Heinz, E., 2003. Plant sphingolipids: structural diversity, biosynthesis, first genes and functions. Biochim Biophys Acta. 1632, 1-15.

Ternes P., Franke S., Zähringer U., Sperling P., Heinz E., 2002. Identification and characterization of a sphingolipid 4-desaturase family. J. Biol. Chem. 277, 25512-25518.

Thompson, J.D., Gibson, T.J., Plewniak, F., Jeanmougin, F., Higgins, D.G., 1997. The ClustalX windows interface: flexible strategies for multiple sequence alignment aided by quality analysis tools. Nucleic Acids Res. 25, 4876-4882.

Wright B.S., Snow J.W., O´Brien T.C., Lynch D.V., 2003. Synthesis of 4-hydroxysphinganine and characterization of sphinganine hydroxylase activity in corn. Archives of Biochemistry and Biophysics 415 184–192.

Zink S., Mehlgarten C., Kitamoto H.K., Nagase J., Jablonowski D., Dickson R.C., Stark M. J.R., Schaffrath R., 2005. Mannosyl-Diinositolphospho-Ceramide, the Major

Yeast Plasma Membrane Sphingolipid, Governs Toxicity of Kluyveromyces lactis Zymocin. Eukaryot. Cell. 4, 879-889.

CONCLUSIONES

Bloque I

1. A partir de semillas en desarrollo de ricino (*Ricinus communis* L.) se han clonado y secuenciado los cDNAs *RcFatA* y *RcFatB* que codifican acil-ACP tioesterasas de tipo A y B, respectivamente. Tanto *RcFatA* como *RcFatB* se encuentran como copia única en el genoma del ricino y los picos máximos de expresión para ambos genes se localizan en estadíos de semillas que coinciden con el periodo de mayor síntesis de aceite.

2. La expresión heteróloga de *RcFatA* y *RcFatB* en *E. coli* alteró el contenido y composición de ácidos grasos de la bacteria, demostrando la producción de proteínas activas en dicho hospedador.

3. La caracterización *in vitro* de las proteínas recombinantes purificadas *Rc*FatA y *Rc*FatB, mostró perfiles de especificidad y eficiencias catalíticas altas para el oleil-ACP, pudiendo explicar ésto el alto contenido de ácidos grasos C18 encontrados en el aceite de semillas de ricino.

4. A partir de nueces de macadamia variedad cate (*Macadamia tetraphylla* L. Johnson) se han clonado y secuenciado los cDNAs *MtFatA* y *MtFatB* que codifican acil-ACP tioesterasas de tipo A y B, respectivamente.

5. La caracterización de los parámetros cinéticos de *Mt*FatA y *Mt*FatB purificadas tras ser expresadas heterologamente en *E. coli*, mostró que MtFatA presenta la mayor especificidad por 16:1-ACP medida en FatAs purificada hasta la fecha, demostrando el rol de esta enzima en el alto contenido de ácidos grasos n-7 en nueces de macadamia. Por el contrario *Mt*FatB mostró un perfil de afinidad por substrato y de eficiencias catalíticas acorde con lo demostrado en otras plantas anteriormente.

6. Se ha aislado y caracterizado la línea mutante para los genes *fata1* y *fata2* de Arabidopsis (*fata1/fata2*), la cual, aunque no presentó diferencias fenotípicas evidentes, mostró bajos niveles de expresión de ambos genes y una actividad tioesterasa reducida respecto a la línea control Col-0.

7. La reducción en la actividad tioesterasa de la línea *fata1/fata2* provocó un descenso en la cantidad de lípidos de la planta respecto a Col-0 debido a la disminución del flujo de síntesis lipídica.

8. El incremento porcentual de ácido linolénico y ácidos grasos de cadena larga a expensas del descenso de los ácidos grasos oleico y linoleico en la línea *fata1/fata2* respecto a Col-0, se debe en mayor medida a que los genes codificantes para la linoleato desaturasa (LDS) y elongasas de ácidos grasos (FAE) no están controlados por el flujo metabólico intraplastidial.

9. El cDNA *HaFatA* ha sido modificado mediante mutagénesis dirigida y los diferentes alelos obtenidos fueron expresados en *E. coli*, purificados y caracterizados bioquímicamente. El alelo Q215W puso de manifiesto una mayor eficiencia catalítica por todos los substratos ensayados, por el contrario, el alelo T182W mostró una actividad casi nula.

10. Aunque el contenido total de ácidos grasos en hojas de tabaco expresando transitoriamente el alelo Q215W, no aumentó respecto a los controles, la cantidad total de triacilglicéridos aumentó dos veces respecto a hojas expresando el alelo silvestre *HaFatA* y cuatro veces respecto a las que expresaban el alelo T182W.

11. El incremento relativo de ácidos grasos saturados en hojas de tabaco expresando el alelo Q215W respecto a los controles se debe a la afinidad relativa de la acil-ACP tioesterasa respecto a las enzimas que incorporan moléculas de acil-ACP a la ruta procariota, la cual es mayoritaria en hojas.

Bloque II

12. A partir de hojas de girasol (*Helianthus annuus* L.) se ha clonado y secuenciado el cDNA *HaPLDα* codificante de la actividad fosfolipasa D. *HaPLDα* se encuentra como copia única en el genoma del girasol y se expresa en todos los tejidos estudiados aunque su expresión es mayor en tejidos verdes (hoja, tallo y cotiledón).

13. La actividad del producto proteico de *HaPLDα* expresado heterologamente y purificado, depende del pH, la concentración de $CaCl_2$ y de la adición de un surfactante, siendo el pH 6.5 y las concentraciones de 10mM de $CaCl_2$ y 5mM de SDS las determinadas como óptimas para el ensayo de actividad. No existieron diferencias de afinidad por diferentes substratos a excepción de PI, el cual no pudo ser hidrolizado.

14. Los niveles de expresión de *HaPLDα* generalmente correlacionaron bien con las actividades PLD medidas en extractos de girasol, a excepción de semillas de 14 días después de floración y cotiledones, apuntando a una posible regulación postranscripcional.

Bloque III

15. Usando hojas de girasol, se ha clonado y secuenciado el cDNA *HaSC4H* que codifica para una Δ4-hidroxilasa de esfingolípidos. La expresión de *HaSC4H* se detecta sobre todo en tejidos vegetativos siendo los cotiledones en desarrollo los órganos de la planta con mayor expresión.

16. La expresión heteróloga de *HaSC4H* en una cepa mutante de *S. cerevisiae* deficiente en la actividad de hidroxilación, provocó la complementación de la mutación de la levadura al detectarse LCBs trihidroxilados en el perfil de esfingolípidos.

17. A partir de hojas de girasol, se ha clonado y secuenciado el cDNA *HaSLD2* que codifica para una Δ8-desaturasa de esfingolípidos. La expresión de *HaSLD2* se diferencia de la Δ8-desaturasa anteriormente clonada *HaSLD1* debido a que la expresión de *HaSLD2* es prácticamente específica de semillas en desarrollo.

18. La actividad Δ8-desaturasa fue corroborada al expresar el clon *HaSLD2* en una cepa silvestre de *S. cerevisiae* y aparecer LCBs con insaturaciones en su perfil de esfingolípidos.